

Monday Morning, August 3, 2026

International Workshop on Gallium Oxide and Related Materials (IWGO-6)

Room ESJ 0202 - Session IWGO-MoM1

Plenary Session I

Moderators: James Speck, University of California Santa Barbara, Marko Tadjer, U.S. Naval Research Laboratory

8:00am IWGO-MoM1-1 Breakfast

8:45am IWGO-MoM1-10 Welcome & Sponsor Thank You

9:00am IWGO-MoM1-13 **PLENARY: Single Crystals and Wafers of β -Ga₂O₃, β -(Al_xGa_{1-x})₂O₃, and r-GeO₂**, **Zbigniew Galazka**, Leibniz-Institut für Kristallzüchtung, Germany **INVITED**

Ultra-wide bandgap (UWBG) oxide materials attract a considerable scientific and technological attention in the research community to boost the development of next generation power devices capable of switching high voltages. The development chain includes single crystal growth, substrates preparation, homo- and heteroepitaxial film growth, device fabrication in different architectures, study of physical properties of obtained materials, and characterization of the devices. This requires a multidisciplinary approach interconnecting science and technology.

During this talk, I will overview melt growth methods applied for β -Ga₂O₃ and β -(Al_xGa_{1-x})₂O₃ single crystals [1-3], their structural quality, and wafers. I will also highlight epitaxial film growth of β -Ga₂O₃ and β -(Al_yGa_{1-y})₂O₃ on β -(Al_xGa_{1-x})₂O₃ substrates by Metal-Organic Vapor Phase Epitaxy (MOVPE) [4, 5]. Ultra-high purity β -Ga₂O₃ single crystals grown by the Czochralski method and their features will be described as well. Additionally, doping of Czochralski-grown β -(Al_xGa_{1-x})₂O₃ single crystals with different 4+ elements will reveal their impact on electrical conductivity at high Al content (>20 mol.%).

The discussion will also cover rutile-GeO₂ (r-GeO₂) single crystals grown by a modified Top-Seeded Solution Growth (TSSG) with prepared epi-ready wafers [6, 7].

Finally, a comparison of basic physical properties of the discussed β -Ga₂O₃, β -(Al_xGa_{1-x})₂O₃, and r-GeO₂ single crystals and wafers might be useful for further development directions.

Acknowledgements: The work was financially supported by the following grants from the Bundesministerium für Bildung und Forschung (BMBF) nos. 03VP03712 and 16ES1084K, German Research Foundation (DFG) nos. 491040331 and 555506919, Senatsausschuss Wettbewerb (SAW) no. K417/2021, and ONRG no. N629092412105.

[1] Z. Galazka; J. Appl. Phys. 131 (2022) 031103.

[2] Z. Galazka; "Growth of bulk β -Ga₂O₃ single crystals" in "Comprehensive Semiconductor Science and Technology 2nd Ed.", Ed. R. Fornari, Elsevier (2025).

[3] Z. Galazka; IEEE Trans. Semicond. Manuf. 38 (2025) 796-802.

[4] S. Bin Anooz et al.; J. Phys. D: Appl. Phys. 59 (2026) 015308.

[5] S. Bin Anooz et al.; J. Vac. Sci. Technol. A 44 (2026) 032702.

[6] Z. Galazka et al.; J. Appl. Phys. 133 (2023) 035702.

[7] Z. Galazka et al.; Adv. Mater. Interfaces (2024) 2400122.

*Author for correspondence: zbigniew.galazka@ikz-berlin.de

9:45am IWGO-MoM1-22 **Plasma-Treatment Based (Near) Surface Doping of Semiconducting Oxides**, **Oliver Bierwagen**, Paul-Drude Institute for Solid State Electronics, Germany; **Piero Mazzolini**, University of Parma, Italy **INVITED**

The control of charge carrier concentration in (ultra-)wide bandgap oxide semiconductors usually involves the substitutional incorporation of foreign dopant atoms during growth or post growth by ion implantation or dopant in-diffusion. Above-room temperature growth or annealing processes are required for these approaches and often the dopant effect gets partially compensated by the formation of native point defects.

This talk will discuss a completely different approach based on two different room-temperature surface plasma treatments that induce free carrier systems in undoped (ultra-)wide bandgap oxide semiconductors.

In the first part, the creation of near-surface electron systems in *n*-type oxides, such as In₂O₃, SnO₂, and different polymorphs of Ga₂O₃ are

discussed in detail. For example, the resulting electron systems in undoped κ -Ga₂O₃ exhibited an unprecedentedly high electron mobility above 25 cm²/Vs at sheet/volume carrier concentrations around 2x10¹⁴ cm⁻²/4x10¹⁹ cm⁻³, and a similar carrier system was induced in a semi-insulating Mg-doped β -Ga₂O₃ substrate. The thermal stability of these electron systems is discussed and a native-point-defect based doping mechanism is proposed. That the discussed feature can also be a bug, is further highlighted by the unintentional creation of an electron system during sputter deposition of a dielectric SiO₂ layer on a homoepitaxial β -Ga₂O₃ layer.

The creation and thermal stability of a surface hole system in the *p*-type oxide NiO is demonstrated in the second part and shown to be related to surface charge transfer doping.

The presented approaches may provide an easy way of scouting the charge-carrier-transport potential of novel oxide semiconductors before elaborating substitutional doping, and will be tested against further topical and novel oxide semiconductors.

The presented body of work has been accumulated over more than ten years and we acknowledge all contributors, including, Marko Perestjuk, Ivana Lapsanska, Carmine Borelli, Andrea Ardenghi, Theresa Berthold, Melanie Budde, Marcel Himmerlich, Christian Golz, Abbas Tahraoui.

10:10am IWGO-MoM1-27 **Lattice Defects in β -Ga₂O₃ Crystals and Power Devices**, **Yongzhao Yao**, Mie University, Japan **INVITED**

Lattice defects in β -Ga₂O₃ significantly degrade the performance and reliability of Ga₂O₃-based devices. Establishing effective strategies to reduce such defects requires comprehensive knowledge of their three-dimensional spatial distribution as well as their structural characteristics. This information can be obtained through a combination of advanced characterization techniques, including transmission electron microscopy (TEM), phase-contrast microscopy, X-ray topography, and related X-ray imaging methods. In this work, we focus on the visualization and characterization of lattice defects and the evaluation of their impact on Ga₂O₃ power devices. We review recent results from our research group, where multiple X-ray imaging techniques—namely reflection and transmission X-ray topography (XRT), X-ray reticulography (XRR), and X-ray laminography (XRL)—have been employed to reveal structural defects such as dislocations, nano-voids, and domain boundaries in β -Ga₂O₃ crystals. Furthermore, reflection and transmission XRT has been extended to enable real-time observation of power devices under forward and reverse bias conditions (operando observation), allowing direct investigation of defect dynamics under external stimuli.

International Workshop on Gallium Oxide and Related Materials (IWGO-6)

Room ESJ 0202 - Session IWGO-MoM2

Epitaxial Growth and Doping Control I

Moderators: Oliver Bierwagen, Paul-Drude Institute for Solid State Electronics, Yuichi Oshima, National Institute for Materials Science

11:05am IWGO-MoM2-38 **Toward 150mm Ga₂O₃ Epitaxy by HVPE**, **Jacob Leach**, **Caroline Reilly**, **Heather Splawn**, KYMA TECHNOLOGIES, INC **INVITED**

The key to realizing the full potential of Ga₂O₃-based devices for medium voltage (>1kV) power switching applications lies in large part in the ability to grow thick (>20 microns) and simultaneously lightly doped (<1x10¹⁶ cm⁻³) drift layers with high crystalline quality. To date, the only option for preparing such thick layers on diameter-scalable (001)-oriented freestanding Ga₂O₃ substrates is halide vapor phase deposition (HVPE). Our previous work focused on the development of thick homoepitaxial layers on 2" substrates by HVPE which could be controllably doped throughout the ranges of interest for power electronics device designers, i.e. from ~5x10¹⁵ cm⁻³ to ~3x10¹⁶ cm⁻³ [1]. In this work, we report on the growth of commercially relevant Ga₂O₃ epilayers grown on 100mm and 150mm substrates using HVPE. Figures below show a photograph of an as-grown ~20 μ m thick epilayer as well as a N_D-N_A free carrier concentration map showing good doping control in the range of ~1-2x10¹⁶ cm⁻³ over a 100mm substrate. Initial results from similar epilayers grown on 150mm substrates will be presented as well as an outlook on the commercial landscape for thick epilayers of Ga₂O₃.

Acknowledgements

This technology was primarily supported by the Microelectronics Commons Program, a DoW initiative, under award number N00164-23-9-G059. The

Monday Morning, August 3, 2026

fundamentals had no role in study design, data collection or analysis, or preparation of the manuscript. **Distribution Statement A: Approved for public release. Distribution is unlimited.**

[1] Leach et al. GOX 2025, Salt Lake City UT, USA, 5 August 2025.

11:30am IWGO-MoM2-43 MOCVD Growth of (011) β -Ga₂O₃ up to 20 μ m: Defect Optimization and Device Impact, Md Mosarof Hossain Sarkar, Dong su Yu, The Ohio State University; Jiawei Liu, SUNY at Buffalo; Sadikul Alam, Mehidi Hassan, The Ohio State University; Yuki Ueda, Chia-Hung Lin, Kohei Sasaki, Novel Crystal Technology, Japan; Jinwoo Hwang, The Ohio State University; Uttam Singiseti, SUNY at Buffalo; Hongping Zhao, The Ohio State University

β -Ga₂O₃ has emerged as a promising semiconductor for vertical power electronics. However, achieving high-quality thick β -Ga₂O₃ drift layers with smooth surface morphology and well-controlled low doping remains a long-standing challenge. In HVPE growth of thick (001) β -Ga₂O₃, post-growth chemical-mechanical polishing (CMP) is typically required to achieve adequate surface smoothness for device processing.

In this study, (011) β -Ga₂O₃ films up to 20 μ m thick were grown on (011) β -Ga₂O₃ substrates at growth rates of 2.86–5.5 μ m/h. Atomic force microscopy (AFM) measurements revealed smooth surfaces with RMS roughness of 0.48–1.05 nm (5x5 μ m²), among the lowest reported for comparable thicknesses. X-ray diffraction (XRD) confirmed high crystalline quality, with rocking curve FWHM of 13.6 arcsec (on-axis) and 29.2 arcsec (off-axis), indicating low threading dislocation density. Dent-type defects increased with thickness but were mitigated by incorporating a buffer layer. Secondary ion mass spectrometry (SIMS) indicated low background levels of C, H, and Si, near the detection limit.

Substrate pre-treatment and growth conditions were optimized to suppress dent-type defects. The incorporation of acid treatment, in-situ annealing, buffer layers, and pulse-flow growth layer led to a reduction of defect density by over an order of magnitude. Schottky barrier diodes (SBDs) were fabricated on the MOCVD-grown (011) β -Ga₂O₃ drift layers, as shown in Fig. 1(a). The forward J–V characteristics exhibit near-ideal behavior with an ideality factor of $\eta = 1.02$, Schottky barrier height of $\phi_b = 1.47$ eV, and turn-on voltage of $V_{on} = 1.11$ V (defined at 1 A/cm²). The forward current density exceeded 1250 A/cm² at 5 V. Reverse-bias measurements yielded a breakdown voltage of ~640–740 V, which is expected to be further improved through optimized field-management designs in future work.

Overall, these results demonstrate that high-quality thick (011) β -Ga₂O₃ drift layers can be achieved by MOCVD with effective defect control, enabling strong potential for high-performance vertical power devices.

11:45am IWGO-MoM2-46 Colossal Bandgaps: Growing Si-Doped α -(Al_xGa_{1-x})₂O₃ Films with $E_g \leq 7$ eV with s-MBE, Jacob Steele, Debiditya Bhattacharya, Kazuki Nomoto, Cornell University; M. K. Indika Senevirathna, Clark Atlanta University; Huili "Grace" Xing, Debdeep Jena, Darrell G. Schlom, Cornell University

One emerging ultrawide bandgap material that is closely related to Ga₂O₃ is α -(Al_xGa_{1-x})₂O₃, which has a tunable E_g ranging 5.4 – 8.6 eV. Despite theory predicting silicon to be a shallow n type donor over the range of 5.4 – 7.5 eV[1], achieving active donors has proven to be extremely difficult. This challenge has led to only molecular-beam epitaxy (MBE)[2], metal-organic chemical vapor deposition (MOCVD)[3], and mist chemical vapor deposition (CVD)[4] having produced any conductive films with $x > 0$.

We previously have demonstrated that an uncommon variant of MBE, suboxide MBE (S-MBE), can be utilized to grow α -(Al_xGa_{1-x})₂O₃ with excellent structural quality[5], as well as α -Ga₂O₃ with record electronic properties[6]. In this work, we report a multistep S-MBE technique that reliably produces conductive Si-doped α -(Al_xGa_{1-x})₂O₃ thin films with S-MBE. The technique produces conductive α -(Al_xGa_{1-x})₂O₃ thin films with $x \leq 0.58$ ($E_g = 7.0$ eV).

[1] D. Wickramaratne, J.B. Varley, & J.L. Lyons, *Appl. Phys. Lett.* **121**, 042110 (2022).

[2] H. Okumura, and J.B. Varley, *Jpn. J. Appl. Phys.* **63**(7),075502 (2024).

[3]H. Okumura et al., *Jpn. J. Appl. Phys.* **63**(5), 055502 (2024).

[4] G.T. Dang, et al. 2020, *AIP Adv.* **10**, 115019

[5] J. Steele, et al., *APL Mater.* **12**(4), 041113 (2024).

[6] J. Steele, et al. *APL Mater.* **13**, 101117 (2025).

12:00pm IWGO-MoM2-49 Fast Step-Flow Growth on Highly Offcut (100) Ga₂O₃ Substrates, M Brooks Tellekamp, National Renewable Energy Laboratory; Drew Haven, David Joyce, Luxium Solutions; Henry Garland, John Mangum, National Renewable Energy Laboratory; Kevin Schulte, Anna Sacchi, Matthew Young, Andriy Zakutayev, national renewable Energy Laboratory

The (100) surface of Ga₂O₃ is highly desirable from a device and epitaxy standpoint – bulk growth of (100) material is more scalable than (010), the surface is nearly lattice-matched to p-type partner NiO, and Al₂O₃ incorporates at higher concentrations without phase separation. More importantly, the impact ionization coefficients along the [100] direction are minimized while the dielectric constant is maximized, leading to the highest possible critical fields. This is advantageous compared to the current state of the art, (001), due to reduced surface defects and increased possible breakdown voltage. However, the epitaxial growth rate on (100) surfaces is less than 10% of other faces due to weak bonding and favorable desorption, and on-axis (100) growth easily forms twin domains. Recent demonstrations have shown growth rate improvements from 0.4 nm/min to 1.5 nm/min by growing on (100) wafers that are offcut 6° in the -c direction.¹ These films show step-flow growth from (20-1) step-edges and high electron mobility due to suppressed twins. Despite these exciting results, offcuts greater than 6° have not been explored due to the waste associated with grinding and polishing large offcuts.

In this talk we will discuss the molecular beam epitaxy (MBE) growth and properties of β -Ga₂O₃ grown on (100) substrates offcut in the -c direction up to 13.4°. These large offcuts are enabled by edge-fed film-defined growth (EFG) where the offcut is grown into the surface by pulling the crystal through the EFG die with the seed crystal rotated by the desired offcut angle. We will demonstrate that 13.4° offcut substrates still exhibit a terraced (100) surface, and that a >10x increase (>5 nm/min) in growth rate is achieved. Despite the large offcut angle we will demonstrate step-flow growth with RMS roughness values below 2 nm RMS, even after 600 nm of growth. As previously reported on lower offcuts, we observe reversal of substrate twin domains around the (001) direction at the substrate-epitaxial interface. This increase in growth rate, along with careful control of impurity levels, leads to record-low (by MBE) unintentional doping densities of < 2E15 cm⁻³ on 13.4° offcut wafers and < 5E15 cm⁻³ on 11.1° offcut wafers. We will also demonstrate (Al_xGa_{1-x})₂O₃ films grown on highly offcut substrates are monoclinic up to $x = 0.33$. This work establishes highly offcut (100) β -Ga₂O₃ as a viable and scalable alternative substrate orientation for power electronic devices.

12:15pm IWGO-MoM2-52 Record High Mobility with Observation of Quantum Oscillations at Low Temperature for 2DEGs in MOCVD Grown β -(Al_xGa_{1-x})₂O₃/ β -Ga₂O₃ Heterostructures, Joshua Buontempo, Cameron Gorsak, Pushpanshu Tripathi, Hari Nair, Cornell University

The ultra-wide bandgap (~ 4.8 eV) and high estimated breakdown field strength (8 MV/cm) of β -Ga₂O₃ make it a promising material for radio frequency applications [1]. One of the main material limitations that hinders device performance is a low maximum room temperature mobility (~ 200 cm²/Vs) [2]. This is further exacerbated once dopants are introduced into the β -Ga₂O₃ lattice, as scattering from ionized and neutral impurities further reduces the electron mobility [2, 3]. One approach to increase the carrier mobility, while retaining high carrier densities, is to implement modulation doping in a heterostructure. The spatial separation of the impurity atoms from the charge carriers in a triangular quantum well results in the formation of a high mobility 2-dimensional electron gas (2DEG) channel [4, 5].

In this work, we utilize triethylaluminum (TEAl) and triethylgallium (TEGa) for the source of Al and Ga, respectively, to grow β -(Al_xGa_{1-x})₂O₃/ β -Ga₂O₃ heterostructures by MOCVD. TEAl and TEGa pyrolyze via β -hydrogen elimination [6], enabling minimal carbon incorporation at a relatively low substrate temperature of 650 °C, which is essential for mitigating the formation of compensating gallium vacancies while maintaining high crystalline quality and low surface roughness. As-grown films exhibit room-temperature mobilities as high as 165 cm²/Vs at a sheet density of ~ 1.8 × 10¹² cm⁻². The films exhibits record low-temperature mobility for a β -(Al_xGa_{1-x})₂O₃/ β -Ga₂O₃ 2DEG as high ~ 2914 cm²/Vs at 45 K.

Additionally, from Shubnikov–de Haas (SdH) oscillations below 5 K, we extract a 2DEG density of 1.7 × 10¹² cm⁻², in agreement with transport data. We extract a cyclotron effective mass, $m^* = 0.308 \pm 0.004 m_e$, which agrees with the calculated conduction band non-parabolicity in β -(Al_xGa_{1-x})₂O₃/ β -Ga₂O₃ and the estimated position of E_f above the conduction band

Monday Morning, August 3, 2026

minimum [7]. This work affirms the viability of MOCVD using TEAl and TEGa for growing high-quality gallium oxide-based heterostructures.

References

- [1] Higashiwaki et al., AAPPS Bull. 32(1), 2022.
- [2] Ma et al., Appl. Phys. Lett. 109, 2016.
- [3] Jena et al., Oxford Univ. Press, 2022.
- [4] Shieh et al., J. Vac. Sci. Technol. B 12, 1994.
- [5] Kudo et al., Jpn. J. Appl. Phys. 33, 1994.
- [6] Smith et al., J. Inorg. Nucl. Chem. 29(3), 1967.
- [7] Peelaers et al., Appl. Phys. Lett. 111, 2017.

Monday Afternoon, August 3, 2026

International Workshop on Gallium Oxide and Related Materials (IWGO-6)

Room ESJ 0202 - Session IWGO-MoA1

Defects Science I

Moderators: John Lyons, Naval Research Laboratory, Matthew McCluskey, Washington State University

2:00pm **IWGO-MoA1-1 Toward Quantitative Modeling of Temperature-Dependent Defect Physics in β -Ga₂O₃**, *Elif Ertekin*, University of Illinois; *Michael Scarpulla*, University of Utah; *Joel Varley*, Lawrence Livermore National Lab; *Nasim Alem*, Penn State University; *Channyung Lee*, *Grace McKnight*, University of Illinois; *Aaditta Arnab*, University of Utah **INVITED** β -Ga₂O₃ is a promising semiconductor for next-generation power electronics due to its ultrawide band gap and high critical breakdown field. While first-principles methods have provided substantial insight into its ground-state properties, many of the key processes governing synthesis and device operation occur at elevated temperatures, where defect thermodynamics, diffusion, and electron-phonon interactions become central. In this presentation, I will discuss efforts to develop a quantitatively predictive description of these temperature-dependent effects, with the goal of achieving direct and reliable agreement with experiment.

Temperature plays a dual role in β -Ga₂O₃, simultaneously influencing defect populations and enabling mass transport. The low-symmetry monoclinic structure gives rise to complex, anisotropic diffusion pathways for both native defects and impurities, with migration governed by a competition between interstitial, interstitialcy, and trap-limited mechanisms. When coupled with the strong temperature dependence of defect formation energies, including contributions from chemical potentials, band gap renormalization, and vibrational entropy, this leads to significant changes in predicted dopability and compensation behavior under realistic growth and annealing conditions.

These same thermodynamic and kinetic effects extend beyond point defects. Under conditions of elevated temperature and nonstoichiometry, polymorphic transformations become accessible, and the formation of γ -Ga₂O₃ within β -Ga₂O₃ can be understood in terms of vacancy-mediated pathways and configurational entropy contributions to phase stability. Such mechanisms are consistent with experimental observations of nanoscale γ -phase inclusions and interfacial layers.

Temperature also directly modifies the electronic structure through lattice expansion and electron-phonon coupling, producing substantial band-edge shifts across device-relevant temperature ranges. Taken together, these effects highlight the interconnected roles of temperature, defects, and lattice dynamics in determining the behavior of β -Ga₂O₃, and underscore the importance of incorporating finite-temperature physics into predictive modeling of ultrawide-band-gap semiconductors.

2:25pm **IWGO-MoA1-6 Characterization of β -Ga₂O₃ Deep Acceptor/ n^- Junction Diodes Grown by Molecular Beam Epitaxy**, *Steve Rebollo*, *Wolfgang Buchmaier*, *Sriram Krishnamoorthy*, *James Speck*, UC Santa Barbara

β -Ga₂O₃ lacks p-type conductivity in part due to the lack of shallow acceptors. Despite this, deep acceptor doping is of interest because deep acceptor doped layers can be used to create potential energy barriers in devices. Unlike shallow dopants, which are always fully ionized at room temperature, the ionization of deep dopants may change with operating conditions which may impact device performance. Here, we investigate the electrical properties of β -Ga₂O₃ deep acceptor/ n^- junction diodes.

An epitaxial stack consisting of a 320 nm thick, 3×10^{17} cm⁻³ Si-doped n^- layer followed by a 20 nm thick, 8×10^{19} cm⁻³ Mg-doped layer was grown by plasma-assisted molecular beam epitaxy (PAMBE) on a Sn-doped, n^- (001) β -Ga₂O₃ substrate. Metal-oxide-catalyzed epitaxy (MOCATAXY) was used to enable high quality growth. A wet-etch only process with hot-H₃PO₄ was used to co-fabricate both mesa deep-acceptor/ n^- junction diodes and planar Schottky barrier diodes (SBDs). Ni/Au was used to contact the Mg-doped and n^- layers while Ti/Au was used as a backside ohmic contact. The band diagram for virgin devices is similar to that of a pn diode.

The deep acceptor/ n^- diodes exhibit rectifying behavior. Compared to a SBD, which has a minimum ideality factor of 1.1, a specific on-resistance of 6.0 m Ω cm², and a turn-on voltage of 0.8 V, the deep acceptor/ n^- diode has a minimum ideality factor of 1.9, an $R_{on,sp}$ of 24.9 m Ω cm², and a turn-on voltage of 2.4 V. The virgin deep acceptor/ n^- diode exhibits a built-in voltage of 3.1 V as determined from capacitance-voltage measurements. The V_{bi} increased to 3.6 V when the measurement was repeated following the

initial IV measurements. The IV and CV characteristics remain unchanged over the span of 5 weeks. The V_{bi} further increases to 4.5 V following a proper burn-in (5 V for 60 s). The CV characteristics are unaffected by AC frequency or by large pre-soak voltages.

The observed behavior is attributed to deep acceptor states trapping electrons when the diode is turned on. This increases the depletion region width and built-in voltage when compared to virgin devices. Detrapping appears to be a slow process. It is hypothesized that the diode is a majority carrier device with overflow electrons that reach the Ni/Au contact contributing to current flow. The quadratic turn-on behavior implies space-charge limited transport, but additional experiments are required to confirm this. Of note, the V_{bi} demonstrated here is significantly larger than what has been demonstrated in β -Ga₂O₃ SBDs and heterojunction devices. The large V_{bi} and the stable device characteristics suggest that Mg may be a promising deep acceptor candidate for β -Ga₂O₃ devices.

2:40pm **IWGO-MoA1-9 Identification and Suppression of Carbon-Related Trap States and Carrier Compensation in MOCVD-Grown β -Ga₂O₃**, *Miranda Carver*, *Hemant Ghadi*, *Lingyu Meng*, *Dong Su Yu*, *Hongping Zhao*, *Aaron Arehart*, *Steven Ringel*, Ohio State University

Beta-phase gallium oxide (β -Ga₂O₃) is a promising ultra-wide-bandgap semiconductor for next-generation power and high-frequency devices due to its large bandgap (~4.8 eV), high theoretical breakdown field (>8 MV/cm), and availability of melt-grown native substrates. Epitaxial growth by metal-organic chemical vapor deposition (MOCVD) produces high-quality β -Ga₂O₃ layers with low background impurity concentrations [1]. The conventional precursor, triethylgallium (TEGa), yields material with excellent mobility but is limited to growth rates below 3 μ m/hr, which constrain vertical device architectures that require thick drift layers [1,2]. Trimethylgallium (TMGa) enables faster growth rates (up to ~10 μ m/hr); however, faster growth with TMGa is often accompanied by unintentional compensation from extrinsic impurities (e.g. carbon). Previous work shows that increasing O₂ flow during growth can mitigate this compensation while maintaining high growth rates [3]. In this study, we investigate the effects of oxygen in MOCVD TMGa-based growth of β -Ga₂O₃ to identify compensating defects in the bandgap using quantitative defect spectroscopy.

Si-doped β -Ga₂O₃ epilayers were grown on Sn-doped (010) EFG substrates via MOCVD using TMGa at a growth rate of 6.1 μ m/hr while varying the O₂ flow from 800 to 3000 sccm. Growths were performed at 950 °C and 60 Torr with constant TMGa and SiH₄ flow rates. Schottky barrier diodes with 8 nm Ni were fabricated for defect characterization. All devices exhibited rectifying behavior and a quality factor ($Q = \omega C/G$) >10, indicating good diode characteristics for defect measurements. The net ionized carrier concentration extracted from C-V measurements varied from 3×10^{17} cm⁻³ to 4×10^{18} cm⁻³ with increasing O₂ flow despite a constant SiH₄ flow, suggesting increased compensation at lower oxygen flow rates. Deep level transient spectroscopy (DLTS) measurements revealed two traps with a dominant state near $E_c - 0.6$ eV, with the concentration decreasing monotonically with increasing O₂ flow. Deep level optical spectroscopy (DLOS) measurements revealed states at $E_c - 1.6$ eV, $E_c - 2.2$ eV, and $E_c - 4.4$ eV, with the $E_c - 1.6$ eV trap exhibiting the strongest dependence on O₂ flow, decreasing in concentration as the O₂ flow increased. The correlated reduction of the $E_c - 0.6$ eV and $E_c - 1.6$ eV traps with increasing O₂ flow suggests that both are associated with carrier compensation that is suppressed under oxygen-rich growth conditions. Further details will be presented at the conference.

[1] Z. Feng, Appl. Phys. Lett. 114(25), 250601 (2019).

[2] S. Bin Anooz, Appl. Phys. Lett. 116(18), 182106 (2020).

[3] L. Meng, Crystal Growth & Design 22(6), 3896–3904 (2022).

2:55pm **IWGO-MoA1-12 Deep Trap States in Mg/N Co-Implanted β -Ga₂O₃ Current Blocking Layers Revealed by Thermally Stimulated Current Spectroscopy**, *Hitoshi Takane*, *Yusuke Yamashita*, Toyota Central R&D Labs., Inc., Japan; *Fenfen Fenda Florena*, *Hironobu Miyamoto*, *Kohei Sasaki*, Novel Crystal Technology, Inc., Japan; *Daigo Kikuta*, Toyota Central R&D Labs., Inc., Japan

Deep acceptor doping to form a quasi-p-type current blocking layer (CBL) in β -Ga₂O₃ via ion implantation is crucial for achieving both high-voltage blocking and enhancement-mode operation [1]. Mg/N co-implantation has been proposed, achieving a significant improvement in current blocking capability compared with Mg- or N-implantation alone [2]. Since deep traps that compensate free carriers strongly affect CBL performance, their properties need to be clarified to optimize the fabrication process and ensure device reliability. In this study, we performed thermally stimulated

current (TSC) spectroscopy to examine deep traps in Mg/N co-implanted CBLs. The TSC study revealed four trap levels in the Mg/N co-implanted CBLs.

To form CBLs in β -Ga₂O₃, N-implantation ([N]: 1.2×10¹⁹ cm⁻³, 650-nm box profile) and Mg/N co-implantation ([Mg]: 6.0×10¹⁸ cm⁻³, 300-nm box profile, [N]: 6.0×10¹⁸ cm⁻³, 650-nm box profile) were carried out, followed by thermal annealing at 900 or 1000°C under an O₂ atmosphere for 30 min. Reverse *I*-*V* measurements (up to -200 V) at room temperature showed that the Mg/N co-implanted samples exhibited superior current blocking capability compared with the N-implanted samples.

We performed the TSC measurements for both samples. The Mg/N co-implanted CBLs showed clear TSC spectra, whereas such spectra could not be obtained for the N-implanted samples due to high dark leakage current. For the Mg/N co-implanted CBLs, we extracted trap energy levels by two methods. One is to fit the spectra based on Eq. (1) [3], where E_T is the energy level of deep traps.

$$I = I_0 \{-E_T/kT - kD_T/\delta T^4 e^{-E_T/kT} \times [1 - 4kT/E_T + 20(kT/E_T)^2]\} \quad (1)$$

The other method is direct extraction from the peak temperature (T_m) with Eq. (2) [4].

$$E_T = kT_m \ln(T_m^4/\delta) \quad (2)$$

Four trap levels near the conduction band minimum (E_C) were identified at $E_C - E_T \sim 0.72, 0.83, 0.93,$ and 1.02 eV. The values obtained by the two methods were in good agreement, supporting the reliability of the extracted energy levels. The trap levels at $E_C - E_T \sim 0.72$ and 1.02 eV may correspond to the previously reported E2* and E3 traps, respectively, which are likely associated with implantation-induced damage [3].

This paper is based on results obtained from a project, JPNP22007, commissioned by the New Energy and Industrial Technology Development Organization (NEDO).

[1] K. Zeng, *J. Phys. Mater.* **8** 031002 (2025). [2] F.F. Florena *et al.*, will be presented at IWGO-6 (2026). [3] M. Pavlovic *et al.*, *JAP* **84**2018 (1998). [4] B. Wang *et al.*, *JAP* **125**, 105103 (2019). [5] A.Y. Polyakov *et al.*, *JVST A* **40**, 020804 (2022).

Author for correspondence: Hitoshi.Takane.xp@mosk.tytlabs.co.jp

3:10pm IWGO-MoA1-15 Effects of 230 MeV Ca Swift Heavy Ion Irradiation on β -Ga₂O₃ Schottky Diodes, Yanzhen Zhao, Ohio State University; *Cale Overstreet*, University of Tennessee, Knoxville; *Hemant Ghadi*, *Quentin Shuai*, Ohio State University; *Kay-Obbe Voss*, GSI Helmholtz Centre For Heavy Ion Research; *Maik Lang*, University of Tennessee, Knoxville; *Steven Ringel*, *Aaron Arehart*, Ohio State University

Radiation exposure can degrade semiconductor device performance and lead to failure. β -Ga₂O₃ is a promising material for aerospace applications due to its ultra-wide bandgap (~4.8 eV) and strong atomic bonding [1]. While previous studies have examined the radiation response of β -Ga₂O₃ devices, heavy-ion-induced damage remains relatively underexplored [1]. Heavy ions can introduce displacement damage and generate defects degrading device performance. Therefore, investigating radiation-induced trap formation is important.

A systematic investigation of displacement damage in halide vapor phase epitaxy (HVPE)-grown β -Ga₂O₃ Schottky diodes was conducted under 230 MeV Ca irradiation up to relatively high fluence. The net carrier concentration decreases with irradiation fluence with a carrier removal rate (CRR) of 2.5×10^6 cm⁻¹. To identify the radiation-induced defects, deep-level transient and optical spectroscopies (DLTS/DLOS) were performed. Lighted C-V (LCV) measurements were used to improve trap concentration accuracy for the DLOS levels. Based on the combination of measurements, the $E_C - 0.70$ eV and $E_C - 0.80$ eV traps showed negligible trap concentration changes, whereas three DLOS-identified levels ($E_C - 2.0$ eV, $E_C - 3.0$ eV, and $E_C - 4.4$ eV) increased with radiation fluence. The trap concentrations-fluence dependence yields introduction rates of 8.4×10^4 and 6.1×10^5 for $E_C - 2.0$ and $E_C - 3.0$, and 1.4×10^6 cm⁻¹ for DLOS optical feature $E_C - 4.4$ eV, respectively. The results establish a defect spectrum for radiation damage in β -Ga₂O₃, are consistent with the CRR, overall require high fluences for obvious changes, and provide insight for radiation-tolerant devices design.

[1] J. Kim, S. J. Pearton, C. Fares, J. Yang, F. Ren, S. Kim, and A. Y. Polyakov, *Journal of Materials Chemistry C* **7**, 10 (2019).

3:25pm IWGO-MoA1-18 Machine Learning Quantification of Dislocation Defects in Ga₂O₃ Using X-Ray Topography, James Gallagher, NRL; *Christian Reimann*, Rigaku, Germany; *Caroline Reilly*, *Jacob Leach*, *Heather Splawn*, Kyma Technologies; *Nadeemullah Mahadik*, *Marko Tadjer*, *Karl Hobart*, *Michael Mastro*, NRL

Ga₂O₃ is a promising ultra-wide bandgap semiconductor, as it is one of the least expensive to manufacture while maintaining a high breakdown voltage, resistance to radiation, and the ability to operate at high temperatures. In many maturing semiconductors, defects are present in concentrations exceeding 10³ cm⁻². These defects often reduce the reliability of devices and lead to unpredictable performance. To both learn the effect of defects on performance and optimize the manufacturing of Ga₂O₃ wafers, quick, non-destructive methods for defect mapping are needed. Multiple techniques exist and are well known; however, the defect quantity can easily exceed 10⁴ cm⁻². To rapidly quantify the defects, computational algorithms are needed. However, since defects vary in size, shape, and intensity, pattern-matching algorithms are unreliable. This work discusses using machine learning techniques to evaluate the concentration of defects in Ga₂O₃, with a focus on evaluating defects using X-Ray topography (XRT) images.

Figure 1a shows an XRT image of a (001) Ga₂O₃ wafer using the $g=[-204]$ reflection. Defects are clearly oriented with a dislocation line direction of $\epsilon=[010]$. These are likely edge dislocations, as the imaging vector g is perpendicular to the dislocation line ϵ [1]. Applying a U-Net model yields the image in Figure 1b, where white pixels indicate a high probability of belonging to a defect. Figure 1c shows a contour plot circling the predicted locations on the original image. This model can evaluate high-resolution (<4 μ m/pixel) wafer-scale images in minutes on a standard desktop computer. Figures 1d-1f demonstrate the model's application at a wafer scale. At such scales, the model maps defects with high accuracy, and most disagreements between the model's output and manual labeling arise from the subjective nature of defining defect boundaries.

[1] Y. Yao, Y. Tsusaka, K. Sasaki, A. Kuramata, Y. Sugawara, and Y. Ishikawa, "Large-area total-thickness imaging and Burgers vector analysis of dislocations in β -Ga₂O₃ using bright-field x-ray topography based on anomalous transmission," *Applied Physics Letters*, vol. 121, no. 1, p. 012105, Jul. 2022, doi: 10.1063/5.0098942.

**International Workshop on Gallium Oxide and Related Materials (IWGO-6)
Room ESJ 0202 - Session IWGO-MoA2**

Defects Science II

Moderators: Emmanouil Kioupakis, University of Michigan, **Hartwin Peelaers**, University of Kansas

4:10pm IWGO-MoA2-27 Advancing Understanding in Conductivity Control in Ga₂O₃ Polymorphs and Alloys Through Atomistic Simulations, Joel Varley, Lawrence Livermore National Laboratory **INVITED**

Exploiting chemical and structural control of gallium oxide (Ga₂O₃) through doping, alloying, and epitaxy is an attractive way of further expanding the properties of this promising ultra-wide bandgap platform for next-generation power electronics. For example, Ga₂O₃ exhibits a number of (metastable) polymorphs with superior properties to the thermodynamically favored β -phase, and alloying with other elements like In and Al alloys can lead to tunability of the band gap to potentially access higher power device figures of merit, analogous to the III-nitride system but spanning a much larger range of bandgaps exceeding 8 eV eV.[1,2] Here we survey the current understanding of dopability, common trap levels, and other types of in Ga₂O₃ and related alloys, focusing on their potential optical and electrical consequences from insights gained through first-principles-based calculations employing hybrid functionals. Specifically, we discuss what is known about the influence of crystal structure and composition on the prospects of donor doping and electrical compensation, as well the role(s) of native defects and impurities incorporated through growth and processing steps. We summarize the behaviour predicted for a number of conventional dopants and lesser-explored dopants and impurities that can impact the performance of Ga₂O₃-related materials and devices.[3-8] These results provide guidance for understanding the roles of different defect populations in the family of Ga₂O₃ polymorphs and related alloys.

This work was performed under the auspices of the U.S. DOE by Lawrence Livermore National Laboratory (LLNL) under contract DE-AC52-07NA27344.

Monday Afternoon, August 3, 2026

4:35pm IWGO-MoA2-32 **High-Throughput, High-Resolution, Three-Dimensional Observation of Threading Dislocations in β -Ga₂O₃ Using Phase-Contrast Microscopy**, *Yukari Ishikawa, Daiki Katsube*, Japan Fine Ceramics Center, Japan; *Yongzaho Yao*, Mie Univ., Japan Fine Ceramics Center, Japan; *Koji Sato*, Japan Fine Ceramics Center, Japan; *Kohei Sasaki*, Novel Crystal Technology, Japan

Wafer-scale, depth-resolved inspection of threading dislocations remains a critical challenge in the development of β -Ga₂O₃ ultrawide-bandgap semiconductors. We report a laboratory-implementable, nondestructive approach for high-throughput, high-resolution, three-dimensional visualization of threading dislocations using phase-contrast microscopy (PCM). PCM can be implemented in a conventional laboratory environment under ambient conditions and achieves millisecond-scale acquisition of each field of view, providing a practical and scalable platform for rapid wafer-level inspection. The detection capability of PCM is quantitatively validated through direct comparison with synchrotron radiation X-ray topography (SR-XRT), demonstrating excellent correspondence exceeding 96% in identical regions. PCM further offers superior lateral spatial resolution, enabling the separation of closely spaced dislocations. By systematically shifting the focal plane, depth-resolved imaging of dislocation propagation through the crystal thickness is achieved, allowing three-dimensional reconstruction of dislocation networks. Projection analysis of sequential PCM images reveals dislocation trajectories and their crystallographic characteristics. These results establish PCM as an accessible and growth-relevant platform for wafer-scale, three-dimensional dislocation evaluation in β -Ga₂O₃, opening a pathway toward process feedback and reliability-oriented materials engineering.

4:50pm IWGO-MoA2-35 **Origin of Donor Compensation in (Al_xGa_{1-x})₂O₃ Alloys**, *Sierra Seacat, Hartwin Peelaers*, University of Kansas

Many Ga₂O₃ devices require the formation of heterostructures to confine charge carriers. Typically, monoclinic AlGaO alloys are used for this purpose, as the larger bandgap of Al₂O₃ results in an alloy with a conduction-band offset relative to Ga₂O₃ enabling charge carrier confinement. However, intentional *n*-type doping can be difficult to achieve in these alloys, with donor compensation observed in alloys with 25% Al content or higher when doped with Si. The source of this compensation cannot be ascribed to Si alone, as density functional theory (DFT) calculations predict that Si should remain shallow up to 70% Al content. This implies that another defect is acting as a compensating acceptor.

Here, we propose cation vacancies as the source of donor compensation in monoclinic AlGaO alloys. Using DFT with the HSE06 hybrid functional, we calculate the formation energies of cation vacancies in monoclinic Al₂O₃ and AlGaO₃ as compared to the Si donor. We find that the split vacancy configuration is also the lowest energy vacancy in Al₂O₃ and AlGaO₃. By determining the point where this vacancy becomes lower in energy than Si at the CBM as a function of alloy composition, we predict that vacancies will compensate donor doping for 16% Al content or greater under O-poor conditions and are therefore the likely source of donor compensation in monoclinic AlGaO [1].

[1] S. Seacat and H. Peelaers, <https://doi.org/10.48550/arXiv.2602.02879> (2026).

International Workshop on Gallium Oxide and Related Materials (IWGO-6)

Room Concourse - Session IWGO-MoP

IWGO Poster Session I

Moderators: **Esmat Farzana**, Iowa State University, **Katie Gann**, Naval Research Laboratory

IWGO-MoP-1 Anisotropic Wet Etching of β -Ga₂O₃ using TMAH, **Takayoshi Oshima**, NIMS, Japan

This study demonstrates advanced surface treatment and microfabrication techniques for β -Ga₂O₃ using TMAH etching. (i) Mild etching of (001) substrates with 2.38 wt% TMAH (a standard photolithographic developer) at 25–40 °C transforms relatively rough, CMP-finished surfaces into atomically flat step-and-terrace morphologies [1]. On (010) substrates, aggressive etching with 25 wt% TMAH at 90 °C reveals significant crystallographic anisotropy. (ii) Specifically, pronounced lateral etching along the [001] direction facilitates the undercutting of dry-etched mesa structures to form β -Ga₂O₃/air-gap structures, such as air-bridges and cantilevers [2]. (iii) Furthermore, the high etch resistance perpendicular to the (-201) plane allows for the refinement of dry-etched trenches, transforming rough, slanted sidewalls into smooth, vertical (-201) facets [3]. These results provide straightforward pathways for the surface preparation, the development of high-performance β -Ga₂O₃ MEMS and fin/trench-based power devices.

This work was supported by ARIM program (JPMXP1225NM5079) and JSPS KAKENHI (JP24K01368).

[1] T. Oshima, *Jpn. J. Appl. Phys.* **64**, 088001 (2025). [2] T. Oshima, *Appl. Phys. Express* **18**, 116501 (2025).

[3] T. Oshima, *AIP Advances* **16**, 025145 (2026).

IWGO-MoP-2 Electrical Characterization of 1D P–N Heterojunctions with Axial and Core–Shell Architectures, **Roman Yatskiv**, Institute of Photonics and Electronics of the Czech Academy of Sciences, Czechia

One-dimensional wide-bandgap heterostructures have attracted increasing interest in recent years because of their significant potential applications in future optoelectronic devices. We developed a novel technique to investigate the electrical properties of individual nanorods [1], nanostripes [2], or axial/core–shell p–n junctions [3,4] using a nanomanipulator in the chamber of a scanning electron microscope. In contrast to conventional approaches, this method eliminates the use of extensive processing chemistry and allows the observation of morphological changes in situ during electrical characterisation.

Figure 1 (a) individual CuI/ZnO core–shell heterojunction in contact with a gold electrode; **(b)** experimental setup for the electrical measurement of a single core–shell CuI/ZnO NR heterojunction; **(c)** representative room-temperature I–V characteristics of an individual CuI/ZnO core–shell heterojunction.

1. S. Tiagulskiy, O. Černohorský, N. Bašinová, R. Yatskiv, J. Grym, *Materials Research Bulletin*, **164** (2023) 112286.
2. P. Wojnar, S. Chusnutdinow, A. Kaleta, M. Aleszkiewicz, S. Kret, J.Z. Domagala, P. Ciepielewski, R. Yatskiv, S. Tiagulskiy, J. Suffczyński, A. Suchocki, T. Wojtowicz, *Nanoscale*, **16** (2024) 19477–19484.
3. S. Tiagulskiy, R. Yatskiv, H. Faitová, Š. Kučerová, J. Vaniš, J. Grym, *Materials Science in Semiconductor Processing*, **107** (2020) 104808.
4. S. Tiagulskiy, R. Yatskiv, M. Sobanska, K. Olszewski, Z.R. Zytkeiwicz, J. Grym, *Nanoscale*, **17** (2025) 8111–8117.

*Author for correspondence: yatskiv@ufe.cz

IWGO-MoP-3 Enhancement of Breakdown Voltage in β -Ga₂O₃/NiO Heterojunction Diodes by Modulating p–NiO/p+NiO Widths, **SinSu Kyoung, SangHun Kim**, Powercubesem Inc., Republic of Korea

β -Ga₂O₃ has attracted great attention in power electronics because of its ultra-wide bandgap, which allows high breakdown voltage and excellent power device performance. However, it is still difficult to fabricate p–n junction devices based on β -Ga₂O₃ because reliable p-type doping in β -Ga₂O₃ is not easily achieved. One possible solution is to form heterojunctions using p-type oxide semiconductors such as NiO. [1–2]

In this study, we show that changing the widths of the p–NiO and p+NiO layers can significantly improve the breakdown voltage of β -Ga₂O₃/NiO

heterojunction diodes. The device was fabricated using an n-type β -Ga₂O₃ wafer with a cathode electrode on the backside. On the top surface, p–NiO and p+NiO layers were stacked sequentially and covered with an anode electrode to form a double-layer heterojunction diode.

To investigate the effect of the device structure, the widths of the p–NiO and p+NiO layers were systematically varied. When both layers had the same width, the device showed a breakdown voltage of ~326 V. However, when the width decreased toward the top, making the p+NiO layer narrower than the p–NiO layer, the breakdown voltage increased significantly to ~670 V.

This improvement is related to the reduction of electric field crowding near the junction edge due to electric field dispersion in the width-modulated structure. These results indicate that controlling the lateral structure of p-type layers is an effective method for improving the reverse voltage performance of β -Ga₂O₃ heterojunction diodes. Further optimization of the device structure is expected to enhance the device performance.

IWGO-MoP-4 Metal-Catalyst-Dependent Growth of β -Ga₂O₃ Nanowires on Sapphire for Solar-Blind UV Photodetectors, **JungBok Lee, MinSeok Jang, HeeJin Kim, JuEun An, HoJun Lee**, Pusan National University, Republic of Korea

β -Ga₂O₃ has emerged as a promising ultra-wide-bandgap semiconductor for solar-blind ultraviolet (UV) photodetectors owing to its large bandgap, high breakdown field, and excellent thermal stability. In this study, β -Ga₂O₃ nanowires were synthesized on sapphire substrates by Pulsed Laser Deposition (PLD) using different metal catalysts, including Au, Ag, Cu, Ni, and Ti, in order to investigate the influence of catalyst species on nanowire growth and device performance. SEM analysis revealed clear catalyst-dependent differences in nanowire density, morphology, and size distribution, indicating that the choice of metal catalyst strongly affects nucleation and growth behavior. Structural characterization by XRD and Raman spectroscopy confirmed the formation of β -Ga₂O₃ nanowires on sapphire substrates. Based on the as-grown nanowire networks, metal–semiconductor–metal (MSM) photodetectors were fabricated and evaluated under UV illumination. The devices exhibited a distinct photoresponse under 254 nm excitation, while the response under longer-wavelength UV illumination was relatively weaker, demonstrating selective solar-blind UV sensitivity. Among the investigated catalysts, the Ag-assisted β -Ga₂O₃ nanowires showed the most enhanced photoresponse and the highest photo-to-dark current contrast, indicating superior photodetection behavior compared with the other catalyst-assisted samples. The improved performance is attributed to catalyst-dependent variations in nanowire growth characteristics and interfacial charge transport. These results demonstrate that metal-catalyst engineering is an effective route for tuning β -Ga₂O₃ nanowire growth and improving the performance of solar-blind UV photodetectors, providing useful insight for future wide-bandgap oxide optoelectronic devices.

IWGO-MoP-5 Epitaxial Growth of Si Doped β -(In_xGa_{1-x})₂O₃ Thin Films on (010) β -Ga₂O₃ Substrates, **Aoi Saito**, Kyoto Institute of Technology, Japan; **Hiroki Miyake**, MIRISE Technologies Corporation, Japan; **Hiroyuki Nishinaka**, Kyoto Institute of Technology, Japan

β -Ga₂O₃ has a large bandgap of approximately 4.8 eV and bulk substrates can be fabricated by melt-growth methods, making it a promising candidate for power device applications. Whereas β -(Al_xGa_{1-x})₂O₃/ β -Ga₂O₃ heterostructures have been the primary focus for β -Ga₂O₃-based HEMT structures [1], β -(Al_xGa_{1-x})₂O₃/ β -(In_yGa_{1-y})₂O₃ heterostructures have recently attracted attention due to the expectation of a larger band offset. Nevertheless, reports on the high-quality growth of β -(In_xGa_{1-x})₂O₃ remain scarce, and understanding its physical properties is essential for HEMT applications. In particular, since β -(In_xGa_{1-x})₂O₃ serves as the channel layer, understanding its electrical properties is important. In this study, Si doping in β -(In_xGa_{1-x})₂O₃ was investigated using the mist CVD method, which has been successfully used for crystal growth in our group [2].

Figure 1 shows the XRD 2 θ – ω measurement results for samples with In concentrations of 1.8 and 3 vol.% in the solution. As shown in Fig. 1, a diffraction peak accompanied by clear fringes was observed for the sample with an In concentration of 1.8 vol.%, indicating the growth of a thin film with high crystallinity. In contrast, when the In concentration was 3 vol.%, the fringes disappeared, and degradation of crystallinity due to lattice relaxation was observed. Figure 2 shows the electron mobility as a function of In concentration with [Si]/[Ga]=0.1 at.%. As shown in Fig. 2, the mobility decreases with increasing In concentration, indicating that the In composition notably influences the carrier transport properties, likely due to alloy scattering.

[1] Zhang et al., Appl. Phys. Lett. 112, 173502 (2018).

[2] H. Nishinaka, et al., Sci. Technol. Adv. Mater. 25 (2024).

IWGO-MoP-6 Dependence of Substrate Orientation the β -Ga₂O₃ Single Crystal Layer Grown by the Flux Method, Kentaro Ishida, Toshinori Taishi, Shinshu University, Japan

β -Ga₂O₃ is one of the most promising wide-bandgap semiconductor materials, with a bandgap 4.5 times wider and a breakdown voltage 25 times higher than that of silicon. Since it melts at atmospheric pressure, it is possible to grow low-cost bulk single crystals. Furthermore, device fabrication requires epitaxial growth, a technique for growing thin films on a substrate. Currently, epitaxial growth of β -Ga₂O₃ is primarily performed using vapor-phase methods such as HVPE. In recent years, the manufacture of certain high-voltage power devices has required thick epitaxial layers of β -Ga₂O₃. In this study, the solution growth of β -Ga₂O₃ using fluxes composed of MoO₃ alone or with the addition of Li₂CO₃ was investigated.

IWGO-MoP-7 Characterization of β -Ga₂O₃ Epitaxial Layers Using Time-Resolved Photoluminescence, Mahiro Ishikawa, Takuma Ishihara, Kazuki Shimazoe, Nagoya Institute of Technology, Japan; Kohei Sasaki, Novel Crystal Technology, Japan; Masashi Kato, Nagoya Institute of Technology, Japan

β -Ga₂O₃ has an ultrawide bandgap and has been attracting attention as a next-generation power-semiconductor device material [1]. To ensure reliability in β -Ga₂O₃ devices, it is important to investigate the impact of defects. We investigated evaluation of β -Ga₂O₃ epitaxial wafer using photoluminescence (PL), which is non-destructive, non-contact technique.

(001) oriented β -Ga₂O₃ wafers with epitaxial layer thickness of 5, 10 or 15 μ m were used as samples. For evaluation, PL spectra and time-resolved PL (TR-PL) measurements were carried out using a 266 nm laser under the conditions of a pulse width of 1 ns and an excitation light intensity of 0.6 mW. These measurements were conducted both of epitaxial layer (Epi side) and substrate (Sub side) sides.

Figure 1 shows PL spectra the samples. For Sub side, a weaker emission was observed compared to those from Epi side for all the samples. On Epi side, the thicker the epitaxial layer, the stronger the light emission. The sample with an epitaxial layer thickness of 15 μ m exhibited emission at wavelengths of approximately 500 nm and 560 nm, but none was observed in the samples with epitaxial layers of 5 and 10 μ m. Figure 2 shows TR-PL decay curves. The TR-PL decays were faster on Sub side than on Epi side. The decays can be broadly divided into two components: fast decay with a small time constant, and the proportion of the slow decay component in Epi side depends on the epitaxial layer thickness. These results demonstrate that the time constant of the slow component would reflect crystalline quality of the epitaxial layers.

This paper is based on results obtained from a project, JPNP22007, commissioned by the New Energy and Industrial Technology Development Organization (NEDO).

Figure 1. PL spectra

Figure 2. TR-PL decay curves

[1] M. Higashiwaki: Phys. Status. Solidi. Rapid. Res. Lett. Vol15, Issue11, 5 August (2021)

* Author for correspondence: cnj13011@ict.nitech.ac.jp [mailto:cnj13011@ict.nitech.ac.jp]

IWGO-MoP-8 Crack-Free Dicing of β -Ga₂O₃ Substrates, Michael Liao, APEX Microdevices; Mark Goorsky, University of California Los Angeles; Piyush Shah, APEX Microdevices

It is widely known that β -Ga₂O₃ substrates are mechanically fragile and cleaves easily along the (100) and (001) planes. Dicing by wafer sawing β -Ga₂O₃ substrates into coupons, dies, or chips has been reported to be a challenging task as edges of β -Ga₂O₃ are susceptible to cracking. The damaged edges from wafer sawing cracks and in some cases distort the substrate so severely that a significant area adjacent to the edge becomes unusable for either epitaxy or wafer bonding. In the case of (001) and (100) substrates, the surface also delaminates at uncontrolled depths along the thickness of the substrate upon cracking at the edges. We demonstrate successful crack-free dicing for various orientations of β -Ga₂O₃ substrates by employing pulsed UV laser dicing. The edges of wafer-saw coupons are structurally characterized and directly compared to edges of laser diced coupons, primarily the impact of each edge type on direct wafer bonding yield and exfoliation via light-atom ion implantation. Laser diced coupons produce sharp, clean edges that do not distort the substrate that would

reduce wafer bonding yield. In fact, entire \sim cm scale, laser-diced β -Ga₂O₃ coupons yield \sim 100% fully bonded areas when bonded to 4H-SiC substrates including areas up to the edge of the sample. On the other hand, cracks and delamination from wire sawed edges hinder wafer bonding altogether. Interestingly, wafer saw edges and cracks greatly impact the nucleation mechanics of light-atom ion implantation for the exfoliation and transfer of thin films. The cracks and damage induced by the wafer saw process serve as nucleation sites for the implanted light atoms to nucleate and grow to induce surface blistering or exfoliation (which would have induced layer transfer if bonded prior to annealing). However, these surface blisters appear much earlier than expected compared to the blisters in the rest of the uncracked bulk material. Control over the timing and uniformity of exfoliation is important for producing consistent thin-film β -Ga₂O₃ composite substrates. Mitigating damage and lattice distortion at substrate edges are important for either subsequent coupon processing or for dicing dies or chips from processed wafers.

The authors acknowledge the support from Air Force SBIR Phase II program. TPOC Dr. Thaddeus Asel.

IWGO-MoP-9 Silicon Implantation Doping for Channel Definition of UID Alpha and Beta Ga₂O₃ Lateral MESFET Transistors, Aniol Vellvehí i Llovet, Institut de microelectrònica de Barcelona (IMB-CNM-CSIC), Spain; Amador Perez Tomas Perez Tomas, Institut de Microelectrònica de Barcelona (IMB-CNM-CSIC), Spain

Ion implantation is a key technique for achieving local, CMOS-compatible doping profiles in Ga₂O₃ power devices. This approach has been proven in β -Ga₂O₃, but its implementation in α -Ga₂O₃ remains challenging due to the limited thermal stability of the α -phase [1]. Extending this process to α -Ga₂O₃ is particularly attractive due to its wider bandgap (\sim 5.3 eV) and a potential critical electric field of \sim 10 MV/cm, compared to \sim 8 MV/cm in the β -phase [2], [3]. In this work, the same MESFET fabrication flow was applied to both alpha and beta-Ga₂O₃ in order to directly compare their compatibility with ion-implantation-based channel engineering and to identify material-dependent limitations. The α -phase samples consisted of 200 nm of α -Ga₂O₃ grown and stabilized on m-plane sapphire, while the β -phase samples consisted of 500 nm of β -Ga₂O₃ grown on (-201) β -Ga₂O₃ substrates. Si implantation defined the channel region, and an Al₂O₃ cap layer was deposited before annealing to protect the surface and preserve the α -phase [4]. After activation, the cap was removed from the S/D contact regions and Ti/Au metallization was used to complete the devices. A Si⁺ implantation was used also to decrease the contact resistance under the source/drain metallization. In β -Ga₂O₃, Si donors were successfully activated after annealing at 950 °C, yielding functional lateral MESFETs with reproducible performance. In contrast, α -Ga₂O₃ required a wide annealing study from 500 °C to 1100 °C to balance donor activation with phase stability. The Al₂O₃ cap layer helped to preserve the α -phase up to approximately 700 °C, but this temperature was still insufficient to activate the implanted Si donors. When annealing above this limit, where activation would nominally occur (\sim 900 °C) [5], the α -layer underwent a rapid α -to- β transformation accompanied by structural degradation. This prevented any electrical conduction through the implanted region and ultimately inhibited the free carrier control for operational α -Ga₂O₃ MESFETs via ion implantation. In summary, these results confirm the robustness of implanted-channel engineering in β -Ga₂O₃, while highlighting the fundamental limitations of ion-implantation-based channel engineering in α -Ga₂O₃ due to its limited thermal stability.

IWGO-MoP-10 Temperature-dependent Characteristics of HVPE-grown β -Ga₂O₃ Schottky Contacts with Different Metals, Eito Hatayama, Kazutaka Kanegae, Hajime Takayama, Michihiro Shintani, Hiroyuki Nishinaka, Kyoto Institute of Technology, Japan

β -Ga₂O₃ is a promising material for next-generation low-power switching devices due to its high breakdown electric field. Understanding the temperature dependence of carrier transport and Schottky barrier properties is crucial for practical device operation and reliability. We investigated the electrical characteristics of HVPE-grown β -Ga₂O₃ vertical Schottky diodes (SBDs) using different Schottky electrodes from 95 K to 408 K.

Si-doped n-type (001) β -Ga₂O₃ homoepitaxial layers, with a net donor density of 4×10^{16} cm⁻³, were grown via halide vapor phase epitaxy on an n⁺-type substrate. Ni and Cu Schottky electrodes were formed on the epitaxial surface. C-V and I-V characteristics of the SBDs were evaluated. The Schottky barrier heights (ϕ_{B0}) was determined from C-V characteristics, while the ideality factor (n) and the apparent Schottky barrier height (ϕ_B)

were extracted from *I-V* characteristics using thermionic emission (TE) models.

The temperature dependence of ϕ_{BO} for Ni ($\phi_{BO,Ni}$) and Cu ($\phi_{BO,Cu}$) are evaluated. At each temperature, $\phi_{BO,Ni}$ was ~ 0.3 eV higher than $\phi_{BO,Cu}$, consistent with the difference in their work functions. Extracted temperature coefficient (α) for $\phi_{BO,Ni}$ and $\phi_{BO,Cu}$ were -5.9×10^{-4} and -7.0×10^{-4} eV/K, respectively. The obtained coefficients are consistent with the typical values reported for other metals (such as Pt and Ni), confirming that they reflect the intrinsic temperature dependence of the bandgap.

As for the carrier transport, n approached unity above approximately 200 K, confirming TE dominance. Below 200 K, n increases while ϕ_B decreases with decreasing temperature. Specifically, at around 100 K, n reached 2.58 for Ni and 1.57 for Cu. The onset temperatures for the increase in n and decrease in ϕ_B were lower for Cu than for Ni, reflecting the difference in their work function. However, deviations at lower temperatures seem to suggest that considering tunneling and/or patch effects is necessary.

IWGO-MoP-11 Effect of Ion Charge and Implantation Dosage on Damage Recovery and Band Gap Narrowing in Sn-Implanted β -Ga₂O₃. *Kishor Upadhyaya*, KAUST, Saudi Arabia; *D.M. Esteves, Marco Peres, Katharina Lorenz*, Instituto Superior Técnico, Portugal; *Iman Roqan*, KAUST, Saudi Arabia

We report a study on the effect of the ion charge state (Sn^+ and Sn^{++}) and the implantation dosage on the structural damage recovery and optical absorption properties of β -Ga₂O₃ thin films grown using PLD. The high resolution x-ray diffraction (HRXRD) curves reveal that the FWHM of the implanted films are restored indicating good damage recovery while displaying transition from compressive strain into tensile strain as the implantation dosage increases. Atomic force microscopy (AFM) analysis reveals the reduction in the surface roughness value from 15.86 nm to 9.01 nm as the dosage increases indicating that the crystallite-merging becomes more efficient with the dosage. Raman spectroscopy shows that the peaks < 300 cm⁻¹ representing translational motions of Ga-chain disappear in higher dosage and Sn^{++} implanted films. The optical band gap shown by Tauc narrows from 4.22 eV in undoped film to 3.99 eV in $Sn^+ : 1 \times 10^{15}$ cm⁻² implanted film due to shallow donor levels with band tail of implanted films extending deeper into the band gap suggesting formation of deeper states due to implantation. High resolution transmission electron microscope (HR-TEM) and differential phase contrast (DPC) mapping show that undoped films contain elongated crystallite domains throughout the film while the implanted films contain smaller crystallite domains with large number of grain boundaries extending up to 150 nm deep from the surface. These findings provide crucial insights in understanding the band gap modification and structural variations due to implantation which are important since they affect the optoelectronic properties of the film and in turn the device performances

IWGO-MoP-12 Electrical Stability of Cr₂O₃/ β -Ga₂O₃ Heterojunction Diodes (HJDs) with Orientation-Dependent Breakdown Electric Field. *Yizheng Liu, Haochen Wang, Carl Peterson, Chinmoy Saha, James Speck, Chris Van de Walle, Sriram Krishnamoorthy*, University of California at Santa Barbara

This work reports the superior electrical stability of Cr₂O₃/ β -Ga₂O₃ heterojunction diodes (HJDs) compared with co-fabricated NiO_x/ β -Ga₂O₃ HJDs and explores the orientation-dependent breakdown electric field ($E_{Br,||}$) of Cr₂O₃/ β -Ga₂O₃ HJDs fabricated on five commercially available β -Ga₂O₃ orientations. The HJDs are fabricated on highly doped n-type bulk substrates and exhibit breakdown electric field anisotropy across various orientations with the highest $E_{Br,||}$ value obtained at 12.9 MV/cm on (110) β -Ga₂O₃. Type-II band alignment between Cr₂O₃ and β -Ga₂O₃ is also reported by first-principles calculations.

The Cr₂O₃/(001) HVPE β -Ga₂O₃ HJD fabrication begins with a backside Ti/Au (50/150 nm) Ohmic metallization on n⁺ β -Ga₂O₃ bulk substrate using e-beam evaporation followed by a 60-seconds rapid thermal annealing (RTA) at 470 °C in N₂. A p⁻ and p⁺ Cr₂O₃ stack is reactively sputtered on HVPE β -Ga₂O₃ drift region with a pre-patterned photoresist liftoff mask by optical lithography. Following the Cr₂O₃ deposition, a Ni/Au/Ni (50/50/150 nm) anode cap/metal hard mask stack is deposited via e-beam evaporation. The fabricated HJDs are later dry-etched ~ 2 μ m into the β -Ga₂O₃ drift region below the heterojunction interface using inductively coupled plasma (ICP) for edge termination. Similar fabrication process is also applied to NiO_x/(001) HVPE β -Ga₂O₃ HJDs for stability comparison and Cr₂O₃/n⁺ β -Ga₂O₃ HJDs for breakdown electric field analysis.

The as-fabricated Cr₂O₃/ β -Ga₂O₃ HJDs exhibit similar electrical characteristics compared to NiO_x-based HJDs in terms of forward current density (~ 125 A/cm² at 5 V), differential specific on-resistance ($R_{on,sp} \sim 12$ m Ω ·cm²), and breakdown voltages (~ 2 kV) on 7.48- μ m thick drift region with 9.45×10^{15} cm⁻³ apparent charge density. The NiO_x/ β -Ga₂O₃ HJDs show significant forward current density degradation (< 1 A/cm² at 5 V) after 10-days of ambient exposure while that of Cr₂O₃/ β -Ga₂O₃ HJDs remains relatively constant. It is qualitatively determined that the sheet resistance (R_{sh}) degradation of sputtered NiO_x causes forward current density reduction in the ambient conditions, and water (H₂O) vapor in the ambient air is the main agent that increases the sheet resistance of NiO_x thin film from reactive sputtering. Cr₂O₃/ β -Ga₂O₃ HJDs fabricated on n⁺ β -Ga₂O₃ bulk substrates reveal $E_{Br,||}$ anisotropy across five orientations of β -Ga₂O₃ with (110) orientation exhibiting the highest breakdown electric field value at 12.9 MV/cm. Relative permittivity values used for $E_{Br,||}$ values extraction are found using first-principles calculations.

IWGO-MoP-13 Direct Atomic Layer Processing (DALP®): Spatially Localized, Multi-Material Fabrication for Next-Generation Devices from Discovery to Manufacturing. *Mira Baraket*, ATLANT 3D Nanosystems, Denmark

Progress in next-generation advanced electronic and functional devices, based on complex heterostructures and advanced materials integration, is increasingly constrained by the rigidity of conventional thin-film processing and patterning workflows. While these approaches deliver high material quality and uniformity, they offer limited flexibility for spatially localized, multi-material fabrication, three-dimensional thickness engineering, and rapid experimentation at the nanoscale within a single process flow.

ATLANT 3D introduces Direct Atomic Layer Processing (DALP®), a nanofabrication technology enabling digitally controlled, spatially localized deposition of multiple materials with atomic-scale precision. DALP allows different materials to be deposited sequentially and locally in a unified workflow, enabling manufacturing of complex material stacks, heterostructures, interfaces, and thickness gradients without intermediate lithographic patterning steps.

This presentation describes the DALP process architecture and its role in both combinatorial materials discovery and targeted device manufacturing for next-generation devices. By enabling programmable material placement, controlled thickness variation, and repeatable execution within a single platform, DALP supports accelerated materials exploration while also enabling the direct production of device-ready structures as part of broader manufacturing flows. Representative examples include multi-material nanoscale structures for advanced semiconductor and functional material applications, where precise interface control, spatial selectivity, repeatability, and manufacturability are critical. DALP expands the accessible design space of nanoscale fabrication and provides a direct pathway from materials discovery to device-ready, manufacturable structures.

IWGO-MoP-14 NiO/Ga₂O₃ Heterojunction Rectifiers with Reverse Breakdown Voltage > 8.1 kV. *Hsiao-Hsuan Wan, Jian-Sian Li, Chao-Ching Chiang, Katharina Loske, Travis Anderson*, University of Florida; *Aman Haque*, The Pennsylvania State University; *Marko Tadjer*, Naval Research Laboratory, USA; *Jacob Leach, Caroline Reilly*, Kyma Technologies; *Fan Ren*, University of Florida

Vertical Ga₂O₃ heterojunction diodes (HJDs) were fabricated and systematically studied to evaluate the impact of lateral contact geometry on forward and reverse device performance. The devices were formed on 32 μ m thick, lightly doped (8.6×10^{15} cm⁻³) β -Ga₂O₃ drift layers grown by halide vapor phase epitaxy on heavily doped n⁺ substrates. A NiO/Ni/Au heterojunction anode was employed together with dielectric edge termination using an 80 nm SiO₂ / 45 nm SiN field-plate structure. Three device designs with different field plate dimensions ($D = 10, 20,$ and 30 μ m) between the first- and second-layer contact metals were investigated. Capacitance-voltage measurements confirmed uniform drift-layer doping, while forward *I-V* characteristics showed comparable saturation currents and turn-on voltages for all designs. Increasing D resulted in a reduction in on-resistance and a significant suppression of reverse leakage current at low to moderate reverse bias. The optimized device with $D = 30$ μ m exhibited the highest breakdown voltage of approximately 8.1 kV, compared with 5.5 kV and 4.5 kV for $D = 20$ μ m and $D = 10$ μ m, respectively. These results demonstrate that lateral contact spacing is a critical design parameter for electric-field management and breakdown enhancement in Ga₂O₃ heterojunction diodes.

IWGO-MoP-15 P-Type Li_yNi_{1-x-y}Mg_xO for β -Ga₂O₃ Heterojunction Power Device Applications, Madani Labeled, You Seung Rim, Sejong University, Republic of Korea

Ultrawide bandgap (UWBG) semiconductors are promising for high-power electronics; however, reliable p-type doping in β -Ga₂O₃ is fundamentally hindered by its flat O 2p-derived valence band [1], which results in large hole effective mass, low mobility, and strong self-trapping [2]. As a result, high-performance β -Ga₂O₃ p-n junctions require external p-type UWBG materials, though most oxide candidates suffer from low mobility [3] or unfavorable band alignment [4]. Here, we report Li_yNi_{1-x-y}Mg_xO as a novel p-type UWBG semiconductor grown by co-sputtering with controlled Mg incorporation for β -Ga₂O₃-based power devices. XRD and XPS confirm successful Mg substitution and improved crystallinity. The bandgap widens from 4.27 to 5.44 eV with increasing Mg power. While hole concentration decreases (1.72×10^{18} to $\sim 10^{16}$ cm⁻³), hole mobility dramatically improves from 0.798 to 33.39 cm²V⁻¹s⁻¹. DFT calculations using VASP attribute this enhancement to reduced localization of valence band edge states. Heterojunction devices achieve breakdown voltages up to -1450 V and reduced on-resistance (8.83 m Ω .cm²). Despite increased band offset, the reduced turn-on voltage at higher Mg content is explained by Mg-induced trap-assisted tunneling. These results establish Li_yNi_{1-x-y}Mg_xO as a promising p-type contact for high-performance β -Ga₂O₃ UWBG power electronics.

IWGO-MoP-16 Multi-Kilovolt Vertical NiO/Ga₂O₃ P-N Heterojunction Diodes with Ring-Assisted Junction Termination Extension, Kanghee Shin, Sejong University, Republic of Korea; Ho Jung Jeon, Seoul National University, Republic of Korea; Jang Hyeok Park, Madani Labeled, You Seung Rim, Sejong University, Republic of Korea

To achieve high breakdown voltage (V_{BR}) of Ga₂O₃ power devices, edge termination (ET) is essential because of electric field (E -field) crowding at the main junction edge, which results in premature breakdown [1]. Among various ET technologies, junction termination extension (JTE) is widely used in commercial power devices due to its simple formation by single-step p-type ion implantation or diffusion. However, selective p-type doping in Ga₂O₃ remains significantly challenging [2]. To this end, Ga₂O₃ power devices commonly rely on a sputtered p-type nickel oxide (NiO) as an alternative material for JTE formation. Notably, NiO has a wide bandgap of ~ 3.8 eV and tunable conductivity [3]. Nevertheless, NiO single-zone JTE (SZ-JTE) exhibits large variations since its effective JTE dose depends on both doping concentration (N_{JTE}) and thickness (t_{JTE}). As a result, small deviations in both NJTE and tJTE can degrade JTE's blocking capability, resulting in a narrow process window and premature breakdown [4]. Here, we proposed a ring-assisted JTE (RA-JTE) for vertical NiO/Ga₂O₃ p-n heterojunction diodes (HJDs). The RA-JTE consists of a sputtered NiO JTE layer augmented with multiple NiO floating field rings. In addition, the multiple p⁺-NiO rings are designed with their spacing gradually increasing away from the main junction. Owing to this design, RA-JTE can suppress peak E -field at the main junction edge and promote a more uniform E -field distribution, resulting in a V_{BR} exceeding 3 kV. TCAD simulations further indicate that RA-JTE preserves a more uniform E -field profile under JTE dose deviations, offering improved robustness compared with SZ-JTE. These results suggest that RA-JTE is a promising ET method for Ga₂O₃ power devices with enhanced process tolerance.

[1] H. Gong *et al.*, IEEE Electron Device Lett. **45**, 1421(2024).

[2] S. J. Pearton *et al.*, Appl. Phys. Rev. **12**, 031336 (2025).

[3] Y. Ma *et al.*, Adv. Elect. Mater. **11**, 230062 (2025).

[4] W. Sung *et al.*, IEEE Electron Device Lett. **37**, 1609(2016).

*Author for correspondence: youseung@sejong.ac.kr

IWGO-MoP-17 Wafer-Scale Heteroepitaxy of Sn-Alloyed ϵ -Ga₂O₃ on Sapphire via Low-Pressure Mist-CVD, Yan Wang, Chee Keong Tan, Hong Kong University of S&T (GZ), China

The industrial deployment of metastable ϵ -Ga₂O₃ on sapphire is currently impeded by intrinsic crystallographic incompatibility and the difficulty of achieving macroscopic homogeneity via solution-based growth techniques. When grown on a strictly hexagonal substrate like sapphire, the inherent symmetry mismatch inevitably induces the formation of three equivalent 120°-rotational domains, which act as carrier scattering centers and severely broaden the X-ray rocking curve (XRC) full-width at half-maximum (FWHM). Furthermore, the complex interplay of precursor mist flow and evaporation dynamics in Mist-CVD often leads to non-uniform thickness and quality gradients. To address these limitations, we implement a synergistic uni-element engineering strategy via Tin (Sn) alloying [1]. Beyond its conventional role as a dopant, we demonstrate that heavy Sn

alloying effectively modulates the cation sublattice, promoting a structural evolution from the ordered orthorhombic phase toward a pseudo-hexagonal symmetry. This symmetry regulation significantly mitigates the lattice misfit with the substrate, culminating in an ultranarrow (004) XRC FWHM of 0.04°. TEM investigations reveal a rapid lattice recovery mechanism, where initial interfacial disorder is annihilated within a few nanometers. Furthermore, we successfully surmounted the uniformity barriers typical of Mist-CVD, realizing superior wafer-level consistency with a thickness deviation of merely ~ 2 nm across a 2-inch wafer. This work identifies Sn-alloyed ϵ -Ga₂O₃ as a versatile and high-fidelity template, offering a simplified single-source route for the scalable manufacturing of next-generation electronics.

IWGO-MoP-18 MOCVD-grown 12 μ m Thick Sn Doped (001) β -Ga₂O₃ Layers with Extremely Low Free Charge Concentrations, Akash Patnaik, UVSQ – CNRS, France; Corinne Sartel, UVSQ – CNRS, France; Yunlin Zheng, INSP, Sorbonne Université, France; Thomas Ribault, Yves Dumont, Ekaterine Chikoidze, UVSQ – CNRS, France

The ever-increasing demand in energy necessitates efficient power converters, with high power handling capability. β -Ga₂O₃ based diodes are promising devices for the next generation high voltage power-switching applications, owing to large bandgap of Ga₂O₃. To attain large blocking voltage, the β -Ga₂O₃ drift layer of vertical diodes should be thick (>10 μ m) with around 10¹⁶cm⁻³ free carriers. There are several reports of thick unintentionally doped or low Si doped β -Ga₂O₃ layer with nearly 10¹⁶cm⁻³ carrier concentration for PiN or SBD diode applications. Majority of those films were grown using HVPE growth technique. Interestingly, up to our knowledge there has been no report of thick (>10 μ m) β -Ga₂O₃ epilayers doped with Sn(tin) having less than 10¹⁶cm⁻³ free carrier concentrations, grown using MOCVD. The challenges, in having low Sn doped β -Ga₂O₃ and eventually low carriers, stems from "wrong" site occupancy of Sn in crystal lattice or compensating defect formation, resulting in resistive films. In this work, we report 12 μ m thick homoepitaxial β -Ga₂O₃ film with 6 \times 10¹⁶cm⁻³ Sn dopants (SIMS) on Sn-doped β -Ga₂O₃ (001) substrate grown in a RF-heated horizontal MOCVD reactor (MR Semicon). Growth temperature was T=875°C with TMGa and TEsSn as Gallium and Sn precursor, respectively. The rocking curves comparison for (002) reflection of our epilayers, with (002) reflection of commercially available Sn-doped β -Ga₂O₃ substrate from NCT, Japan is performed. The full-widths at half maximum (FWHMs) of our epilayer (0.020°) is comparable to the commercially available substrate (0.026°), suggesting its high structural quality. Capacitance-Voltage measurement is performed on the grown sample, using Hg-probe. The extracted charge concentration ($N_d - N_a$) from the CV plot, in the frequency range of 0.1MHz to 1MHz, is calculated to be around 6 \times 10¹⁵cm⁻³. Thus, up to our knowledge, we demonstrate for the first time, 12 μ m thick MOCVD grown Sn: β -Ga₂O₃ epilayers, with very low charge concentration $n < 10^{16}$ cm⁻³, necessary for high power PiN diode fabrication.

IWGO-MoP-19 Structural Properties of Mist CVD Grown Rutile GeO₂ Thin Films on TiO₂ Substrates, Kazuki Shimazoe, Shota Ishiyama, Nagoya Institute of Technology, Japan; Hiroyuki Nishinaka, Kyoto Institute of Technology, Japan; Masashi Kato, Nagoya Institute of Technology, Japan

Rutile-structured germanium dioxide (r-GeO₂) has attracted considerable attention as a high-power switching device material owing to its high breakdown field (7.0 MV/cm), capability for ambipolar doping, and feasibility of bulk crystal growth using flux-based techniques [1]. However, these substrates are not commercially available yet; therefore, heterogeneous substrates, such as TiO₂ and sapphire, have been utilized to grow r-GeO₂. Lattice mismatches between r-GeO₂ and these heterogeneous substrates can induce phase separation with amorphous and α -quartz phases [2]. This study investigated the insertion of buffer layers to reduce lattice mismatch. Rutile structured Ge_xSn_{1-x}O₂, which has compositions that can be lattice-matched to both r-GeO₂ and TiO₂, was employed as a buffer layer. The Ge_xSn_{1-x}O₂ buffer layer consisted of six layers, each with a Ge composition from 70% to 95% in increments of 5%, gradually reducing the lattice mismatch.

GeO₂ and graded Ge_xSn_{1-x}O₂ buffer layers were grown by mist chemical vapor deposition (CVD). Figure 1 shows scanning electron microscopy (SEM) images and the inverse pole figure (IPF) map obtained from electron backscatter diffraction (EBSD) analysis of GeO₂ thin films on a (001) TiO₂ substrate with and without a graded buffer layer. In addition to rutile phase, α -quartz phase was detected on bare TiO₂ substrates, as shown in Figure 1 (a)-(c). The IPF map of the rutile phase is predominantly red (Figure 1 (b)), corresponding to the (001) plane, which is consistent with the substrate orientation and suggests epitaxial growth. In contrast, the IPF map in Figure

1 (c) exhibits color gradation, suggesting polycrystalline growth of α -quartz phase. As shown in Figure 1 (e), only signals attributed to (001) oriented rutile phase were observed, indicating that single-phase r - GeO_2 growth was achieved by a graded $\text{Ge}_x\text{Sn}_{1-x}\text{O}_2$ buffer layer. These results revealed that reducing the lattice mismatch is effective for the growth of single-phase r - GeO_2 thin films on TiO_2 substrates.

[1] K. Bushick, et al., *Appl. Phys. Lett.* **117**, 182104 (2020)

[2] I. Rahaman, et al., *ACS Appl. Electron. Mater.* **7**, 2848–2854(2025)

IWGO-MoP-20 Epitaxy of b -($\text{Al}_x\text{Ga}_{1-x}$) $_2\text{O}_3$ on (001) b - Ga_2O_3 Substrates by MOCVD, Indraneel Sanyal, AIXTRON Ltd., UK; Dan Lamb, Ciaran Llewellyn, Shreyasi Maitra, Saptarsi Ghosh, Swansea University, UK; Andrew Pakes, K.B.K Teo, AIXTRON Ltd., UK

β -($\text{Al}_x\text{Ga}_{1-x}$) $_2\text{O}_3$ has emerged as a highly promising ultra-wide-bandgap semiconductor for multi-kV power electronics. Key challenges—including particle formation, parasitic gas-phase reactions, and controllable Al incorporation—are typically addressed by tuning conventional MOCVD parameters such as VI/III ratio, reactor pressure, and growth temperature. We identify the precursor reaction zone path length, before impingement on the substrate, as an independent and selective process variable. This geometric parameter modulates the residence time without significantly affecting surface-directed mass transport or surface reaction kinetics, because the concentration boundary layer thickness remains unchanged.

We tested this hypothesis in an AIXTRON CCS 3 × 2" MOCVD reactor. Two gas-phase Al fractions—22% TMAI/(TMAI+TMGa) for samples A and B, and 52% for samples C and D were combined with two showerhead-substrate gaps: 6 mm (A, C) and 15 mm (B, D). This matrix was designed to isolate whether precursor reaction zone path length meaningfully affects Al incorporation and particle formation.

XRD measurements show the dominant β - Ga_2O_3 (002) substrate peak near 31.7°, accompanied by a lower-angle feature near 30.4° consistent with the rotated-domain (-401) reflection previously reported for MOCVD growth on (001) β - Ga_2O_3 substrates. Notably, the β -($\text{Al}_x\text{Ga}_{1-x}$) $_2\text{O}_3$ layers exhibit a strong rotated-domain contribution as well, while a distinct alloy (002) peak at ~32.3–32.4° is much weaker to be clearly resolved. This absence is attributed to the requirement for coherently strained films and the potential complications of alloy inhomogeneity or Al segregation. Therefore, Al incorporation can be more reliably estimated from the separation $\Delta(2\theta)_{(401)}$. Using this approach, we estimate solid-phase Al fractions of ~22% (A), ~12% (B), ~42% (C), and ~35% (D). These results show that, at fixed TMGa, TMAI flows, reducing the gap consistently increases incorporated Al while simultaneously suppressing particle formation, as confirmed by optical microscopy.

Quantitative transport modelling incorporating the actual reactor geometry shows that the mean residence time in the parasitic reaction zone ($T > 250$ °C) increases from 5.1 ms at 6 mm gap to 12.8 ms at 15 mm gap—providing 2.5× more time for deleterious TMAI + O_2 oxidation reactions, which preferentially deplete TMAI relative to TMGa. Importantly, concentration boundary layer calculations show that δ_c remains constant—approximately 1.19 mm for TMAI and 0.94 mm for TMGa—across both gap settings. This confirms that surface-directed mass transport and reaction kinetics are not affected by the gap variation.

IWGO-MoP-21 Performance Enhancement of β - Ga_2O_3 Deep-Ultraviolet Photodetectors via Al_2O_3 Passivation, Hee Won Shin, Jang Hyeok Park, You Seung Rim, Sejong University, Republic of Korea; Si-Young Bae, Pukyong National University, Republic of Korea

Deep-ultraviolet (DUV) photodetectors have attracted considerable attention for applications such as flame detection, space exploration, and sterilization monitoring [1]. Among various materials, β - Ga_2O_3 is a promising candidate for solar-blind photodetectors owing to its ultrawide bandgap (~4.8 eV), which enables selective absorption in the solar-blind region [2].

In this work, β - Ga_2O_3 -based DUV photodetectors were fabricated using epitaxial thin films grown by mist chemical vapor deposition (Mist-CVD) [3]. The Mist-CVD technique offers several advantages, including a simple non-vacuum process, cost-effectiveness, and the ability to grow high-quality epitaxial films.

The effects of atomic layer deposition (ALD)-deposited Al_2O_3 passivation on the electrical and photoresponse characteristics of the devices were systematically investigated. Prior to passivation, the devices exhibited shifted and asymmetric I–V characteristics due to surface defects and trap states. After applying the Al_2O_3 passivation layer, the I–V curves shifted

toward the origin and became more symmetric, indicating effective suppression of surface trap states.

Furthermore, the I–T characteristics also showed a noticeable improvement. Before passivation, the devices showed a triangular-shaped response with a pronounced persistent photoconductivity (PPC) effect [4]. In contrast, after Al_2O_3 passivation, the I–T curves exhibited a square-shaped response with fast rise and decay times, indicating effective suppression of the PPC effect.

The device performance was significantly enhanced following passivation, with responsivity increasing from 2.67×10^{-2} A/W to 2.20 A/W – an improvement of approximately two orders of magnitude. Simultaneously, the on/off ratio rose from 3.63×10^2 to 6.84×10^4 due to the simultaneous reduction in dark current and increase in photocurrent.

These results demonstrate that Al_2O_3 passivation effectively suppresses surface trap states and significantly enhances the electrical stability and photoresponse performance of β - Ga_2O_3 -based DUV photodetectors.

[1] C. Avila-Vendano, J. A. Carvajal-Fresno, and M. A. Quevedo-Lopez, *IEEE Sensors J.* **21**, 14815 (2021)

[2] Z. Galazka, *Semicond. Sci. Technol.* **33**, 113001 (2018)

[3] K. Uno, M. Ohta, and I. Tanaka, *Appl. Phys. Lett.* **117**, 052106 (2020)

[4] S. Hullavarad, N. Hullavarad, D. C. Look, and B. Clafin, *Nanoscale Res. Lett.* **4**, 1421–1427 (2009)

+Author for correspondence: youseung@sejong.ac.kr

IWGO-MoP-22 Suppression of Twin Nucleation in Bulk β - Ga_2O_3 Using Wide-Width Seeds, Won-Jae LEE, Dong-Eui University, Republic of Korea; Eun-Seo LEE, Dong Eui University, Republic of Korea; Eun-Jeong An, Sang-Jin Bae, Ho-Gyun Yun, Jung-Gon Kim, Kwang-Hee Jung, Mi-Seon Park, Dong-Eui University, Republic of Korea; Dong-Jin Lee, Jin-Ki Kang, AXEL, Republic of Korea

In the growth of bulk β - Ga_2O_3 crystals by the edge-defined film-fed growth (EFG) method, twin defects frequently arise during the shouldering stage. This phenomenon is initiated when the degree of supercooling at the growth interface reaches the energy threshold required for twin nucleation as the expanding crystal diameter perturbs thermal stability. The resulting twin defects disrupt the structural integrity of the crystal and significantly degrade the efficiency of the devices [1].

In this study, we propose an optimized growth process using a wide-width seed that corresponds to the die width, thereby fundamentally suppressing twin formation by bypassing the diameter expansion stage. Initially, a (-101)-oriented β - Ga_2O_3 ingot was grown using a conventional seed (Figure 1(a)); although it appeared to be a single crystal to the naked eye, polarized microscopy (Figure 1(b)) and HRXRD θ - 2θ scans (Figure 1(c)) revealed distinct twin boundaries and crystallographic non-uniformity within the same ingot.

To resolve this issue, a wide-width seed fabricated by the vertical Bridgman (VB) method was introduced (Figure 1(d)). Since the seed width matches the die, it facilitates immediate vertical growth, enhancing interface stability and effectively eliminating the conditions for twin nucleation. Consequently, a twin-free single-crystalline β - Ga_2O_3 ingot was successfully grown (Figure 1(e)), and microscopy after polishing (Figure 1(f)) confirmed that twin defects were completely suppressed, resulting in a high-quality crystalline state.

IWGO-MoP-23 Comparison of NiO/ β -Ga₂O₃ Heterojunction Diodes Fabricated Using Planar and Confocal RF Magnetron Sputtering Systems, Wojciech Hendzelek, Łukasiewicz Research Network-Institute of Microelectronics and Photonics, Warsaw University of Technology- Institute of Microelectronics and Optoelectronics,, Poland; *Aleksandra Wójcicka*, Łukasiewicz Research Network-Institute of Microelectronics and Photonics, Warsaw University of Technology- Institute of Microelectronics and Optoelectronics, Poland; *Aneta Gołębiowska*, Łukasiewicz Research Network-Institute of Microelectronics and Photonics, Poland; *Jarosław Tarenko*, *Oskar Sadowski*, *Maciej Kamiński*, Łukasiewicz Research Network-Institute of Microelectronics and Photonics, Warsaw University of Technology - Institute of Microelectronics and Optoelectronics, Poland; *Marcin Guza*, *Marek Wzorek*, Łukasiewicz Research Network-Institute of Microelectronics and Photonics, Poland; *Justyna Wierzbicka*, Łukasiewicz Research Network-Institute of Microelectronics and Photonics, Warsaw University of Technology - Institute of Microelectronics and Optoelectronics, Poland; *Krzysztof Czuba*, *Anna Szerling*, *Andrzej Taube*, Łukasiewicz Research Network-Institute of Microelectronics and Photonics, Poland

Application of p-type conductive oxides, such as nickel oxide (NiO) allows to produce high quality, high voltage, and low leakage current gallium oxide (β -Ga₂O₃) power diodes. NiO active layers are often deposited using reactive magnetron sputtering method, and process parameters can affect both material and resulting power devices properties. However, there is a lack of direct comparison of different magnetron sputtering configurations for deposition of p-type NiO layers for β -Ga₂O₃ devices. Here, in this work, properties of vertical NiO/ β -Ga₂O₃ heterojunction diodes (HJDs) obtained by confocal and planar sputtering magnetron system were compared. The devices were fabricated on n⁺- β -Ga₂O₃ epi layers (N_b~6.5x10¹⁵cm⁻³) grown by HVPE on bulk (001) β -Ga₂O₃ substrates. The NiO/Ni/Au anodes were fabricated using lift-off photolithography and deposition of 100 nm NiO layers by means of RF magnetron sputtering using ceramic NiO target. Nickel oxide layers were deposited with different oxygen contents in the Ar/O₂ gas mixture equal to 0, 10, 20, 30% in both planar down pO₂ (oxygen partial pressure) and confocal down fO₂ (oxygen partial flow) sputtering magnetron systems. Diodes with a NiO layer deposited in pure Ar atmosphere were characterized by Schottky-like or double-barrier I-V characteristics. Devices with a NiO layer from a confocal magnetron sputtering possess a lower ideality factor (n = 1.02), higher forward current over 200 A/cm² and breakdown voltage over 1600V as compared to diodes produced with a NiO layer obtained from a planar system. However, it shows "double-barrier" like forward characteristics. Higher breakdown voltage can be associated with higher energy bandgap (E_g=3.71 eV) as well as higher resistivity of layers deposited using confocal sputtering system. Devices with NiO layer deposited in a reactive atmosphere (pO₂ = fO₂ = 10-30%) were characterized by a typical p-n heterojunction characteristics with higher turn-on voltages. Higher forward current and breakdown voltage were observed for HJDs fabricated means of confocal magnetron sputtering system as compared to planar one. Ideality factors as low as n~1,15 were obtained for all diodes, regardless of oxygen partial flow. This work has been partially supported by the Wide Bandgap (WBG) Pilot line, which is funded jointly by the Chips Joint Undertaking, through the European Union's Digital Europe programme and Horizon Europe programme, as well as by the participating states Italy, Sweden, Poland, Finland, Austria, France and Germany, under Grant Agreement n. 101183211

IWGO-MoP-24 A Non-Van Der Waals Platform for Deep-Subwavelength Twist-Polaritonics Based on β -Ga₂O₃ Nanoflakes, Debo Hu, National Center for Nanoscience and Technology, China

Twist-polaritonics provides precise control of light-matter states through the stacking of atomically smooth, anisotropic layers but has been restricted to van der Waals (vdW) crystals. Non-vdW crystals, despite their symmetry-broken dielectric responses ideal for exotic polaritons, are difficult to thin into suitable flakes due to their rigid 3D bonding networks, thus limiting the implementation of deep-subwavelength twist-polaritonics. Here, we establish a non-vdW polaritonic platform using ultrathin, single-crystalline β -Ga₂O₃ nanoflakes synthesized by exploiting its anisotropic bonding hierarchy on the quasi-layered (100)B plane. These flakes exhibit deep-subwavelength polariton confinement beyond $\lambda/20$. Moreover, their atomic-scale flatness enables the assembly of twisted bilayers, in which we observe a topological transition of the polariton dispersion from hyperbolic to elliptical, directly controlled by the twist angle. This work positions β -Ga₂O₃ as a high-performance nanophotonic platform beyond the vdW family, while proposing that anisotropic bonding

hierarchy provides a general strategy to unlock non-vdW twist-polaritonic functionality in a wide range of bulk crystals.

IWGO-MoP-25 Engineering Considerations for the Growth of Sb-Doped Sn_{0.4}Ge_{0.6}O₂ Thin Films, Avery-Ryan Ansbro, Yi Liang, Pat Kezer, Manasi Londhe, John Heron, University of Michigan, Ann Arbor

Rutile germanium dioxide (r-GeO₂) has drawn a lot of attention due to its large bandgap, structural stability, and high thermal conductivity. Enhanced stability offered through alloying with SnO₂ makes these rutile structured oxides excellent candidates for next generation power electronic devices. Due to rutile oxides only recently being recognized as ultra-wide bandgap semiconducting materials, potential dopant and contact materials remain speculative.

In this work, we confirm Sb as an effective dopant in single crystal r-Sn_{0.4}Ge_{0.6}O₂ thin films grown on (10-10)-oriented sapphire substrates. Through variation of doping concentrations from 0.03-3.3%, we identify lower and upper doping limits for thin films. Additionally, we can achieve carrier densities up to 1.7 x 10²⁰ cm⁻³ and mobilities up to 33 cm²/Vs at room temperature. Challengingly, it is observed that under oxygen rich annealing conditions, germanium vacancies can act as electron sinks, drastically reducing carrier mobilities and rendering films insulating. We confirm that Sb can still behave as an effective donor so long as annealing occurs under reduced oxygen environments. Our work establishes optimized conditions for synthesizing Sb-doped thin films using pulsed laser deposition and the interplay between electron transport and deposition conditions.

IWGO-MoP-26 Characterization and Light Emission of CBLs with Varying Nitrogen Implantation Doses for β -Ga₂O₃ Devices, Kohei Ebihara, Tetsuro Hayashida, Munetaka Noguchi, Rina Tanaka, Ryuji Sakai, Hiroshi Watanabe, Masaki Taya, Tatsuro Watahiki, Mitsubishi Electric Corporation, Japan

β -Ga₂O₃ has an ultrawide bandgap of 4.7 eV and superior material properties that make it a promising candidate for next-generation power devices. However, realization of effective p-type doping in β -Ga₂O₃ remains a significant challenge, limiting the performance of devices. To address this issue, current-blocking layers (CBLs) with deep levels introduced by nitrogen (N) ion implantation have been proposed as an alternative to p-type wells. In this study, CBL test element groups (CBL-TEGs) with varying N implantation doses were fabricated to evaluate CBL performance and reduce leakage current. Light emission analyses were performed to identify the leakage locations and elucidate the leakage mechanism.

CBL-TEGs have an epitaxial layer grown on a β -Ga₂O₃ (001) substrate, with a carrier concentration of 1.0 x 10¹⁶ cm⁻³ and a thickness of 10 μ m. N ion implantation was performed to create a box profile with a depth of 0.8 μ m. Total N doses were 4.0 x 10¹³, 4.0 x 10¹⁴, and 4.0 x 10¹⁵ cm⁻². An n⁺ layer with a depth of 0.2 μ m was formed by silicon (Si) ion implantation. Following N and Si implantations, annealing was performed at 900 °C for 30 min. and 1 min., respectively. The top and bottom electrodes were formed by depositing Ti/Au with thicknesses of 20/230 nm. Finally, the top electrode was patterned, and the samples were annealed at 470 °C for 1 min.

The reverse-bias characteristics of the CBL-TEGs with various N doses were measured. Increasing the N dose effectively reduces the leakage current. Specifically, for the sample with a dose of 4.0 x 10¹⁵ cm⁻², the leakage current remained below 2 x 10⁻⁵ A/cm², a substantial improvement over previously reported values. After that, plan-view images of light emission and the emission spectrum under leakage condition were obtained. Clear emission is observed from the n⁺ region surrounding the top electrode for the 4.0 x 10¹³ cm⁻² sample, indicating that leakage current was distributed throughout the CBL under the entire n⁺ region. An emission peak near 700 nm (1.77 eV) suggests electron transitions involving the deep level. For the 4.0 x 10¹⁴ cm⁻² sample, emission from the n⁺ region around the electrode was observed, as with the case for the 4.0 x 10¹³ cm⁻² sample. In contrast, for the 4.0 x 10¹⁵ cm⁻² sample, emission was confined to the edge of the n⁺ region. These observations indicate that a N dose of 4.0 x 10¹⁵ cm⁻² effectively suppresses leakage through the CBL under the n⁺ region.

Acknowledgement: This study is based on results obtained from a project, JPNP22007, commissioned by the New Energy and Industrial Technology Development Organization (NEDO).

IWGO-MoP-27 Homoepitaxial Growth of β -Ga₂O₃ Using a Novel High-Density Oxygen Radical Source (HD-ORS) for MBE and PVD, Arun Kumar Dhasiyan, Nagoya University, Japan; Tomoki Takeda, Naofumi Kato, NU-Rei Co., Ltd, Japan; Naohiro Shimizu, Osamu Oda, Masaru Hori, Nagoya University, Japan

β -Ga₂O₃ has gained strong interest for power electronics because of its advantages over Si, SiC, and GaN. Homoepitaxy on β -Ga₂O₃ substrates is especially important, as it enables films with the highest crystalline quality. Among available techniques, Molecular Beam Epitaxy (MBE) offers atomic-level precision and excellent interface control, but its growth rate is limited by volatile Ga₂O formation. Achieving (001) homoepitaxy at low temperatures is difficult for any method. Overcoming the growth-rate limitation requires a more efficient oxygen plasma source capable of further oxidizing Ga₂O into solid β -Ga₂O₃. A high-density plasma is therefore essential.

To address this, we developed a High-Density Oxygen Radical Source (HD-ORS) that uses a mixture of ozone and oxygen to generate atomic oxygen for both MBE and Physical Vapor Deposition (PVD). Ozone was chosen instead of O₂ because its peak dissociation energy is an order of magnitude lower, and its dissociation produces singlet oxygen (¹D), which is significantly more reactive than triplet oxygen (³P).

This study demonstrates homoepitaxial β -Ga₂O₃ growth on Sn-doped Ga₂O₃ substrates by MBE using the HD-ORS. Optimal growth was achieved at a substrate temperature of 300 °C. We further show homoepitaxial β -Ga₂O₃ growth by PVD using both a commercial Low-Impedance Antenna Inductively Coupled Plasma (LIA-ICP) source and the HD-ORS. Notably, the HD-ORS enabled stable and reproducible (001)-oriented homoepitaxy on (001) substrates, achieving a growth rate of 1 μ m/h—an order of magnitude higher than typical Ga₂O₃ growth rates obtained by conventional MBE.

IWGO-MoP-28 Lock-in Infrared Thermography Techniques for Thermal Characterization of Ultra-Wide Bandgap Semiconductors, Ethan Scott, Jessica Reyes, University of Virginia; Jeffrey Braun, John Gaskins, Laser Thermal; Marko Tadjer, Navel Research Laboratory; Patrick Hopkins, University of Virginia

Ultra-Wide Bandgap (UWBG) semiconductors offer excellent performance for high-power applications. Their physical properties enable high critical breakdown fields, and their strong atomic bonds make them inherently stable at elevated temperatures. However, despite this potential, the performance of UWBG devices is still limited by material quality, defect density, and doping challenges, which also directly affect thermal performance. For materials such as gallium oxide, which naturally exhibit low thermal conductivity, any further reduction poses a significant engineering challenge. Therefore, accurate assessment of thermal performance is critical. Thermoreflectance techniques are among the most prevalent methods for measuring the thermal conductivity of UWBG substrates and films, offering excellent spatial resolution. However, they often require a mirror-like surface and a thin metal optothermal transducer. For example, as-deposited films can have a surface roughness incompatible with thermoreflectance, which necessitates sample polishing or membrane fabrication. In cases where samples have a thickness-dependent structure (e.g., a nucleation layer), polishing the top surface can affect the apparent measured thermal conductivity. Lock-in infrared thermography (LIT) provides an alternative approach, using a similar analysis to thermoreflectance while not strictly requiring a transducer layer and being insensitive to surface roughness. In this talk, we detail the advantages and limitations of LIT, demonstrating that it is well-suited for measurements of high-thermal-conductivity substrates and offers potential for higher measurement throughput.

IWGO-MoP-29 Reverse Leakage Reduction of β -Ga₂O₃ Schottky Barrier Diode by Ex-Situ Mg Annealing Diffusion, Zhiyu Xu, Jia Wang, Haitao Wang, Hiroshi Amano, Nagoya University, Japan

This work studies the leakage current characteristics of Ga₂O₃ Schottky barrier diodes (SBDs) employing metallic magnesium (Mg) as an *ex-situ* diffusion source for Schottky barrier engineering. The epitaxial structure consists of a 5 μ m unintentionally doped (UID) β -Ga₂O₃ layer ($n \approx 2.6 \times 10^{16}$ cm⁻³) grown by hydride vapor-phase epitaxy (HVPE) on a (001)-oriented n-type Sn-doped β -Ga₂O₃ substrate (NCT). A 10 nm thick Mg layer was deposited by sputtering on patterned regions, followed by liftoff. The Mg diffusion process was performed by thermal annealing at various temperatures in O₂ or N₂ ambient for different durations. The wafers were then cleaned by acid to remove Mg residue and other amorphous compound formed during annealing. Ni/Au Schottky contact was deposited on the Mg-treated mesa regions by e-beam evaporation, and an Al backside

contact was subsequently deposited by sputtering. No edge termination or passivation was applied in these SBDs. A reference sample without Mg annealing process was also fabricated.

The forward and reverse *J-V* measurement results for 200 μ m diameter SBD are shown in Fig. 1. Under forward bias, almost all SBDs have the same behavior as the reference device except that annealing at 800°C shows an increased turn-on voltage. Compared to the annealing in N₂ ambient, the annealing process of Ga₂O₃ in O₂ ambient better suppresses the reverse leakage current with stable device performance. It was found that with thin Mg deposition thickness of 10nm, the mild annealing temperature of 600-650°C shows lower leakage current compared to annealing at higher temperature of 800°C. Furthermore, extending the annealing time from 5 minutes to 10 minutes at 650°C increases the reverse leakage, indicating that Mg diffusion needs to be controlled such that there exists a window for moderate Mg diffusion concentration for the optimized reverse leakage characteristics of Mg-annealed β -Ga₂O₃ SBD.

IWGO-MoP-30 In-situ Reflectometry for Monitoring Growth Rate, Surface Morphology, and Doping in MOVPE Homoepitaxy of β -Ga₂O₃, Kolja Haberland, LayTec AG, Germany; Ta-Shun Chou, NextGO Epi UG, Germany; Andreas Fiedler, Adreas Popp, Saud Bin Anooz, Raimund Grüneberg, Jana Rehm, Arub Akhtar, Institut für Kristallzüchtung IKZ, Germany

The MOVPE growth of gallium oxide remains challenging, as precise control of layer thickness, surface morphology, and doping levels is required to produce device-grade epitaxial wafers for lateral and vertical transistors and to enable scaling to larger wafer sizes. In-situ optical metrology methods such as pyrometry and reflectometry therefore play an important role in understanding and controlling the growth process [1]. For fundamental studies, gallium oxide layers can be grown heteroepitaxially on sapphire substrates. Due to the refractive index contrast between the film and the substrate, strong Fabry-Pérot oscillations appear in the reflectance signal, enabling straightforward determination of growth rate and layer thickness. However, transistor applications require growth on native gallium oxide substrates, resulting in homoepitaxy where the refractive index contrast is minimal and Fabry-Pérot oscillations are largely suppressed.

In this work, we demonstrate that in-situ reflectometry can nevertheless provide critical growth information during homoepitaxial growth. Small variations in refractive index enable extraction of growth rate and layer thickness using an autocorrelation-based analysis of the reflectance signal. In addition, short-wavelength reflectometry at 280 nm provides a sensitive method for real-time monitoring of surface roughness during growth, independent of the substrate material. Furthermore, we present results on the determination of doping levels in Si-doped gallium oxide using in-situ reflectometry. Significant refractive index changes with doping level are observed and attributed to plasmonic effects described by the Drude approximation. This enables correlation of doping levels with the in-situ reflectance signal, demonstrating the potential of optical in-situ metrology for real-time monitoring of doping during MOVPE growth.

With such in-situ monitoring, independent of the substrate and even the MOVPE tool, the growth can be precisely monitored.

[1] Journal of Crystal Growth 603 (2023) 127003

Author for correspondence: kolja.haberland@laytec.de

IWGO-MoP-31 Epitaxial β -(Al_xGa_{1-x})₂O₃ Thin Films Grown on (100) β -Ga₂O₃ by MOVPE, Deborah Kern, Martin Handweg, Ta-Shun Chou, Saud Bin Anooz, Martin Schmidbauer, Andreas Popp, Andreas Fiedler, Leibniz Institute for Crystal Growth, Germany

One major drawback of Ga₂O₃ is its low electron mobility. To overcome this limitation in homoepitaxial β -Ga₂O₃, a modulation-doped β -(Al_xGa_{1-x})₂O₃/Ga₂O₃ heterostructure has been proposed to induce a high-mobility two-dimensional electron gas (2DEG) at the interface, which can be used in high electron mobility transistors (HEMT). However, a comprehensive understanding of the growth mechanisms, as well as the surface and reaction behavior of aluminum-alloyed gallium oxide layers is still lacking.

We report on the growth of fully strained epitaxial thin layers (15-60 nm thickness) of β -(Al_xGa_{1-x})₂O₃ on β -(100) Ga₂O₃ with an offcut angle of 4° by metal-organic vapor phase epitaxy (MOVPE) with an Al content around 40%. With increasing the Ga flow, the growth rate increased linearly up to approximately 30 nm/min at constant Al flow (Fig. 1a). With a higher Ga flow, a smoother surface with a step-bunching morphology with less particles is observed (Fig. 1b). The Al content in the layers stayed roughly constant with increasing Ga flow, might suggesting that a Ga wetting-layer is formed. The Ga wetting layer influences adatom diffusion, allowing Al adatoms to migrate over the Ga-rich surface and incorporate into the

crystal lattice, effectively “sinking” from the adlayer to form a thin layer. Thus, Ga acts as a surfactant for the growth of β -(Al_xGa_{1-x})₂O₃, possibly attributed to a metal-exchange catalysis mechanism similar to the reported In-catalyzed Ga₂O₃ growth via MBE.[1]

This work is an important step toward understanding the growth of Al-alloyed heterostructures for achieving high-efficiency HEMT devices.

[1] P. Vogt, O. Brandt, H. Riechert, J. Lähnemann, O. Bierwagen, PRL **119**, 196001 (2017).

IWGO-MoP-32 NiO/ β -Ga₂O₃ Vertical Pin Diodes with Low Leakage and Size Dependent Transport Characteristics, Tom Miccittis, Institute of Electronics, Microelectronics and Nanotechnology (IEMN), France

β -Ga₂O₃ has emerged as a promising ultra-wide bandgap semiconductor for high-voltage power electronics due to its large bandgap (~4.8 eV) and high critical electric field. However, the absence of reliable p-type doping remains a key limitation for the realization of bipolar devices. One approach to overcome this challenge consists of using p-type oxides to form heterojunction PIN structures with n-type Ga₂O₃.

In this work, vertical Ni_{1-x}O/ β -Ga₂O₃ PIN diodes were fabricated on Si-doped β -Ga₂O₃ substrates with a 10- μ m-thick n⁻ Ga₂O₃ drift layer ($N_D \approx 10^{16}$ cm⁻³). The Ni_{1-x}O layer used to form the heterojunction was optimized in a companion study focusing on the electrical properties of p-type Ni_{1-x}O thin films. A 3 μ m-deep mesa structure was implemented to mitigate electric field crowding at the device periphery and improve the overall electrical performance.

Electrical characterization was performed on devices with anode diameters ranging from 80 μ m to 450 μ m. Forward measurements show rectifying behavior with a turn-on voltage of approximately 1.9 V. The forward current density increases with the device diameter, while smaller diodes exhibit reduced current density. This size dependence suggests that forward transport is not purely limited by bulk series resistance but is influenced by perimeter-related effects and non-uniform carrier injection at the Ni_{1-x}O/ β -Ga₂O₃ heterojunction.

Reverse measurements reveal low leakage current densities in the 10⁻⁷–10⁻⁸ A/cm² range and a diameter-dependent breakdown behavior, where larger devices exhibit earlier breakdown, likely due to electric-field crowding at the device periphery, combined with increased sensitivity to local defects in larger-area devices.

Temperature-dependent measurements further reveal a transition from injection-limited transport in small devices to drift-limited conduction in larger diodes. While larger diodes exhibit a decrease of forward current with increasing temperature, consistent with mobility degradation in the Ga₂O₃ drift layer, smaller devices show a thermally activated current increase, suggesting injection-limited transport at the heterojunction.

A benchmark of leakage current density versus breakdown voltage is presented and compared with reported Ni_{1-x}O/ β -Ga₂O₃ heterojunction diodes. These results highlight the competitive among the lowest reported leakage performance of the proposed devices and provide insights into the transport mechanisms governing the scaling of vertical Ga₂O₃ heterojunction power diodes.

IWGO-MoP-33 Electronic and Electrical Properties of Mg_xNi_{1-x}O Thin Films Deposited by Rf Magnetron Sputtering, Harunobu Yasuda, Shunya Matsui,

Takayuki Akiba, Tomohiro Yamaguchi, Tohru Honda, Department of Electrical Engineering and Electronics, Graduate School of Engineering, Kogakuin University, Japan; Hironobu Miyamoto, Kohei Sasaki, Novel Crystal Technology, Japan; Takeyoshi Onuma, Department of Electrical Engineering and Electronics, Graduate School of Engineering, Kogakuin University, Japan β -Ga₂O₃ is known as a novel material for power electronics. [1,2] We have been focusing on Mg_xNi_{1-x}O alloy as a material for pn heterojunction with β -Ga₂O₃. Electric property, bandgap, and band alignment have been reported for Mg_xNi_{1-x}O with $x \leq 32\%$. [2,3] In this study, Mg_xNi_{1-x}O films were deposited by RF magnetron sputtering for $x \leq 0.58$, and their electronic and electrical properties were evaluated.

Mg_xNi_{1-x}O films were deposited by RF magnetron sputtering in an O₂ atmosphere at an ambient temperature. A NiO target and c-plane sapphire or quartz glass substrate were set with a distance of 3 cm. To alloy with MgO, the NiO target was co-sputtered with 0 to 16 pieces of 10×10 mm² square-shaped MgO substrates. RF power and sputtering pressure were fixed at 150 W and 0.75 Pa, respectively. Since sputtering rate decreased with increasing the number of MgO substrate, sputtering time was varied in a range 10-30 minutes to adjust film thickness in a range 106-140 nm. Resistivity was measured by the four-point probe method with van der

Pauw configuration. Mg composition was quantified by energy dispersive X-ray spectrometry. Optical transmittance spectra were measured by UV-Vis spectrophotometer. Valence band offset (ΔE_v) at the MgNiO/sapphire interface was determined by X-ray photoelectron spectroscopy.

As shown in Fig. 1, room temperature resistivity increased monotonically with increasing x. All the films were confirmed to show a p-type conductivity by Seebeck effect measurement. Absorption edge E_{edge} , which was determined by the Tauc plot, increased with x in a range 3.69-4.28 eV. The Tauc plot showed additional onset in a range 3.74-5.49 eV. The former is attributed to O 2p to Ni 3d charge transfer transition, and the latter is originated from valence to conduction band transition giving bandgap E_g . [5] ΔE_v decreased with x in a range 2.31-1.57 eV. The results may imply that breakdown voltage is expected to be higher for large x with maintaining low on-voltage.

This work was supported in part by the New Energy and Industrial Technology Development Organization (NEDO), subsidized by project No. JPNP22007. [1] M. Higashiwaki *et al.*, J. Phys. D: Appl. Phys. **50**, 333002 (2017). [2] K. Sasaki, Appl. Phys. Express **17**, 090101 (2024). [3] M. Murayama *et al.*, IWGO4, (2022), Pos 1-41. [4] T. Onuma *et al.*, IWGO5, (2024), TuP_46. [5] T. Saitoh *et al.*, Appl. Phys. Lett. **112**, 041904 (2018). [6] A. M. E. Raj *et al.*, Cryst. Res. Technol. **42**, 867 (2007).

IWGO-MoP-34 Improved Structural and Electrical Properties of MOCVD-Grown β -Ga₂O₃/Sapphire Films with Compositionally-Graded (Al_xGa_{1-x})₂O₃ Buffer, Filip Gucmann, Sai Gurukrishna Vadlamudi, Kristina Hušeková,

Edmund Dobročka, Peter Nádaždy, Dagmar Gregušová, Iryna Kozak, Ondrej Pohorelec, Institute of Electrical Engineering, Slovak Academy of Sciences, Slovakia; Matej Mičušík, Polymer Institute, Slovak Academy of Sciences, Slovakia; Igor Piš, Milan Ťapajna, Institute of Electrical Engineering, Slovak Academy of Sciences, Slovakia

We report on β -(Al_xGa_{1-x})₂O₃/ β -Ga₂O₃ (AlGaO/GaO) heterostructures grown on c-plane sapphire by liquid-injection MOCVD. AlGaO buffers were compositionally-graded with varying starting Al content (5, 15, 30 at. %) via novel fully-autonomous liquid precursor dosing to achieve linear gradient for mitigation of the lattice mismatch. As opposed to our previous results, Si-doped GaO films grown on AlGaO buffers exhibited improved crystallinity: GaO X-ray rocking curve showed best FWHM of ~1.6°, while only ~0.9° for AlGaO buffer with 5% Al content. However, signs of phase separation were observed for AlGaO films with 15% and 30% Al content. Significantly improved was RT electron mobility $\mu_e \sim 8$ cm²/Vs at $n_e \sim 1.3 \times 10^{19}$ cm⁻³ ($\rho = 0.078$ Ω -cm) compared to the films prepared directly on sapphire which showed $\mu_e \sim 0.6$ -1.7 cm²/Vs and strong electron localization. Depletion-mode MOSFETs showed output current of ~9 mA/mm but did not fully pinch-off (before gate dielectric breakdown) without gate recess. Further, strong suppression of parasitic (310)-oriented crystallites, previously achieved via the use of off-cut substrates, was observed for 5% Al content AlGaO buffers, while only minor content was observed in subsequently-grown GaO films. Implementing the AlGaO buffer led to several times larger GaO grains than previously; RMS surface roughness of AlGaO and GaO films were 3.8 and 11 nm, respectively. We further evaluate electronic structure, depth-resolved chemical composition, stoichiometry, and electric transport properties via photoluminescence, X-ray photoelectron spectroscopy, elastic recoil detection analysis, and low-T I-V measurements, respectively.

IWGO-MoP-35 Reduction of Si Impurities in β -Ga₂O₃ Homoepitaxial Films Grown by Mist-CVD, Yuki Isobe, Kyoto University, Japan; Yuki Yamamoto, OXIDE Corporation, Japan; Hirokazu Izumi, Hyogo Prefectural Institute of Technology, Japan; Takeru Wakamatsu, Kyoto University, Japan; Kentaro Kaneko, Ritsumeikan University, Japan; Shizuo Fujita, Katsuhisa Tanaka, Kyoto University, Japan

β -Ga₂O₃, one of the ultra-wide-bandgap semiconductors with a bandgap of 4.6-4.9 eV, has attracted attention because of its potential applications for power electronics. Thus far, the control of carrier concentration in the range of 5×10^{17} cm⁻³ to 2×10^{20} cm⁻³ has been achieved for thin films obtained by mist-CVD [1]. However, compared to other growth processes, the carrier concentration remains relatively high. The carrier concentration below 10^{17} cm⁻³ is required for achieving a breakdown voltage above 1 kV. This is partly because unintentional impurities such as Si are incorporated into thin films during the growth process. In this work, an attempt was made to reduce the concentration of unintentional impurities, especially, Si by inner-wall coating of silica tube used for the thin film growth and cleaning of substrate surface prior to the preparation of β -Ga₂O₃ thin films on β -Ga₂O₃ substrates.

Figure 1 shows SIMS profiles of Si in thin films and substrates before and after the cleaning of substrate surface with hydrofluoric acid and inner-wall

coating of silica glass tube. It is clear that the concentration of Si was reduced by both treatment with hydrofluoric acid and inner-wall coating. Figure 2 depicts relationship between electron mobility and carrier concentration obtained by the Hall effect measurements. The carrier concentration was reduced by both hydrofluoric acid treatment and inner-wall coating. For the thin film grown in the silica glass tube the inner-wall of which was coated with both Ga₂O₃ and Al₂O₃, the carrier concentration is decreased to $6.3 \times 10^{16} \text{ cm}^{-3}$, and the electron mobility reaches $129 \text{ cm}^2\text{V}^{-1}\text{s}^{-1}$.

This work was supported by the New Energy and Industrial Technology Development Organization (NEDO) under project JPNP21005.

[1] T. Ogawa et al., Jpn. J. Appl. Phys. 62, SF1016 (2023).

IWGO-MoP-36 Prospects of Safe and Cost-Effective Mist CVD for Homoepitaxial Growth and Devices of β -Ga₂O₃, Shizuo Fujita, Takeru Wakamatsu, Yuki Isobe, Hikaru Ikeda, Kyoto University, Japan; Yuji Ando, Hidemasa Takahashi, Ryutarō Makisako, Nagoya University, Japan; Tetsuzo Ueda, Panasonic, Japan; Jun Suda, Katsuhisa Tanaka, Kyoto University, Japan; Hidetaka Sugaya, Panasonic, Japan

Mist CVD has evolved as a safe and cost-effective method for growing oxide thin films such as those used for transparent conductors, passivation layers, and coating films. However, its application to the growth of device-quality semiconductor layers has hardly been investigated, as it is considered inferior to MOCVD or MBE in terms of source purity and the potential for impurity incorporation. At Kyoto University, based on the experience that β -Ga₂O₃ films grown on β -Ga₂O₃ substrates exhibit good surface morphology and crystallinity, owing to homoepitaxy, efforts have been made to reduce residual impurities in β -Ga₂O₃ films. Recently, the donor concentration became controllable in the order of 10^{17}cm^{-3} , where the breakdown voltage could be >800 V.

To demonstrate the potential applications of mist CVD-grown β -Ga₂O₃ films in devices, we presented successful operation of MESFETs with the gate length (L_G) of 2 μm [1], followed by those with a L_G of 0.45 μm and an effective gate width (W_G) of 150 μm showing a current gain cut-off frequency (f_T) and a maximum oscillation frequency (f_{max}) of 8.3 and 18.4 GHz, respectively [2]. In this presentation, we demonstrate advanced RF characteristics of MESFETs with larger W_G showing higher power and gain.

We used a (010)-oriented 2-inch β -Ga₂O₃ substrate grown by the vertical Bridgeman method. The substrate was divided into four pieces on which the growth was performed by mist CVD. The β -Ga₂O₃ epitaxial layer was Ge-doped and had a thickness of 61 nm. The electron concentration and mobility were estimated at $1.5 \times 10^{18} \text{ cm}^{-3}$ and $85 \text{ cm}^2/\text{Vs}$, respectively, based on the Hall effect measurements. The MESFETs were fabricated at the C-TEFs of Nagoya University using stepper lithography. The L_G and W_G were 0.4 and 600 μm , respectively. An example of the DC characteristics revealed the maximum drain current and transconductance of 93 mA/mm and 33 mS/mm, respectively, at the drain voltage of 10 V. An amplifier using the MESFET showed a maximum output power of 19 dBm (80 mW), a linear gain of 10dB, and a maximum added efficiency of 15% at 2.48 GHz by placing the matching circuit near the device. The output power was more than six times higher than that of our previous device [2] owing to the larger gate width. However, the drain current is not high enough, and overcoming this is one of our future objectives. Nevertheless, these results encourage the use of mist CVD may as a cost-effective device fabrication technology.

We acknowledge Novel Crystal Technology, Inc. for supplying a 2-inch β -Ga₂O₃ substrate.

[1] H. Takane et al., Appl. Phys. Express 16, 081004 (2023); [2] H. Ikeda et al., Jpn. J. Appl. Phys. 64, 108002 (2025).

IWGO-MoP-37 Quaternary (Al_xSc_yGa_{1-x-y})₂O₃ for Lattice-Matched β -Ga₂O₃ Heterostructures, Kazuki Koreishi, Institute of Science Tokyo, Japan; Kodai Niitsu, National Institute for Materials Science, Japan; Takuto Soma, Tohoku University, Japan; Kohei Yoshimatsu, Akira Ohtomo, Institute of Science Tokyo, Japan

Bandgap engineering of β -Ga₂O₃ has been widely investigated for enhancing Baliga's figure of merit of the materials and for developing heterojunction-based devices. These studies employed the heteroepitaxy of a ternary (Al_xGa_{1-x})₂O₃ (AGO) alloy; however, a phase-pure and high-quality AGO epitaxial layer is practically limited to an Al content of approximately 20% and a certain layer thickness due to the lattice mismatch. In contrast, a quaternary (Al_xSc_yGa_{1-x-y})₂O₃ (ASGO) is expected to exhibit a wider tunability of the bandgap energy (E_g) and layer thickness owing to its lattice matching to β -Ga₂O₃. Here, we have investigated the crystal structures and

E_g of ASGO powders and thin films for future heterojunction-based power-device applications.

The four lattice parameters of the ASGO powder samples are identical to those of β -Ga₂O₃ when x/y is between 1.5 and 3.2. We thus prepared several ASGO films with the lattice-matched x/y range on β -Ga₂O₃ (100) by using pulsed-laser deposition. The lattice-matched ASGO (100) epilayer exhibited superior crystallinity as confirmed by a sharp reflection from the thin film in x-ray diffraction reciprocal space maps. The estimated E_g of the ASGO (100) films determined by electron energy loss spectroscopy varied from 4.5 to 5.8 eV while maintaining the lattice matching to β -Ga₂O₃.

IWGO-MoP-38 Photoemission Electron Microscopy for Imaging Defects, Andrew Winchester, Min-Yeong Kim, Ory Maimon, National Institute for Science and Technology (NIST); Dinusha Mudiyansele, Houqiang Fu, Arizona State University; Sang-Mo Koo, Kwangwoon University, Republic of Korea; Qiliang Li, George Mason University; Sujitra Pookpanratana, National Institute for Science and Technology (NIST)

β -Ga₂O₃ has potential for use in high-power electronics due to its unique properties and facile crystalline growth. Commercial realization of β -Ga₂O₃ power electronics will require intimate knowledge of performance-limiting structural and extended defects. Here, we use photoemission electron microscopy (PEEM) and spectroscopy to measure the surface electronic properties and observe spatial inhomogeneities of β -Ga₂O₃ substrates and homoepitaxy films.

The electronic properties of β -Ga₂O₃ substrates with (010), (001), and (-201) orientations are measured and show nanoscale electronic variations on all three facets that correspond to local regions of different doping and gap state density (Fig 1 a-c). The work function and ionization potential of the (010) surface are substantially lower than the other two orientations (Fig 1 d), which is consistent with reported differences in Schottky barrier heights.¹

In (010) β -Ga₂O₃ homoepitaxially grown via hydride vapor phase epitaxy (HVPE), extended structural defects are observed. We observe two types of linear, surface defects aligned along the [001] crystal axis. One defect consists of a micrometer-sized particle and a tail of protruding material, while the other is a groove in the surface. The large particle is a Ga-rich phase that is likely present early in the HVPE growth that disrupts the surface, while the groove defect appears purely structural in nature.²

1. Fu et al. IEEE Trans. Electron Devices 65, 3507–3513 (2018).
2. Kim et al., Appl. Phys. Lett. 126, 231605 (2025).

* Author for correspondence: sujitra@nist.gov

IWGO-MoP-39 First-Principles and Thermodynamic Study of (Al_xGa_{1-x})₂O₃ Growth by PA-MBE, Rie Togashi, Sophia University, Japan; Akira Kusaba, Kyushu University, Japan; Masataka Higashiwaki, Osaka Metropolitan University/NICT, Japan; Yoshinao Kumagai, Tokyo University of Agriculture and Technology, Japan

Ga₂O₃ and (Al_xGa_{1-x})₂O₃ alloys have attracted attention as materials for next-generation high-power devices. In this study, the composition dependence of the formation enthalpy, ΔH , of (Al_xGa_{1-x})₂O₃ alloys in the α and β phases was investigated by first-principles calculations. For simplicity, the calculated results were approximated using a regular solution model. Based on these results, thermodynamic analysis was performed for plasma-assisted molecular beam epitaxy (PA-MBE) growth of (Al_xGa_{1-x})₂O₃.

For β -(Al_xGa_{1-x})₂O₃, three Al occupation models were considered: octahedral-site occupation (β -oct), random occupation of octahedral and tetrahedral Ga sites (β -rand), and tetrahedral-site occupation (β -tet). The results indicate that Al preferentially occupies the octahedral site. The composition-dependent formation enthalpies for α - and β -(Al_xGa_{1-x})₂O₃ were approximated using the regular solution model, $\Delta H = \Omega x(1-x)$. The fitted Ω values were 511 cal/mol-cation for β -oct, 3021 cal/mol-cation for β -tet, and 2108 cal/mol-cation for α -(Al_xGa_{1-x})₂O₃, corresponding to critical temperatures (T_c) of -145, 487, and 257 °C, respectively. The low T_c for β -oct suggests that compositional separation is unlikely within the β phase.

The relationship between the gas-phase composition ratio, $R_{\text{Al}} (=P^{\circ}_{\text{Al}}/P^{\circ}_{\text{III}})$, and the solid-phase Al composition x was also investigated under various oxygen input partial pressures. Under O-rich growth conditions, R_{Al} was nearly equal to x . In contrast, under metal-rich growth conditions, x shifts toward Al₂O₃-rich compositions with increasing R_{Al} because the input Ga becomes Ga₂O(g) and remains in the gas phase. The calculated results agree well with the experimental data. These results indicate that, under the present PA-MBE conditions, the growth of (Al_xGa_{1-x})₂O₃ is thermodynamically limited.

Monday Evening, August 3, 2026

This work was supported in part by the Collaborative Research Program of Research Institute for Applied Mechanics, Kyushu University.

[1] T. Ohtsuki, J. Vac. Sci. Technol. A **41**, 042712 (2023).

IWGO-MoP-40 Benchmarking Gate Charge in Gallium Oxide Transistors, Daniel Dryden, Air Force Research Laboratory

Gate charge Q_G is a useful metric for understanding and predicting the switching speed and loss of high-voltage power switches, but is difficult or impossible to directly measure on-wafer for ultra-wide band gap devices due to their extremely low gate charges and fast switching speeds. New methods for extracting Q_G are therefore necessary in order to effectively benchmark Ga_2O_3 devices. We have explored three means of estimating gate charge: split C-V, s-parameter extraction, and geometric approximation. The geometric method provides a conservative order-of-magnitude estimate of Q_G . Q_G from split C-V measurements are in good agreement with datasheet values for COTS parts and agree within an order of magnitude with the $Q_{G,geometric}$ for lateral Ga_2O_3 devices. S-parameter extraction agrees well with split C-V data and has a lower noise floor, improving accuracy for small-periphery devices. Work is ongoing to correlate these values to transient switching measurements and to determine the best practices for accurate Q_G extraction. Overall, these methods provide a useful suite of techniques for researchers looking to benchmark switching performance for small, UWBG devices with low Q_G .

IWGO-MoP-41 Defect Characterization of Czochralski Grown Gallium Oxide, Aleksander Imhof, Nadeemullah Mahadik, Naval Research Laboratory; Marko Tadjer, naval research Laboratory; Robert Lavelle, Pennsylvania State University

The high electrical breakdown strength, ease of melt-growth, and high Baliga's figure of merit of beta-phase gallium oxide (β - Ga_2O_3) make it a desirable ultra-wide-bandgap semiconductor material for the fabrication of next-generation power devices [1]. β - Ga_2O_3 's material characteristics make it a competitive with other wide-bandgap materials GaN and SiC [2,3]. Wafer quality is crucial to the future development and adoption of β -devices as dislocations and other structural defects have negative impacts on their performance and reliability. Characterization of the different β -production methods has already begun in an effort to understand and mitigate dislocations [4,5,6].

This work focuses on the characterization of defects in an axial slice from seed to dome of β - Ga_2O_3 commercially grown by SYNOPSIS using the Czochralski (CZ) method. High resolution x-ray topography (XRT) was used to observe threading dislocations that propagate throughout the slice. To obtain clear XRT images, the sample surfaces were subjected to chemical-mechanical polishing (CMP) to remove damage introduced during mechanical processing prior to XRT observation. Figure 1 shows two XRT images taken with $g = 912$ and $g = 605$. Note that the horizontal lines that appear in Fig. 1(a) do not appear in Fig. 1(b). Using contrast analysis, the invisibility criterion, the Burgers vectors of these horizontal lines must contain a component. As the growth direction for CZ grown β - Ga_2O_3 is these striations can be characterized as threading screw dislocations as their Burgers vector and dislocation direction are parallel. Using the data, it was calculated that the density of the TSDs on the seed side was $\sim 1000/cm^2$ which dropped to $\sim 400/cm^2$ on the dome side. It was observed that the TSDs either annihilated, converted to basal plane dislocations (BPDs), or combined into a single TSD. The white circular contrasts in Fig 1(a) are basal plane dislocations and their density in the slice also decreases from seed side to dome. The average density dropped from $\sim 400/cm^2$ to $\sim 100/cm^2$. Finally, the long dislocations in these images are threading mixed dislocations TMDs as their line direction changes as they migrate through the slice and they appear in both Fig 1(a) and 1(b) The density of the TMDs once again drops from seed side to dome side, with the averages of $\sim 150/cm^2$ and $\sim 50/cm^2$ respectively. Further details of the defects and their evolution will be presented.

IWGO-MoP-42 Adsorption Controlled Growth and Doping of α -(Al,Ga) $_2O_3$ by Suboxide Molecular Beam Epitaxy, Sushma Raghuvansy, Marco Schowalter, Alexander Karg, Martin Samuel Williams, Manuel Alonso-Orts, Andreas Rosenauer, Martin Eickhoff, University of Bremen, Germany; Patrick Vogt, Paul-Drude-Institut für Festkörperelektronik Leibniz-Institut im Forschungsverbund Berlin, Germany

Among ultra-wide bandgap (UWBG) semiconductors Ga_2O_3 is a promising candidate for application in high-power electronic devices due to its high breakdown field [1]. To further widen the bandgap, alloying with isoelectric Al is a viable strategy. Because of the limited solubility of Al in β - Ga_2O_3 , α - Ga_2O_3 is the preferred polymorph for such investigations. Being

isostructural to Al_2O_3 , α - Ga_2O_3 allows for Al-alloying over the entire composition range [2].

In this contribution we investigate the growth of α -(Al_xGa_{1-x}) $_2O_3$ layers by plasma-assisted suboxide molecular beam epitaxy (S-MBE) in combination with the presence of the growth-enhancing additive Indium on the surface. Using these approaches, a comparative study of the Al-alloying of α - Ga_2O_3 on m-plane Al_2O_3 is presented. The findings pave the way to investigate the incorporation of donors into the α -(Al_xGa_{1-x}) $_2O_3$ layers. Furthermore, we take the concept of Vogt et al. [3] into account, to use a low temperature α - Ga_2O_3 buffer layer to suppress the defect formation in the desired conductive layer on top. In this framework we study doping with Sn, Ge, and Si for layers at different Al-concentrations. The incorporation of the dopants and their electrical activity are examined in relation to structural and morphological characteristics, analyzed by using high-resolution X-ray diffraction (XRD), atomic force microscopy, X-ray photoelectron spectroscopy (XPS), and scanning transmission electron microscopy (STEM).

Tuesday Morning, August 4, 2026

International Workshop on Gallium Oxide and Related Materials (IWGO-6)

Room ESJ 0202 - Session IWGO-TuM1

Substrate Development and Material Quality I

Moderators: Masataka Higashiwaki, Osaka Metropolitan University/NICT, Yoshinao Kumagai, Tokyo University of Agriculture and Technology

8:00am IWGO-TuM1-1 Breakfast

8:30am IWGO-TuM1-7 Invited Paper, Lynn Petersen, Office of Naval Research **INVITED**

8:55am IWGO-TuM1-12 Cost Analysis of Gallium Oxide Wafer Production and Challenges and Strategies for Cost Reduction, Akito Kuramata, Takuya Igarashi, Shinya Watanabe, Novel Crystal Technology, Inc., Japan; Chia-Hung Lin, Novel Crystal Technology, Inc., Taiwan; Kohei Sasaki, Kimiyoshi Koshi, Novel Crystal Technology, Inc., Japan **INVITED**

Gallium oxide has attracted significant attention as a promising material for next-generation power devices, and intensive research and development efforts on wafer and device technologies are being conducted worldwide toward its practical implementation. Applications are expected primarily in the medium- to high-voltage range, including wind power generation, photovoltaic systems, high-voltage direct current power transmission, energy storage systems, railway traction, fast charging for electric vehicles, and AI data centers.

In recent years, the rapid emergence of Chinese manufacturers has led to a substantial decline in the prices of SiC wafers and SiC power devices. For gallium oxide power devices to achieve commercial viability, they must outperform SiC not only in device performance but also in cost competitiveness. From this perspective, aggressive reduction of wafer manufacturing costs is of critical importance.

In this report, we analyze the cost structure of gallium oxide wafers and identify the key challenges that must be addressed to achieve future cost reductions. Furthermore, we discuss potential concrete strategies to overcome these challenges. Finally, we present the results of cost simulations estimating the extent to which wafer costs could be reduced after implementing the proposed measures.

*Author for correspondence: kuramata@novelcrystal.co.jp

9:20am IWGO-TuM1-17 Dawn of a 7 eV Semiconductor: Si-doped α -(Al_xGa_{1-x})₂O₃, Darrell Schlom, Cornell University **INVITED**

For 65 years the highest bandgap semiconductor known has been cubic boron nitride (c-BN), with a bandgap (E_g) of 6.4 eV [1,2]. In the last few years this situation has changed, and a new semiconductor has emerged with higher E_g : α -(Al_xGa_{1-x})₂O₃. The first glimpse of this promising new semiconductor was conducting Si-doped α -(Al_xGa_{1-x})₂O₃ with $E_g = 6.2$ eV in 2020 [3]. This was followed by the prediction that silicon would be a shallow dopant in α -(Al_xGa_{1-x})₂O₃ for E_g up to 7.5 eV [4]. Then in 2024 Okumura's group showed conductivity up to $E_g = 6.9$ eV in Si-doped α -(Al_xGa_{1-x})₂O₃ [5,6]. Using a different growth technique—suboxide MBE (S-MBE) in which pre-oxidized molecular beams of the constituents, i.e., Ga₂O and SiO for the growth of Si-doped α -(Al_xGa_{1-x})₂O₃—and a sequence of buffer layers, we achieve conductivities more than 100 million times higher at $E_g \leq 7.0$ eV. In these structures we observe room-temperature mobilities as high as 90 cm²/(V·s) for α -Ga₂O [7]. Using a Si-doped α -(Al_{0.51}Ga_{0.49})₂O₃ channel layer with $E_g = 6.7$ eV, we fabricate Schottky diodes and MESFETs. Our results demonstrate the widest bandgap semiconductor in which active electronic device behavior utilizing controlled carrier transport and field-effect modulation has been achieved [8].

[1] R.H. Wentorf, "Preparation of Semiconducting Cubic Boron Nitride," *J. Chem. Phys.* **36** (1962) 1990–1991.

[2] R.M. Chrenko, "Ultraviolet and Infrared Spectra of Cubic Boron Nitride," *Solid State Commun.* **14** (1974) 511–515.

[3] G.T. Dang, Y. Tagashira, T. Yasuoka, L. Liu, and T. Kawaharamura, "Conductive Si-doped α -(Al_xGa_{1-x})₂O₃ Thin Films with the Bandgaps up to 6.22 eV," *AIP Adv.* **10** (2020) 115019.

[4] D. Wickramaratne, J.B. Varley, and J.L. Lyons, "Donor Doping of Corundum (Al_xGa_{1-x})₂O₃," *Appl. Phys. Lett.* **121** (2022) 042110.

[5] H. Okumura, A. Fasson, and C. Mannequin, "Si-doped (AlGa)₂O₃ Growth on *a*-, *m*- and *r*-Plane α -Al₂O₃ Substrates by Molecular Beam Epitaxy," *Jpn. J. Appl. Phys.* **63** (2024) 055502.

Tuesday Morning, August 4, 2026

[6] H. Okumura, and J.B. Varley, "MOCVD Growth of Si-doped α -(AlGa)₂O₃ on *m*-Plane α -Al₂O₃ Substrates," *Jpn. J. Appl. Phys.* **63** (2024) 075502.

[7] J. Steele, J. Chen, T. Burrell, N.A. Pieczulewski, D. Bhattacharya, K. Smith, K. Gann, M.O. Thompson, H.G. Xing, D. Jena, D.A. Muller, M.D. Williams, M.K. Indika Senevirathna, and D.G. Schlom, "Growth of Conductive Si-Doped α -Ga₂O₃ by Suboxide Molecular-Beam Epitaxy," *APL Mater.* **13** (2025) 101117.

[8] This work was performed in collaboration with J. Steele, D. Bhattacharya, K. Nomoto, N.A. Pieczulewski, P. Sorenson, M. Ramesh, I. Shukla, S. Das, V-A. Ha, F. Giustino, B. Mazumder, M.K. Indika Senevirathna, M. Schubert, D.A. Muller, H.G. Xing, and D. Jena.

9:45am IWGO-TuM1-22 Demonstration of 150 mm (001) β -Ga₂O₃ Substrates Grown by EFG Method, Sho Hasegawa, Kimiyoshi Koshi, Yuki Ueda, Ryoichi Sakaguchi, Novel Crystal Technology, Inc., Japan; Isao Sakamoto, Novel Crystal Technology, Inc, Japan; Keita Konishi, Makoto Mizui, Yu Yamaoka, Shinya Watanabe, Kohei Sasaki, Akito Kuramata, Novel Crystal Technology, Inc., Japan

While 100-mm (001) β -Ga₂O₃ substrates are commercially available and have been successfully utilized in high-voltage, high-current devices, scaling the substrate diameter from 100 mm to 150 mm is essential for full-scale mass production. In this study, we report the growth of 150-mm (001) β -Ga₂O₃ single crystals using the edge-defined film-fed growth (EFG) method, along with the successful fabrication of 150-mm (001) substrates.

10:00am IWGO-TuM1-25 Bulk Single Crystal Growth of β -Ga₂O₃ with Automatic Diameter Control System Specialized for the OCCC Method, Masanori Kitahara, Taketoshi Tomida, FOX Corporation, Japan; Vladimir Kochurikhin, Gushchina Liudmila, C&A Corp, Russian Federation; Yasuhiro Shoji, Kei Kamada, FOX Corporation, Japan; Koichi Kakimoto, Tohoku University, Japan; Akira Yoshikawa, FOX Corporation, Japan

The Oxide Crystal Growth using a Cold Crucible (OCCC) method is scalable, crucible-free growth technique. We have previously reported the growth of oxide single crystals, including 2-inch-diameter β -Ga₂O₃, by taking advantage of the OCCC method [1,2]. With simulation-assisted optimization of growth parameters such as oscillator frequency [3], single crystal growth was successfully demonstrated. However, manual diameter control based on visual observation has made it difficult to achieve smooth seeding and shoulder formation, posing a major challenge for long-length bulk crystal growth. In this study, a dedicated automatic diameter-control (ADC) system was developed, and its application to β -Ga₂O₃ bulk single-crystal growth is reported

Experimental: β -Ga₂O₃ crystal growth was conducted using an OCCC system equipped with a water-cooled copper basket with a 150 mm diameter and an induction heating system with a 60 kW oscillator capacity. High-purity (99.999%) β -Ga₂O₃ powder was used as the starting material, and growth was performed in an air atmosphere. A β -Ga₂O₃(100) seed crystal was rotated at 2-5 rpm with a pulling rate of 1–4 mm/h.

Result: ADC system specialized for the OCCC method has been developed for the first time in the world. Smooth ADC step growth following the prescribed diameter was achieved from seeding through the shoulder, body, and tail parts, resulting in the successful growth of a bulk single crystal with a 30 mm diameter and 50 mm-long body. The dedicated ADC makes it possible to achieve crystal mass production in a way analogous to the conventional Cz method. Initial assessments using X-ray rocking curve (XRC) mapping of representative wafers confirm high crystallinity with narrow FWHM values across the surface, indicating minimal mosaicity. The crystallinity, including dislocation density and electrical properties of the grown crystals will be discussed in detail during the presentation.

[1] A. Yoshikawa et al., *Scientific Reports*, **14**, 1: 14881 (2024).

[2] K. Kamada et al., *Crystals* **2023**, **13**, 921.

[3] K. Kakimoto et al., *J. Cryst. Growth*, vol. 622, p. 127029 (2023).

*Author for correspondence: kitahara@fox-tech.co.jp

10:15am IWGO-TuM1-28 Development of High-Quality 4" β -Ga₂O₃ (010) Wafer via the VB Method, Yuki Yamamoto, Shigenori Shimizu, OXIDE, Japan; Kensuke Mizukoshi, Takashi Nishinoiri, Ceratec Japan Co., Ltd., Japan; Toshinori Taishi, Keigo Hoshikawa, Shinshu Univ., Japan

Most commercially available β -Ga₂O₃ wafers are grown by the edge-defined film-fed growth (EFG) method; however, circular wafers are limited to the (001) or (201) orientations. In contrast, the vertical Bridgman (VB) method enables the growth of circular wafers with (100), (010), and (001) orientations, and the growth of 4-inch-diameter single crystals has been reported. In this study, Fe-doped [010] β -Ga₂O₃ single crystals with a

8:00 AM

Tuesday Morning, August 4, 2026

diameter of 4 inches were grown by the VB method. The obtained crystals were sliced and polished to fabricate (010)-oriented wafers. X-ray topography and X-ray rocking curve measurements were carried out for evaluation. The grown crystal exhibited a constant-diameter region of 30 mm without twins or cracks. A 500 μm thick wafer was obtained by slicing and polishing. Although wafer warpage was observed after single-side polishing. The warpage was reduced after double-side polishing. The full width at half maximum obtained from X-ray rocking curve measurements was approximately 15 arcsec. Reflection X-ray topography showed diffraction contrast over the entire wafer area, indicating that the wafer is free from not only twins and cracks but also low angle grain-boundaries.

International Workshop on Gallium Oxide and Related Materials (IWGO-6)

Room ESJ 0202 - Session IWGO-TuM2

Substrate Development and Material Quality II

Moderators: Zbigniew Galazka, Leibniz Institute for Crystal Growth, Kohei Sasaki, Novel Crystal Growth

11:00am **IWGO-TuM2-37 Defect Complexes and β -to- γ Phase Boundaries in Si-implanted Ga_2O_3** , Naomi Pieczulewski, Katie Gann, Cornell University; Thaddeus Asel, Brenton Noesges, Air Force Research Laboratory, Materials and Manufacturing Directorate, USA; Michael Thompson, David Muller, Cornell University

INVITED

Multislice electron ptychography is used to resolve the three-dimensional atomic structure of Si-implanted $\beta\text{-Ga}_2\text{O}_3$, containing both transformed β -phase and residual γ -phase, enabling direct characterization of defect structures and β - γ phase boundary. We provide the first three-dimensional experimental evidence of interstitial-vacancy complexes in $\beta\text{-Ga}_2\text{O}_3$. Analysis of the β -to- γ phase transformation reveals a shared oxygen sublattice that facilitates localized transformation by a continuous transformation or a martensitic-like transition. Experimental evidence shows gradual displacement of Ga atoms can evolve into ordered interstitial defect chains forming $\gamma\text{-Ga}_2\text{O}_3$ through a static oxygen sublattice, indicating a continuous transformation. This relationship is described by a coincidence lattice, from which a structural model of the γ -phase is constructed. Additionally, we identify implant-damaged regions where we observe dislocation formation and lattice strain of the oxygen sublattice, indicating a non-continuous mechanism. By overcoming the limitations inherent to conventional scanning transmission electron microscopy, multislice electron ptychography directly resolves the β - γ crystallographic relationship at the nanoscale, providing critical experimental insight into defect-mediated phase evolution in Ga_2O_3 .

11:25am **IWGO-TuM2-42 Thulium-doped Gallium Oxide Scintillators: Growth and Characterization**, Marko Tadjer, Lee Mitchell, Naval Research Laboratory; Robert Lavelle, Pennsylvania State University Applied Research Laboratory; Alex Lebedinsky, University of Houston; Darshana Wickramaratne, Evan Glaser, Naval Research Laboratory; Katie Gann, Tia Gray, National Research Council; Alan Jacobs, James Spencer Lundh, Steven Bennett, Naval Research Laboratory; Matthew Krohn, Pennsylvania State University Applied Research Laboratory; Bernard Philips, Naval Research Laboratory; Kumar Saurabh, P. Shiv Halasyamani, University of Houston; Karl Hobart, Naval Research Laboratory

Versatility in melt growth capabilities for $\beta\text{-Ga}_2\text{O}_3$ provide not only for excellent material availability but also for a wide range of dopants in these crystals including shallow donors such as Si and Ge, deep donors and acceptors, and other rare earth dopants investigated for applications such as neutron detectors and scintillators [1, 2]. In this work, we report float zone (FZ) growth of rare earth thulium (Tm) doped $\beta\text{-Ga}_2\text{O}_3$. Whereas Tm-doped $\beta\text{-Ga}_2\text{O}_3$ deposition has been reported via several techniques (e.g., PLD), single-crystal growth of Tm-doped $\beta\text{-Ga}_2\text{O}_3$ has not been reported [3, 4].

The crystal growth was performed in an optical FZ furnace (Crystal Systems Co.). O_2 was flowed through the chamber at a rate of 50 mL/min at a pressure of 3.5 bar. The feed and seed rods were rotated in opposite directions at a rate of 15 rpm, and the growth rate was 5.0 mm/h. The entire crystal growth process took approximately 11 hours. FZ $\beta\text{-Ga}_2\text{O}_3$ crystal dimensions were about 11.6 mm in diameter and 57.6 mm in length, reproduced over several growths to-date with good repeatability. This method was used to grow crystals of Tm-doped Ga_2O_3 with a Tm concentration of up to 1%. Here, we show a 0.01% Tm doped crystal (0.0206g of Tm_2O_3 in 100g of Ga_2O_3). The Tm concentration of 10^{19} cm^{-3} was

measured via X-ray fluorescence and further quantified via SIMS. Prior to slicing, the Tm-doped $\beta\text{-Ga}_2\text{O}_3$ boule was mounted on a three-axis goniometer and oriented for slicing into (010) samples. The orientation of the boule was corrected by modifying the goniometer axes to align with the (010) Laue reference. After final chemical-mechanical polishing (CMP), the surface topography of the substrates was evaluated via optical profilometry. The substrates were also characterized by high-resolution XRD by collecting (020) X-ray rocking curves. First-principles calculations were also performed, confirming Tm acts as a deep donor in $\beta\text{-Ga}_2\text{O}_3$. EPR spectroscopy confirmed these samples were conductive via the unintentional incorporation of Si shallow donors. The double numerical integration of the Lorentzian EPR line shapes yields a concentration of uncompensated shallow donors (i.e., $N_D - N_A$) of $8 \times 10^{16} \text{ cm}^{-3}$. Scintillation counts were obtained from one sample using various radioactive sources. Characteristic gamma rays from low energy isotopes such as Am-241 (59.5 keV), Cd-109 (88 keV), and Co-57 (122 keV) were easily observed. Further details will be presented at the workshop.

[1] C. Prasad et al., Mater. Today Phys. **35**,101095 (2023).

[2] D. Valdes et al., APL Mater. **13**, 041116 (2025).

[3] Q. Guo et al., Thin Solid Films **639**, 123 (2017).

[4] Z. Chen et al., Appl. Phys. Expr. **14**, 081002 (2021).

11:40am **IWGO-TuM2-45 Growth of $\beta\text{-Ga}_2\text{O}_3$ Crystals by Piling-Down EFG Method with a Raw Material Supply System**, Yuki Ueda, Novel Crystal Technology Inc., Japan; Kimiyoshi Koshi, Sho Hasegawa, Kohei Sasaki, Akito Kuramata, Novel Crystal Technology, Inc., Japan

We have successfully commercialized 4-inch $\beta\text{-Ga}_2\text{O}_3$ single-crystal substrates and demonstrated the feasibility of 6-inch substrates using the edge-defined film-fed growth (EFG) method. However, increases in crystal diameter and length require larger and more expensive iridium (Ir) crucibles to accommodate the greater volume of raw materials, posing a significant cost challenge. Therefore, to reduce the total Ir required for crystal growth, we have developed a novel EFG method based on a pulling-down growth technique with continuous feeding of raw materials. In this study, we attempted to use the developed method to grow approximately 2-inch $\beta\text{-Ga}_2\text{O}_3$ crystals.

A droplet of Ga_2O_3 melt supplied onto the die passed through a slit formed in the die and subsequently reached the seed crystal. Crystal was grown at a pulling-down rate of approximately 10 mm/h in a mixed N_2/O_2 atmosphere (2 vol% O_2) with continuous feeding of raw materials. As a result, an approximately 2-inch $\beta\text{-Ga}_2\text{O}_3$ crystal was successfully obtained. The full width at half maximum (FWHM) of the x-ray rocking curve (XRC) 002 peak for a {001} sample prepared from the crystal center was 27 arcsec, comparable to that of conventional EFG crystals. On the other hand, x-ray diffraction (XRD) measurements of the {010} samples revealed that the crystallinity deteriorates as growth proceeds. This may be attributed to the temperature gradient increasing inside the furnace during growth.

11:55am **IWGO-TuM2-48 Redefining $\beta\text{-Ga}_2\text{O}_3$ Smart Cut™ Through Optimized Ion Implantation**, Adrien Roth, Guillaume Gelineau, Lucas Colonel, Frédéric Mazen, Frédéric Milési, Florence Madeira, Nicolas Troutot, CEA-Leti, France; David Eon, CNRS, France; Julie Widiez, CEA-Leti, France

Wide bandgap semiconductors are widely used for high-efficiency power electronics, but their bulk crystal growth remains costly and energy-intensive [1]. In this context, $\beta\text{-Ga}_2\text{O}_3$ has emerged as a promising alternative thanks to its ability to be grown from a liquid phase [2]. However, its very low thermal conductivity ($0.15 \text{ W}\cdot\text{cm}^{-1}\cdot\text{K}^{-1}$) strongly limits heat dissipation, hindering the widespread adoption of Ga_2O_3 -based power devices in industry [3]. To address this limitation, we investigate the transfer of (001)-oriented $\beta\text{-Ga}_2\text{O}_3$ layers, leveraging the availability of large-area (4-inch) substrates for process development, whereas prior studies mainly focused on the 2-inch (-201) orientation [4-7]. The process based on the Smart Cut™ technology, consists of implanting the bulk substrate with light ions, bonding it to the carrier substrate, and performing a fracture annealing that leads to the transfer [8].

First, we investigate the blistering process in $\beta\text{-Ga}_2\text{O}_3$, a necessary preliminary step to confirm the possibility of achieving Smart Cut™. Then, we perform fracture tests on the samples, replacing the carrier substrate with a $4\mu\text{m}$ SiO_2 deposited layer, which acts as a stiffener for the layer transfer. In this study, we compare three ion implantation conditions: He^+ , H^+ and an optimized H^+ implantation process. All three types of implantations resulted in blistering of $\beta\text{-Ga}_2\text{O}_3$. However, the optimized H^+ implantation enables blistering at a lower implantation dose and annealing temperature than conventional H^+ implantation, while maintaining a higher

Tuesday Morning, August 4, 2026

crystalline quality than for He⁺ implantation. In terms of blister morphology, H⁺ implantation produces a high density of small-diameter blisters with few exfoliations and no coalescence. The other two types of implantations produce larger-diameter blisters with coalescence and exfoliations. These two ion implantation processes also allowed the fracture of a thin layer of β -Ga₂O₃ with transfer yields of 79 % of the sample surface for He⁺ implantation and 95 % for optimized H⁺ implantation.

This optimized condition, used in the Smart Cut™ process, enable the fabrication of the first

β -Ga₂O₃/ β -Ga₂O₃ homostructure on 4-inch (001) wafers, with a 97% transfer yield and 730nm transferred layer thickness. The presence of surface microdefects is under investigation to improve the subsequent heterostructure fabrication.

[1]Yeboah et al., Intell. Sustain. Manuf.,2025

[2]Huang et al., Eur. Phys. J. Spec. Top.,2025

[3]Kohei Sasaki, APEX 17,2024

[4]Xu et al., ACS Appl. Electron. Mater.,2022

[5]Cheng et al.,2020

[6]Shen et al., Sci. China Mater.,2023

[7]Liao et al., ECS Trans., Vol. 112,2023

[8]Widiez et al., Vol. 223,2025

12:10pm IWGO-TuM2-51 HCl-based Halide Vapor Phase Epitaxy and HCl Gas Etching on (-112) β -Ga₂O₃ Substrates, Takayoshi Oshima, Yuichi Oshima, NIMS, Japan

We investigated the (-112) orientation—which is perpendicular and close to the (100) and (011) planes, respectively and corresponds to the fundamental {100} planes of the fcc oxygen sublattice in β -Ga₂O₃ [1]—as a novel platform for homoepitaxial growth and plasma-free gas etching.

Homoepitaxy was performed using HCl-based halide vapor phase epitaxy (HVPE). The resulting epilayer was single crystalline with tilt and twist spreads comparable to those of the substrate. Although slit-like pits sandwiched by vertical (100) facets—similar to those previously reported for epilayers grown on (011) substrates [2]—were observed on the surface, the pit-free regions exhibited a step-and-terrace morphology with a root-mean-square (RMS) roughness as small as 0.10 nm. Notably, the unintentional Cl impurity concentration in the epilayer was as low as $2 \times 10^{15} \text{ cm}^{-3}$, substantially lower than $1 \times 10^{16} \text{ cm}^{-3}$ observed in the layer simultaneously grown on a (001) substrate. Such atomically flat epitaxial surface and low Cl impurity incorporation are highly advantageous for device applications.

Selective-area HCl gas etching was conducted using a SiO₂ mask in the same HVPE system. The resulting etched structures reflected crystal anisotropy. The side etching was minimized when the mask windows were aligned along the [02-1] direction due to the formation of (100) facets with the lowest surface energy density. Along the trench direction, the (100) sidewalls were exceptionally flat and perfectly vertical. The vertical etch rate of the (-112) plane was approximately 50 times higher than the lateral etch rate of the (100) plane, enabling high-precision patterning of fin and trench structures.

This work was supported by ARIM (JPMXP1225NM5079),JSPS KAKENHI (JP24K01368), NEDO (No. JPNP22007).

[1] T. Oshima, Jpn. J. Appl. Phys. **65**, 038003 (2026).

[2] Y. Oshima and T. Oshima, Sci. Technol. Adv. Mater. **26**, 2585551 (2025).

Tuesday Afternoon, August 4, 2026

International Workshop on Gallium Oxide and Related Materials (IWGO-6)

Room ESJ 0202 - Session IWGO-TuA1

Heterogeneous Integration and other WBG and UWBG Oxides Beyond Ga₂O₃

Moderators: Andrew Green, AFRL, Man Hoi Wong, The Hong Kong University of Science and Technology

2:00pm **IWGO-TuA1-1 Heterogeneous Gallium Oxide Integration and Vertical Device Technology**, *Martin Kuball*, University of Bristol, UKINVITED
Gallium Oxide (Ga₂O₃) devices offer potential to outcompete SiC technology though have still to prove their true potential including device reliability. We demonstrate pathways to enable heterogenous Ga₂O₃ growth on alternative substrates including Si, furthermore challenges and solutions to overcome in vertical device technology, including mitigation of trap states for improve device reliability.

2:25pm **IWGO-TuA1-6 >10 kV Vertical NiO_x/(011) β-Ga₂O₃ HJDs with PFOM >2.3 GW/cm²**, *Yizheng Liu*, Carl Peterson, Chinmoy Saha, University of California at Santa Barbara; *Marko Tadjer*, Naval Research Laboratory; *Sriram Krishnamoorthy*, University of California at Santa Barbara

We report the fabrication and characterization of vertical NiO_x/β-Ga₂O₃ heterojunction diodes (HJDs) on 20-μm-thick/low-doped HVPE-grown (011) β-Ga₂O₃ with breakdown voltage beyond 10 kV, differential specific on-resistance ($R_{on,sp}$) at 43 mΩ·cm², and power figure of merit (PFOM) exceeding 2.3 GW/cm² on 60-μm dia. device. The parallel-plane breakdown electric field ($E_{Br,||}$) is extracted to be >5.3 MV/cm.

The NiO_x/(011) HVPE β-Ga₂O₃ HJD fabrication begins with a backside Ti/Au (50/350 nm) Ohmic metallization on n⁺ β-Ga₂O₃ bulk substrate using e-beam evaporation followed by a 60-seconds rapid thermal annealing (RTA) at 470 °C in N₂. A ~28 nm of p⁻ NiO_x is deposited on HVPE β-Ga₂O₃ drift region with a pre-patterned photoresist liftoff mask by optical lithography. Following the first layer NiO_x deposition, a self-aligned p⁺⁺ NiO_x (~20 nm) contact layer is reactively sputtered. Then, a Ni/Au/Ni (50/100/150 nm) anode cap/metal hard mask stack is deposited via e-beam evaporation. The fabricated HJDs are later dry-etched ~2 μm into the β-Ga₂O₃ drift region below the heterojunction interface using BCl₃ inductively coupled plasma (ICP) at 200 W for edge termination. A ~1.5-μm-thick SiO₂ field plate oxide is sputtered conformally on the HJDs, then a Ni/Au (50/300 nm) field plate metal stack with 20-μm edge extension (L_{FP}) is deposited on the oxide via e-beam evaporation to conclude the device fabrication.

The mesa-isolated/field plated (MI/FP) HJD with 60-μm dia. dimension shows rectifying behavior with an on/off ratio of 10¹⁰ and turns on at ~2 V forward bias with an on-state current density >60 A/cm². The capacitance-voltage (C-V) characteristics of the HJD reveals a built-in potential of 2.2 V and an average apparent charge density at 1.8×10¹⁵ cm⁻³. The 60-μm dia. device exhibits a breakdown voltage > 10 kV with a corresponding $E_{Br,||}$ >5.3 MV/cm. MI/FP HJDs with 100-μm dia. also exhibits breakdown voltages at 6.5-7.3 kV. The $R_{on,sp}$ of the 60-μm dia. device is at 43 mΩ·cm², giving rise to a PFOM > 2.3 GW/cm², which approaches the material limit of 4H-SiC. The HJDs across various diode dimensions (60-μm dia. to 1-mm dia.) show consistent $R_{on,sp}$ values which indicates that there is no current spreading and the extracted $R_{on,sp}$ is accurate. The pulsed current-voltage (I-V) measurements with <1% duty cycle show that the 1-mm dia. HJD accomplishes >1.5 A absolute current value at 9 V on thick and low-doped HVPE-grown β-Ga₂O₃, which is comparable to the I-V characteristics of co-fabricated Schottky barrier diode (SBD) counterpart, indicating that the vertical MI/FP HJD is able to fully exploit the on-state potential of the epitaxial drift region.

2:40pm **IWGO-TuA1-9 Semiconductor Properties of Epitaxial NiGa₂O₄ Spinel That Forms at Ga₂O₃/NiO Interfaces**, *Kingsley Egbo*, *Anna Sacchi*, *M. Brooks Tellekamp*, *Andriy Zakutayev*, National Laboratory of the Rockies

β-Ga₂O₃ is one of the most promising ultra-wide band gap semiconductor materials due to its combination of intrinsic semiconductor properties and manufacturing scalability. Considering the difficulties associated with p-type doping of β-Ga₂O₃, alternative strategies involving the heteroepitaxial growth of p-type oxide layers have been explored as potential substitutes. For example, the use of p-NiO contacts to β-Ga₂O₃ has led to a demonstration of vertical power diodes with breakdown voltages over 10 kV. Our recent work has shown that the NiO/Ga₂O₃ may become unstable above 400 °C temperature, leading to uncontrolled formation of NiGa₂O₄ at

the interface. Such high temperatures may be present due to intentional heating for NiO growth or unintentional hot spots during high-power operation, exacerbated by low thermal conductivity. However, the NiGa₂O₄ structure and properties remains relatively unknown due to the thinness of this naturally formed interphase.

This presentation will report on the intentional epitaxial growth and semiconductor properties of NiGa₂O₄ spinel layers that naturally form at Ga₂O₃/NiO interfaces used in electronic devices. Cubic spinel NiGa₂O₄ films of 10-50 nm thicknesses and low surface roughness (~ 2 nm) were grown using pulsed laser deposition at the α-Al₂O₃ and β-Ga₂O₃ substrate temperatures in the 300-900 °C. The optical absorption onset (3.6-3.9 eV) and thermal conductivity (4-9 W m⁻¹ K⁻¹) vary systematically with substrate temperature due to varying Ni and Ga cation ordering on the spinel lattice. The valence band offset between NiGa₂O₄ and β-Ga₂O₃ is determined to be 1.8 eV. The NiGa₂O₄-based p-n heterojunction devices on Ga₂O₃ (001) substrates with 10⁸ rectification ratio and 1.4 V turn-on voltage maintaining this diode behavior up to 600 °C operating temperature. These results highlight the potential of NiGa₂O₄ as a p-type interlayer to increase the performance and reliability of Ga₂O₃-based devices in high-power and high-temperature applications.

2:55pm **IWGO-TuA1-12 Breaking the 6 eV Barrier: Colossal Bandgap Electronics with Si Doped α-(Al_xGa_{1-x})₂O₃ by S-MBE**, *Debaditya Bhattacharya*, *Jacob Steele*, *Kazuki Nomoto*, *Naomi Pieczulewski*, Cornell University; *Preston Sorensen*, University of Nebraska - Lincoln; *Madhav Ramesh*, Cornell University; *Indika Senevirathna*, Clark Atlanta University; *Mathias Schubert*, University of Nebraska - Lincoln; *David Muller*, *Huili Grace Xing*, *Darrell Schlom*, *Debdeep Jena*, Cornell University

Establishing a new material as a viable semiconductor platform can be done by meeting three fundamental criteria: the demonstration of controllable doping with mobile carriers, a measurable bandgap, and the successful fabrication of rectifying junctions or observation of transistor action. In this work, we demonstrate that Si-doped α-(Al_xGa_{1-x})₂O₃ grown by suboxide molecular-beam epitaxy on sapphire fulfills these three criteria [1-3]. Hall effect measurements verify semiconductor behavior through controllable n-type conduction. Vacuum UV ellipsometry confirms a channel bandgap of 6.71

Leveraging this platform, we realize the first CBG “AlphaDiodes” and “AlphaFETs.” The diodes exhibit an on-off ratio > 10⁷ and a lateral breakdown field of ~12 MV/cm - among the highest values recorded for any semiconductor. The Pd-gated AlphaFETs demonstrate enhancement-mode (normally-off) operation with a threshold voltage of ~1 V, proving that the channel potential can be effectively modulated via electrostatic gating despite the extreme bandgap. While current density is currently limited by contact and access resistance at the regrown interfaces, the combined evidence of Hall transport, optical bandgap, and transistor action establishes α-(Al_xGa_{1-x})₂O₃ as a practical platform for high-voltage, high-efficiency electronics.

Crucially, this platform utilizes m-plane sapphire substrates. Sapphire offers a unique trifecta of benefits: it is an abundant, low-cost material produced at a massive industrial scale (with crystals reaching diameters up to 640 mm) [4], and its high structural quality allows for the growth of high-purity epitaxial layers. By achieving these device milestones on a native, readily available substrate, we break the historical bottleneck of small-scale, high-cost synthesis that has previously hindered ultra-wide bandgap materials like diamond and c-BN, providing a clear path for the scalable adoption of colossal bandgap semiconductors.

[1] Steele, J., et al. (2025). *APL Materials*, 13, 101117

[2] Steele, J., et al. (2024). *APL Materials*, 12, 041113

[3] Jinno, R., et al. (2021). *Science Advances*, 7, eabd5891

[4] Kang Sen, et al. (*J. Synth. Cryst.*), 50, 1397–1401 (2021)

3:10pm **IWGO-TuA1-15 Thin-Film β-Ga₂O₃ Composite Substrates for Thermal Management Solutions**, *Michael Liao*, APEX Microdevices; *Mark Goorsky*, University of California Los Angeles; *Piyush Shah*, APEX Microdevices

We demonstrate successful fabrication of single-crystalline β-Ga₂O₃ composite substrates on either 4H-SiC or diamond for thermal management of high-power electronic devices. Direct wafer bonding, without the use of bonding interlayers, at room temperature with ~kPa of applied pressure is employed to heterogeneously integrate β-Ga₂O₃. Prior to bonding, β-Ga₂O₃ substrates are implanted with light-atoms to induce exfoliation and transfer of single-crystalline β-Ga₂O₃ films to a handle substrate such as 4H-SiC and diamond upon annealing. Leveraging our

previous efforts on β -Ga₂O₃ exfoliation [1-3] and CMP [4], we continue to improve and expand key processing steps towards pristine thin-film β -Ga₂O₃ composite substrates for different β -Ga₂O₃ orientations including, but not limited to, (001), (010), and (100). We also develop post-bond wafer-stock removal (lapping and polishing) processes for achieving β -Ga₂O₃ composite substrates that require thicker β -Ga₂O₃ films that currently may not be commercially feasible via ion implantation (i.e., > 1 MeV). Thermal transport measurements comparing bulk β -Ga₂O₃ vs composite substrates subjected to the same heating conditions show a ~5 \times lower temperature rise and an effective thermal conductivity ~5 to ~10 times higher than bulk β -Ga₂O₃ depending on the film thickness. Thermal boundary conductance values for the β -Ga₂O₃|4H-SiC and β -Ga₂O₃|diamond interfaces are ~120 MW/(m²K) and ~75 MW/(m²K), respectively, which are on the same order achieved via β -Ga₂O₃ heteroepitaxy reported in the current literature. Unlike heteroepitaxy, which limits the β -Ga₂O₃ orientation typically to twinned (201) or polycrystalline depending on the substrate, wafer bonding bypasses limitations associated with heteroepitaxy to achieve structures with control over material combination and crystal orientation without sacrificing crystalline quality. To test robustness, thermal cycling of our β -Ga₂O₃ composite substrates from room temperature up to 1000 °C show no degradation in the thermal transport across the interface. Subsequent homoepitaxial growth of device layers on these composite substrates will be presented.

The authors acknowledge the support from Air Force SBIR Phase II program. TPOC Dr. Thaddeus Asel.

References

- [1] M. E. Liao, et al., ECS J. Solid State Sci. Technol., 8(11), P673 (2019).
- [2] M. E. Liao, et al., J. Vac. Sci. Technol. A, 41, 063203 (2023).
- [3] M. E. Liao, et al., ECS Trans., 112(3), 269 (2023).
- [4] M.E. Liao, et al., J. Vac. Sci. Technol. A, 41, 013205 (2023).

International Workshop on Gallium Oxide and Related Materials (IWGO-6)

Room ESJ 0202 - Session IWGO-TuA2

Defects Science III & Thermal Management

Moderators: Martin Kuball, University of Bristol, Heather Splawn, KYMA TECHNOLOGIES, INC.

3:55pm **IWGO-TuA2-24 Conductive Al₂O₃ with Ohmic Contacts via Ion Implantation**, Alan Jacobs, Katie Gann, James Lundh, Daniel Pennachio, Darshana Wickramaratne, Karl Hobart, Michael Mastro, Naval Research Laboratory

Interest in β -Ga₂O₃ and β -Al_xGa_(2-x)O₃ has been driven by both the ultra-wide bandgap, enabling step-change improvements in device figures of merit, as well as the availability and scalability of melt-grown oxide substrates. Recent interest has extended this regime into α -Al_xGa_(2-x)O₃ for bandgap tunability toward the ultimate potential of α -Al₂O₃ at nearly 9eV. Here we report on generation of conductive Al₂O₃ via ion implantation with ohmic contacts and low thermal activation energy of resistivity suggesting a shallow dopant or impurity band conduction.

Conductive α -Al₂O₃ has been previously reported with silicon doping by both ion implantation and growth by MBE[1-2]. Reported as-grown conductivity was minimal but increased to ~0.1mA at 100V after annealing at 1400°C. Reports of ion implanted samples exhibited conductivity ~1 μ A at 100V after annealing at 1300°C, which reduced at higher anneal temperatures.

Here, bulk sapphire wafers were blanket implanted with silicon, or silicon and oxygen at doses of 1.08 \times 10¹⁵ and 1.62 \times 10¹⁵ cm⁻² respectively, with oxygen intending to maintain stoichiometry. As-implanted, the silicon doped material exhibited a faint coloration by eye while co-implanted material appeared slightly darker. After annealing in N₂ or Ar ambient at 1000°C for 10 minutes, the material darkened, whereas material annealed in vacuum turned transparent. Samples had Ti/Au (20/200nm) contacts with isolation regions formed by Ar/Cl reactive ion etch. Isolation current across a trench remained at the noise floor of ~10 fA up to 10 V.

Linear transmission-line measurements of silicon doped films exhibit sheet and specific contact resistances of 206 k Ω /□ and 3.8 \times 10⁻⁴ Ω cm⁻² respectively. Films co-doped with both silicon and oxygen were measured at 75.0 k Ω /□ and 7.5e \times 10⁻⁵ Ω cm⁻² respectively. Van der Pauw

measurements taken at up to 500°C exhibit a low activation energy of ~57 meV. Thermal activation may exhibit two regimes: low temperature (100-400°C) at 49 meV and a high temperature regime (400-500°C) at 90 meV warranting further investigation. Van der Pauw measurements of unimplanted material exhibits no measurable current until high temperatures, exceeding 120 G Ω /□ until ~800°C and exhibiting a high thermal activation energy of ~1.31 eV from 800-950°C. X-ray diffraction shows strain recovery and significant reduction of gross point defect populations after annealing at 1000°C.

[1] Hironori Okumura 2022 *Jpn. J. Appl. Phys.* **61** 125505. DOI: 10.35848/1347-4065/aca196

[2] Hironori Okumura et al. 2021 *Jpn. J. Appl. Phys.* **60** 106502. DOI: 10.35848/1347-4065/ac21af

*Author for correspondence: alan.g.jacobs3.civ@us.navy.mil

4:10pm **IWGO-TuA2-27 In-Situ X-Ray Topography Observation of Behavior of Dislocations in β -Ga₂O₃(001) Schottky Barrier Diode During Applying Voltage**, Daiki Katsube, Japan Fine Ceramics Center, Japan; Yongzhao Yao, Mie University, Japan; Daiki Wakimoto, Hironobu Miyamoto, Kohei Sasaki, Akito Kuramata, Novel Crystal Technology, Japan; Yukari Ishikawa, Japan Fine Ceramics Center, Japan

In the next-generation power semiconductor β -Ga₂O₃, the impact of dislocations on device performance remains unclear, and understanding dislocation behavior during device operation is a critical issue. In this study, we performed in-situ observation of dislocation behavior in a β -Ga₂O₃(001) Schottky barrier diode (SBD) under applied voltage using in-situ X-ray topography (XRT) technique.

Monochromatic X-rays (11.27 keV, KEK-PF) were used to conduct in-situ XRT observations of a β -Ga₂O₃(001) SBD device during applying voltage. The SBD had a vertical device structure with voltage applied between the surface and backside electrodes. In-situ XRT observations were performed in a reflection geometry from the surface electrode side of the SBD. The diffraction condition $g = 316$, which enables observation of all in-plane dislocations, was employed.

Figure 1 shows the XRT image of the SBD. To enable reflection XRT observation of dislocations within the device, the surface electrode (region outlined by yellow lines) was fabricated with a thickness of 100 nm, thinner than that of a conventional SBD. In contrast, the electrode pad (indicated by a blue circle) was deposited with a conventional electrode thickness (approximately 1 μ m). Voltage was applied to the electrode pad through wiring that appears as black shadow-like lines in the image, connected to the surface electrode. The white and black lines visible in the image correspond to dislocations present in the SBD. During applying voltage, in-situ observation revealed that dislocations moved. Among the dislocations moving, most of them were located near the thin film electrode edge, and moved toward the thin film electrode edge.

4:25pm **IWGO-TuA2-30 Killer Defects in (011) HVPE-Grown β -Ga₂O₃ Schottky Barrier Diodes Studied by Synchrotron X-ray Topography and Emission Microscopy**, Masanori Eguchi, Synchrotron Light Application Center, Saga University, Japan; Shotaro Nakaniwa, Makoto Sato, Niloy Chandra Saha, Department of Electrical and Electronic Engineering, Saga University, Japan; Chia-Hung Lin, Kohei Sasaki, Novel Crystal Technology, Japan; Makoto Kasu, Department of Electrical and Electronic Engineering, Saga University, Japan

β -gallium oxide (β -Ga₂O₃) possesses an ultra-wide bandgap of 4.8 eV and a high breakdown field of 8 MV/cm. Therefore, it is expected to become a promising material for high-power, highly efficient electronic devices. However, crystal defects, so-called killer defects in β -Ga₂O₃, cause reverse leakage current and lower off-state breakdown voltage in Schottky barrier diodes (SBDs). The (011) surface was reported to exhibit lower defect density than the (001) surface. Therefore, in this study, we elucidate the killer defects in (011) β -Ga₂O₃ SBDs and find that microcracks along the [100] direction are killer defects.

4:40pm **IWGO-TuA2-33 Impact of Bias Dependent Joule Heating on Gallium Oxide Lateral Transistors via Deep UV Thermal Imaging**, Dominic Myren, University of Connecticut; Daniel Dryden, Air Force Research Laboratory; Cameron Gorsak, Hari Nair, Cornell University; Ahmad Islam, Andrew Green, Air Force Research Laboratory; Georges Pavlidis, University of Connecticut

As Gallium Oxide (Ga₂O₃) lateral transistors are advanced toward high-voltage and high-power switching regimes, self-heating driven by bias-dependent Joule dissipation emerges as a critical limitation to performance and reliability. In contrast to established Gallium Nitride technology, the

Tuesday Afternoon, August 4, 2026

relatively low thermal conductivity of Ga₂O₃ exacerbates localized thermal accumulation, particularly under non-uniform electric field distributions. This work experimentally investigates the impact of bias conditions on the Joule heating profile in lateral Ga₂O₃ transistors [1] and captures the transient evolution of thermal hotspots across operational regimes relevant to high power electronics.

Direct mapping of the Ga₂O₃ channel temperature is not trivial when leveraging traditional methods for thermal characterization.[2] Due to its inherent wide band gap (≈ 4.6 eV), optical techniques require probing wavelengths in the Deep Ultraviolet (DUV) range to directly measure the surface temperature. Any sub-bandgap excitation will result in depth averaged temperature measurements that extend into the Gallium oxide substrate and underpredict the peak temperature. While nanoparticle Raman thermometry can overcome this challenge, it is a point measurement which features low throughput for channel thermal mapping. This study presents a newly developed DUV wide field thermoreflectance imaging microscope that can transmit wavelengths down to 260 nm with sub-micron spatial resolution and a 50 \times objective.

The gate voltage is varied from partially depletion (-3.5 V) to fully open channel conditions (0 V). In parallel, the drain voltage is adjusted to match the same average power density across the device. Pronounced thermal confinement is observed near the gate (56% elevated peak temperature rise when increasing the drain voltage from 10 to 21.5 V). These findings establish a direct correlation between bias-dependent electric field profiles and transient thermal behavior in gallium oxide devices. The study underscores the necessity of incorporating electro-thermal co-design strategies, including field management and device geometry optimization, to mitigate localized overheating. Deep UV thermal imaging proves to be a powerful diagnostic tool for resolving nanoscale thermal phenomena in ultra-wide bandgap semiconductors, providing critical insight into reliability challenges as gallium oxide transistors are scaled toward next-generation high-power applications. [1] D. M. Dryden et al., APL Electronic Devices 2, 026108 (2026) [2] D. Myren et al., Appl. Phys. Lett. **126**, 200502 (2025).

4:55pm **IWGO-TuA2-36 Engineered Substrates for Ga₂O₃ Vertical Power Devices**, *Caroline Reilly*, Kyma Technologies, Inc.; *Sean O'Leary*, Modern Microsystems, Inc.; *Emma Rocco*, US Naval Research Laboratory; *Craig McGray*, Modern Microsystems, Inc.; *Marko Tadjer*, *Karl Hobart*, US Naval Research Laboratory; *Heather Splawn*, *Jacob Leach*, Kyma Technologies, Inc. The ability of Ga₂O₃ to handle thermal loads has been questioned due to its relatively low thermal conductivity. While it has yet to be seen what thermal problems arise in high voltage power switching applications, parallel efforts to mitigate this risk include packaging solutions and approaches such as engineered substrates. Engineered substrates have been developed for other semiconductors (i.e. SOI, QST™, SmartSiC™) and provide performance and/or supply chain benefits over bulk substrates. In the case of Ga₂O₃, using SiC as an underlying carrier wafer could reduce substrate thermal resistance by 50x. While efforts have shown the feasibility of Ga₂O₃-SiC composite wafers, this work seeks to prepare Ga₂O₃-SiC composite wafers for high voltage vertical Ga₂O₃ devices. Beyond the primary goal of a thermally conductive substrate, this application necessitates additional considerations towards interface electrical conductivity and the ability to grow Ga₂O₃ on the engineered substrate.

Bonding of 2" Ga₂O₃ to n-type 100mm SiC has been conducted utilizing interlayers expected to be both thermally and electrically conductive, such as n-Si, TiN_x, and ITO. As-bonded wafers have shown areal yields of >80%, with thinned composite wafers having 60% or greater areal yields. Polished composite wafer coupons have been prepared with remaining Ga₂O₃ thicknesses $\sim 2\mu\text{m}$ and surface roughness < 1 nm. Interface thermal resistances of ~ 23 m²K/GW have been measured, such that the interface provides a negligible thermal barrier. Electrical conductivity measurements through full-thickness bonded Ga₂O₃-SiC wafers indicate that ITO is a promising interlayer, providing significantly less resistance than alternatives. Initial growth results on composite wafers have produced layers with similar roughness as those grown on bulk Ga₂O₃. More details on the composite wafer preparation, electrical and thermal conductivity, and growth results will be presented at the conference.

Acknowledgements

This technology was primarily supported by the Microelectronics Commons Program, a DoW initiative, under award number N00164-23-9-G059. The funders had no role in study design, data collection or analysis, or preparation of the manuscript.

Tuesday Evening, August 4, 2026

International Workshop on Gallium Oxide and Related Materials (IWGO-6)

Room Concourse - Session IWGO-TuP

IWGO Poster Session II

Moderator: Nidhin Kurian Kalarickal, Arizona State University

IWGO-TuP-1 Observation of the 2 eV Defect in Nitrogen Doped Ga₂O₃ by DLTS, Jian Li, Core4ce LLC; Brenton Noesges, Prescott Evans, Air Force Research Laboratory, Materials and Manufacturing Directorate, USA; Jacob Breakfield, Zach Weber, Nolan Hendricks, Andy Green, Air Force Research Laboratory; Adam Neal, Tadj Asel, Shin Mou, Air Force Research Laboratory, Materials and Manufacturing Directorate, USA

We demonstrate that the deep-level transient spectroscopy (DLTS) technique (conventional capacitance mode, samples in the dark) can routinely detect and characterize defects with activation energies >1 eV under judiciously selected experimental conditions in the temperature-rate space. Our DLTS results (Figure 1) are comparable to previous work [1], where the ~2.0 eV defect in nitrogen-implanted *b*-Ga₂O₃ was observed only by deep-level optical spectroscopy (DLOS) but not by DLTS of which conditions were less tuned towards detecting large activation energies. This augmented DLTS capability could enable full-bandgap defect study of general wide-bandgap semiconductors (e.g., GaN and SiC with E_g~3.3 eV) and is particularly relevant to understanding the effects of compensating acceptors in *b*-Ga₂O₃, whose activation energies are often large.

We apply this DLTS capability to investigate various species and preparation methods of compensating acceptors in *b*-Ga₂O₃ (e.g., N and Fe, ion implantation with various annealing conditions vs *in situ* doping) which are necessary for the optimization of semi-insulating substrates, buffers, and blocking layers critical to device behaviors such as breakdown, dynamics, and dispersion.

IWGO-TuP-2 Cathodoluminescence Study of Rutile GeO₂ Grown via Mist CVD, Kazuki Shimazoe, Shota Ishiyama, Nagoya Institute of Technology, Japan; Kazutaka Kanegae, Hiroyuki Nishinaka, Kyoto Institute of Technology, Japan; Masashi Kato, Nagoya Institute of Technology, Japan

Ultrawide bandgap (~4.6 eV) rutile germanium dioxide (*r*-GeO₂) has attracted significant attention as a high-power switching device material owing to its large breakdown field (~7 MV/cm) and ambipolar doping ability. Schottky barrier diode and transistor operations have been reported using *r*-GeO₂ thin films and bulk substrates, respectively [1,2]. Defect characterization is essential for achieving reliable device operation. Cathodoluminescence (CL) is powerful technique to examine defect-related luminescence in wide bandgap semiconductors. This study investigated CL properties of GeO₂ thin films to understand the defects.

Mist chemical vapor deposition (CVD) was utilized for growth of GeO₂ thin films. (001) TiO₂ was used as the growth substrate. Graded Ge_xSn_{1-x}O₂ buffer layers were inserted to grow single-phase *r*-GeO₂. The details of the graded buffer layer have been reported elsewhere [3]. Figure 1 shows the CL spectra of *r*-GeO₂ grown on a graded Ge_xSn_{1-x}O₂ buffer layer, along with the spectrum of the graded buffer layer alone for comparison. Luminescence peaks attributed to *r*-GeO₂ were observed around 2.2, 3.8, and 4.4 eV. The peak around 2.2 eV is close to the peak attributed to oxygen deficient centers [4]. The luminescence around 4.4 eV is relatively close to the bandgap of *r*-GeO₂ (~4.6 eV) although its transition is forbidden. One possibility is luminescence originating from isoelectronic traps associated with carbon impurities derived from the mist CVD precursor (C₆H₁₀Ge₂O₇). The incorporation of carbon into *r*-GeO₂ was confirmed by energy dispersive X-ray spectroscopy. Another possibility is that non-ideal crystallinity, such as defects or strain in the film, breaks the selection rules, thereby enabling forbidden transition to be observed. In the presentation, we will discuss more detailed CL results using temperature dependent spectra.

[1] K. Kanegae, et al., Appl. Phys. Express 18 041001 (2025). [2] K. Tetzner, et al., IEEE Electron Device Lett., 47, 566-569(2026). [3] K. Shimazoe, et al., Appl. Phys. Express 17, 105501 (2024). [4] H.-J. Fitting, et al., J. Non-Cryst. Solids 279, 51-59 (2001).

*Author for correspondence: shimazoe.kazuki@nitech.ac.jp

IWGO-TuP-3 Temperature Dependent Switching Characteristics of p-NiO/β-Ga₂O₃ Heterojunction Mosfets Under Cryogenic Conditions, Joonhui Park, Taejun Park, Yusup Jung, Taiyoung Kang, Sinsu Kyoung, PowerCubeSemi. Inc., Republic of Korea

The development of power semiconductor devices capable of reliable operation under cryogenic conditions is increasingly important for extreme-Tuesday Evening, August 4, 2026

environment applications such as deep-space electronics, cryogenic sensing, and quantum technologies. β-Ga₂O₃, with its ultra-wide bandgap (~4.8 eV) and high critical electric field (~8MV/cm), has emerged as a promising material for next-generation high-voltage power electronics. However, the switching characteristics of β-Ga₂O₃-based transistors under cryogenic conditions remain insufficiently understood.

In this work, a β-Ga₂O₃ heterojunction field-effect transistor (HJ-FET) incorporating a p-type NiO gate layer was fabricated to form a p-n heterojunction on an n-type β-Ga₂O₃ channel. Temperature-dependent electrical characteristics were systematically investigated from room temperature to cryogenic temperatures (~-160 °C). As temperature decreased, the drain current gradually decreased and the threshold voltage shifted positively due to carrier freeze-out in the β-Ga₂O₃ channel. Meanwhile, the subthreshold slope improved from 224 mV/dec at room temperature to approximately 100~117 mV/dec under cryogenic conditions, accompanied by a significant enhancement in the on/off current ratio from ~10⁵ to ~10⁹. Despite the presence of gate leakage at low temperatures, the device maintained clear switching behavior with stable gate modulation.

These results demonstrate the feasibility of β-Ga₂O₃ heterojunction MOSFETs operating under cryogenic environments and provide insight into the low-temperature switching behavior of β-Ga₂O₃ power devices for extreme-environment electronic applications

IWGO-TuP-4 Influence of Sapphire Substrate Orientation on Epitaxial Rutile GeO₂ Thin Film Solar-Blind Photodetector Properties, Eriks Dipsans, Edvards Strods, Sven Oras, Annamarija Trausa, Jevgenijs Gabrusenoks, Edgars Butanovs, Institute of Solid State Physics, University of Latvia

Rutile GeO₂ (*r*-GeO₂) has recently emerged as a promising ultrawide-bandgap (E_g~4.7 eV) semiconductor due to its potential use as a solar-blind UV-C range photodetector and its theoretically predicted ambipolar doping, which implies unique device fabrication possibilities. However, producing phase pure *r*-GeO₂ still remains challenging due to many unknown variables both in substrates and deposition methods [1]. In this work, pulsed laser deposition process for *r*-GeO₂ thin film growth on a-, m- and r-plane sapphire substrates was demonstrated in 350 – 425 °C temperature range, and film crystallinity and morphology optimization was performed. X-ray diffraction (XRD), X-ray photoelectron spectroscopy, scanning and transmission electron microscopies, atomic force microscopy (AFM), Raman spectroscopy and ellipsometry were used for the as-grown film characterization. XRD analysis revealed that (101)-orientated *r*-GeO₂ films were obtained on a- and r-plane sapphire substrates, while (002) orientation for m-plane substrate was observed. At optimized deposition conditions for each substrate orientation, XRD omega scan peak full width at half maximum and root mean square AFM surface roughness scan yielded results of 0.66°/5.1 nm, 0.50°/2.7 nm and 1.20°/6.9 nm for a-, m- and r-plane substrates, respectively. Furthermore, photodetector devices fabricated on these films exhibited peak responsivities 1.76 mA/W, 1600 mA/W and 5.77 mA/W for a-, m- and r-plane substrates, accordingly. It was observed that the responsivity peak wavelength at 220-230 nm for all the prepared films corresponds to a value significantly larger than the optical bandgap, which merits to be investigated further.

IWGO-TuP-5 Effect of Unintentional Si Impurities on F-doped β-Ga₂O₃ Thin Films Grown by Mist CVD, Ichiro Seike, Kyoto Institute of Technology, Japan; Hiroki Miyake, MIRISE Technologies Corporation, Japan; Hiroyuki Nishinaka, Kyoto Institute of Technology, Japan

Controlling carrier concentration by doping is important for device applications of β-Ga₂O₃, which has attracted attention as a next-generation power device material. Si, Ge, and Sn have been actively studied as n-type dopants substituting the Ga site. However, there have been few experimental reports on F substituting the O site, even though theoretical calculations suggest that F is a shallow donor. Establishing the Osite doping technology in β-Ga₂O₃ is important because it may be possible to further improve conductivity by dual doping, which has been reported in ZnO and SnO₂. In this study, we report on the effect of unintentional Si impurities in F-doped β-Ga₂O₃ thin films.

Figure 1(a) and (b) show the concentration of incorporated elements in F-doped β-Ga₂O₃ thin films grown using a quartz and an alumina tube in the reaction chamber, respectively. In the case where the quartz tube is used, Si concentration in the thin film is about 2×10²⁰ cm⁻³, which is much larger than the F concentration of about 2×10¹⁸ cm⁻³. Since the carrier concentration calculated from Hall effect measurement at room temperature is 1.3×10²⁰ cm⁻³, it is suggested that Si contributes as a donor. This is considered to be due to the incorporation of a large amount of

Tuesday Evening, August 4, 2026

Si originating from the quartz tube as a result of the etching effect of F. On the other hand, when an alumina tube is used, Si concentration was reduced to $2 \times 10^{18} \text{ cm}^{-3}$, a reduction of approximately two orders of magnitude compared to the quartz tube. Considering the carrier concentration of $1.6 \times 10^{19} \text{ cm}^{-3}$ by Hall effect measurement, it is thought that F contributes as a donor, unlike in the case of the quartz tube.

IWGO-TuP-6 First Demonstration of p-type LiGa₅O₈ UWBG Thin Films by MOCVD, Dong Su Yu, Mingxuan Wu, Binzhi Liu, Md Mosarof Hossain Sarkar, Kaitian Zhang, Jinwoo Hwang, Hongping Zhao, The Ohio State University

Ultrawide bandgap (UWBG) LiGa₅O₈ with spinel cubic structure was recently discovered as a p-type material [1]. Due to the lack of native p-type Ga₂O₃, p-LiGa₅O₈ is considered as a promising candidate to form Ga₂O₃/LiGa₅O₈ pn junctions. Previously, the growth of p-LiGa₅O₈ has been demonstrated via mist-CVD [1].

In this work, we achieve the first successful growth of p-LiGa₅O₈ via metalorganic chemical vapor deposition (MOCVD). Triethylgallium (TEGa), lithium-tert-butoxide (LiOtBu), and high-purity oxygen are used as the Ga, Li and O precursors, respectively. Both c-sapphire and GaN-on-sapphire are used as substrates. X-ray diffraction measurements indicate the formation of peaks consistent with the cubic spinel LiGa₅O₈ phase. Cross-sectional scanning transmission electron microscopy revealed well-crystallized LiGa₅O₈ thin films with lattice structures consistent with the cubic spinel. X-ray photoelectron spectroscopy analysis confirmed the lithium incorporation in samples with relatively high Li molar flow rates. Electrical transport properties were probed using room temperature Hall measurements. The as-grown films show a wide range of resistivity depending on the MOCVD growth condition. For a selected series of samples, the Hall measurements show p-type conduction with hole concentrations on the order of $\sim 10^{18} \text{ cm}^{-3}$ and mobility around $\sim 10 \text{ cm}^2/\text{V}\cdot\text{s}$.

Results from this work demonstrate the feasibility of LiGa₅O₈ growth by MOCVD and provide initial insight into growth conditions and carrier transport in this material system. The present study proposes a promising route to integrate p-LiGa₅O₈ with Ga₂O₃ power device technologies.

IWGO-TuP-7 Fabrication and Characteristics of α -Ga₂O₃-Based Schottky Barrier Diodes on Sapphire Substrates for Microwave Rectenna Applications, Takeru Wakamatsu, Kyoto University, Japan; Yasuo Ohno, Laser Systems Inc., Japan; Hikaru Ikeda, Shizuo Fujita, Kyoto University, Japan; Tomomi Hiraoka, Laser Systems Inc., Japan; Kentaro Kaneko, Ritsumeikan University, Japan; Katsuhisa Tanaka, Kyoto University, Japan

Rectennas are key devices in microwave wireless power transfer converting RF to DC using a rectifier and an antenna. To obtain higher conversion efficiency of a rectifier, the product of R_{on} (on-resistance) and C_{off} (capacitance in the off-state) should be minimized. Ga₂O₃ is a promising material owing to its high breakdown field (E_c), since there is the relationship $R_{\text{on}}C_{\text{off}} = 2V_{\text{out}}/\mu E_c^2$, where μ denotes the mobility. Furthermore, sapphire substrates are suitable for RF applications due to their low dielectric loss, and therefore rectifiers made of α -Ga₂O₃, which is grown on sapphire using mist CVD, can enable the integration of a rectifier, an antenna, and a matching circuit onto a single chip. In this presentation, we demonstrate the fabrication and RF characteristics of α -Ga₂O₃ Schottky barrier diodes (SBDs) for use in rectennas.

α -Ga₂O₃ SBDs consisting of n^- and n^+ layers, with an anode diameter of 4 μm , were fabricated on sapphire substrates by mist CVD with Ge doping. C-V measurements revealed the net donor concentrations of 4×10^{17} and $8 \times 10^{18} \text{ cm}^{-3}$ for the n^- and n^+ layers, respectively. The anode is connected to the anode pad via an air bridge to minimize $R_{\text{on}}C_{\text{off}}$. The I-V characteristics of the SBD indicated an ideality factor of 1.07, an on-resistance of 210 Ω , and a breakdown voltage of 41.4 V. The capacitance in the off-state (C_{off}) was estimated to be 0.02 pF based on the S-parameters in the off-state.

A full-wave rectifier circuit comprising 16 SBDs arranged in a 4'4 configuration was fabricated and used for RF characterization. A 2.45 GHz microwave signal was delivered to the rectifier circuit via an RF probe. The input power to the rectifier circuit (P_{in}) and the reflected power (P_{ref}) were measured using directional couplers. The output power (P_{out}) was obtained from the DC output voltage (V_{out}) across the 1 k Ω load resistance (R_{load}) as $P_{\text{out}} = V_{\text{out}}^2/R_{\text{load}}$. The results revealed a conversion efficiency of 13.9 % at an input power of 1.7 W. However, the efficiencies are significantly underestimated due to on-chip measurements without a matching circuit, resulting in high reflectance. We created a circuit model using the S-parameters of a single SBD and incorporating an impedance-matching circuit; this predicted a conversion efficiency of 67 % at an input power of 1

W. These results encourage the use of α -Ga₂O₃ SBDs on sapphire for RF rectennas for microwave wireless power transfer systems.

A part of this work was supported by MIC under a grant entitled "R&D of ICT Priority Technology (JPMI00316): Next-Generation Energy-Efficient Semiconductor Development and Demonstration Project (in collaboration with MOEJ)."

IWGO-TuP-8 Gigantic Space Charge Limited Currents and Thermal Effects in Si-Fe-doped Ga₂O₃ Devices, Pierre Gallarday, Aniol Vellvehí, INSTITUTE OF MICROELECTRONICS OF BARCELONA - (IMB-CNM-CSIC), Spain; Verena Leitgeb, Department Microelectronics, Materials Center Leoben Forschung GmbH (MCL), Austria; Miquel Vellvehí, Josep Montserrat, INSTITUTE OF MICROELECTRONICS OF BARCELONA - (IMB-CNM-CSIC), Spain; Barbara Kosednar-Legenstein, Lisa Mitterhuber, Elke Kraker, Anton Köck, Department Microelectronics, Materials Center Leoben Forschung GmbH (MCL), Austria; José Rebollo, Amador Pérez-Tomás, INSTITUTE OF MICROELECTRONICS OF BARCELONA - (IMB-CNM-CSIC), Spain

Currents, far in excess of ohmic currents, can be drawn through thin, relatively perfect insulating crystals being the solid-state analog of space charge limited current (SCLC) phenomena in a vacuum diode. SCLC is most relevant in materials with low intrinsic carrier density and weak screening, such as organic semiconductors, insulators, and wide bandgap materials, where it helps probe mobility and defect states. Two basic requirements were established to observe SCLC in low conducting materials: (i) at least one of the contact must be ohmic to provide an excess of carriers ready to enter the material and (ii) the studied material has to be relatively free from trap states.

In this work, we investigate the electro-thermal behaviour due to unusual and gigantic SCLC transport of an (010)-oriented high-resistivity compensated Fe-doped β -Ga₂O₃ as-received single crystal with a compensating shallow Si-implant and lateral concentric metal ohmic contacts (Ti/Au). The Si-channel implantation (depth $\sim 300\text{nm}$) was defined via BOX profile technique with energies of 200 keV, 95 keV, 60 keV, 30 keV and 10 keV, and with doses in the range of 1.28×10^{13} - 0.6×10^{12} ions/cm². Physical characterization includes XRD and Raman –showing no implantation structural effect- while thermal analysis is done by Time-Domain Thermo Reflectance (TDTR). TDTR reveals a substantial reduction in thermal conductivity within the implanted layer (12.5 W/mK - implanted vs 20.2 W/mK - bulk), attributed to lattice disorder and increased phonon scattering.

A simplified analytical model describing the spatial distribution of electric field and volumetric Joule heating under SCLC conditions shows good agreement with electrical measurements, i.e., current is proportional to V^2 and inversely to L^3 for the applied voltage and spacing between electrodes, respectively. We ascribe it to a SCLC phenomenon (Mott-Gurney) in cylindrical coordinates:

$$I = \theta \cdot (9\pi/4) \cdot \epsilon_s \cdot \mu \cdot d_{\text{ch}} \cdot (V^2/[F \cdot r_0^2])$$

(θ - current enhancement factor, ϵ_s - dielectric permittivity, μ - carrier mobility, d_{ch} - conductive channel depth, F - geometrical correction in function of inner (r_i) and outer (r_o) radius). The interplay between SCLC conduction and non-uniform electric field distribution produces highly localized Joule heating, leading to pronounced temperature gradients and premature thermal breakdown at relatively low applied voltages. These findings reveal unusual enhanced electro-thermal effects in β -Ga₂O₃ devices which provides better understanding of the SCLC phenomena but may also have novel potential applications in areas such as solid-state local heating or surfaces including self-cleaning/antibacterial functional aspects.

IWGO-TuP-9 Conductive Si-doped β -Ga₂O₃ by Atomic Layer Deposition and Annealing, Katie Gann, Benjamin Greenberg, Daniel Pennachio, Naval Research Laboratory; Jeffrey Woodward, Naval research Laboratory; Alan Jacobs, Emma Rocco, Boris Feygelson, Rachael Myers-Ward, Karl Hobart, Michael Mastro, Naval Research Laboratory

While many methods for growth of high-quality Si-doped Ga₂O₃ have been developed, epitaxial thin film growth often requires etching and complicated processing for device fabrication. This process could be simplified by conformal deposition methods, but are often limited by low crystal quality. Atomic layer deposition (ALD) of Si-doped Ga₂O₃, with trimethylgallium and ozone precursors was performed at a $T_{\text{sub}} = 220^\circ\text{C}$ on semi-insulating (010) β -Ga₂O₃ substrates, with 399 cycles of Ga₂O₃ and 1 cycle of Si, yielding a film thickness of 28 nm by ellipsometry and an average Si concentration of $9.5 \times 10^{19} \text{ cm}^{-3}$. Characterization by HRXRD suggests the as-deposited film is amorphous. Annealing at 900 $^\circ\text{C}$ for 10 minutes under an N₂ ambient results in conductive films with a mobility of

49 cm²/Vs and an estimated carrier concentration of 8.4×10¹⁸ cm⁻³ (roughly 9% active). XRD shows an unexpected peak around 64.2°, often attributed in literature to the 440 reflection of the γ-phase, which is considered to have a common oxygen lattice and continuous phase transformation with the β-phase. Annealing at 1000 °C resulted in the disappearance of this secondary XRD peak, but the film became insulating.

HAADF-STEM studies of the 900 °C annealed film revealed a crystallization front from the substrate, with half of the deposited film epitaxially registered with the substrate with no evidence of the original interface. Roughly ~15 nm near the free surface appeared crystalline and either of a different phase or orientation of β-Ga₂O₃. While viewing down the [001] zone axis (ZA) of the substrate, the surface region of the ALD film was identified as the [010] ZA of β-Ga₂O₃ (with [001] oriented in the surface normal), rather than any orientation of the γ-phase. While the observation of a different orientation of the β on a β-Ga₂O₃ substrate is surprising, the orientation of this thin film layer is such that the oxygen lattice is continuous, with the FCC-like stacking preserved between the two orientations. The 20-4 reflection, which corresponds with the [001] direction, is also located at 64.2°, indicating the secondary XRD peak is likely due to this orientation of β-Ga₂O₃. The observation of the common oxygen lattice suggests that the continuous transformation between β and γ phase enables this formation of a different orientation. Imaging of the electrically insulating 1000 °C annealed film showed complete recrystallization of the lattice with no evidence of a substrate-film interface. The lack of conductivity suggests either Si segregated during crystallization or compensating defects formed.

IWGO-TuP-10 Atomic Scale Investigation of (100) Twin Boundary in EFG-Grown Sn-Doped β-Ga₂O₃, Mehdi Hassan, Binzhi Liu, Jinwoo Hwang, Ohio State University

This work presents an atomic scale investigation of the detailed structure of twin boundaries in an EFG-grown Sn-doped β-Ga₂O₃ with 0.5 mol% Sn doping. It has been known that the twin structure of β-Ga₂O₃, a highly anisotropic monoclinic crystal, not only involves the typical mirror symmetry, but also includes a lattice translation component along the twin boundary, possibly on the order of 1/4 or 1/2 of the unit cell [1]. More recent computational studies have also proposed detailed atomic structures of twin boundaries [2]. However, a detailed experimental analysis is still necessary to gain a comprehensive understanding of the formation mechanism of twins during EFG growth. In this work, we used high-resolution scanning transmission electron microscopy (STEM) to investigate such details.

Optical reflection and Electron backscatter diffraction (EBSD) was first utilized to locate the TB region. Then STEM results from the prepared FIB lamellae reveal two key aspects of the twin boundary structure. First, the structures are consistent with those predicted by Mengen et al. [2], namely (100)A and (100)B types, but the experimental results reveal specific aspects of the boundary that have not been considered in the calculations. First, there is a notable atomic scale strain near the boundary, showing deviation from the bulk structure. Second, this apparent strain at the interface makes the twin boundary effectively an alternating twin boundary that consists of both (100)A and (100)B types, as shown in Fig. 1a. Our results suggest that, besides the energetics of the twin boundaries in β-Ga₂O₃, there are additional factors involving mismatch between the crystals, which result in the strain near the twin boundary observed in this study. The details of the twin boundary structure, strain, and a possible explanation of how this leads to two types of boundaries separated by only a few nanometers will be discussed in this presentation.

IWGO-TuP-11 Optimized CMP Processing and Subsurface Damage Control for High-Quality (010) β-Ga₂O₃ Single Crystals, Won-Jae Lee, Eun-Jeong An, Eun-Seo Lee, Sang-Jin Bae, Ho-Gyun Yun, Kwang-Hee Jung, Jung-Gon Kim, Mi-Seon Park, Dong-eui university, Busan, Republic of Korea; Jin-Ki Kang, Dong-Jin Lee, Axel, Republic of Korea

The post-processing crystalline quality of β-Ga₂O₃ single crystals grown by the vertical Bridgman (VB) method was evaluated. Raman spectroscopy revealed that while the (001) and (100) planes exhibited excellent crystallinity, high full width at half-maximum (FWHM) values for the A_g(3) phonon mode was observed on the (010) surface. Furthermore, as shown in Fig. 1(a), high-resolution X-ray diffraction (HR-XRD) analysis of the (010) plane and its asymmetric (310) plane showed a consistent trend, with the (010) surface exhibiting significantly higher FWHM values. These discrepancies in crystallinity were confirmed to originate from orientation-specific subsurface damage (SSD). The lower mechanical strength of the

(010) plane makes it susceptible to fracture propagation during processing, resulting in deeper SSD than other orientations [1].

In this study, a systematic three-step chemical mechanical polishing (CMP) process was developed to effectively eliminate this deep SSD. The first CMP step used a slurry containing ~3 μm diamond and alumina abrasives with the pad A; the second CMP step used a 72 nm colloidal silica slurry with pad A; and the third CMP step used the same slurry as the second CMP step with pad B. In each step, material removal rates (MRRs) of 5, 3, and 2 μm/h, respectively. As shown in Fig.1 (b) and (c), HR-XRD analysis conducted after all processing steps confirmed the complete removal of the SSD, with the FWHM ultimately reaching 33 arcsec. Atomic force microscopy (AFM) revealed an average roughness (Ra) of 0.116 nm, indicating a surface roughness suitable for epitaxial substrates.

IWGO-TuP-12 Heat-resistant Characteristics of Li doped NiO Films Deposited by RF Magnetron Sputtering, Shunya Matsui, Harunobu Yasuda, Tomohiro Ymaguchi, Tohru Honda, Department of Electrical Engineering and Electronics, Kogakuin University, Japan; Hironobu Miyamoto, Kohei Sasaki, Novel Crystal Technology, Japan; Takeyoshi Onuma, Department of Electrical Engineering and Electronics, Kogakuin University, Japan

β-Ga₂O₃ is expected as a next-generation material to replace existing Si and SiC, but achieving p-type conductivity remains elusive^[1,2]. NiO is a possible alternative for the p-type material. However, the heat-resistance of undoped NiO is limited to around 200°C^[3]. In this study, impact of deposition conditions on resistivity in RF magnetron sputtering of lithium-doped NiO and their heat-resistant characteristics are shown.

24.4-227-nm-thick NiO:Li films were deposited on c-plane sapphire or quartz glass substrates for 5 minutes in an Ar and O₂ mixture atmosphere at an ambient temperature. To dope Li atoms, a NiO target was co-sputtered with 3 or 5 pieces of f=10 mm LiNiO₂ pellets. RF power, sputtering pressure, and O₂ ratio [O₂/(Ar+O₂)] were varied in ranges of 75-300 W, 0.25-1.50 Pa, and 0-50%, respectively. ρ was measured by the four-point probe method with van der Pauw configuration for 5×5 mm² square-shaped devices. Thermal annealing was conducted using tubular furnace at temperatures T_{anneal} of 400, 500, 600, and 700°C for 20 minutes in an oxygen atmosphere with a flow rate of 0.5 L/min.

Li concentrations were evaluated by secondary ion mass spectrometry to be 1.8×10²¹ and 1.0×10²² cm⁻³ for the as-deposited films with 3 and 5 pellets, respectively. As shown in Fig. 1, as-deposited 5-pellet films exhibited ρ=5.26×10⁻²-7.27×10⁻²Ω·cm. In contrast, as-deposited 3-pellet films exhibited monotonical decrease in ρ from 1.72×10⁰ to 9.18×10⁻²Ω·cm with increasing O₂ ratio. After the thermal annealing, ρ for the 5-pellet films almost unchanged below T_{anneal}=600°C, but it significantly increased at T_{anneal}=700°C. For the 3-pellet films, ρ increased up to the value obtained for the as-deposited film with O₂ ratio of 0% below T_{anneal}=600°C, but it also significantly increased at T_{anneal}=700°C. Seebeck effect measurements showed p-type conductivity for all the films. The results brought us to determine heat-resistance temperature being around 600°C. The heat-resistance of the NiO thin film was improved through Li doping.

The authors would like to thank Prof. S. Aikawa for his help with the sputtering equipment. This work was supported in part by the New Energy and Industrial Technology Development Organization (NEDO), subsidized by project No. JPNP22007.

[1] M. Higashiwaki *et al.*, J. Phys. D: Appl. Phys. **50**, 333002 (2017). [2] K. Sasaki *et al.*, Appl. Phys. Express **17**, 090101 (2024). [3] H. Yasuda *et al.*, The 85th JSAP Autumn Meeting, 8p-P10-24 (2025).

IWGO-TuP-13 Heavy-Ion Microprobe Induced Parasitic Channel in Ga₂O₃ MOSFETs, Adam Neal, Air Force Research Laboratory, Materials and Manufacturing Directorate, USA; Daram Ramdin, Core4ce; Eric O'Quinn, University of Tennessee Knoxville; Adam Charnas, Air Force Research Laboratory, Materials and Manufacturing Directorate, USA; Kay-Obbe Voss, GSI Helmholtzzentrum für Schwerionenforschung, Germany; Cale Overstreet, University of Tennessee Knoxville; Cameron Gorsak, Hari Nair, Cornell University; Andrew Green, Air Force Research Laboratory, Sensors Directorate; Thaddeus Asel, Shin Mou, Air Force Research Laboratory, Materials and Manufacturing Directorate, USA; Maik Lang, University of Tennessee Knoxville

The development of the first ultrawide-bandgap β-Ga₂O₃ transistor in 2012 has spurred intensive research into material properties and device optimization for the development of advanced electronics. Space applications of β-Ga₂O₃ are of particular interest due to the established susceptibility of Si, SiC and GaN to single event-burnout effects due to heavy ion collisions. Experiments elucidating the effects of heavy-ion

irradiation on β -Ga₂O₃ transistors are just beginning to be reported, and such studies are critical to inform the design and implementation of Ga₂O₃ power switches and amplifiers in space. In this study, 192 MeV ⁴⁰Ar and 1182 MeV Au species were used to perform spatially resolved “microprobe” characterization of Ga₂O₃ MOSFETs. Single ions are shot into the device with a lateral spatial resolution of ~0.5 micron by 0.5 micron, together with in-situ electrical characterization, to map the most sensitive regions of the device. We find that these lateral Ga₂O₃ MOSFETs do not suffer catastrophic single event burnout up to average electric fields of at least 0.66 MV/cm for 192 MeV ⁴⁰Ar or 0.05 MV/cm for 1182 MeV Au, but they experience significant threshold voltage shifts due to accumulated micro-dosing effects when the heavy ions impact the channel region. Analysis of I-V curves indicates a radiation-induced activation of the parasitic channel at the substrate-epi interface in these Ga₂O₃ devices causing significant negative threshold voltage shifts, where the parasitic channel was otherwise well controlled through appropriate surface treatment prior to epitaxial growth. This study points to the need for additional buffer engineering to mitigate parasitic channel formation at the substrate-epi interface for rad-hard Ga₂O₃ transistors.

IWGO-TuP-14 Large-Area, UVC Passive Pixel Sensors based on Heteroepitaxial β -Ga₂O₃, Hyojung Kim, SiSung Yoon, GeonWook Yoo, Soongsil University, Republic of Korea

Ultraviolet-C (UVC) sensors are essential optoelectronic devices for fire detection, sterilization, environmental monitoring, and defense systems, as they detect signals that cannot be obtained by visible or infrared sensors [1, 2]. In this study, we demonstrated a β -Ga₂O₃ UVC passive pixel sensor (PPS) by integrating a β -Ga₂O₃ transistor and a large-area metal-semiconductor-metal (MSM) photodetector (PD) on a single pixel.

Fig. 1 (a) shows schematic and layout of the fabricated β -Ga₂O₃ PPS. Fig. 1(b) presents the I-V characteristics of the MSM PD (1x1 mm²), where the dark current of 6.5 pA and a 250 nm photocurrent of 0.5 μ A were measured at 20 V, resulting in a photo-to-dark contrast ratio of 10⁵. Fig. 1 (c) shows a peak responsivity of 1.9 A/W at 250 nm with a UV/visible rejection ratio ($R_{250\text{ nm}} / R_{400\text{ nm}}$) of 2.8x10⁵. Fig. 2(a) presents transfer characteristic of the fabricated Ga₂O₃ transistor for V_{DS}=1, 10 V. The threshold voltage was extracted to be 3.5 V, and on/off ratio was 10⁷; Fig. 2(b) shows output characteristic. R_{on} was extracted to be 0.42 k Ω -mm. Fig. 3 illustrates semi-log scale output I-V characteristics of the PPS with/without UVC (250 nm) irradiation. The gate electrode of transistor was used for a selected (SEL) signal, and drain electrode was used for an output signal. For a fixed V_{SEL} of 3 V, V_{OUT} was swept from 0 to 7 V. In the dark state, the output current was ~90 pA, whereas under UVC irradiation, it increased to 6.2 nA. The β -Ga₂O₃ PPS showed good UVC response with a dark-to-photo current ratio of ~60 under irradiation of 250 nm UVC.

In summary, we demonstrated a homogeneous integration of β -Ga₂O₃ UVC PPS with a β -Ga₂O₃ MSM PD and a transistor. The MSM exhibited a high responsivity of 1.9 A/W and rejection ratio of 2.8x10⁵, while the transistor showed a threshold voltage of 3.5 V for enhancement-mode and R_{on} of 0.42 k Ω -mm. The integrated PPS achieved a distinct UV response with an on/off ratio of 60. These results can provide a method to realize a monolithic integration of the heteroepitaxial β -Ga₂O₃ UVC PPS and its array toward UVC imaging.

IWGO-TuP-15 Heteroepitaxial Growth of β -Ga₂O₃ on High-Angle Off-Cut Sapphire via MOCVD: Optimization through Minimum Oxygen Distance Simulations, Hyeon-Yun Kim, JungHun Choi, Ji-Hyeon Park, Dae-woo Jeon, Korea Institute of Ceramic Engineering and Technology, Republic of Korea

Beta-gallium oxide (β -Ga₂O₃) is a premier ultra-wide bandgap semiconductor (> 4.9 eV) tailored for advanced high-power devices and solar-blind photodetectors. While homoepitaxial techniques on native substrates have matured, the exorbitant expense of single-crystal β -Ga₂O₃ severely restricts its commercial viability. Consequently, the heteroepitaxial deposition of β -Ga₂O₃ on sapphire via metal-organic chemical vapor deposition (MOCVD) has become a focal point of research, offering a highly scalable and economically viable pathway.

In this study, we investigate strategies to mitigate lattice mismatch and suppress the formation of rotated domains during the heteroepitaxy of β -Ga₂O₃ on sapphire. We utilized a-plane off-cut sapphire substrates to enforce structural symmetry and align these domains. While conventional approaches typically report optimal growth near a 6° off-cut, our research systematically expanded the experimental range from 6° to 16°, revealing a positive trend of improving crystallinity at these higher off-cut angles. To interpret the underlying mechanism driving this tendency at angles above 6°, we conducted comprehensive simulations based on the minimum

oxygen-to-oxygen (O-O) distance between the sapphire substrate and the β -Ga₂O₃ layer. By elucidating these interactions, this work establishes an optimized framework for enhancing the crystal quality of β -Ga₂O₃ on highly off-cut sapphire, ultimately advancing the commercial viability of cost-effective UWBG power semiconductor devices.

IWGO-TuP-16 Defect- and Dopant-engineered p-type Conductivity in Epitaxial ZnGa₂O₄ Spinel Oxide Thin Films, Mohammad M. Afandi, Young Min Park, Gyeong Ryul Lee, Roy B. Chung, Kyungpook National University, Republic of Korea

Spinel ZnGa₂O₄ (ZGO) is an ultrawide-bandgap (UWBG) oxide with high optical transparency, large breakdown fields, tunable electrical conductivity, and strong chemical stability, making it a promising candidate for high-power and extreme-environment electronics. However, achieving stable p-type conductivity remains challenging due to the self-compensation of acceptor defects in oxide semiconductors. In this study, epitaxial ZGO thin films were grown on c-plane α -Al₂O₃ substrates via mist chemical vapor deposition, with the Zn/Ga precursor ratio systematically controlled to regulate defect formation in the spinel lattice.

Structural analysis confirms the formation of highly crystalline, single-phase epitaxial films with smooth surfaces. Electrical characterization reveals stable p-type conductivity with a hole mobility of 4.43 cm² V⁻¹ s⁻¹ and hole concentration on the order of 10¹⁵ cm⁻³ at room temperature, attributed to intrinsic self-doping arising from cation non-stoichiometry and antisite defects, supported by cation state analysis. In addition to intrinsic defect engineering, extrinsic acceptor doping using Li and Ni was preliminarily explored to further tune the electrical properties. These results highlight the importance of defect engineering in spinel oxides and establish ZGO as a promising p-type UWBG semiconductor for next-generation high-power and optoelectronic devices.

IWGO-TuP-17 Remote Epitaxy of α -Ga₂O₃ via Polycrystalline MoS₂, Gyeong Ryul Lee, Young Min Park, Roy Chung, Kyungpook National University, Republic of Korea

Among various studies on thin film growth mediated by two-dimensional (2D) materials with van der Waals bonding in the vertical direction, research on remote epitaxy has gained significant attention, beginning with the use of single-crystalline graphene. [1] Although graphene is the most extensively studied van der Waals material to date, its limited direct synthesis on various substrates and the potential damage during the transfer process pose challenges for large-area fabrication and broader material integration. Among 2D materials, transition metal dichalcogenides (TMDs), which possess a characteristic sandwich-like structure, have been reported to be synthesized over large areas using solution-based methods. [2,3] Notably, the remote epitaxial growth of ZnO nanorods using MoS₂ as a mediating layer has been demonstrated. [4] In this study, polycrystalline MoS₂ with a sandwich structure was directly synthesized on sapphire substrates with a corundum structure via a solution-based process. Using this MoS₂ layer, α -Ga₂O₃, a polymorph of Ga₂O₃ with the same crystal structure as the underlying sapphire substrate was successfully grown via remote epitaxy. To investigate the growth mechanism of Ga₂O₃ through remote epitaxy, we analyzed the microcrystal formation in the early stages of growth on both bare sapphire and MoS₂-coated substrates with varying MoS₂ thicknesses, and compared the crystalline quality of the resulting thin films. Scanning transmission electron microscopy (STEM) analysis revealed that the film began to grow as a single crystal from the interface. Finally, through exfoliation of the grown films, it was confirmed that single-crystalline Ga₂O₃ was obtained without damaging the underlying 2D MoS₂ layer.

IWGO-TuP-18 β -Ga₂O₃ Growth on Single Crystal Diamond (111), Arpit Nandi, University of Bristol, UK; Arnab Mondal, Ankush Bag, Indian Institute of Technology Guwahati, India; Martin Kuball, University of Bristol, UK

Gallium oxide (Ga₂O₃) enables highly efficient power electronics due to its ultra-wide bandgap and high critical electric field (8 MV/cm). However, its lack of p-type doping and poor thermal conductivity limit high-power device performance. Overcoming this requires heterointegrating Ga₂O₃ with p-type substrates such as SiC and, especially, diamond, which provides a >200-fold increase in thermal conductivity [1,2].

We report the epitaxial growth of β -Ga₂O₃ thin films on diamond substrates using a close-injection showerhead metal-organic chemical vapour deposition method. Growth on diamond in oxygen-rich environments is complicated by rapid surface oxidation of the substrate, often leading to self-exfoliation or peel-off; thus, a two-step growth approach was adopted. A low-temperature (Al_xGa_{1-x})₂O₃ (AGO6) buffer layer was used to protect the diamond surface and as a strain-relief layer, followed by high-

temperature growth of the Ga₂O₃ epitaxial layer [3]. Initial growth of (Z01) β-Ga₂O₃ on (001) diamond showed two-sets of in-plane grain variants. Analysing the in-plane relationship between variants, we find that using offset (111) diamond reduces these variants. Textured epitaxy of (Z01) β-Ga₂O₃ was confirmed using XRD. φ-scans showing increased peak separation, and reduced in-plane variants with an improved epi-layer FWHM of 0.9° on (111) diamond, down from the 1.5–1.9° typical of (001) substrates. AFM showed coalescence with a surface roughness of 4.4 nm for an area of 10x10 μm². We also report β-Ga₂O₃ on diamond photodetectors delivering 17.15 A/W responsivity, a PDCR of 2.8x10³, a 2.8x10¹³ Jones detectivity and an external quantum efficiency of 83.2%; this radiation-tolerant pairing is promising for space applications

IWGO-TuP-19 Suboxide-MBE Growth of β-Ga₂O₃ on Metallic Ru(001), Martin Samuel Williams, Marco Schowalter, Aman Baunthiyal, Alexander Karg, Sushma Raghuvansy, Jens Falta, Andreas Rosenauer, Martin Eickhoff, Manuel Alonso-Orts, Universität Bremen, Germany

The use of backside (BS) contacts for power distribution (BSPD) and even signal routing is gaining attention in physical design optimisation for its capacity to improve performance and power efficiency, while reducing cell height – presenting future routes for continued scaling of integrated circuits at smaller nodes [1]. BSPD and BS signal routing have enabled the implementation of 4-track standard-cell libraries, resulting in up to a 15% power reduction and a 35% area reduction compared to a 6-track library with BSPD only [2]. When combined with the ultra-wide bandgap of monoclinic β-Ga₂O₃, and consequently its high breakdown field, this approach presents an avenue for future efficient high-power devices.

Molecular beam epitaxy (MBE) enables the growth of crystalline β-Ga₂O₃ on substrates such as sapphire. However, it entails complex two-step growth kinetics – exhibited by the formation and desorption of the volatile Ga₂O suboxide in Ga-rich conditions – and low growth rates. Alternatively, suboxide MBE (S-MBE) simplifies growth of β-Ga₂O₃ to a single step, enabling more stable and higher growth rates in the suboxide-rich adsorption-controlled regime. Furthermore, S-MBE allows for epitaxial growth at lower temperatures – facilitating the growth of β-Ga₂O₃ on Ru while minimising oxidation of the metallic surface.

The growth of β-Ga₂O₃ on RF-sputtered Ru [3] is studied across a wide stoichiometry range, from φ_{Ga2O}/φ_O = 0.05 to φ_{Ga2O}/φ_O = 10, with nucleation in suboxide-rich growth aided by the inclusion of an initial buffer layer in stoichiometric growth conditions. (-201)-oriented β-Ga₂O₃ is observed to form across the investigated parameter space. The vertical conductivity of unintentionally and intentionally Si-, Sn- and Ge-doped films is studied, utilising the Ru film as a BS contact. Finally, Ru is demonstrated as a replacement for a lower distributed Bragg reflector in vertical optical cavities, exhibiting an as-deposited reflectance surpassing 70% over the near-UV and visible spectral range.

- [1] Xie *et al.*, 2024 IEEE Symposium on VLSI Technology and Circuits (2024)
- [2] Kedilaya *et al.*, IEEE J. Explor. Solid-State Comput. Devices Circuits **11** (2025)
- [3] Baunthiyal *et al.*, APL Mater. **13**, 4 (2025)

IWGO-TuP-20 Gd Incorporation in β-Ga₂O₃ Grown by Suboxide MBE: Towards Ultraviolet Emission and Luminescent Thermometry, Martin Samuel Williams, Marco Schowalter, Alexander Karg, Mahmoud Elhajhasan, University of Bremen, Germany; Marcus Rohnke, University of Giessen, Germany; Carsten Ronning, University of Jena, Germany; Gordon Callsen, Andreas Rosenauer, Martin Eickhoff, Manuel Alonso-Orts, University of Bremen, Germany

β-Ga₂O₃ has emerged as a promising ultra-wide bandgap semiconductor for next-generation power electronics and solar-blind photonics. Rare-earth doping offers an attractive route to introduce spectrally well-defined optical transitions. In particular, Gd³⁺ exhibits intra-4f transitions in the UV-B spectral region. The Stark manifold of Gd³⁺, consisting of a single ground state and split excited multiplets, is largely insensitive to small crystal-field variations due to shielding of the 4f electrons by the outer 5s and 5p orbitals, while remaining responsive to larger symmetry changes such as those between Ga₂O₃ polymorphs. In addition, this manifold enables temperature-dependent population redistribution among crystal-field split levels, which can be exploited for high-precision luminescent thermometry [1].

Our recent work [2] studied Gd implantation in β-Ga₂O₃ thin films grown by atomic layer deposition (ALD) and molecular beam epitaxy (MBE). Detailed photoluminescence (PL) spectroscopy revealed a well-resolved manifold of four lines in the UV-B originating from the electronic transitions from the

Stark splitting of the ⁶P_{7/2} excited state to the ⁸S_{7/2} ground level of Gd³⁺. These results indicated that the transition energies in implanted β-Ga₂O₃:Gd films are largely independent of the growth method (for the undoped β-Ga₂O₃ films) and of the annealing conditions in the Gd-implanted layers, reflecting the weak sensitivity of the 4f electronic states to such small variations in the host crystal environment

In this work, we extend these studies to epitaxially grown Ga₂O₃:Gd layers synthesized by suboxide molecular beam epitaxy (S-MBE) [3]. Growth was performed under adsorption-controlled and oxygen-rich conditions. Structural characterization by reflection high-energy electron diffraction (RHEED) and X-ray diffraction (XRD) confirms the formation of crystalline β-Ga₂O₃ layers, while XRD and depth-resolved X-ray photoelectron spectroscopy (XPS) provide evidence for successful Gd incorporation into the films. These results demonstrate the feasibility of in-situ Gd incorporation during suboxide MBE growth and establish a platform for studying rare-earth optical properties in epitaxial Ga₂O₃, enabling direct comparison with implanted samples [2] and opening pathways towards engineered UV-B emitters and temperature-sensing photonic devices.

References

- [1] D. Yu, (...), M. Suta, Light Sci. Appl. **10**, 236 (2021).
- [2] M. S. Williams, (...), M. Alonso-Orts, Mater. Today Phys. **54**, 101731 (2025).
- [3] P. Vogt, (...), J. S. Speck, APL Mater. **9**, 031101 (2021).

IWGO-TuP-21 Epitaxial Growth of κ(ε)-Ga₂O₃ Thin Films on 4H-SiC Substrates by Mist Chemical Vapor Deposition, Taisei Oya, Kazuyuki Uno, Wakayama University, Japan

Gallium oxide (Ga₂O₃) faces challenges in achieving stable p-type conductivity and possesses relatively low thermal conductivity. One promising strategy to overcome these limitations is heteroepitaxial growth on 4H-SiC, whose high thermal conductivity and p-type conductivity can compensate for the intrinsic weaknesses of Ga₂O₃. However, reports on Ga₂O₃ heteroepitaxy on 4H-SiC substrates remain limited [1-3]. In this study, epitaxial growth on 4H-SiC substrates was carried out using mist chemical vapor deposition (mist-CVD), resulting in the formation of κ(ε)-phase Ga₂O₃ thin films. The growth results are presented, and the potential of this heteroepitaxial system is discussed.

Ga₂O₃ films were grown by mist CVD using a mixed precursor solution of [GaCl₃]=0.02 M and [Hacac]=0.06 M. The 4H-SiC (0001) substrates were pretreated by SPM (H₂SO₄:H₂O₂=3:1) cleaning and subsequent 10% of HF etching to obtain surfaces with a bilayer step structure. We then varied the substrate temperature to identify the temperature range in which continuous Ga₂O₃ thin films can be formed. In addition, we tracked how the growth mode of the crystal evolves with increasing film thickness.

Thin-film growth was not observed on the carbon face of 4H-SiC, and no film was obtained on 4° off-axis substrates. In contrast, thin-film growth was confirmed on the Si face of 4H-SiC(0001) on-axis substrates. According to X-ray diffraction measurements, crystalline film growth started at temperatures above 550°C, whereas continuous thin-film formation was achieved at temperatures above 600°C. At a growth temperature of 600°C, a κ(ε)-phase film initially grew coherently on the substrate and was subsequently followed by the formation of a lattice-relaxed layer. At a film thickness of approximately 300 nm, the XRC FWHM decreased, indicating improved crystalline orientation. At a growth temperature of 700°C, the β phase initially grew coherently on the substrate, followed by the formation of the κ(ε) phase after lattice relaxation. When the film thickness reached approximately 300 nm, the XRC FWHM decreased, indicating improved crystalline orientation, like the behavior observed for films grown at 600°C.

The coherent growth of κ(ε)-Ga₂O₃ in ultrathin films with thicknesses of 20–30 nm suggests its potential application as a dielectric layer in MOSFETs. Furthermore, the improvement in crystalline orientation for films thicker than 300 nm indicates the feasibility of κ(ε)-Ga₂O₃ for vertical device applications.

- [1] N. Nepal *et al.*, J. Vac. Sci. & Technol. **A38**, 063406 (2020), [2] F. Hrubisak *et al.*, J. Vac. Sci. & Technol. **A41**, 042708 (2023), [3] C.-W. Ku *et al.*, Appl. Surf. Sci. Adv. **24**, 100661 (2024).

IWGO-TuP-22 Stability and Interlayer Formation at Epitaxial p-type Oxides/Ga₂O₃ Interfaces, *Anna Sacchi, Michelle Smeaton*, National Laboratory of the Rockies; *Shivashree Shivamade Gowda*, University of Virginia; *Krishna Acharya*, Colorado School of Mines; *Steven R. Spurgeon*, National Laboratory of the Rockies; *Patrick Hopkins*, University of Virginia; *Vladan Stevanovic*, Colorado School of Mines; *Brooks Tellekamp, Andriy Zakutayev*, National Laboratory of the Rockies

Ga₂O₃ interfaces with p-type oxides are relevant for heterojunction device applications in power electronics. Among these, NiO [1] and Cr₂O₃ [2] are considered the most promising. To date, most studies on Ga₂O₃ based heterojunctions have focused primarily on device optimization rather than on the fundamental understanding of interface dynamics and long-term stability. This work aims to provide a deeper understanding of NiO/Ga₂O₃ and Cr₂O₃/Ga₂O₃ interfaces. A detailed growth campaign for NiO and Cr₂O₃ has been conducted via pulsed laser deposition on Ga₂O₃ substrates with two different orientations, *i.e.*, (001), and (-201). X-ray diffraction evaluated material quality and epitaxial relationship, revealing two possible different orientations of the epilayers depending on the nominal out-of-plane substrate orientation, *i.e.*, (111) NiO and (001) Cr₂O₃ aligned to Ga₂O₃ (101) and (-201) when grown on (001) or (-201) oriented Ga₂O₃, respectively. The detected two-fold epitaxial relationship is explained in terms of equivalence of the oxygen and gallium sublattices for the (101) and (-201) Ga₂O₃ planes. This finding also provides a useful methodology to characterize epilayers on an asymmetric substrate. Transmission electron microscopy (TEM) further validates the XRD results and expands the investigation of interface stability, addressing the potential formation of interfacial layers [3] under thermal treatments that simulate long-term high-temperature operation. Finally, thermoreflectance measurements were conducted to probe heat transport across the interfaces, examining the influence of substrate and epilayer orientation as well as the presence of any interfacial layers.

IWGO-TuP-23 Structural Properties of Sn-Doped β -Ga₂O₃ Thin Films Grown on Off-Axis Sapphire Substrates by Mist Chemical Vapor Deposition, *Jae-Hyeok LIM, Yun-Ji SHIN, Tae-Yong Park, Seong-Min JEONG*, Korea Institute of Ceramic Engineering and Technology, Republic of Korea; *Chang-Mo KANG*, Pusan National University, Republic of Korea; *Si-Young BAE*, Pukyong National University, Republic of Korea

β -Ga₂O₃ is an ultra-wide bandgap semiconductor that has attracted significant attention for next-generation power electronic devices. Heteroepitaxial growth on sapphire substrates is promising due to its cost-effectiveness and scalability; however, the severe lattice mismatch often leads to poor crystalline quality and phase instability. In this study, the effect of substrate off-axis angle on the structural properties of Sn-doped β -Ga₂O₃ thin films was systematically investigated.

β -Ga₂O₃ thin films (~1.5 μ m) were grown on c-plane sapphire substrates using a mist CVD process. Both on-axis and 7° off-axis substrates were employed, and Sn doping concentrations (UID, 1%, and 4%) were varied to examine their influence on structural and optical properties. The films were characterized by HR-XRD, AFM, and UV-Vis spectroscopy.

The 7° off-axis substrate significantly improved crystalline quality, reducing the rocking-curve FWHM from 2600–3700 arcsec (on-axis) to ~1600–1700 arcsec. Although increasing Sn incorporation led to crystalline degradation, the off-axis films maintained β -phase stability even at 4% doping. In contrast, on-axis films exhibited phase instability, evidenced by the disappearance of β -phase peaks and the emergence of secondary phases, suggesting a phase transition. AFM analysis revealed improved surface uniformity for off-axis films, although local roughening appeared at higher doping levels. UV-Vis measurements revealed a gradual bandgap narrowing with increasing Sn concentration. Notably, on-axis films exhibited a more pronounced decrease (~4.42 eV), whereas off-axis films retained higher bandgap values (~4.69–4.77 eV), indicating reduced defect-induced band tailing.

These results demonstrate that off-axis substrates effectively enhance crystalline quality and suppress Sn-induced phase degradation, likely through step-flow growth and improved strain relaxation, providing a viable route for scalable growth of high-quality Sn-doped β -Ga₂O₃ on cost-effective sapphire substrates.

IWGO-TuP-24 Enhanced Surface Engineering and Deep Mesa Etching in Vertical Ru-Si-O/ β -Ga₂O₃ Schottky Diodes, *Aleksandra Wojcicka*, Lukaszewicz Research Network - Institute of Microelectronics and Photonics, Poland

Realizing gallium oxide potential in vertical Schottky barrier diodes (SBDs) requires precise anisotropic dry etching, which simultaneously introduce near-surface damage and defect states, making subsequent wet etching

equally important for surface engineering, as both steps strongly affect device performance. Despite extensive studies on wet etching treatments for β -Ga₂O₃ Schottky contacts, no universally optimal surface preparation procedure has been established, since the results depends on crystal orientation and metallization scheme. This remains particularly relevant for amorphous Ru-Si-O Schottky contacts, as their high work function (5.6 eV) makes them attractive for high-power β -Ga₂O₃ devices.

In this work, to investigate the effect of post-etch wet surface treatment, five types of Schottky diode samples were prepared: non-etched, plasma-etched, and plasma-etched samples subsequently treated with 25%wt. TMAH, Piranha solution, or H₃PO₄ prior to Ru-Si-O/Au anode deposition on the surface of (001) β -Ga₂O₃ epilayers ($n \sim 1 \times 10^{16} \text{ cm}^{-3}$, $\sim 10 \mu\text{m}$). Surface engineering by H₃PO₄ and TMAH resulted in effective Schottky barrier heights of $\Phi_B = 1.95 \pm 0.02 \text{ eV}$ and $1.99 \pm 0.03 \text{ eV}$, respectively, while the ideality factors were $n = 1.07 \pm 0.01$ and $n = 1.06 \pm 0.02$. Moreover, the breakdown voltage increased from approximately 950 V to up to ~1600 V. Subsequently, the BCl₃/Ar RIE-ICP etching process was optimized by tuning the pressure (5–30 mTorr), table RF power (0–100 W), and Ar content (0–60%), with the constant ICP power fixed at 1200 W, temperature of 20 °C, and the total gas flow at 40 sccm. The etching tests were performed through a 200 nm thick Ni mask. The optimized conditions were then combined with the previously developed post-etch wet-treatment procedure to fabricate three vertical Schottky diodes with target mesa depths of 0.8, 1.2, and 1.6 μm . The optimized post-etch treatment and mesa-etching process enabled vertical Ru-Si-O/ β -Ga₂O₃ Schottky diodes with breakdown voltages exceeding 2 kV.

This work has been partially supported by the Wide Bandgap (WBG) Pilot line, which is funded jointly by the Chips Joint Undertaking, through the European Union's Digital Europe programme and Horizon Europe programme, as well as by the participating states Italy, Sweden, Poland, Finland, Austria, France and Germany, under Grant Agreement n. 101183211.

IWGO-TuP-25 Effect of Oxygen Ambient During Cool-Down on Nio/Ga₂O₃ Heterojunction Diodes, *Ai Ho, Cheng-Han Li, Ray-Hua Horng*, National Yang Ming Chiao Tung University (NYCU), Taiwan; *Ying-Hao Chu*, National Tsing Hua University, Taiwan

Gallium oxide (Ga₂O₃) has recently attracted significant attention as an ultra-wide bandgap semiconductor due to its large bandgap (4.7 - 4.9 eV) and high critical breakdown electric field (8 MV/cm), which enable a Baliga figure of merit (BFOM) as high as 3444. However, achieving p-type Ga₂O₃ remains a major challenge because of the difficulty in incorporating acceptor dopants and the limited generation and transport of holes. Furthermore, the relatively flat valence band structure leads to a large hole effective mass, resulting in low hole mobility. To address this issue, nickel oxide (NiO) has been widely used to form heterojunctions with Ga₂O₃, demonstrating a feasible approach in previous studies. In this work, we further investigate the impact of oxygen introduction during the cool-down process following metal-organic chemical vapor deposition (MOCVD) growth of Ga₂O₃. The differences between samples with and without oxygen introduction are systematically analyzed through electrical characterization. Overall, oxygen introduction enhances device breakdown characteristics and switching performance, which is further supported by material analysis using X-ray photoelectron spectroscopy (XPS).

IWGO-TuP-26 Sn-Induced Defect Engineering in β -Ga₂O₃: A Combined Experimental and First-Principles Study, *Vijay Kumar Gudelli*, King Abdullah University of Science and Technology, India; *Andres E Castano Hurtado*, King Abdullah University of Science and Technology (KAUST), Colombia; *Kishor Upadhyaya*, King Abdullah University of Science and Technology (KAUST), India; *Iman S Roqan*, King Abdullah University of Science and Technology, Saudi Arabia

β -Ga₂O₃, an ultrawide-bandgap semiconductor with a very high critical electric field, has strong potential for high-power electronic and optoelectronic devices but requires precise defect engineering to realize its full capabilities. This study presents a combined theoretical-experimental framework for understanding substitutional doping via Sn incorporation in epitaxial β -Ga₂O₃, clarifying the charge-compensation mechanisms and the associated optical signatures. Using advanced computational workflows that couple the ShakenBreak toolkit [1] for robust defect relaxation across charge states with the doped code for thermodynamic stability analysis, we systematically map Sn incorporation at the crystallographically distinct Ga (tetrahedral) and Gall (octahedral) sites. Density functional theory shows that the octahedral Sn_{Gall} configuration has markedly lower formation energies (by ~0.5–1 eV relative to tetrahedral Sn_{Ga} across relevant Fermi

levels and chemical potentials), leading to site-selective doping that tunes shallow donor levels near the conduction-band minimum and deep optical centres. These results are then used as input to DefectPL [2] for configuration-coordinate modelling of photoluminescence (PL) and photoluminescence excitation (PLE) spectra, enabling quantitative predictions of zero-phonon lines, phonon sidebands, and vibronic line shapes without empirical fitting. The calculated PL features are similar to our experimental measurements. By combining automated defect discovery, construction of formation-energy diagrams, and spectroscopic simulation, this work resolves site-specific doping behaviour in β -Ga₂O₃, addresses key gaps in defect thermodynamics, and outlines guidelines for designing materials for extreme-environment applications that require coupled electrical and optical control.

[1] I. Mosquera-Lois, S. R. Kavanagh, A. Walsh and D. O. Scanlon, ShakeNBreak: Navigating the defect configurational landscape, *Journal of Open Source Software* 7 (80), 4817 (2022).

[2] D. Manoj, M. Shibu and Abhishek Kumar Singh, Carbon with Stone-Wales defect as quantum emitter in h-BN, *Phys. Rev. B* 111, 104109 (2025).

IWGO-TuP-27 Investigation of NiO/Ga₂O₃ Heterojunction PN Diodes by using HF Surface Treatment, Ray Hua Horng, National Yang Ming Chiao Tung University (NYCU), Taiwan

This study explores the potential of Ga₂O₃ for high-power electronic devices. To achieve this, we fabricated a lateral p-NiO/n-Ga₂O₃ heterojunction PN diode. The fabrication process is used by MOCVD to grow the n-type Ga₂O₃ on a sapphire, followed by sputtering to grow the p-type NiO. Material characterization was performed using XRD, SEM, and AFM. XRD results indicated good epitaxial quality of the β -Ga₂O₃, and the surface grain boundary morphology was analyzed using SEM and AFM. In this study, HF surface treatment was applied to remove dangling bonds and residual Cl from dry etching, thereby enhancing the device's breakdown voltage. The results show that the fabricated diode with HF surface treatment exhibits excellent on/off ratio of 5.1×10^6 and breakdown voltage of 1.96 kV. These findings confirm that the HF surface treatment is an effective method for fabricating high-quality Ga₂O₃ devices.

IWGO-TuP-28 Mechanism and Mitigation of Step-Bunching Instability in Homoepitaxial (100) β -Ga₂O₃ Thin Films, Ta-Shun Chou, Saud Bin Anooz, Zbigniew Galazka, Jana Rehm, Arub Akhtar, Martin Albrecht, Andreas Fiedler, Andreas Popp, Leibniz Institute for Crystal Growth, Germany

Step-bunching is a classical morphological instability observed in nearly all epitaxially grown material systems, typically serving as a source of structural defects. This phenomenon results in increased surface roughness that hinders the quality of electrical contacts and degrades physical properties, such as the mobility of a two-dimensional electron gas (2DEG). (100) β -Ga₂O₃ as a promising plane for large-scale wafer production (up to 6-8 inches), generally requires high offcut angles to achieve the desired step-flow morphology with low defect density. In this context, step-bunching serves as a critical instability that dictates the transition between a smooth, atomically flat surface (step flow growth) and a faceted or defective film.

In this study, we identified two distinct step-bunching morphologies occurring under conditions of high doping concentration and low Ga supersaturation. We propose separate formation mechanisms to explain these observations: the first is attributed to the local pinning effect of adsorbed dopants or impurities (type 1, Figure 1) [1], while the second is characterized as a 'terrace-loading instability.' (type 2, Figure 2). This instability arises independently of impurities as a direct consequence of intrinsic growth dynamics and the Ehrlich-Schwoebel (ES) barrier. It emerges specifically when supersaturation levels exceed the system's capacity to efficiently incorporate growth species into the steps. Based on these mechanisms, we developed a mitigation strategy that stabilizes step advancement by tuning the Ga supersaturation at the growing step front. This approach maintains the desired step-flow morphology across a wide doping range (10^{16} cm⁻³ to 10^{19} cm⁻³) while preserving high carrier mobilities.

Figure 1. Step-bunching type 1, step-pinning type observed while doping above 10^{18} cm⁻³. [1]

Figure 2. Step-bunching type 2, terrace-loading type observed due to an increase in local supersaturation.

[1] Chou et al., *Appl. Phys. Lett.* 126, 022101 (2025).

IWGO-TuP-29 α -Ga₂O₃ Thin Film Grown on Micropatterned Sapphire Substrate, Kotaro Etokoro, Kyoto University, Japan; *Takeru Wakamatsu, Yuki Isobe*, Kyoto University, Japan; *Kentaro Kaneko*, Ritsumeikan university, Japan; *Katsuhisa Tanaka*, Kyoto University, Japan

α -Ga₂O₃ is one of the promising materials for power-switching devices because of its large bandgap of $E_g = 5.3$ eV [1]. Recently, high quality α -Ga₂O₃ epilayers and heterostructures have been prepared on sapphire substrates. Due to the large in-plane lattice mismatch between the film and the substrate, however, α -Ga₂O₃ epilayers grown on sapphire substrates in general suffer from the formation of dislocations with a density of about 10^{10} cm⁻² [2]. In this study, an attempt was made to grow α -Ga₂O₃ films with a reduced density of dislocations on sapphire substrates, for which lens-shaped micropatterns without hollow were fabricated before the film growth.

We fabricated micropatterns in which micro-cylinders (designed diameter was 2 μ m) were arranged at different periods (designed center-to-center distances were 3, 4, and 6 μ m) to construct a hexagonal lattice on the surface of sapphire substrate (10 x 10 mm² square, c-plane) by photolithography and dry-etching. We prepared α -Ga₂O₃ films on the patterned substrates using the mist-CVD process with the growth time of 30 to 300 min. α -Ga₂O₃ was grown on each cylinder with a shape of hexagonal truncated pyramid with the top being the c-plane (0001). For the case of the film grown for 300 min, the facet of c-plane was lost, and the pyramidal shape resulted. In contrast, for the film grown on the substrate patterned with a period of 3 and 4 μ m, the surface of the film, which was the c-plane, became flat and uniform.

X-ray diffraction ω -rocking curve was obtained to examine the crystallinity of the films. We calculated the threading dislocation (TD) density from the full width at half maximum of the diffraction lines [3]. The total density of TD, including screw and edge dislocations, was an order of 10^{10} cm⁻² for the film grown on the substrate without any patterns, while the TD density was reduced to 10^8 cm⁻² when the patterned substrate was used.

This work was supported by MIC under a grant entitled "R&D of ICT Priority Technology (JPMI00316): Next-Generation 14 Energy-Efficient Semiconductor Development and Demonstration Project (in collaboration with MOEJ)."

[1] D. Shinohara and S. Fujita, *Jpn. J. Appl. Phys.* 47, 7311 (2008).

[2] K. Kaneko et al., *Jpn. J. Appl. Phys.* 51, 020201 (2012).

[3] T. C. Ma et al., *Appl. Phys. Lett.* 115, 182101 (2019).

*Author for correspondence: etokoro.kotaro.88a@st.kyoto-u.ac.jp

IWGO-TuP-30 Stabilization of Rutile GeO₂ on R- and M-Plane Al₂O₃ by Plasma-Assisted Molecular Beam Epitaxy, Alexander Karg, Satjawoot Phiw-Ondee, Manuel Alonso-Orts, Martin Samuel Williams, Marco Schowalter, Andreas Rosenauer, Martin Eickhoff, University of Bremen, Germany; *Patrick Vogt*, Paul-Drude-Institut für Festkörperelektronik Leibniz-Institut im Forschungsverbund Berlin, Germany

Rutile germanium dioxide (r-GeO₂), possessing a bandgap of approximately 4.6 eV [1], has recently emerged as a promising material among ultra-wide bandgap (UWBG) semiconductors for applications in high-power electronic devices. Compared to other UWBG oxide semiconductors such as β -Ga₂O₃, r-GeO₂ exhibits a significantly higher thermal conductivity. Furthermore, while Ga₂O₃ can only be doped n-type, both n- and p-type conductivity are predicted for r-GeO₂ [2], a very rare yet desirable property of UWBG semiconductors.

Regarding the epitaxial growth of r-GeO₂, only a limited number of reports exist. In this contribution we focus on molecular beam epitaxy (MBE), for which initial studies employed a graded buffer approach on r-TiO₂ or r-plane Al₂O₃ substrates. In contrast to these studies, we do not use either a pure GeO₂ or Ge source - instead, a powder mixture of both. This approach allows for the evaporation of GeO at significantly lower cell temperatures below 650°C while still achieving commonly used fluxes.

Concerning the layer sequence, we present an alternative concept to stabilize r-GeO₂: Following the growth of SnO₂ and Ge_xSn_{1-x}O₂ buffer layers on m- and r-plane Al₂O₃ substrates, controlled Sn-etching and GeO-exposure of the growth surface are used to enable nucleation of pure r-GeO₂. A comprehensive analysis of the growth parameter space is presented using high-resolution X-ray diffraction (XRD), atomic force microscopy, X-ray photoelectron spectroscopy and scanning transmission electron microscopy (STEM). The nucleation mechanism of GeO₂ is also discussed.

Tuesday Evening, August 4, 2026

[1] M. Laped et al, *Materials Today*, **83**, 513-537(2025)

[2] S. Chae et al, *Appl. Phys. Lett.* **114**, 102104(2019)

IWGO-TuP-31 Deep-Etch Mesa Edge Termination for β -Ga₂O₃ Schottky Barrier Diodes, *Charlotte Conway*, *Aditya K Bhat*, *Sai Charan Vanjari*, University of Bristol, UK; *Jacob Mitchell*, *Jay Burnett*, *Kerry Roberts*, *Huma Ashraf*, KLA Corporation UK Ltd, UK; *Matthew Smith*, *Xiao Tang*, *Martin Kuball*, University of Bristol, UK

The full potential of vertical β -Ga₂O₃ Schottky Barrier Diodes (SBDs) is yet to be reached due to premature breakdown caused by electric field crowding at the Schottky contact edge. Efficient edge termination is essential to realise devices with near theoretical performance: providing higher breakdown voltages and greater efficiency than wide bandgap devices such as SiC [1]. This work explores the solution of deep mesa etching, reducing field crowding at the anode edge. While such edge termination has been realised in other materials [2,3], achieving deep etches in Ga₂O₃ has been challenging [4]. There is also disagreement whether optimal performance occurs in Ga₂O₃ when the trench reaches the full depth of the depletion layer [2], or if there is a shallower saturation depth [4].

This work demonstrates deep etch trenches in Ga₂O₃ in excess of 10 μ m depth for mesa edge termination, using a novel etch approach. The etch rate exceeds 400nm/min – over 8 times faster than standard methods. We have realised over 10 μ m deep etch and demonstrated it on a circular SBD. We determine optimal trench depth and placement to achieve the most favourable edge termination and thus enhanced electrical characteristics. The distance between trench and anode edge are varied and the electrical device performance compared. TCAD simulations show a deeper trench gives better electric field uniformity, with 10 μ m depth demonstrating superior field suppression. In simulation, there is little difference in electric field profile of mesa SBDs on a 5 μ m and 10 μ m epitaxial drift layer. This is tested experimentally by electrical testing of SBDs fabricated at different etch depths on 5 μ m and 10 μ m drift layers. The results deepen understanding of mesa edge termination, leading to its integration in more complex device designs, e.g. trench SBDs – potentially giving breakdown voltages higher than the 4kV previously demonstrated [5].

[1] A.J. Green et al. *Applied Materials*, 10(2), 2022

[2] H. Fukushima et al, *Applied Physics Express*, 12(2):026502, 2019.

[3] C. Han et al, *IEEE Transactions on Electron Devices*, 62(4):1223–1229, 2015.

[4] S. Dhara et al, *Applied Physics Letters*, 121(20), 2022.

[5] A.K. Bhat et al. *Applied Physics Letters*. 127, 113501 (2025)

IWGO-TuP-32 Plasma-Assisted MBE of β -Ga₂O₃/NiO Heterojunctions, *Andy Séguret*, Université Grenoble-Alpes, CEA, Grenoble INP, IRIG, PHELIQS, France; *Marty Volant*, Université Grenoble-Alpes, CEA, IRIG, MEM, France; *Fabien Jourdan*, Université Grenoble-Alpes, CEA, Grenoble INP, IRIG, PHELIQS, France; *Yann Genuist*, Université Grenoble-Alpes, CNRS, Grenoble INP, Institut Néel, France; *Hervé Roussel*, Université Grenoble Alpes, CNRS, Grenoble INP, LMGP, France; *Hanako Okuno*, Université Grenoble-Alpes, CEA, IRIG, MEM, France; *Eirini sarigiannidou*, Université Grenoble Alpes, CNRS, Grenoble INP, LMGP, France; *Vincent Consonni*, 2. Université Grenoble Alpes, CNRS, Grenoble INP, LMGP, France; *Eva Monroy*, *Julien Bosch*, Université Grenoble-Alpes, CEA, Grenoble INP, IRIG, PHELIQS, France

With the growing demand for power electronics, ultra-wide-bandgap materials such as diamond, AlN, and Ga₂O₃ are emerging as candidates to surpass the performance limits of SiC and GaN. Among them, β -Ga₂O₃ is particularly attractive due to its 4.9 eV bandgap and breakdown field exceeding 8 MV/cm, resulting in high power-device figures of merit. However, its low hole mobility[1] and unintentional n-type conductivity[2] necessitate an alternative p-type material for rectifying devices. NiO is well suited for this role, as it is naturally p-type, wide bandgap, and forms a staggered type-II heterojunction with Ga₂O₃. In this context, plasma-assisted molecular beam epitaxy (PAMBE) offers high purity, precise thickness control, low growth temperatures, and sharp interfaces, enabling the growth of low-defect and high-performance heterostructures.

Here, we report PAMBE growth of Ga₂O₃ on AlN templates on c-plane sapphire at temperatures between 580 and 780 °C. Although β -Ga₂O₃ has a monoclinic structure, its (-201) plane exhibits hexagonal symmetry with a reduced in-plane lattice mismatch to the (0001) III-nitride surface (~2.4% along [010] β -Ga₂O₃ || [11-20]AlN [3]). In situ RHEED supports this epitaxial relationship and indicates lattice relaxation within the first few nanometers of growth.

We then demonstrate PAMBE growth of NiO on Al₂O₃ and (001) Ga₂O₃ substrates over a temperature range of 530–730 °C. Electron microscopy and atomic force microscopy reveal the deposition of an approximately 100 nm-thick NiO layer with a remarkably flat surface. X-ray diffraction measurements show that the films adopt the (111) and (133) rocksalt NiO orientations on Al₂O₃ and Ga₂O₃ respectively, and confirm the epitaxial nature of the growth.

[1] Linpeng Dong et al., *J. Alloys Compd.*, 712, 379–85, (2017)

[2] Ling Li et al., *Superlattices Microstruct.* 141, 106502, (2020)

[3] A. Seguret et al., *ACS Mater. Lett.* 7, 660 (2024)

IWGO-TuP-33 Long-Term Performance of Gallium Oxide-Based Hydrogen Sensors at 600°C, *William Callahan*, National Laboratory of the Rockies; *Kingsley Egbo*, Headway Technologies; *Anna Sacchi*, *Davi Febba*, National Laboratory of the Rockies; *Anna Staerz*, *Ryan O'Hayre*, Colorado School of Mines; *Brooks Tellekamp*, *Andriy Zakutayev*, National Laboratory of the Rockies

Electronic devices capable of functioning at elevated temperatures are essential for enhancing efficiency and safety across a broad spectrum of applications, spanning industrial, transportation, and energy sectors. Such high-temperature environments are frequently coupled with additional challenging conditions, such as low-oxygen or strongly reducing atmospheres.

Among the most fundamental devices required for these environments are gas sensors, which can detect abrupt shifts in environmental conditions and warn of impending hazards. Identifying and evaluating gas sensor materials and stacks that can dependably function over extended periods under these demanding high-temperature conditions is a challenging yet critical component of device development.

In this presentation, I will outline our methodology for long-term characterization of high-temperature gallium oxide devices operating as hydrogen sensors in harsh conditions. I will cover the range of device architectures that were evaluated and detail the testing procedures that were employed, including our demonstration of 1,000 hours of continuous operation of a Pt/Cr₂O₃:Mg/Ga₂O₃ hydrogen sensor at 600°C.

IWGO-TuP-34 Investigation of the Effect of Heated-H₃PO₄ on Fin Sidewall Roughness and Electrical Performance, *Xin Zhai*, University of Michigan, Ann Arbor; *Jay Burnett*, *Kerry Roberts*, KLA-Tencor, UK; *Edward Walsby*, KLA-Tencor; *Huma Ashraf*, KLA-Tencor, UK; *Rebecca Peterson*, University of Michigan, Ann Arbor; *Elaheh Ahmadi*, University of California Santa Barbara

Vertical β -Ga₂O₃ trench diodes and FinFETs have attracted considerable interest for power-switching applications because they offer several advantages, including the no requirement for p-type doping, compatibility with enhancement-mode operation, and the potential to increase breakdown voltage without enlarging device area. These device concepts typically rely on high quality fin sidewall surface. In this work, we investigate the effect of post-etch treatment (PET) after chlorine-based dry etching of β -Ga₂O₃ focusing on how heated-H₃PO₄ influence the resulting profiles and sidewall roughness [1]. Under optimized etch conditions, we further assess the quality of the fin sidewall roughness through capacitance-voltage (C-V) characterization. **Fig. 1** compared the Ga₂O₃ fin sidewall morphology before and after hot phosphoric-acid PET for 20mins at 120 °C. **Fig. 1 (a)** and **(b)** show dry-etched fins without any subsequent smoothing, with fins oriented along [010] in **(a)** and [100] in **(b)**. Following the heated-H₃PO₄ treatment, the [010] aligned fin in **Fig. 1(c)** displays a smoother and more uniform sidewall compared with **Fig. 1(a)**, indicating that hot phosphoric acid serves as an effective chemical polishing step for this orientation without appreciable Ga₂O₃ consumption. This improvement is consistent with the electrical data in **Fig. 2**, where the treated sample exhibits a higher accumulation capacitance, whereas the untreated sample shows signatures of Fermi-level pinning. In contrast, for the [100] aligned fin, the post-treated sidewall in **Fig. 1(d)** appears similar roughness with the corresponding untreated case in **Fig. 1(b)**, suggesting that the same treatment is less advantageous for the [100] orientation.

IWGO-TuP-35 Band Alignment of NiO_x/ β -Ga₂O₃(001) Heterojunction Consistently Determined by I-V, C-V, and IPE Measurements, *Akihira Munakata*, University of Tokyo, Japan; *Hironobu Miyamoto*, *Kohei Sasaki*, Novel Crystal Technology, Inc., Japan; *Takuya Maeda*, University of Tokyo, Japan

NiO_x/ β -Ga₂O₃ heterojunction diodes (HJDs) are promising for high-power applications. However, their current transport mechanism and band

alignment remain unclear [1–4]. In this work, the NiO_x/β-Ga₂O₃ HJDs are fabricated, and the current transport and the interface properties are investigated by capacitance-voltage (C-V), current-voltage (I-V), and internal photoemission (IPE) spectroscopy measurements.

The net donor concentration of the β-Ga₂O₃ epitaxial layer was 4.3×10¹⁶ cm⁻³. From the C-V measurements, the built-in potential of 2.29 eV was obtained. The potential barrier height ($e\phi_{b,C-V}$) from the fermi level to the conduction band minimum of β-Ga₂O₃ at the interface was obtained as 2.41 eV. The forward I-V characteristics showed an ideality factor of 1.06, suggesting the thermionic emission (TE) and/or diffusion transport. Assuming that the recombination rate near the interface is high enough, the I-V characteristics were analyzed by the TE model, and the barrier height ($e\phi_{b,I-V}$) of 2.36 eV was extracted. Notably, $e\phi_{b,I-V}$ shows excellent agreement with $e\phi_{b,C-V}$. The photocurrent spectroscopy measurements were also performed. The photocurrent spectrum showed a clear linearity in the modified Fowler plot ($Y^{1/3}$ vs $h\nu$) [5, 6], resulting in the direct extraction of $e\phi_{b,IPE}$ as 2.44 eV. The band alignment of NiO_x/β-Ga₂O₃ was consistently obtained by C-V, I-V and IPE measurements. The reverse I-V characteristics of the HJD demonstrated a breakdown voltage of 1415 V (maximum parallel-plane breakdown field of 4.2 MV/cm). The leakage current under high reverse voltage may originate from the electron tunneling from the NiO_x valence band.

[1] H. Luo *et al.*, *IEEE Trans. Electron Devices* **68**, 3991 (2021). [2] Y. Deng *et al.*, *Appl. Surf. Sci.* **622**, 156917 (2023). [3] F. Zhou *et al.*, *Nat. Comm.* **14**, 4459 (2023). [4] J. Zhang *et al.*, *Nat. Comm.* **13**, 3900 (2022). [5] E. O. Kane, *Phys. Rev.* **127**, 131 (1962). [6] J. I. Panvoke and H. Schade, *Appl. Phys. Lett.* **25**, 53 (1974).

IWGO-TuP-36 AlN Mesa Sidewall Passivation Enables Thermally Stable Reverse Blocking in Vertical β-Ga₂O₃ Power Diodes, Ganesh Mainali, Nuzhat Yousef, King Abdullah University Of Science and Technology, Saudi Arabia; Dhanu Chettri, Haicheng Cao, Leo Raj Solay, King Abdullah University Of Science, Saudi Arabia; Xiaohang Li, King Abdullah University Of Science and Technology, Saudi Arabia

Ultra-wide-bandgap β-Ga₂O₃ has emerged as a leading candidate for next-generation high-voltage power electronics due to its large bandgap (~4.8 eV) and high critical electric field (~8 MV·cm⁻¹). However, the performance of vertical β-Ga₂O₃ Schottky barrier diodes (SBDs) remains fundamentally limited by surface- and edge-related leakage arising from mesa isolation, particularly under high electric field and elevated temperature conditions.

In this work, we demonstrate AlN mesa sidewall passivation as an effective strategy to suppress reverse leakage and enhance electrothermal stability in vertical β-Ga₂O₃ SBDs. The AlN-passivated devices exhibit unchanged forward transport, maintaining thermionic-emission-dominated conduction with a peak current density of ~148 Acm⁻² and a specific on-resistance of ~10 mΩcm², comparable to unpassivated devices. In contrast, reverse characteristics show orders-of-magnitude reduction in leakage current, with breakdown voltage improving from 586–681 V to 1.19–1.34 kV (refer Fig. 2 (b)).

Temperature-dependent measurements (25 °C – 400 °C) reveal a pronounced difference in leakage mechanisms (refer Fig. 2 (c) and (d)). The unpassivated diode exhibits strong thermally activated leakage with an activation energy of ~1.4 eV, consistent with barrier modulation and surface-assisted conduction (refer Fig. 3 (a)). In contrast, the AlN-passivated device demonstrates near temperature-independent reverse leakage, indicating effective suppression of surface states and stabilization of the Schottky barrier at the mesa edge.

Electrothermal TCAD simulations further show that AlN passivation reduces peak localized Joule heating at the mesa edge by ~25%, from ~68×10⁶ to ~51×10⁶ W·cm⁻³, while redistributing heat into the bulk drift region (refer Fig. 3(b) and (c)). This reduction in electrothermal feedback directly correlates with the observed suppression of leakage and enhanced breakdown stability.

The improvement is attributed to the combined effects of: surface state passivation, electric field redistribution at the mesa perimeter, enhanced thermal conduction at the sidewall interface. Unlike multi-layer dielectric field-plate approaches, this work demonstrates that a single conformal AlN layer is sufficient to achieve substantial improvements in both electrical and thermal performance. These results establish mesa sidewall electrostatic engineering using AlN as a scalable and effective pathway toward high-voltage, high-temperature β-Ga₂O₃ power devices for next-generation energy conversion systems.

IWGO-TuP-37 Deep-Acceptor-Mediated Inversion Enabling Normally-Off β-Ga₂O₃ MOSFETs without Epitaxy, Sarit Dhar, Tamara Isaacs-Smith, Auburn University; Jacob Lawson, Charles Ebbing, Chase Kitzmiller, Joseph Merrit, Air Force Research Laboratory, USA

The absence of shallow p-type dopants in β-Ga₂O₃ limits realization of normally-off MOSFET architectures analogous to those used in Si and SiC power devices. In this work, enhancement-mode lateral field-effect transistors are demonstrated on Mg-compensated semi-insulating (010) β-Ga₂O₃ substrates without epitaxial regrowth. The devices exhibit threshold voltages exceeding 2.5 V and inversion-channel field-effect mobilities of ~45 cm²/V·s at room temperature. Preliminary switching measurements indicate microsecond-scale turn-on and turn-off with nearly symmetric rise and fall times. The observed switching behavior is primarily limited by external parasitics, the device gate length and associated capacitances. Surface inversion arises from band-bending-induced ionization of deep Mg acceptors, enabling electron channel formation despite the absence of mobile holes. This mechanism differs fundamentally from conventional inversion in Si and SiC, where shallow acceptor doping provides a hole-rich p-body. In β-Ga₂O₃, the ultra-wide bandgap enables enhancement-mode operation through field-induced ionization of compensating deep acceptors. These results establish a new regime of transistor operation in ultra-wide-bandgap semiconductors governed by deep-level compensation and provide a pathway for monolithic integration of depletion- and enhancement-mode Ga₂O₃ power devices on semi-insulating substrates. Acknowledgement: This work was supported by the Auburn University RSP program and Air Force Research Laboratory. + Author for correspondence: sarit_dhar@auburn.edu

IWGO-TuP-38 Achievement of SiO₂/β-Ga₂O₃ (001) MOS Interface with Low in Terface State Density by Employing ALD with O₃ as an Oxidant and Low-temperature (600°C) Post-deposition Annealing, Atsushi Tamura, Hayama Imaida, Koji Kita, University of Tokyo, Japan

[Introduction] While a high-temperature (1000°C) O₂ annealing has been reported to efficiently reduce interface state density (D_{it}) in SiO₂/β-Ga₂O₃ MOS structures probably by removing oxygen deficiencies in the stack [1], it leads to serious drawbacks including the change in dopant profiles and a significant decrease in carrier density in β-Ga₂O₃ [2]. Therefore, it is essential to develop a low-temperature process to form SiO₂/β-Ga₂O₃ MOS interfaces. Taking into account of the necessity of oxygen deficiency removal as mentioned above, one of the keys is a selective oxidation of the SiO₂/β-Ga₂O₃ near-interface region. Therefore, atomic layer deposition (ALD) of SiO₂ is an attractive option because it enables us to tune the degree of oxidation in the initial stage of the film growth. In this study, we investigated the influence of oxidant supply conditions in ALD on the characteristics of SiO₂/β-Ga₂O₃ MOS interfaces with low-temperature (600°C) post-deposition annealing (PDA).

[Experimental] 11 nm-thick-SiO₂ films were deposited on n-type β-Ga₂O₃ (001) epi-wafers (N^D ~10¹⁶cm⁻³) at 300°C via ALD using TDMAS as a precursor. The initial 3 nm of SiO₂ was deposited using either O₂-remote-plasma-ALD or thermal-ALD employing O₃ as an oxidant, followed by an additional 8 nm of plasma-ALD. In the thermal-ALD, two kinds of O₃-doses per cycle (high or low-dose controlled by changing gas supply pulse duration) were employed. After PDA at 600°C in 0.1% O₂/N₂, Au gate electrodes were deposited.

[Results and Discussions] The sample fabricated via thermal-ALD with a high-dose of O₃ shows the minimum hysteresis width in the C-V curve among three samples. Regarding the energy distributions of D_{it}, its D_{it} is approximately one-third of that of the plasma-ALD sample, achieving approximately 1×10¹¹ eV⁻¹cm⁻² at 0.2 eV below the conduction band edge. These results indicate that a sufficient O₃ supply to promote the oxidation of the near-interface region while avoiding plasma damage would be beneficial for reducing interface defect density with PDA at 600°C. Such a beneficial influence of employing O₃ as an ALD oxidant seems consistent with our previous results on Al₂O₃/β-Ga₂O₃ stacks [3]. This abstract is partly based on results obtained from a project, JPNP22007, commissioned by the New Energy and Industrial Technology Development Organization (NEDO).

[1] K. Kita *et al.*, *ECS Trans.* **92**, 59 (2019). [2] T. Kobayashi *Appl. Phys. Lett.* **126**, 012108 (2025). [3] A. Tamura *et al.*, *Int. Workshop on Dielectric Thin Films for Future Electron Dev.* **2025**, Sendai, Japan.

IWGO-TuP-39 Gallium Oxide-Based Photonic Memory Transistor for Nonvolatile Optoelectronic Applications, Jiatong Dong, King Abdullah University of Science and Technology, China; *Iman Roqan*, King Abdullah University of Science and Technology, Saudi Arabia

Gallium oxide (Ga_2O_3), as an ultra-wide bandgap semiconductor, has attracted significant attention for next-generation power electronics and solar-blind optoelectronic devices. In this work, we report a photonic memory transistor based on Ga_2O_3 integrated on a field-effect transistor platform, demonstrating its potential for nonvolatile optoelectronic memory applications. The device was fabricated by depositing Ga_2O_3 thin films onto the transistor using PVD, followed by standard lithography and metallization processes. Upon ultraviolet (UV) illumination, the device exhibits photoresponse enabling memory behavior without continuous power supply. The charge trapping and detrapping processes in Ga_2O_3 , likely associated with intrinsic defects such as oxygen vacancies, play a key role in the memory effect. Electrical characterization shows that the device demonstrates a memory window, high on/off ratio, and stable retention characteristics. The photo-programming and electrical erasing operations were systematically investigated, revealing tunable switching behavior and good repeatability. In addition, the dependence of the memory performance on illumination intensity and gate bias was analyzed to clarify the underlying physical mechanisms. These results highlight the feasibility of Ga_2O_3 -based optoelectronic memory devices and provide insights into defect-engineered photonic memory functionalities. This work opens up new opportunities for integrating sensing and memory in a single wide-bandgap semiconductor platform.

[1] H. Chang et al., *APL Materials* 13(6), 2024.

[2] C. Chen et al., *IEEE Electron Device Letters*. 42. 1492-1495. (2021)

* Author for correspondence: Jiatong.dong@kaust.edu.sa

IWGO-TuP-40 Vertical Trench-Mos Barrier Diode on (001) β - Ga_2O_3 with Trench Formation by Hot H_3PO_4 Treatment, Aaron Adams, KBR/AFRL

β - Ga_2O_3 is poised as the semiconductor of the future for efficient power electronic devices due to the high predicted electric field strength and availability of shallow donors. However, the lack of p-type doping means a well-rectifying diode with low forward losses likely necessitates trench formation for sidewall junctions with RESURF effect to suppress leakage current [1]. To avoid performance penalties from bulk or interface states introduced during dry etching, it is desirable to find a damage free etch. Hot H_3PO_4 has highly anisotropic etch rates in β - Ga_2O_3 [2], making it a suitable candidate for a plasma-free trench formation process. This work demonstrates trench-MOS barrier diodes (TMBDs) fabricated with a wet-only trench etch.

Devices were fabricated on a $\sim 11.3 \mu\text{m}$, $2.5 \times 10^{16} \text{cm}^{-3}$ Si-doped HVPE layer grown on n+ (001) substrate by Novel Crystal Technology. Trench structures were patterned with subtractively defined SiO_2 mask, with 2-4 μm SiO_2 stripes nominally aligned to [100]. The sample was submerged for 120 minutes in H_3PO_4 at 150 °C. SiO_2 was removed by BOE; 50 nm of Al_2O_3 was deposited by PEALD; Al_2O_3 vias were lithographically patterned and BCl_3 dry etched; finally, top-side anode and back-side cathode contacts were formed by patterned Pt/Au and blanket Ti/Au, respectively.

After wet etching, symmetric sidewalls ($48^\circ \angle$ (001)) appeared, nominally parallel to {035} planes. The etch stop on {035} could be due to high atomic density from coplanar Ga_I sites and coplanar O_I sites or octahedral Ga site bond geometry, with $\text{Ga}_{II}-\text{O}_I$ and $\text{Ga}_{II}-\text{O}_{II}$ bonds that are nearly in plane. The etch-resistant surface indicates a chemically stable surface suitable for critical device junctions. Etch depth was limited by the formation of the {035} facet; while the (001) field etched $\sim 2 \mu\text{m}$, the narrower trenches were shallower due to etch termination when {035} planes met to form a "V".

DC I-V characteristics were measured at room temperature, and TMBDs of varying geometry were compared to a cofabricated planar Schottky diode. The TMBDs show slightly higher $R_{\text{on,sp}}$ than the SBD, from 2.5 to 3.9 $\text{m}\Omega\text{-cm}^2$ due to the current choking of the fin structure. Conversely, the TMBDs with larger trench width (and thereby depth) showed greater leakage current reduction, with leakage largely in the noise and V_{bk} increased from 215 V to 1122 V. Due to the dry etch via, a small hysteresis of < 200 mV in the forward I-V was observed in all devices. TMBDs showed no additional hysteresis, indicating a high-quality interface suitable for trench-based device structures in β - Ga_2O_3 .

IWGO-TuP-41 Challenges and Solutions in Mist-CVD of Ga_2O_3 Heteroepitaxial Films, Roman Yatskiv, Institute of Photonics and Electronics of the Czech Academy of Sciences, Czechia

Mist chemical vapor deposition (mist-CVD) has recently attracted interest as a facile, cost-effective, and environmentally friendly method for the deposition of Ga_2O_3 films [1]. We address selected challenges and issues that hinder the fabrication of high-quality Ga_2O_3 epitaxial films [2]. First, based on numerical simulations of the gas flow (Fig. 1b), we demonstrated that the use of a fan to introduce atmospheric air into the horizontal growth reactor avoids the formation of vortices and mist velocity fluctuations, which develop when a conventional carrier-gas delivery system is employed. Second, we experimentally proved that when the thickness of Ga_2O_3 increases, a multiphase epitaxial film forms, presumably due to enhanced thermal stress (Fig. 1c). Finally, we experimentally investigated the effects of growth temperature and precursor type on phase formation (Fig. 1d).

Figure 1 (a) Schematic of the mist-CVD system for the growth of Ga_2O_3 ; **(b)** temperature velocity and pressure fields in the mist-CVD reactor modelled using COMSOL; **(c)** schematic illustration of the critical thickness for processing at 550 °C; and **(d)** schematic illustration of the influence of the growth temperature and precursor type on phase formation.

[1] K. Kaneko, K. Uno, R. Jinno, S. Fujita, Prospects for phase engineering of semi-stable Ga_2O_3 semiconductor thin films using mist chemical vapor deposition, *J. of Applied Physics*, **131** (2022) 090902.

[2] A.V. Vasin, R. Yatskiv, O. Černohorský, N. Bašínová, J. Grym, A. Korchovyj, A.N. Nazarov, J. Maixner, *Materials Science in Semiconductor Processing*, **186**, 109063 (2025).

* Author for correspondence: yatskiv@ufe.cz

Wednesday Morning, August 5, 2026

International Workshop on Gallium Oxide and Related Materials (IWGO-6)

Room ESJ 0202 - Session IWGO-WeM1

Plenary Session II

Moderators: **Martin Albrecht**, Leibniz Institute for Crystal Growth, **Huili (Grace) Xing**, Cornell University

8:00am IWGO-WeM1-1 Breakfast

8:45am **IWGO-WeM1-10 PLENARY: From Crystal Growth to Power Devices: The Evolution of Gallium Oxide Technology**, **Kohei Sasaki**, Novel Crystal Technology, Inc., Japan

INVITED

Gallium oxide has attracted significant attention as an ultra-wide-bandgap semiconductor with the potential to enable power devices with lower losses than conventional Si, SiC, and GaN technologies [1]. Over the past 17 years, I have been engaged in research on gallium oxide power devices.

In the early 2000s, this research field was still in its infancy, attracting only a limited number of researchers from different parts of the globe. Device prototypes were fabricated on small crystal pieces of only a few millimeters in size, and demonstrations were limited to extremely small-area devices carrying currents on the order of milliamperes. Since then, remarkable progress has been achieved. Today, 6-inch gallium oxide substrates are becoming available [2], and device technologies have advanced to the point where 100-A-class devices can be demonstrated. In parallel, the research community has expanded significantly and is now estimated to exceed 1,000 researchers worldwide.

In terms of epitaxial growth, molecular beam epitaxy was initially the dominant technique; however, alternative methods such as halide vapor phase epitaxy (HVPE) and metal-organic chemical vapor deposition have been developed to enable thick epitaxial layers suitable for vertical power devices. Using HVPE-grown epitaxial wafers, recent demonstrations have included 1.8-kV trench MOS-type Schottky barrier diodes and 10-kV-class FinFETs with performances comparable to state-of-the-art SiC devices. Further improvements, such as electric field management using heterojunctions with p-type NiO, are expected to unlock performance levels beyond the reach of SiC devices in the near future.

Another long-standing challenge has been the high substrate cost associated with the use of expensive noble-metal crucibles. Recently, several metal crucible-free bulk growth techniques have been reported, suggesting promising pathways toward cost reduction [3, 4].

In this keynote, I will reflect on the 17-year evolution of gallium oxide research, from its early stages to the present, and offer my perspective on its future directions.

This work was partially based on results obtained from a project, JPNP22007, commissioned by the New Energy and Industrial Technology Development Organization (NEDO).

[1] K. Sasaki, *Applied Physics Express*: **17**, 090101 (2024). [2] S. Hasegawa et al., *Proc. JSAP Spring Meeting, 2026*, 17p-W9_324-7. [3] Y. Ueda et al., *Proc. JSAP Spring Meeting, 2026*, 16p-W9_324-14. [4] Novel Crystal Technology, Inc., "Successful development of a crystal growth method that significantly reduces the amount of precious metals used," Press Release, Jan. 14, 2026.

9:30am **IWGO-WeM1-19 Homoepitaxial Growth of β -Ga₂O₃ Using HVPE and MOVPE**, **Yoshinao Kumagai**, Tokyo University of Agriculture and Technology, Japan

INVITED

β -Ga₂O₃ has attracted considerable attention as a power device material owing to its high breakdown field of ~ 8 MV/cm [1]. Furthermore, the availability of large-area single-crystal substrates grown by various melt-growth methods [2–6] has promoted extensive research on the fabrication of substrates with homoepitaxial layers having controlled conductivity. Our research group has conducted extensive studies on two homoepitaxial growth techniques capable of medium-to-high growth rates, namely halide vapor phase epitaxy (HVPE) [7–11] and metalorganic vapor phase epitaxy (MOVPE) [12–14], which are applicable to the growth of homoepitaxial layers for both lateral and vertical device structures.

In HVPE, GaCl and O₂ served as sources, enabling homoepitaxial growth on (001) substrates at atmospheric pressure with growth rates of 0.4–19 $\mu\text{m/h}$, yielding high-purity layers [7,8]. Si and N concentrations were controlled in the ranges of 1×10^{16} – 3×10^{18} and 3×10^{18} – 1×10^{21} cm^{-3} by intentional SiCl₄ [9] and NH₃ [11] doping, respectively, although the growth rate strongly depended on the substrate orientation [10]. In MOVPE, trimethylgallium and O₂ were used as sources, enabling homoepitaxial

growth of high-purity layers at 0.9–16 $\mu\text{m/h}$ under reduced pressure and high O/Ga supply ratios [12,14], comparable to HVPE. Si concentrations were controlled in the range of 2×10^{15} – 2×10^{19} cm^{-3} by intentional tetramethylsilane doping [13]. In this talk, the growth mechanisms of β -Ga₂O₃ in HVPE and MOVPE, as well as the progress in homoepitaxial growth, the current status including device applications, and challenges, will be presented.

This work was supported by MIC under a grant entitled "R&D of ICT Priority Technology (JPMI00316): Next-Generation Energy-Efficient Semiconductor Development and Demonstration Project (1st and 2nd periods) (in collaboration with MOEJ)."

- [1] M. Higashiwaki et al., *Appl. Phys. Lett.* **100**, 013504 (2012).
- [2] A. Kuramata et al., *Jpn. J. Appl. Phys.* **55**, 1202A2 (2016).
- [3] E. Ohba et al., *J. Cryst. Growth* **556**, 125990 (2021).
- [4] Z. Galazka, *J. Appl. Phys.* **131**, 031103 (2022).
- [5] X. Gao et al., *J. Alloy. Compd.* **987**, 174162 (2024).
- [6] A. Yoshikawa et al., *Sci. Rep.* **14**, 14881 (2024).
- [7] K. Nomura et al., *J. Cryst. Growth* **405**, 19 (2014).
- [8] H. Murakami et al., *Appl. Phys. Express* **8**, 015503 (2015).
- [9] K. Goto et al., *Thin Solid Films* **666**, 182 (2018).
- [10] K. Goto et al., *Appl. Phys. Lett.* **120**, 102102 (2022).
- [11] K. C. Kakuta et al., *Jpn. J. Appl. Phys.* **64**, 100906 (2025).
- [12] J. Yoshinaga et al., *Appl. Phys. Express* **16**, 095504 (2023).
- [13] J. Yoshinaga et al., *Appl. Phys. Express* **18**, 055503 (2025).
- [14] Y. Terauchi et al., *Jpn. J. Appl. Phys.* **64**, 125503 (2025).

9:55am **IWGO-WeM1-24 Characterization of Shallow and Deep Level Defects in β -(Al_xGa_{1-x})₂O₃ Bulk Crystals**, **Andreas Fiedler**, Leibniz-Institut für Kristallzüchtung, Germany

INVITED

β -Ga₂O₃ alloyed with aluminum has a larger bandgap which can be used in heteroepitaxy to generate an interface 2-dimensional electron gas (2DEG) due to the suitable band alignment. Such structures can potentially be used in high electron mobility transistors (HEMT). For a better understanding of the material a detailed defect investigation on Czochralski grown bulk crystals was carried out. Details on crystals growth, crystal structural quality, and properties can be found elsewhere [1, 2].

In this work, we investigated unintentionally doped single crystals with varying aluminum concentration and report on a shift of activation energies for multiple deep defect states. The electron mobility values are significantly decreasing with increasing Al content, most likely due to an increase in the scattering of optical phonons caused by the lattice mismatch and an increased alloy scattering [1]. The activation energies of the majority carriers are in the range of 20 meV to 30 meV but showing no strong influence by the Al-content.

To gather information about deep level states, Deep-Level Transient Spectroscopy (DLTS) was performed in the temperature range from 20K to 800K. We found three major peaks of deep level states with a significant shift to higher ionization energies regarding to the conduction band edge with increasing Al incorporation. The most prominent peak, which is consistent with the previously reported iron based deep acceptor state (E₂) [3], shifts from around 0.7 eV to 1eV with increasing [Al] from 0% to 20%.

Concluding, the electrical properties of β -Ga₂O₃ and the aluminum alloyed β -(Al_xGa_{1-x})₂O₃ are comparable. While we do not observe a shift of activation energy for the primary shallow donor silicon, we can observe a clear shift of the ionization energies of deep states to higher energies with increasing aluminum content in the alloy. However, this shift of the ionization energy is comparably low to the shift of the overall band gap. This study can give insights in the applicability of the scissor function in DFT calculations of defect states in the β -(Al_xGa_{1-x})₂O₃ alloy.

- [1] Z. Galazka et al.; *J. Appl. Phys.* **133**, 035702 (2023)
- [2] Z. Galazka et al.; *Adv. Mater. Interfaces* **12**, 2400122 (2024)
- [3] M. E. Ingebrigtsen *et al.*, *APL* **112**, 042104 (2018)

International Workshop on Gallium Oxide and Related Materials (IWGO-6)

Room ESJ 0202 - Session IWGO-WeM2

Epitaxial Growth and Doping Control II

Moderators: Ahmad Islam, AFRL, Sriram Krishnamoorthy, University of California Santa Barbara

10:50am **IWGO-WeM2-35 Structural and Electrical Properties of c -plane α -Ga₂O₃ Grown on High-quality α -Cr₂O₃ Templates by HVPE**, Yuichi Oshima, Takayoshi Oshima, National Institute for Materials Science, Japan; Shiyu Xiao, Kazuto Murakami, Katsuhiro Imai, Takahiro Tomita, NGK INSULATORS, LTD, Japan

α -Ga₂O₃ is a promising power semiconductor material; however, due to its metastable nature, high-quality bulk substrates are not available. Consequently, epitaxial growth of α -Ga₂O₃ has mainly been performed on sapphire substrates with large lattice mismatch, resulting in high dislocation densities. Recently, high-quality α -Cr₂O₃ templates, which exhibit a small in-plane lattice mismatch of approximately -0.45% with c -plane α -Ga₂O₃, have attracted significant attention. Epitaxial growth of α -Ga₂O₃ thin films (<~1 μ m) on α -Cr₂O₃ has been demonstrated using mist CVD [1] and HVPE [2], showing dislocation densities on the order of 10⁷ cm⁻², about three orders of magnitude lower than those on sapphire substrates [1].

In this study, α -Ga₂O₃ films were grown on high-quality α -Cr₂O₃ templates to thicknesses far exceeding previously reported values, and their crystalline quality and electrical properties were investigated [3]. The films were grown by HVPE at 520 °C with thicknesses ranging from 0.24 to 21 μ m and a growth rate of approximately 14 μ m/h. X-ray diffraction measurements confirmed phase-pure, single-crystalline α -Ga₂O₃. The tilt angle estimated from X-ray rocking curves was close to that of the underlying α -Cr₂O₃ layer and did not increase with film thickness, while the twist angle increased for films thicker than 10 μ m. The dislocation density estimated from etch pit density (EPD) was 5.6×10⁷ cm⁻² for the thinnest film. Although it increased to 3.9×10⁸ cm⁻² for the 21 μ m-thick film, this value remains much lower than that of α -Ga₂O₃ layers of similar thickness grown directly on sapphire (~3×10⁹ cm⁻²).

Furthermore, Si-doped α -Ga₂O₃ films with a thickness of 2 μ m and EPD of ~1(–3)×10⁸ cm⁻² were fabricated and their electrical properties were evaluated by Hall measurements at room temperature. The mobility increased with decreasing carrier concentration, reaching 144 cm²/Vs at a carrier concentration of 1.8×10¹⁸ cm⁻³. This value significantly exceeds previously reported highest mobilities of approximately 52 cm²/Vs for c -plane [4] and 99 cm²/Vs for m -plane α -Ga₂O₃ [5].

[1] K. Yamada et al, the 72nd JSAP Spring Meet. 14-17 Mar, 2025, Noda, Japan, 16p-Y1311-7 (2025).

[2] K. Takeda et al, 44th Electron. Mater. Symp. (EMS-44), Nara, Japan, Oct 15-17, Fr1-12 (2025).

[3] Y. Oshima et al, J. Appl. Phys. 139, 075302 (2026).

[4] H. Son et al, ECS J. Solid State Sci. Technol. 9, 055005 (2020).

[5] T. Wakamatsu et al, Appl. Phys. Lett. 128, 012105 (2026).

* Author for correspondence: OSHIMA.Yuichi@nims.go.jp [mailto:OSHIMA.Yuichi@nims.go.jp]

11:05am **IWGO-WeM2-38 Homoepitaxial Growth on (0-1-1) β -Ga₂O₃ Substrates Using Oxide Vapor Phase Epitaxy**, Tomoka Nishikawa, The University of Osaka, Japan; Chia-Hung Lin, Kohei Sasaki, Akito Kuramata, Novel Crystal Technology, Inc., Japan; Eisho Kishimoto, Tomoyuki Tanikawa, Ryuji Katayama, Shigeyoshi Usami, Masayuki Imanishi, Yusuke Mori, The University of Osaka, Japan

β -Ga₂O₃ has a large bandgap considered suitable for high voltage power devices. Oxide vapor phase epitaxy (OVPE) enables the growth of high-purity films by utilizing Ga₂O gas and H₂O vapor as group-III and group-VI sources, respectively. We previously investigated growth conditions on the (001) and (010) planes by using OVPE; however, as macro steps occurred at the epitaxial surface due to growth rate anisotropy [1], it is necessary to improve the surface flatness by exploring different crystal orientations. In this study, we focus on the (0-1-1) (or (0-1-1)) plane, on which a flat epitaxial surface was obtained by halide vapor phase epitaxy (HVPE) [2]. (0-1-1) growth was carried out by OVPE on an edge defined film fed growth (EFG) substrate and achieved a growth rate of 5.0 μ m/h (thickness: 10 μ m), which is faster than that on the (001) plane (0.40 μ m/h, thickness: 0.80 μ m) under the same conditions. Additionally, the (0-1-1) surface exhibited no

macro-steps (Fig. 1(a)), in clear contrast to the pronounced macro-steps observed on the (001) surface (Fig. 1(b)). This result indicates that the (0-1-1) plane is promising for OVPE growth. An atomic force microscopy (AFM) image (Fig. 1(c)) revealed a root-mean-square (RMS) roughness of 11.2 nm, and streaks on the surface were observed. Pits were rarely observed on the (0-1-1) surface in OVPE (Fig. 2(a)), whereas hillocks appeared on the surface obtained by HVPE [3]. These pits were approximately 4 μ m deep (Fig. 2(b)) and are considered to have facets corresponding to the (-201) and (101) planes. [1] E. Kishimoto et al., Proc. 21st Int. Conf. on Crystal Growth and Epitaxy (ICCGE-21), H26 (2025). [2] K. Goto et al., Appl. Phys. Lett. 120, 102102 (2022). [3] Y. Oshima and T. Oshima, Sci. Technol. Adv. Mater. 26, 1 (2025).

11:20am **IWGO-WeM2-41 Fe Compensation Doping and Interface Stability for Mitigating Interfacial Si Conductivity in MBE-Grown β -Ga₂O₃ Thin Films**, Brenton Noesges, Prescott Evans, Jian Li, CoreAce; Mark Gordon, University of Dayton; Daram Ramdin, CoreAce; Nicholas Sepelak, KBR; Daniel Dryden, Air Force Research Lab, Sensors Directorate; Shin Mou, Adam Neal, Thaddeus Asel, Air Force Research Laboratory, Materials and Manufacturing Directorate

Parasitic conduction from accumulated Si between β -Ga₂O₃ films and substrate remains a persistent challenge for β -Ga₂O₃-based devices, particularly in lateral structures. Efforts to remove this interfacial Si via various etching methods have been mostly successful, however, in oxide molecular beam epitaxy (MBE), such efforts appear unsuccessful due to re-accumulation of Si from within the MBE including the Si dopant source. Instead of Si removal, we demonstrate how a thin layer of Fe-doped β -Ga₂O₃ on the substrate surface can compensate interfacial Si and eliminate the double-channel effect from lateral devices. Secondary ion mass spectrometry (SIMS) and capacitance-voltage (C-V) measurements confirm the Fe confinement to the substrate-film interface and interfacial charge compensation, respectively. Devices fabricated from epitaxial material using this interfacial Fe compensation show no double channel effect in ~97% of structures, significantly improved from device yield of <50% without Fe compensation. These results demonstrate a potential method to mitigate parasitic conduction channels due to interfacial Si in β -Ga₂O₃. While Fe seems initially promising, we are doing further studies on the stability of the interfacial Fe-doped layers to both processing conditions and electrical cycling during device operation. Alternative compensating acceptors including N or Mg need to be explored given the observation of capacitance transients in Fe-doped structures. Overall mitigating this parasitic interface will help improve yield and performance uniformity in fabricated devices.

11:35am **IWGO-WeM2-44 Coherent Growth of α -(Al,Ga)₂O₃ on α -Cr₂O₃ Templates by Mist-CVD**, Riena Jinno, The University of Tokyo, Japan; Shiyu Xiao, NGK Insulators, Ltd, Japan; Takayoshi Oshima, NIMS (National Institute for Materials Science), Japan; Satoshi Iwamoto, The University of Tokyo, Japan; Kazuto Murakami, NGK Insulators, Ltd., Japan; Katsuhiro Imai, Takahiro Tomita, NGK Insulators, Ltd, Japan

α -(Al,Ga)₂O₃ possesses the largest bandgap of 5.4-8.8 eV among (Al,Ga)₂O₃ polymorphs, and electrical conductivity is theoretically expected when the Al composition x is lower than 0.7 [1]. Sapphire substrates are commonly used for the growth of α -(Al,Ga)₂O₃; however, for x <0.7, the critical thickness is less than 50 nm, leading to high dislocation densities and consequently high resistivity [2]. α -Cr₂O₃, which is lattice matched with (Al,Ga)₂O₃, is promising as a substrate for Ga-rich α -(Al,Ga)₂O₃ growth. We previously reported the lattice-matched growth of α -(Al,Ga)₂O₃ using commercial α -Cr₂O₃ substrates, but the α -(Al,Ga)₂O₃ layers inherited the low crystallinity of the substrate [3]. High-quality α -Cr₂O₃/sapphire templates, whose dislocation density is lower than 10⁸ cm⁻², have been realized by a group at NGK Insulators, Ltd. Dislocation density in α -Ga₂O₃ layers grown on the template were lower than 10⁸ cm⁻², which was three orders of magnitude smaller compared to α -Ga₂O₃ films grown on sapphire substrates [4,5]. In this study, we report coherent growth of α -(Al,Ga)₂O₃ on the α -Cr₂O₃/sapphire templates.

(Al,Ga)₂O₃ films were grown on c -plane α -Cr₂O₃/sapphire templates manufactured by NGK Insulators, Ltd using a hot-wall-type mist-CVD system. The Al composition x in the grown films varied from 0.05 and 0.5. A symmetric x -ray diffraction $2\theta/\omega$ scan profile for the samples showed that the successful growth of single-phase α -(Al,Ga)₂O₃ on the α -Cr₂O₃ templates. Reciprocal space mapping revealed that the α -(Al,Ga)₂O₃ films with a film thickness of ca. 50 nm were coherently grown on the α -Cr₂O₃ templates when x was lower than 0.33. Surface atomic force microscopy images of the coherently grown samples revealed smooth surface

Wednesday Morning, August 5, 2026

roughness with root mean square roughnesses smaller than 0.12 nm. When $x = 0.09$ (almost lattice matched to $\alpha\text{-Cr}_2\text{O}_3$), the film was coherently grown on the template when the film thickness was ca. 900 nm. These findings suggest that the $\alpha\text{-Cr}_2\text{O}_3$ template holds promise for the growth of high quality $\alpha\text{-(Al,Ga)}_2\text{O}_3$ in the Ga-rich region, thus paving the way for the development of advanced $\alpha\text{-(Al,Ga)}_2\text{O}_3$ -based heterostructure devices.

This work was partly supported by Grants-in-Aid for Scientific Research (25K17958) and Nippon Sheet Glass Foundation for Materials Science and Engineering.

[1] D. Wickramaratne, *et al.*, Appl. Phys. Lett. **121**,042110P. (2022).

[2] H. Okumura and J. B. Varley, *Jpn. J. Appl. Phys.* **63** 075502.

[3] R. Jinno, *et al.*, IWGO-4, WeP-9 (2024).

[4] M. Watanabe, *et al.*, JSAS Autumn Meet., 20p-A302-9 (2023).

[5] Y. Oshima, *et al.*, J. Appl. Phys. **139**, 075302 (2026).

*Author for correspondence:jinno@iis.u-tokyo.ac.jp

11:50am **IWGO-WeM2-47 Demonstration of Homojunction Ga₂O₃ PiN Diodes with High Bipolar Injection**, *Pierre Gallarday, Aniol Vellvehi, Miquel Vellvehi, José Rebollo, Josep Montserrat*, INSTITUTE OF MICROELECTRONICS OF BARCELONA - (IMB-CNM-CSIC), Spain; *Corine Sartel, Yves Dumont, Ekaterine Chikozide*, Groupe d'étude de la matière condensée (GEMaC) - UVSQ, France; *Amador Pérez-Tomás*, INSTITUTE OF MICROELECTRONICS OF BARCELONA - (IMB-CNM-CSIC), Spain

Gallium oxide (Ga₂O₃) is widely recognized as a premier next-generation, ultra-wide-bandgap (UWBG) semiconductor for energy, power and deep-UV optoelectronics, offering a compelling pathway beyond the limits of Si, SiC, and GaN. However, to fully exploit the benefits of Ga₂O₃ in high-power applications, achieving *p*-type conductivity and, consequently, an effective *p-n* junction is mandatory. This remains as one of the major challenges of the technology.

Ion implantation technique has attracted attention to form stable *p*-type conduction when applied into epitaxial layer in homojunction systems. Very recently, vertical *p-n* junctions using Phosphorous (P) have been reported. This is an unexpected result as, in general, P implantation in $\beta\text{-Ga}_2\text{O}_3$ is regarded as amphoteric and only a deep acceptor. However, when the P doping dose is sufficiently high in the implanted regions, a delocalization-localization regime has been observed typically associated with disordered systems in Anderson-localization physics, i.e., a metal-insulation transition (MIT) at low-T that enables hole transport.

In this work, a homoepitaxial PiN diode was engineered and presents unambiguous high-injection bipolar operation. We apply the recently reported methodology of acceptor extended wavefunctions in disordered system (related to Anderson disorder) via a P implantation route performed on epitaxial highly resistive *p*-type Ga₂O₃ grown via MOCVD on commercial highly conductive Sn-doped (001) substrates. Here, we demonstrate that using a native lightly doped *p*-type intrinsic epi reduces the residual donor and increase bipolar conductivity modulation which results in an easier minority lifetime control. The consistent device demonstration of $8\text{-}6\times 10^{18}$ cm⁻³ free hole depletion and electron-hole plasma adds further evidence that bipolar devices are possible in Ga₂O₃ and confirm that P implantation is a route for implementing homoepitaxial *p-n* junctions.

In summary, our results show that the introduction of native *p*-type conductivity compensates residual donor defects, enhances bipolar conductivity modulation, and enables improved control of carrier lifetime. The reproducible observation of free-hole depletion and electron-hole plasma in the range of $\sim 1\text{-}8\times 10^{18}$ cm⁻³ at room T provides further compelling evidence for the feasibility of bipolar device operation in Ga₂O₃. In unternated devices, it is yet possible to achieve minority carrier lifetimes of 0.1-0.2 ms, current densities above 6000 A/cm², breakdown voltages larger than 500V and on-off ratios of 10⁷. These results open new research avenues toward advanced Ga₂O₃ power electronic devices based on disordered extended waveform concepts.

12:05pm **IWGO-WeM2-50 Uniform Growth of Thick Homoepitaxial $\beta\text{-Ga}_2\text{O}_3$ Layers on 2-inch (010) Substrates by Low-Pressure Hot-Wall MOVPE**, *Yoshiki Iba, Yuma Terauchi*, Tokyo University of Agriculture and Technology, Japan; *Junya Yoshinaga*, TAIYO NIPPON SANSO CORPORATION, Japan; *Yasuhiro Hashimoto*, Sumitomo Metal Mining Co. Ltd., Japan; *Yoshinao Kumagai*, Tokyo University of Agriculture and Technology, Japan

$\beta\text{-Ga}_2\text{O}_3$ is a promising candidate material for next-generation power devices. The growth of thick homoepitaxial layers with controlled conductivity is essential for vertical device fabrication. Recently, our group demonstrated high-speed growth of Si-doped n-type homoepitaxial layers

with a carrier concentration of 2×10^{16} cm⁻³ on $\beta\text{-Ga}_2\text{O}_3(010)$ small-sized substrates (10×15 mm²) by low-pressure hot-wall metalorganic vapor phase epitaxy (MOVPE) [1]. In this study, homoepitaxial growth was carried out on 2-inch $\beta\text{-Ga}_2\text{O}_3(010)$ substrates, and the crystallinity and uniformity of the grown layers were investigated.

A horizontal low-pressure hot-wall MOVPE reactor (TAIYO NIPPON SANSO, FR2000-OX) was used. Si-doped homoepitaxial layers were grown on a 2-inch-diameter Sn-doped $\beta\text{-Ga}_2\text{O}_3(010)$ substrate for 150 min at a reactor pressure of 3.4 kPa and a growth temperature of 1000°C using trimethylgallium (TMGa), O₂, and tetramethylsilane (TMSi) as the Ga, oxygen, and Si dopant sources, respectively, using Ar as the carrier gas.

An approximately 11 μm -thick homoepitaxial layer with a smooth surface was obtained over the entire substrate. The X-ray rocking curves of $\beta\text{-Ga}_2\text{O}_3(020)$ measured at various positions on the 2-inch substrate all exhibited full width at half maximum (FWHM) values in the range of 27–38 arcsec, comparable to those of the original substrate. Furthermore, secondary-ion mass spectrometry measurements revealed a uniform Si doping concentration of approximately 1×10^{16} cm⁻³ at all measured positions, suggesting that the prepared homoepitaxial substrate is suitable for device fabrication.

This work was supported by MIC under a grant entitled “R&D of ICT Priority Technology (JPMI00316): Next-Generation Energy-Efficient Semiconductor Development and Demonstration Project (second period) (in collaboration with MOEJ).”

[1] J. Yoshinaga *et al.*, Appl. Phys. Express **18**, 055503 (2025).

Wednesday Afternoon, August 5, 2026

International Workshop on Gallium Oxide and Related Materials (IWGO-6)

Room ESJ 0202 - Session IWGO-WeA

Advanced Device Scaling and Fabrication Techniques I

Moderators: Siddarth Rajan, The Ohio State University, Yuhao Zhang, University of Hong Kong

2:00pm IWGO-WeA-1 Recent Advances in β -Ga₂O₃ Power and RF Device Technologies, Uttam Singiseti, University at Buffalo

INVITED

The ultrawide-bandgap semiconductor β -gallium oxide (Ga₂O₃) has emerged as a promising material for power electronics, RF, and high-speed switching applications. This talk presents recent advances in Ga₂O₃ device technologies developed by our group. We demonstrate lateral Ga₂O₃ MOSFETs incorporating optimized field-plate designs that achieve beyond-kilovolt breakdown voltages, along with their switching characteristics under electrical stress conditions. The role of in situ Mg-doped MOCVD-grown Ga₂O₃ films as efficient current-blocking layers (CBLs) is discussed. In addition, trench MOSFET architectures incorporating CBLs are presented for high-voltage, high-speed operation targeting grid-level power applications. Strategies for mitigating thermal management challenges in Ga₂O₃ devices are also addressed.

Owing to its high Johnson's figure of merit, Ga₂O₃ is also a strong candidate for high power density RF amplifiers. We report significant improvements in RF power performance using Ga₂O₃ technology. By aggressively scaling gate lengths and gate-source spacing, (Al_xGa_{1-x})₂O₃/Ga₂O₃ heterostructure FETs were fabricated, demonstrating record RF performance. We will also report the radiation tolerance of the RF devices.

2:25pm IWGO-WeA-6 1.5 kV/0.6 A Double Pulse Test Switching Of Cr₂O₃/ β -Ga₂O₃ Heterojunction Diodes With > 3 kV Breakdown Voltages And Record Low Reverse Recovery Charge, Chinmoy Nath Saha, University of California Santa Barbara; Yuzhou Yao, Juchen Yang, The Ohio State University; Yizheng Liu, University of California at Santa Barbara; Pengyu Fu, Shuwei He, The Ohio State University; James S. Speck, University of California at Santa Barbara; Jin Wang, The Ohio State University; Sriram Krishnamoorthy, University of California at Santa Barbara

β -Ga₂O₃ heterojunction diodes (HJD) incorporating different p-type oxides (NiO_x, Cu₂O, Cr₂O₃) have been demonstrated with multi-kV-class breakdown voltages. In this work, we report the first experimental demonstration of kV-class static and switching performance of Cr₂O₃/ β -Ga₂O₃ heterojunction diodes (HJD) with > 3 kV breakdown voltages. The devices were fabricated on (001)-oriented 9.5 μ m thick β -Ga₂O₃ drift layer grown by halide vapor phase epitaxy (HVPE) on a conductive β -Ga₂O₃ substrate. Bi-layer Cr₂O₃ and anode metal (Ni/Au/Ni) were lifted off simultaneously to fabricate the HJD. A 1.5 μ m mesa etch was employed to realize an effective edge termination. The fabricated HJDs exhibited a forward current density of 125 A/cm² at 4.5 V and a differential specific on-resistance of \sim 19 m Ω ·cm². Breakdown voltage of \sim 3.2 kV was achieved for a wide range of device dimensions (diameter = 60-300 μ m) with noise floor reverse leakage up to 2.5-3 kV. This is a significant achievement since breakdown voltage showed no substantial degradation with increasing device dimensions [1]. Based on a punch-through model, the estimated parallel-plane breakdown field approached \sim 4 MV/cm. In addition, the switching performance of β -Ga₂O₃ power diodes is critical for high-frequency power conversion applications. A double pulse test (DPT) was employed, where Ga₂O₃ HJD served as the upper device and a commercially available SiC MOSFET served as the lower switching device. At a reverse voltage of 1.5 kV and a peak forward current of about 0.6 A, the HJD showed a peak reverse recovery current (I_{rr}) of \sim 0.128 A, a reverse recovery time (t_{rr}) of 12.8 ns, and an ultralow reverse recovery charge (Q_{rr}) of 0.74 nC. This is the highest test voltage and lowest reverse recovery charge reported for the β -Ga₂O₃ diode switching test. Additional measurements at 1 kV with peak forward currents ranging from 0.3 to 0.7 A showed relatively stable I_{rr} , t_{rr} , Q_{rr} at 0.1 A, 15 ns, and 0.6 nC, respectively. In comparison with a commercial SiC MPS diode exhibiting Q_{rr} of 41 nC and t_{rr} of 20 ns at 1.2 kV, the Cr₂O₃/ β -Ga₂O₃ HJDs reported here show improved reverse recovery characteristics. In summary, we have achieved > 3 kV breakdown voltages with 4 MV/cm parallel plane electric field for a wide range of device dimensions by fabricating Cr₂O₃/ β -Ga₂O₃ heterojunction diodes (HJD) with an optimized edge termination. The combination of multi-kV static breakdown voltages with sub-nC reverse recovery charge at 1.5 kV test voltage highlights the strong potential of Cr₂O₃/ β -Ga₂O₃ HJDs for future medium-voltage and high-frequency power conversion applications.

[1]. Liu, AIP Advances, **15**, 015114 (2025).

2:40pm IWGO-WeA-9 Sub-Micron β -Ga₂O₃ FinFETs with >700 mA/mm Current Density and >10⁸ ON/OFF Ratio Using Si δ -Doped Channels, Nabisindhu Das, Arizona State University

β -Ga₂O₃ is a promising ultra-wide bandgap semiconductor for RF/mm-wave transistors due to its large critical breakdown field (\sim 8 MV/cm), high saturation velocity (\sim 2 \times 10⁷ cm/s), and availability of bulk substrates. However, achieving high current density and strong electrostatic control in scaled devices remains challenging with uniformly doped channels due to short-channel effects. In this work, we demonstrate sub-micron gated depletion-mode β -Ga₂O₃ FinFETs employing Si δ -doped channels with sheet charge density exceeding 3 \times 10¹³ cm⁻², enabling enhanced carrier confinement and improved device performance. The δ -doped epitaxial structure was grown by MOCVD as shown in Fig.1 (b). Fin structures with 100 nm width and 200 nm spacing were defined using e-beam lithography and ICP-RIE etching (Fig.1 a, c). Ohmic contact regrowth was used to achieve low contact resistance, followed by ALD deposition of a 7 nm Al₂O₃ gate dielectric and fabrication of sub-micron gates ($L_G \approx$ 150 nm). Hall measurements indicate a sheet carrier density of \sim 3.3 \times 10¹³ cm⁻² with mobility of \sim 89 cm²/V·s. Devices exhibit low contact resistance and a sharp doping profile with \sim 4.8 nm FWHM. Transfer characteristics show clear pinch-off with threshold voltage \sim -17 V, subthreshold slope \sim 239 mV/dec, and ON/OFF ratio exceeding 10⁸ with low gate leakage. Output characteristics demonstrate current saturation with peak drain current >700 mA/mm. Pulsed I-V measurements reveal \sim 20% current collapse, indicating the need for improved surface passivation. Small-signal RF measurements yield $f_T \approx$ 6.3 GHz and $f_{MAX} \approx$ 2 GHz. These results highlight the potential of δ -doped β -Ga₂O₃ FinFETs as promising platform for high power RF applications. This work is supported by the Army Research Office UWBG RF center under award No. W911NF2520005

2:55pm IWGO-WeA-12 Over 3 kV Ultra-low Leakage Vertical (011) β -Ga₂O₃ Diodes with Schottky Contact Engineering and High- κ Field Plate, Emerson Hollar, Esmat Farzana, Iowa State University

The β -Ga₂O₃ has achieved great interest for high-power devices due to its large critical breakdown field, shallow dopants, and melt-grown native substrates. To achieve the desired multi-kV β -Ga₂O₃ power switches, vertical devices with low-doped, thick drift layer and minimal defects are essential requirements. However, to date, scaling up the voltage rating of vertical β -Ga₂O₃ devices has remained severely limited due to the presence of killer dislocation defects and unintentional [Cl] impurities that creates difficulties in achieving high-quality thick drift layer (>10 μ m) and lower doping (<8 \times 10¹⁵ cm⁻³) with the existing (001) β -Ga₂O₃ epiwafers grown by halide vapor phase epitaxy (HVPE). To overcome these constraints, the recently emerged HVPE (011) β -Ga₂O₃ epiwafers has brought tremendous potential by offering reduced dislocation effects due to the dislocation being parallel to the (011) plane as well as low unintentional [Cl] impurities [1]. However, due to their early stage, high-power vertical Schottky barrier diodes (SBD) on (011) β -Ga₂O₃ epiwafers are yet to be reported.

In this work, we report high-voltage vertical (011) β -Ga₂O₃ SBDs on HVPE-grown 20 μ m thick drift layer with 1 MHz C-V extracted doping \sim 5 \times 10¹⁵cm⁻³. Two different Schottky contact diodes were co-fabricated with 100 μ m diameters, including Pt/ β -Ga₂O₃ and PtO_x/thin Pt (1.5 nm)/ β -Ga₂O₃. The PtO_x/thin Pt contact merges the benefits of both low turn-on voltage from interfacing Pt while allowing improved reverse blocking by PtO_x [1]. To reduce edge field crowding, we integrated high-permittivity (κ) ZrO₂ field-plate (FP) for both contacts using a stack of sputtered ZrO₂ (226 nm) on interfacing thin ZrO₂ (9 nm) formed by atomic layer deposition to protect the surface from sputter damage. The forward J-V showed excellent transport properties with near unity ideality factor and similar turn-on voltage for both cases. At reverse bias, the SBDs without FP revealed similar breakdown voltage of \sim 1.5 kV for both cases. However, with FP, the PtO_x/thin Pt SBDs showed significantly enhanced breakdown voltage \sim 3.7 kV compared to the Pt ones (2.75 kV) and punch-through field with a peak of 5 MV/cm at FP edge, reaching ZrO₂ breakdown limit. Moreover, the FP PtO_x/thin Pt SBDs demonstrated ultra-low leakage which is order of magnitude lower compared to existing reports of (001) β -Ga₂O₃ SBDs of same 100 μ m diameter at 3 kV operation. **To the best of our knowledge, this is the first report of high-power vertical (011) β -Ga₂O₃ SBDs that shows its great potential to expand the performance limit of low-loss multi-kV β -Ga₂O₃ devices.**

[1] E. J. Hollar and E. Farzana, *Appl. Phys. Lett.* **128**, 053503 (2026).

Wednesday Afternoon, August 5, 2026

3:10pm IWGO-WeA-15 Vertical Ga₂O₃(010) FinFETs Processed with Nitrogen Radical Irradiation, *Zhenwei Wang*, National Institute of Information and Communications Technology, Japan; *Jin Inajima*, *Kohki Tsujimoto*, *Yusuke Teramura*, Osaka Metropolitan University, Japan; *Yoshiki Iba*, *Yuma Terauchi*, Tokyo University of Agriculture and Technology, Japan; *Junya Yoshinaga*, Tokyo University of Agriculture and Technology/TAIYO NIPPON SANSO CORPORATION, Japan; *Takafumi Kamimura*, National Institute of Information and Communications Technology, Japan; *Yoshinao Kumagai*, Tokyo University of Agriculture and Technology, Japan; *Masataka Higashiwaki*, Osaka Metropolitan University/NICT, Japan

We studied the effects of nitrogen (N) radical irradiation on device characteristics of vertical Ga₂O₃(010) fin field-effect transistors (FinFETs). A positive threshold voltage (V_{th}) shift for the nitridated FinFET from the V_{th} value for the non-nitridated one was observed. The in-plane uniformity of V_{th} was also improved for the nitridated FinFETs. Finally, a multi-FinFET with fin width of 300 nm showed superior device characteristics such as a V_{th} of +1.0 V, a specific on-resistance (R_{on}) of 9.5 m Ω cm², a breakdown voltage (V_{br}) of 1,213 V, and a power figure of merit (V_{br}^2/R_{on}) of 0.15 GWcm⁻². These results indicate that N radical irradiation can be a useful technique to fabricate normally-off Ga₂O₃ FinFETs with an excellent in-plane uniformity of device performance.

3:25pm IWGO-WeA-18 Enhancement-Mode Ga₂O₃ CAVETs with Improved Breakdown Voltage by Hot Implantation, *Jun Morihara*, Osaka Metropolitan University, Japan; *Daisuke Matsuo*, *Shun Konno*, *Kosuke Usui*, *Shinya Takemura*, Nissin Ion Equipment Co., Ltd., Japan; *Zhenwei Wang*, National Institute of Information and Communications Technology, Japan; *Romualdo Ferreyra*, Osaka Metropolitan University, Japan; *Kohei Tanaka*, Nissin Ion Equipment Co., Ltd., Japan; *Masataka Higashiwaki*, Osaka Metropolitan University, Japan

Normally-off operation is highly demanded for FETs to ensure fail-safe capability in high-voltage and high-power applications. Enhancement-mode (E-mode) Ga₂O₃ current aperture vertical FETs (CAVETs) fabricated using room-temperature Si- and nitrogen (N)-ion implantations have been demonstrated [1]. Overall on-state device characteristics of the CAVETs were decent; however, the off-state breakdown voltage (V_{br}) was as low as 263 V [1], which could be attributed to the insufficient recovery of crystal damage caused by the implantations. In this work, we employed hot ion implantation to minimize the crystal damage and enhance V_{br} .

We used *n*-Ga₂O₃ (001) epitaxial substrates having an *n*-Ga₂O₃ drift layer grown by halide vapor phase epitaxy. The CAVET fabrication process started with N hot implantation. N ions with a dose of 1×10^{14} cm⁻² were implanted into the *n*-Ga₂O₃ drift layer at 450°C, followed by activation annealing at 1000°C for 20 min in N₂ atmosphere. Subsequently, multiple Si implantations were performed at 300°C to form an *n*-channel layer, *n*⁺-access regions, and *n*⁺-drain and source ohmic regions. The activation annealing of the Si implants was carried out at 800°C for 30 min. A 50-nm-thick Al₂O₃ gate dielectric was formed by atomic layer deposition on the channel layer. Source and drain ohmic electrodes, and gate electrodes were fabricated with Ti/Au and Ti/Pt/Au metal stacks, respectively. The aperture size and the Si-implanted channel area were 20 μ m and 210 \times 25 μ m², respectively.

Drain current–drain voltage (I_d – V_d) characteristics showed that at a gate voltage (V_g) of +6 V, the CAVET exhibited near-linear I_d turn-on behavior in the low V_d range and quasi-saturation at $V_d \sim 20$ V, and reached the maximum I_d of 0.123 kA/cm² at $V_d = 40$ V. The I_d – V_g characteristics at $V_d = 20$ V provided a high I_d on/off ratio of 1×10^{11} , which can be attributed to superior current-blocking capability of the N-implanted region formed by hot implantation. The threshold V_g extracted from linear extrapolation of the I_d – V_g curve was +3.8 V, ensuring the E-mode normally-off operation. The off-state I_d leakage at $V_g = 0$ V monotonically increased with increasing V_d and saturated at $10^{-3} - 10^{-2}$ A/cm² for $V_d > 100$ V. Then, destructive breakdown occurred near the gate electrode edge at $V_d = 756$ V. All on- and off-state device characteristics of the CAVET in this work were superior to those of the previous one [1]. Among the improvements, the most significant was the threefold increase in V_{br} . These results indicate that the hot implantation process is effective in improving endurance of Ga₂O₃ CAVETs.

[1] M. H. Wong *et al.*, IEEE Electron Device Lett. **41**, 296 (2020).

3:40pm IWGO-WeA-21 Enhancement-Mode Vertical β -Ga₂O₃ U-Trench MOSFET with N-doped CBL and MOCVD regrown n⁺ Contact Layers, *Walid Amir*, *Jiawei Liu*, *Surajit Chakraborty*, University at Buffalo-SUNY; *Dongsu Yu*, *Md. Mosarof Hossain Sarkar*, *Hingping Zhao*, Ohio State University; *Uttam Singiseti*, University at Buffalo-SUNY

Due to its large bandgap (~ 4.8 eV) and strong critical electric field (~ 8 MV/cm), β -Ga₂O₃ has drawn a lot of attention as an ultra-wide-bandgap (UWBG) semiconductor for high-power applications. However, because traditional n⁺ contact methods rely on ion implantation followed by high-temperature activation annealing, which increases process complexity and may degrade material quality, the realization of cost effective and low-resistance ohmic connections is still difficult. In this work, we reduce thermal budget while preserving electrical performance by using a regrown n⁺ contact layer to create highly doped contact areas without post-implantation annealing.

The fabrication process started on commercially available Sn-doped (001) β -Ga₂O₃ substrates with a ~ 10 μ m HVPE-grown epitaxial drift layer. The CBL was formed by N-ion implantation at multiple energy levels followed by annealing in N₂ atmosphere to activate the nitrogen dopants. In contrast to the conventional approach of using Si-ion implantation for ohmic contact formation, which requires additional high-dose implantation steps, dedicated masking, and high-temperature activation annealing, this work introduces a regrown Si-doped n⁺ contact layer (~ 75 nm) with a high carrier concentration of $\sim 10^{18}$ cm⁻³ deposited directly by MOCVD epitaxial regrowth.

The ohmic contact quality was validated by transmission line model (TLM) measurements, yielding a transfer length $L_T = 0.13$ μ m, contact resistance $R_C = 0.38$ Ω -mm, sheet resistance $R_{SH} = 1389$ Ω /sq, and specific contact resistivity $\rho_C = 2.65 \times 10^{-7}$ Ω -cm². Transfer characteristics demonstrated normally-off operation with a clear threshold voltage of $V_{TH} = 5$ V and an I_{ON}/I_{OFF} ratio of 8.5×10^5 . From the output (I_D – V_{DS}) characteristics swept with $V_{GS} = 0$ to 20 V in 5 V steps, a peak current density exceeding 100 A/cm² was achieved, with an on-resistance $R_{ON} = 94.6$ m Ω -cm².

Three-terminal off-state breakdown measurements were performed in Fluorinert (FC-40) liquid to suppress air arcing. At $V_{GS} = 0$ V, breakdown voltages of 920 V–980 V were recorded across three representative devices, demonstrating excellent device-to-device uniformity and robust blocking capability. The resulting Baliga figure of merit (BFOM = V_{BR}^2/R_{ON}) makes this work well competitive with state-of-the-art vertical β -Ga₂O₃ devices.

This work demonstrates a high-performance enhancement-mode vertical β -Ga₂O₃ trench-gate MOSFET with N-ion implanted CBL and a simplified ohmic contact scheme based on epitaxial n⁺ regrowth. The regrown n⁺ contact approach offers a practical, cost-effective, and thermally efficient alternative to ion-implanted contacts, without sacrificing electrical performance.

Wednesday Evening, August 5, 2026

International Workshop on Gallium Oxide and Related Materials (IWGO-6)

Room Concourse - Session IWGO-WeP

IWGO Poster Session III

Moderators: Hari Nair, Cornell University, Saurav Roy, North Carolina State University

IWGO-WeP-1 Ultra-Sensitive Arc-Detecting DUV Sensor based on p-NiO/ β -Ga₂O₃ Heterojunction Using p⁺ NiO Interlayer, *Taejun Park, Yusup Jung, Sanghun Kim, TaiYoung Kang, SinSu Kyoung, Powercubesemi, Inc., Republic of Korea*

Ultraviolet (UV) radiation from the sun can be divided into UV-A (320–400 nm), UV-B (280–320 nm), and UV-C (200–280 nm). Among them, UV-C light is strongly absorbed by the ozone layer at the earth's surface, so it is also called solar-blind deep UV light (DUV). The need for DUV sensing is increased because of its properties such as arc discharge detection in power plants and sterilization. And DUV sensor research has been extensively conducted in various fields, including biological and chemical analyses, arc detectors, and flame sensors [1].

In this study, we simply fabricated a DUV sensor based on p-NiO/ β -Ga₂O₃ heterojunction by the RF sputtering system. In addition, the experiment was conducted to investigate the effect of p⁺NiO interlayer on the electrical and photoresponse characteristics of the as-fabricated DUV sensor.

As a result, the as-fabricated DUV sensor with p⁺ NiO interlayer had a low leakage current of 7.34×10^{-9} A, high photocurrent of 4.01×10^{-6} A, fast rise and fall times of 30 and 50 ms were observed under UV-C irradiation at -5V bias. The effect of p⁺NiO interlayer on p-NiO/ β -Ga₂O₃ heterojunction DUV sensor has confirmed their potential for application in DUV and Arc detecting systems, and further research is planned to improve the device characteristics.

IWGO-WeP-2 Electrical Characterization of Mist-CVD HfO_x/ β -Ga₂O₃ MIS Capacitor, *Hayato Tanikawa*, Kyoto Institute of Technology, Japan; *Kazutaka Kanegae, Hiroyuki Nishinaka*, Kyoto Institute of Technology, Japan β -Ga₂O₃ is expected to be used in power switching devices. HfO_x films are one of promising gate dielectrics for β -Ga₂O₃-based devices due to its high dielectric constant. Previous studies have reported HfO_x films deposited by ALD. In this study, mist-CVD was used to deposit HfO_x gate dielectrics. Mist-CVD achieves a deposition rate that is an order of magnitude higher than ALD and does not require vacuum equipment, making it a low-cost technique.

A 40-nm-thick HfO_x film was deposited on HVPE β -Ga₂O₃ epitaxial layers by mist-CVD using the solution gas of O₂, with an O₂/O₃ gas mixture as the carrier gas. The deposition temperature was set to 400°C. The dielectric constant of the mist-CVD HfO_x film was 10.8. Post-deposition annealing (PDA) was performed at 350°C for 10 min in N₂ ambient. Finally, Ni gate and Ohmic electrodes were formed on the HfO_x surface and backside of the β -Ga₂O₃ epitaxial wafer, respectively.

Capacitance-voltage (C-V) characteristics of MIS capacitor were measured at 1MHz. The voltage sweeps were set from -3 V to 7 V (1st sweep) and from 7 V to -3 V (2nd sweep). The experimental C-V curves have a positive voltage shift relative to the ideal curve. Using the flat-band voltage shift of 2.70 V, we extracted a net negative fixed charge density of $Q_f = 6 \times 10^{-7}$ C/cm², which is comparable to the values for ALD HfO_x (10^{-7} to 10^{-6} C/cm²). Hysteresis was observed in the measured C-V characteristics. From the flat-band voltage hysteresis of 0.8 V, we estimated an averaged interface trap density of $D_{it,ave} = 2 \times 10^{11}$ cm⁻² eV⁻¹, which is also comparable to the values for ALD HfO_x (10^{10} to 10^{12} cm⁻² eV⁻¹). With the addition of PDA treatment, Q_f and $D_{it,ave}$ decreased to 4.6×10^{-7} C/cm² and 1.3×10^{11} cm⁻² eV⁻¹, respectively.

In the HfO_x/ β -Ga₂O₃ MIS structure, we successfully formed a HfO_x film by mist-CVD at a higher deposition rate than ALD, with Q_f and $D_{it,ave}$ comparable to those of ALD HfO_x. HfO_x deposited by mist-CVD is a promising gate dielectric for β -Ga₂O₃ power switching devices.

IWGO-WeP-3 Tuning the Conductivity of p-type Ni_{1-x}O Thin Films for Ni_{1-x}O/ β -Ga₂O₃ Heterojunction Power Devices, *Thomas Ribault, Akash Patnaik, Bruno Berini, Corinne Sartel*, CNRS-UVSQ, France; *Yunlin Zheng, Jean-Louis Cantin*, CNRS-INSP, France; *Zurab Kushitashvili, Amiran Bibilashvili*, Institute of Nano et Microelectronics, Tbilisi, Georgia; *Tom Micottis, Farid Medjdoub*, CNRS-I.E.M.N., France; *Ekaterine Chikoidze, Yves Dumont*, CNRS-UVSQ, France

Several research groups in the past, reported NiO/ β -Ga₂O₃ rectifiers performance through empirical optimisation of device structure and edge termination [1-4]. However, a well-established materials-physics framework

for sputtered Ni_{1-x}O thin films remains missing. Present work fills this gap by establishing how reactive RF sputtering deposition at room-temperature controls the structural, chemical, and point defect landscape of Ni_{1-x}O, and which in turn governs Ni_{1-x}O/ β -Ga₂O₃ heterojunction structure band alignment, interface quality, carrier transport, and breakdown capability.

Ni_{1-x}O thin films were deposited using reactive RF magnetron sputtering by varying the O₂ fraction from 0 to 100%, and the applied RF power from 50 to 200 Watts. 20-200 nm thin films were deposited primarily on c-sapphire (0001). The room-temperature resistivity decreases, from 5 Ω .cm (50 W) to 0.9 Ω .cm (200 W), and from 30 Ω .cm (20% O₂) to 0.01 Ω .cm (100% O₂), with ~1nm RMS roughness (AFM). XRD patterns consistently show a cubic NiO (111) phase, and the best crystalline quality obtained between 40-60% O₂. NIR transmittance decreases with increasing O₂ fraction, since Ni vacancy and hole carrier density increases, which enhances free-carrier absorption. Kelvin probe measurements show that the work function of Ni_{1-x}O remains constant at 4.23 eV for films deposited at 20-90% O₂, which implies constant Fermi level, thus, indicating hopping conductivity mechanism with localised carriers. The optimised Ni_{1-x}O thin films with different thicknesses were then deposited on 10 μ m Si: β -Ga₂O₃ (001) epilayers from NCT, Japan. Subsequently, vertical Ni_{1-x}O/ β -Ga₂O₃ heterojunction PiN diodes were fabricated, which exhibits rectifying behaviour with a V_{ON} ~1.9 V and low leakage current densities ~10⁻⁷-10⁻⁸ A/cm². Thus, this study will enable to engineer p-type Ni_{1-x}O film using room-temperature RF sputtering technique, for the realization of high-breakdown voltage β -Ga₂O₃ heterojunction power devices.

References

- [1] S. J. Pearton *et al.*, *A.P.R.*, 5, 011301 (2018)
- [2] J.-S. Li *et al.*, *A.P.L.*, 121, 042105 (2022)
- [3] H. Gong *et al.*, *IEEE*, 67, 8, 3341-3347 (2020)
- [4] A. Taube *et al.*, *M.S.S.P.*, 184, 108842 (2024)

IWGO-WeP-4 Electro-Optical Metrology Development to Probe Deep-Level Traps in β -Ga₂O₃ MOSFETs, *Ory Maimon*, George Mason University; *Neil Moser*, Air Force Research Laboratory; *Pragya Shrestha, Min-Yeong Kim*, National Institute for Science and Technology (NIST); *Sang-Mo Koo*, Kwangwoon University, Republic of Korea; *Greg Liddy, Andrew Green, Kelson Chabak*, Air Force Research Laboratory; *Qiliang Li*, George Mason University; *Sujitra Pookpanratana*, National Institute for Science and Technology (NIST)

Although the performance of β -Ga₂O₃ high power devices as field-effect transistors (FETs) have progressed rapidly in recent years, device performance is hindered by defects and traps. Traditional trap characterization methods are sensitive to shallow traps. High densities of traps can significantly reduce mobility by scattering free carriers. However, the long emission time of deep traps in WBG semiconductors requires the use of optical excitation and novel techniques such as deep-level optical spectroscopy, persistent photo-capacitance, photo-assisted C-V (PCV), and photo-assisted I-V (PIV).

In this work, PCV and PIV with sub-bandgap photon energies, E_hv, is used to study the ionized impurity scattering of deep level traps in a lateral depletion-mode β -Ga₂O₃ FET. The density of interface trap states (D_{it}) in β -Ga₂O₃ FETs was determined between 0.4 eV – 4.4 eV below the conduction band (EC) of β -Ga₂O₃. D_{it} peaks near the band edges, similar to conventional material systems. Based on the results, traps located between EC – 4.0 eV and EC – 3.4 eV are primarily responsible for carrier scattering, reducing the mobility by 50 % – 75 % in these devices. The increased mobility degradation further from the interface is attributed to traps located in the bulk.

Author for correspondence: sujitra@nist.gov

IWGO-WeP-5 The Morphology of the Cr₂O₃ Films Surfaces Analyzed by Multifractal Formalism, *Pavel Butenko*, Ioffe Institute, Russian Federation
It is a completely new state-of-art work that analyses diverse surface morphologies of the Cr₂O₃ films deposited on sapphire substrates by mist CVD via Multifractal formalism.

In this abstract, we characterize the surface relief using Multifractal formalism, which determines a number of geometric features that allow us to evaluate various parameters of multifractality. The conditions under which the film shows the maximum nonlinear complexity of the surface, which is required for its functionality, are found. Contrary to the roughness assessment and the regular fractal approach, the multifractal formalism is able to perform in-depth surface morphology analysis necessary to verify the effectiveness of the surface. This will be useful for various functional

applications, for example, the sensor capability of Cr_2O_3 , which is a promising wide bandgap semiconductor material.

IWGO-WeP-6 Growth of 2-inch n-type $\beta\text{-Ga}_2\text{O}_3$ (011) Single Crystal by the VB Method, Yuki Ueda, Takuya Igarashi, Kimiyoshi Koshi, Sho Hasegawa, Ryoichi Sakaguchi, Taiki Chujo, Ryo Shinagawa, Kohei Sasaki, Akito Kuramata, Novel Crystal Technology, Inc., Japan

Homoeptaxial growth of $\beta\text{-Ga}_2\text{O}_3$ on (011) substrates using the halide vapor phase epitaxy (HVPE) method has attracted attention because it enables high-purity films to be formed that have very flat surfaces. However, the conventional edge-defined film-fed growth (EFG) method is limited in the crystal orientations that can be grown, making large-diameter (011) substrates difficult to obtain. In this study, we attempted to grow a 2-inch $\beta\text{-Ga}_2\text{O}_3$ (011) crystal using the vertical Bridgman (VB) method, which enables a wider variety of crystal orientations to be grown than the EFG method.

(011) seed crystals and sintered Ga_2O_3 raw materials were loaded into a Pt-Rh alloy crucible, and crystal was grown in a resistance-heated VB furnace. The raw material was co-doped with 0.05 at% Sn and 0.005 at% Si. The crystal was grown by lowering the crucible at a rate of 1 mm/h. As a result, we successfully grew a 2-inch n-type $\beta\text{-Ga}_2\text{O}_3$ (011) single crystal using the VB method and fabricated a 2-inch $\beta\text{-Ga}_2\text{O}_3$ (011) substrate. The average full width at half maximum (FWHM) of the x-ray rocking curve (XRC) 022 peak over five points on the substrate was 38 arcsec, indicating high crystallinity. In addition, Hall effect measurements revealed a minimum resistivity of $27 \text{ m}\Omega \cdot \text{cm}$ and showed n-type conductivity.

IWGO-WeP-7 c- In_2O_3 Growth by Oxide Vapor Phase Epitaxy Using In_2O and H_2O Source Gases, Rie Togashi, Takumi Shimazaki, Sophia University, Japan; Masato Ishikawa, Gas-Phase Growth Ltd., Japan

Single-crystalline cubic In_2O_3 (c- In_2O_3) has attracted considerable attention as a wide-bandgap semiconductor material for next-generation optoelectronic devices. For such applications, it is essential to prepare high-quality c- In_2O_3 single-crystal layers with low carrier density and high carrier mobility. In recent years, the growth of single-crystalline c- In_2O_3 layers in the bixbyite phase has been reported using halide vapor phase epitaxy (HVPE) [1]. On the other hand, $\beta\text{-Ga}_2\text{O}_3$ growth using Ga_2O and H_2O source gases has been reported [2]. Based on this oxide-source-gas approach, we investigate c- In_2O_3 growth by oxide vapor phase epitaxy (OVPE) using In_2O and H_2O source gases. In this method, In_2O gas is selectively generated by supplying H_2O vapor over In metal in the source zone. The c- In_2O_3 layer is then formed through the reaction between the generated In_2O gas and additional H_2O vapor in the growth zone. In this study, c- In_2O_3 growth using In_2O and H_2O source gases was investigated through both experiments and thermodynamic analysis.

Thermodynamic analysis was first carried out for the formation of In_2O through the reaction between H_2O gas and In metal in the source zone under atmospheric pressure. The calculated equilibrium partial pressures indicated that In_2O can be generated efficiently at elevated temperatures through the reaction $\text{H}_2\text{O}(\text{g}) + 2\text{In}(\text{l}) = \text{In}_2\text{O}(\text{g}) + \text{H}_2(\text{g})$.

Next, thermodynamic analysis was performed for the formation of c- In_2O_3 through the reaction between In_2O gas and H_2O gas in the growth zone under atmospheric pressure. The driving force for c- In_2O_3 formation was determined from the equilibrium analysis. The results showed that the driving force increased with increasing input partial pressure of In_2O , indicating that the reaction $\text{In}_2\text{O}(\text{g}) + 2\text{H}_2\text{O}(\text{g}) = \text{c-}\text{In}_2\text{O}_3(\text{s}) + 2\text{H}_2(\text{g})$ proceeds in the forward direction.

Based on these considerations, c- In_2O_3 were experimentally grown on (0001) sapphire substrates by OVPE using a home-built horizontal hot-wall quartz glass reactor. The experimentally derived driving forces were in good agreement with the thermodynamic predictions. Under H_2O -rich conditions, however, the experimental result deviated from the theoretical value. This is presumably because, in the present system, the reaction between H_2O and the In metal surface becomes saturated under this condition owing to the limited surface area of the In source. As a result, excess H_2O remains unreacted, and the In_2O supply is limited.

[1] R. Togashi *et al.*, Jpn. J. Appl. Phys., **55**, 1202B3 1-5 (2016). [2] R. Togashi *et al.*, Jpn. J. Appl. Phys. (2026), Accepted.

IWGO-WeP-8 Fabrication and Characterization of (011)-Oriented Substrates by the Vertical Bridgman Method, Dong-Jun Lee, Jinki Kang, AXEL, Republic of Korea

$\beta\text{-Ga}_2\text{O}_3$ has attracted significant attention as a next-generation power semiconductor material due to its ultra-wide bandgap and high critical

electric field. In addition, the availability of melt-grown bulk single crystals makes it a promising candidate for large-area substrate applications. Among various crystallographic orientations, the (011) plane is considered a favorable orientation for vertical power-device structures [1].

However, crystal growth along the (011) direction is more challenging than other orientations due to difficulties in maintaining interface stability and managing thermal stress during growth. Meanwhile, fabrication of (011) substrates from conventionally grown (010) crystals requires off-axis cutting, resulting in an elliptical wafer shape and leading to increased material loss and processing complexity.

In this study, the challenges associated with (011)-oriented $\beta\text{-Ga}_2\text{O}_3$ crystal growth using the vertical Bridgman (VB) method were analyzed, and process strategies to overcome these limitations are proposed. The stability of (011) growth was improved through optimization of key process parameters, including temperature gradient and growth rate.

[1] B. Chen, W. Mu, Y. Liu, P. Wang, X. Ma, J. Zhang, X. Dong, Y. Li, Z. Jia, and X. Tao, CrystEngComm **25**, 2404 (2023).

* Author for correspondence: jinki.kang@gmail.com

IWGO-WeP-9 Characterization of p- Cr_2O_3 /n- Ga_2O_3 Heterojunction Rectifiers, Hannah Masten, Frank Kelly, National Research Council; Chinmoy Nath Saha, Yizheng Liu, University of California at Santa Barbara; Tia Gray, National Research Council; Sriram Krishnamoorthy, University of California at Santa Barbara; Marko Tadjer, Naval Research Laboratory

Recently, sputtered Cr_2O_3 has been demonstrated as an effective, drop-in replacement for sputtered p-NiO which typically exhibits significant instability in electrical conductivity over time [1]. This work reports heterojunction rectifiers of ultra-wide bandgap HVPE (001) $\beta\text{-Ga}_2\text{O}_3$ and novel p-type Cr_2O_3 . Details of Cr_2O_3 deposition were reported in Ref. 1. Prior to Cr_2O_3 deposition, approximately $1 \mu\text{m}$ out of the $10 \mu\text{m}$ thick HVPE Ga_2O_3 epilayer was etched off in BCl_3/Ar plasma (800 W ICP, 5 mT, 20 min etch). The motivation for this plasma etch was to evaluate the potential effect of CMP subsurface damage to rectifier electrical performance. Upon etching, one sample was further annealed in ultra-high vacuum at $700 \text{ }^\circ\text{C}$ for ~ 4 hours to remove plasma etch damage [2]. Thus, three samples were prepared: (1) a control sample (no etch), (2) a BCl_3 -etched sample, and (3) an etched and UHV-annealed sample. Figures 1 and 2 show forward-bias I-V characteristics measured on samples (1) and (3), respectively. For brevity, we do not show the degraded I-V characteristic from sample 2. Figures S1 and S2 report the reverse-bias I-V characteristics as well. Further characterization of these novel heterojunction devices will be presented at the workshop.

IWGO-WeP-10 Temperature Dependent Hall as a Probe for Parasitic Conduction in Gallium Oxide Epitaxial Structures, Joshua Buontempo, Cameron Gorsak, Pushpanshu Tripathi, Hari Nair, Cornell University

$\beta\text{-Ga}_2\text{O}_3$ is a promising material for applications in radio frequency (RF) devices due to its ultra-wide bandgap ($\sim 4.8 \text{ eV}$) and estimated breakdown field strength of 8 MV/cm [1]. The δ -doping technique offers multiple advantages over bulk doping such as fine gate control of highly scaled devices [2]. Growth conditions must be tuned to achieve a sharp controlled doping profile exhibiting high channel mobility [2]. However, unintentional conduction pathways can complicate electrical characterization and obscure the intrinsic transport properties of the δ -doped channel. In this work, we leverage temperature-dependent Hall measurements to parse out the transport of unintentionally doped (UID) buffer layers from the Si δ -doped $\beta\text{-Ga}_2\text{O}_3$ epitaxial layers.

Samples with varying buffer layer thicknesses and carrier concentrations were grown by metalorganic chemical vapor deposition (MOCVD) on (010) $\beta\text{-Ga}_2\text{O}_3$ substrates. Temperature-dependent Hall measurements reveal anomalous carrier density behavior deviating from characteristic single-donor freeze-out. These trends are consistent with the presence of multiple conduction channels [3]. A structure with a sufficiently thin buffer, such that all carriers in the buffer should be fully depleted by the semi-insulating substrate, enables characterization of the δ -doped channel alone. By comparing samples with different buffer configurations, we identify that conductive buffer layers can significantly contribute to measured apparent transport.

These results demonstrate that parallel conduction impacts apparent δ -doped $\beta\text{-Ga}_2\text{O}_3$ transport properties and may lead to misinterpretation if not properly accounted for. These findings highlight temperature-dependent characterization as a method for identifying parasitic conduction pathways and provide insight into epitaxial design strategies for

Wednesday Evening, August 5, 2026

isolating and optimizing the δ -doped channel in high-mobility β -Ga₂O₃ devices.

References

- [1] M. Higashiwaki, "β-Ga₂O₃ material properties, growth technologies, and devices: a review," AAPS Bulletin, vol. 32, no. 1, p. 3, 2022.
- [2] E. F. Schubert, ed., Delta-doping of Semiconductors. Boston, MA: Cambridge University Press, August 2005.
- [3] D. C. Look and R. J. Molnar, "Degenerate layer at GaN/sapphire interface: Influence on hall-effect measurements," Applied Physics Letters, vol. 70, pp. 3377–3379, 06 1997.

IWGO-WeP-11 3D Modeling of EFG β-Ga₂O₃ Crystal Growth: Effect of Process on Crystal Quality, Alex Galyukov, STR US, Inc.; Aleksa Crnobrnja, Andrey Smirnov, STR Europe, Serbia

Gallium oxide (β-Ga₂O₃) has emerged as a highly promising material for power electronics applications, owing to its wide bandgap (4.6–5.3 eV) and high critical breakdown electric field (~8 MV/cm) [1]. The edge-defined film-fed (EFG) growth technique is currently the preferred method for large-scale β-Ga₂O₃ crystal production, as it minimizes the melt free surface area, suppresses oxygen evaporation, and improves melt stoichiometry. Nevertheless, achieving large, high-quality crystals remains challenging due to stringent requirements for the lateral temperature uniformity, precise control of dopant incorporation and thermal stress distribution.

Numerical simulation has become an indispensable tool for understanding and optimizing the EFG growth process, enabling detailed analysis of physical phenomena that are difficult or impossible to access experimentally at the high process temperatures. In this work, we present a comprehensive conjugate 3D model of the EFG β-Ga₂O₃ growth system [2], developed using CGSim3D software. The model accounts for asymmetric features of the furnace geometry. It incorporates 3D temperature distribution throughout the furnace: radiative heat transfer in the semi-transparent crystal, including refraction and internal reflection at the crystal/gas interface. Model includes melt and gas flows with free surface tension and the Marangoni effect, dopant segregation and uniformity over the crystal, 3D thermal stress fields in the growing crystal.

We discuss the effect of modifications in furnace parameters on dopant incorporation uniformity and thermal stress development in the crystal. The results demonstrate practical approaches for optimizing growth conditions to reduce thermal stresses and minimize the risk of dislocation generation, improving yield and resistivity uniformity of β-Ga₂O₃ crystal.

Figure 1. Stress components in β-Ga₂O₃ crystal

Figure 2. Dopant distribution in the melt below the growth interface

- [1] M. Higashiwaki, et al., Appl. Phys. Lett. 100, 013504 (2012).
- [2] Y.-J. Shin et al., Jpn. J. Appl. Phys. 62, SF1022 (2023).

*Author for correspondence: Alex.Galyukov@str-soft.com

IWGO-WeP-12 Multi-Ribbon Growth of Offcut (100) β-Ga₂O₃ by EFG, Kurt Lindquist, David Joyce, Kale Geddis, Drew Haven, Luxium Solutions, LLC; Robert Lavelle, Luke Lyle, Benjamin Dutton, Penn State University

As wide-bandgap semiconductors such as SiC and GaN have seen increasing utilization in high-power applications due to their greater efficiency compared to traditional semiconductors, a search is underway for low-cost and high-efficiency alternatives to the currently available materials. Beta-phase gallium oxide (β-Ga₂O₃) is a promising candidate due to its superior material properties, such as an ultra-wide bandgap (~4.8 eV), high electric breakdown field (8 MV/cm), wide range of shallow *n*-type donors (e.g., Sn, Si, etc.), and excellent Baliga's figure of merit. In addition, β-Ga₂O₃ can be grown directly from the melt, unlike other wide-bandgap materials; this offers a path toward significant cost reductions in substrate manufacturing. However, development of β-Ga₂O₃ is still in the early stages and must overcome significant challenges to be manufactured at an industrial scale. Some notable challenges for bulk crystal growth of β-Ga₂O₃ are the low thermal conductivity and two facile cleavage planes of the β-Ga₂O₃ solid, both of which can prove difficult to overcome when scaling crystal size in three dimensions. Furthermore, the Ga₂O₃ melt decomposes to form

gallium metal, which attacks the iridium crucible and significantly reduces its lifetime.

At Luxium Solutions, we utilize the edge-defined film-fed growth (EFG) method for growth of β-Ga₂O₃ due to its unique ability to address the challenges enumerated above. Unlike many melt growth methods, EFG allows the crucible to be emptied of melt after each growth, preventing the buildup of gallium metal that leads to crucible decomposition. In addition, EFG allows for the growth of thin crystals (ribbons) that are effectively two-dimensional, allowing for substantial thermal transport through the crystal during growth despite its low thermal conductivity. However, iridium remains a large portion of the overall manufacturing cost, as it inevitably degrades from reaction with the oxygen required to suppress decomposition of the Ga₂O₃ melt. Therefore, techniques which can increase the yield of crystals from a single growth will significantly reduce manufacturing costs.

This presentation provides an overview of the development of EFG growth of β-Ga₂O₃ at Luxium Solutions, including an introduction to some of the challenges unique to β-Ga₂O₃. The discussion focuses on β-Ga₂O₃ EFG growth development over the last year, including simultaneous multi-ribbon growth, highlighting some of the challenges intrinsic to multi-ribbon growth and progress toward resolving those challenges. Through this discussion, we will demonstrate how this work enables the production of high-quality, domestically produced β-Ga₂O₃ substrates.

IWGO-WeP-13 Development of Surface Preparation Methods for Insulating and Conductive, Miscut (100) β-Ga₂O₃ Substrates, Robert Lavelle, Luke Lyle, Benjamin Dutton, Connor Beakes, Eric Welp, Scott Pistner, Andrew Balog, Penn State University; Drew Haven, David Joyce, Luxium Solutions; Nasim Alem, Joan Redwing, David Snyder, Penn State University

Encouraging epitaxial growth results on miscut (100) β-Ga₂O₃ substrates have motivated evaluation of this orientation for device applications. In addition to CMP, final substrate preparation is critical for facilitating high-quality epitaxial growth, especially for vicinal surfaces. Previous studies on insulating, Mg-doped substrates used phosphoric acid (H₃PO₄) etching and O₂ annealing steps prior to epitaxial growth. However, implementing this process resulted in significant surface roughening of Fe-doped substrates in this work. There is further motivation to utilize conductive substrates for higher power devices. These substrates also require alternative surface preparation steps as annealing in O₂ can result in passivation of the surface with Ga vacancies and a corresponding decrease in conductivity.

This study establishes surface preparation methods for both insulating, Fe-doped and conductive, Sn-doped miscut (100) β-Ga₂O₃ substrates. For both substrate types, an atomically smooth surface (Sq/rms <0.2 nm) with a uniform step/terrace structure was achieved by CMP followed by annealing at 850-900°C with a dwell time selected based on the miscut angle. For the Fe-doped substrates, reducing the total pressure was observed to be important for mitigating surface contamination with the optional inclusion of a hydrofluoric acid (HF) etching step (Fig. 1a). For the Sn-doped substrates, an epi-ready surface was also achieved by annealing in an inert, Ar atmosphere (Fig. 1b). Surface conductivity was maintained using a low O₂ partial pressure during annealing. However, Sn diffusion was observed, even at a relatively low temperature range, further emphasizing the importance of selecting appropriate surface preparation conditions for the miscut substrates. Overall, this study suggests that the surface ordering mechanism for miscut (100) β-Ga₂O₃ substrates is influenced by the Ga vacancy concentration and formation of defect complexes and/or diffusion via these sites. By controlling the variables that affect the formation/compensation of these vacancies, substrates can be prepared with vicinal surfaces for epitaxial growth.

IWGO-WeP-14 Composition-Dependent Thermal Conductivity of Ge_xSn_{1-x}O₂ Alloys, Xiao Zhang, Emmanouil Kioupakis, University of Michigan, Ann Arbor

GeO₂ is an emerging ultra-wide band gap semiconductor with strong potential for power electronic applications. Alloying GeO₂ with SnO₂, a well-established ultra-wide band gap material, enables tunability of material properties for device applications. Recent studies have demonstrated favorable electronic transport properties in Ge_xSn_{1-x}O₂ alloys, making them promising candidates for next-generation power electronics. However, the thermal conductivity, which directly controls heat dissipation and device reliability of these alloys, remains unexplored.

In this work[1] we investigate the thermal conductivity of Ge_xSn_{1-x}O₂ alloys as a function of composition and temperature using first-principles calculations. Density functional theory is used to determine the electronic

structure, while density functional perturbation theory is applied to obtain phonon properties. The alloy is treated using the virtual crystal approximation while incorporating mass-disorder effects introduced by alloying. The phonon-limited thermal conductivity is then computed by solving the Boltzmann transport equation with the almaBTE software. Our results show that at room temperature, alloy disorder reduces directionally averaged thermal conductivity to values as low as 11 W/m K, i.e., by up to approximately a factor of four compared to the end compounds (41 W/m K for GeO₂ and 29 W/m K for SnO₂). Despite this reduction, the alloy thermal conductivity remains comparable to established ultra-wide band gap power-electronic materials such as Ga₂O₃. We further analyze the combined temperature and composition dependence of thermal transport, providing a compact function to evaluate thermal conductivity of Ge_xSn_{1-x}O₂. Our analysis of phonon mean-free-path distributions indicates that high quality crystalline samples with grain size of at least 400 nm are essential for reaching 80% of ideal thermal conductivity. Our work provides insights into the mechanisms that limit heat transport in Ge_xSn_{1-x}O₂ and offers predictive benchmarks for thermal conductivity to guide rational design of Ge_xSn_{1-x}O₂-based devices.

[1] X. Zhang and E. Kioupakis, Phys. Rev. Materials 9, 064603 (2025)

IWGO-WeP-15 MOCVD Growth and Characterization of β -Ga₂O₃ Field Effect Transistors Grown on 2" (010) Substrates, Will Brand, Fikadu Alema, Agniron Technology; Austin Hickman, Soctera; Andrei Osinsky, Agniron Technology

β -Ga₂O₃ has emerged as a promising material for next-generation power electronics due to its ultra-wide bandgap (~4.9 eV) and high theoretical breakdown field (~8 MV/cm). Among available deposition techniques, metal-organic chemical vapor deposition (MOCVD) has demonstrated strong potential for the growth of high-purity, low-defect β -Ga₂O₃ epitaxial films on native substrates [1]. The use of triethylgallium (TEGa) and trimethylgallium (TMGa) precursors enables the growth of carbon-free films with precise doping control. Resulting materials exhibit exceptional electronic properties, including low-temperature electron mobilities ranging from 10,000 to over 23,000 cm²/V·s and acceptor concentrations as low as 2×10^{13} cm⁻³, exceeding values reported for molecular beam epitaxy (MBE), hydride vapor phase epitaxy (HVPE), and even state-of-the-art SiC and GaN bulk materials [2,3].

This presentation will discuss the growth of β -Ga₂O₃ Field Effect Transistor (FET) structures on (010) substrates using Agniron Agilis 700 MOCVD system, supported by Agniron's SBIR program focused on the growth of FET structures on large area substrates. Growth of β -Ga₂O₃ using this reactor has shown both uniform growth on 2" and 4" substrates and uniform, low roughness surfaces across a 2" (010) substrates. To address parasitic conduction arising from the substrate/epitaxy interface, multiple buffer layer strategies were systematically investigated. While conventional HF pretreatment of the native substrate reduces interfacial silicon contamination, it is often insufficient to fully suppress the formation of a secondary conductive channel. Among the approaches explored, the most effective mitigation of interface charge was achieved through the implementation of a nitrogen-doped buffer layer with doping concentrations on the order of $6-8 \times 10^{18}$ cm⁻³, introduced via dilute NH₃/N₂ during growth. CV extracted N_a-N_a profiles indicate an average channel concentration of 1.6×10^{18} cm⁻³, with no measurable interface charge. Hall effect measurements show that carrier mobility remains comparable to unintentionally doped structures, with only a slight reduction in carrier concentration. A 22-point Hall mapping yields an average mobility of 104 cm²/V·s with a 1 σ non-uniformity of 1.5% across a 1" wafer. Thickness uniformity of 0.83% was achieved across a 2" wafer within the same growth run. Device-level performance, including transistor current density and threshold voltage characteristics, will also be presented.

[1] F. Alema, Journal of Crystal Growth 475, 77 (2017).

[2] G. Seryogin, Appl Phys. Lett. 117, 262101 (2020).

[3] F. Alema, APL Materials 7, 121110 (2019)

IWGO-WeP-16 DRCLS Defects Near LiGa₅O₈/Ga₂O₃ Heterointerfaces, Carlos DeLeon, Kaitian Zhang, Hongping Zhao, Leonard Brillson, Ohio State University

Lithium Gallate (LiGa₅O₈) is a novel semiconductor in high power electronics. In addition to a ~5.5 eV ultrawide bandgap (UWBG), LiGa₅O₈ exhibits p-type conductivity, which oxides like Gallium Oxide (Ga₂O₃) have difficulty achieving. Hence, lattice-matched LiGa₅O₈/Ga₂O₃ heterojunctions could enable UWBG P-N junctions, important for high-power electronics.

However, the novelty of LiGa₅O₈ also means that research to understand how its defects affect its electrical properties is still at an early stage.

Depth Resolved Cathodoluminescence (DRCLS) nanoscale depth analysis of LiGa₅O₈ films grown epitaxially on Ga₂O₃ measured its sub-bandgap optical emissions compared with theory [1] to understand their physical nature. DRCLS of LiGa₅O₈ on Ga₂O₃ revealed characteristic emissions of native defect complexes in both their heterointerface and Cr impurities.

DRCLS identified four primary defect emissions at 1.72 eV, 1.74 eV, 1.79 eV, and 1.84 eV. All four correlate to theoretical charge state transitions (CSTs) [1] and R1/R2 Cr defect features. TEM analysis suggested ~35 nm LiGa₅O₈ film thickness, while DRCLS depth profiles displayed pronounced defect intensity changes around ~50 nm, indicating interfacial-related defects. Thus both 1.72 eV and 1.84 eV defects are low within the LiGa₅O₈ but increase towards the substrate, while the 1.84 eV defect density increases near the free surface as well. Both the 1.74 and 1.79 eV defect features are dominant within the outer 60 nm, consistent with LiGa₅O₈ defects. For the 1.74 eV defect, first-principles CST calculations are consistent with Li_{Ga-tet}. [1] Its intensity decreases strongly but not entirely, extending into the Ga₂O₃ substrate whereas the 1.79 eV intensity decreases even more, indicating this defect is the LiGa₅O₈ film's most prominent defect. The closest CST indicates a Li_{Ga-tet}+Ga_{Li} complex, i.e., an exchange reaction, which is supported by the increased defect density being prominent in the Li rich film. The strong 1.84 eV emission at the free surface and the interface can be related to either a V_{Ga-oct} point defect based on a similar CST energy [1] for both LiGa₅O₈ and Ga₂O₃ or Cr features since Cr is an unintentional impurity in Ga source for both LiGa₅O₈ and Ga₂O₃.

DRCLS of LiGa₅O₈ and Ga₂O₃ heterointerfaces provide both measurement and physical nature of their defects, highlighting the impact of their buried interfaces on their nature and spatial distribution. Further refinement of both DRCLS technique and epitaxial growth of atomically abrupt interfaces are underway.

[1]Klichchupong Dapsamut, Kaito Takahashi, & Walter R. L. Lambrecht J. Appl. Phys. 135, 235707 (2024), <https://doi.org/10.1063/5.0209774>

IWGO-WeP-17 Electric-Field-Limited Breakdown in Oxide/ β -Ga₂O₃ p-n Heterojunction Diodes, Sanjay Gopalan, John Muth, Ki Wook Kim, North Carolina State University

Identifying a viable p-type partner for β -Ga₂O₃ is critical for enabling high-voltage bipolar devices. We evaluate oxide p-type candidates for β -Ga₂O₃ heterojunction (HJ) diodes by comparing NiO, Cr₂O₃, and GeO₂. Density functional theory (DFT) was used to extract band alignments for NiO/ β -Ga₂O₃, Cr₂O₃/ β -Ga₂O₃, and GeO₂/ β -Ga₂O₃. All interfaces exhibit type-II alignment with large valence-band offsets (>2 eV), enabling strong hole blocking and stable junction formation. Cr₂O₃ shows a slightly higher valence-band offset and comparable conduction-band offset to NiO, while GeO₂ exhibits moderate offsets that still support effective carrier confinement. Hybrid-functional fitting of bandgaps produces negligible change in predicted breakdown trends, confirming that device behavior is dominated by field distribution rather than small band-offset variations.

Using DFT-derived parameters, TCAD simulations were performed for NiO/ β -Ga₂O₃, Cr₂O₃/ β -Ga₂O₃, and GeO₂/ β -Ga₂O₃ HJ diodes. Owing to the absence of fully calibrated transport and impact-ionization models for β -Ga₂O₃, breakdown voltage (BV) is defined using a critical electric-field criterion of 8 MV cm⁻¹ in the Ga₂O₃ drift region. This provides a consistent comparative metric while β -Ga₂O₃ TCAD models remain under development. All heterojunctions demonstrate multi-kV blocking capability, with BV primarily limited by edge field crowding. Dielectric termination and field-plate structures redistribute the electric field and significantly enhance BV, with Cr₂O₃/ β -Ga₂O₃ showing slightly higher limits and GeO₂/ β -Ga₂O₃ exhibiting comparable trends under optimized designs.

IWGO-WeP-18 Hot-wall MOCVD Growth on Miscut (100) β -Ga₂O₃ Substrates, Benjamin Dutton, Robert Lavelle, Luke Lyle, Randal Cavaleiro, Connor Beakes, Scott Pistner, Penn State University Applied Research Laboratory; Drew Haven, David Joyce, Luxium Solutions LLC; David Snyder, Penn State University Applied Research Laboratory

Recent results in literature utilizing hot-wall metal organic chemical vapor deposition (HW-MOCVD) to grow β -Ga₂O₃ films have realized high growth-rates (>15 μ m/h) and low impurity incorporation. To date, these studies have mostly focused on (010) or (-201) commercially available substrates; however, films grown on miscut (100) β -Ga₂O₃ substrates by cold-wall MOCVD have encouraged further exploration into this orientation. In this study, HW-MOCVD is established as an effective method for epitaxial growth on (100) β -Ga₂O₃ substrates with miscut values ranging from 2° -

6°+ and doped with donors or acceptors using TMGa as a precursor. AFM scans indicated step-flow growth could be achieved at various miscut angles using the process parameters developed in this work. The effect of miscut angle on extended defect density and morphology was investigated using imaging techniques including optical microscopy and FIB-SEM. Process parameters, such as VI/III ratio, were also shown to demonstrably impact extended defect morphology. Background donor concentrations of the films were measured by Hg probe and SIMS in order to understand the impact of miscut angle on impurity incorporation. Lastly, growth conditions were modulated in pursuit of validating the homogeneity of HW-MOCVD over a 4-inch diameter platen area.

IWGO-WeP-19 Temperature-Optimized Lattice-Matched Epitaxy of UWBG Rutile $\text{Ge}_x\text{Sn}_{1-x}\text{O}_2$ on (001) Rutile TiO_2 , Satyam Patel, Becky (R.L.) Peterson, University of Michigan, Ann Arbor

r- GeO_2 is an emerging ultrawide bandgap (UWBG) semiconductor with predicted n- and p-type conduction, and with higher thermal conductivity and electron mobility than $\beta\text{-Ga}_2\text{O}_3$. [1] Alloying r- GeO_2 with r- SnO_2 forms r- $\text{Ge}_x\text{Sn}_{1-x}\text{O}_2$, enabling tunable lattice parameters and bandgaps. [2] Lattice-matched r- $\text{Ge}_x\text{Sn}_{1-x}\text{O}_2$ /r- GeO_2 heterostructures are attractive for future electronic, optoelectronic, and quantum devices. While r- $\text{Ge}_x\text{Sn}_{1-x}\text{O}_2$ epitaxy has been demonstrated on (001) r- TiO_2 , [3, 4] the growth temperature has not been optimized. Here, we investigate the impact of growth temperature on stoichiometry and crystallinity of lattice-matched r- $\text{Ge}_x\text{Sn}_{1-x}\text{O}_2$ films grown on r- TiO_2 via mist chemical vapor deposition (mist CVD).

In mist CVD, an ultrasonically-generated precursor mist flows into a furnace where it thermally decomposes on the substrate, forming a thin film. We used a 1 Ge to 1.21 Sn precursor ratio to target a $\text{Ge}_{0.422}\text{Sn}_{0.578}\text{O}_2$ alloy composition, which Vegard's law predicts will have relaxed in-plane lattice parameters matching (001) r- TiO_2 . Eight samples were prepared with growth temperature varying from 725 °C to 900 °C. As growth temperature increased, the (002) $2\theta/\omega$ peak shifted to lower angles, indicating an increased out-of-plane lattice parameter, c . Concurrently, the direct-forbidden transition energy redshifted from 4.03 eV to 3.77 eV, due to decreased Ge incorporation and changes in substrate-induced strain.

X-ray diffraction (XRD) reveals an optimal growth window between 750 °C to 775 °C, for which films exhibit the narrowest full width at half maximum (FWHM) in rocking curves and pronounced Laue oscillations in symmetric $2\theta/\omega$ scans. The r- $\text{Ge}_{0.43}\text{Sn}_{0.57}\text{O}_2$ film grown at 775 °C demonstrated the highest growth rate ($> 2 \text{ nm}\cdot\text{min}^{-1}$), the lowest substrate-induced strain, sub-nanometer surface roughness, and superior structural quality, as shown in scanning transmission electron microscopy (STEM) imaging. Reciprocal space mapping, azimuth scans, and nanobeam electron diffraction (NBED) confirm lattice-matched epitaxy of the r- $\text{Ge}_{0.43}\text{Sn}_{0.57}\text{O}_2$ on TiO_2 . In the future, these optimized growth conditions can be used to obtain high quality heterostructures in the $\text{Ge}_x\text{Sn}_{1-x}\text{O}_2$ alloy system.

This work was supported by NSF DMR FuSe awards #2235208 and #2328701.

References: [1] S. Chae *et al.*, Appl. Phys. Lett. **114**(10), 102104 (2019); [2] A.M. Abed & R.L. Peterson, APL Mater. **13**(11), 111115 (2025); [3] H. Takane *et al.*, Phys. Rev. Mater. **6**(8), 084604 (2022); [4] H. Takane *et al.*, Appl. Phys. Express **17**(1), 011008 (2024).

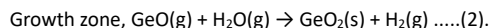
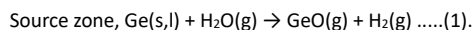
IWGO-WeP-20 Growth of Rutile-Type GeO_2 by Oxide Vapor Phase Epitaxy, Haru Nakano, Shigeyoshi Usami, Masayuki Imanishi, Yusuke Mori, Osaka University, Japan

Rutile-type germanium dioxide (r- GeO_2) has emerged as a promising power semiconductor material; however, achieving high material purity is essential to realize its full breakdown potential in device applications. Although various growth methods have been investigated, further improvements in material purity remain necessary. Recently, we proposed oxide vapor phase epitaxy (OVPE) as a novel technique for producing high-purity oxide thin films (e.g., Ga_2O_3). This method employs metal-oxide vapor as the source material, enabling intrinsically high-purity growth. In this study, we investigated OVPE to the growth of r- GeO_2 . Growth was performed on a (001) r- TiO_2 substrate under conditions determined based on thermodynamic calculations. The formation of r- GeO_2 was confirmed through X-ray diffraction. Scanning electron microscope observations revealed thin-film growth, and cross-sectional SEM indicated a growth rate of approximately 200–500 nm/h. These results indicate that r- GeO_2 can be grown using the OVPE. However, an $\alpha\text{-GeO}_2$ polytype was also detected, and further investigation is required to clarify its origin.

IWGO-WeP-21 Thermodynamic analysis of GeO_2 growth via Oxide Vapor Phase Epitaxy, Shigeyoshi Usami, Masayuki Imanishi, Yusuke Mori, The University of Osaka, Japan

Rutile-type germanium dioxide (r- GeO_2) is one of the candidates for next-generation power semiconductor materials owing to its wide band gap (4.44-4.68 eV) [1], high breakdown electric field ($\sim 7 \text{ MV/cm}$) [2], and predicted ambipolar carrier conduction [3]. Although various thin-film growth methods for r- GeO_2 have been reported [4-6], the development of a high-purity growth technique, which is essential for achieving high breakdown voltage, is still required. Recently, we proposed oxide vapor phase epitaxy (OVPE) as a novel growth technique capable of achieving high-purity oxide thin films (e.g., Ga_2O_3) [7]. This method utilizes metal-oxide vapor as the source material, which is free from impurities originating from metal precursors and thus enables intrinsically high-purity growth. In this study, we investigate the feasibility of GeO_2 growth using OVPE through thermodynamic analysis.

In the OVPE method, metal-oxide vapor generated in the source zone is transported to the growth zone and mixed with an oxidant, resulting in the growth of a solid oxide on a substrate. The chemical reactions involved in GeO_2 growth are shown in Eqs. (1) and (2):



Thermodynamic equilibrium states were calculated by minimizing the Gibbs free energy under given conditions of temperature, partial pressures, and total pressure. First, the temperature dependence of the equilibrium partial pressure (P_{eq}) of GeO(g) and the H_2O -to- GeO conversion efficiency in the source zone were evaluated. The amount of GeO(g) increases with source-zone temperature, and a temperature above 1000 °C is required to achieve a conversion efficiency greater than 90%.

Next, the temperature dependence of the supersaturation for GeO_2 growth at various H_2O partial pressures was evaluated. The supersaturation was derived from the difference between the initial and equilibrium partial pressures of GeO(g) . The temperature range for GeO_2 growth expands with increasing H_2O partial pressure. Comparison with growth temperatures employed in other methods suggests that the rutile phase is achievable by OVPE.

- [1] M. Stapelbroek *et al.*, Solid State Commun. **25**, 959-962 (1978).
- [2] K. Bushick *et al.*, Appl. Phys. Lett. **117**, 182104 (2020).
- [3] S. Chae, J. Lee *et al.*, Appl. Phys. Lett. **114**, 102104 (2019).
- [4] H. Takane *et al.*, Appl. Phys. Lett. **119**, 062104 (2021).
- [5] K. Shimazoe *et al.*, Jpn. J. Appl. Phys. **64**, 050903 (2025).
- [6] F. Golbasi *et al.*, J. Alloys Compd. **1014**, 178591 (2025).
- [7] R. Togashi *et al.*, DOI: 10.35848/1347-4065/ae54ed.

IWGO-WeP-22 Experimental Study of Hf-Doped $\beta\text{-Ga}_2\text{O}_3$ by Floating Zone Method, Myeonggyun Kang, Tohoku University, Japan, Republic of Korea; Kei Kamada, Hisato Suezumi, Masanori Kitahara, Satoshi Ishizawa, Kikito Murakami, Yuui Yokota, Masao Yoshino, Akira Yoshikawa, Tohoku University, Japan

Introduction: Czochralski (Cz) and Edge-Defined Film-Fed Growth (EFG) methods inevitably require the use of expensive Ir crucibles and, as the market price of Ir rises, there is a strong demand for economically viable alternatives [1]. Here, our laboratory has proposed the Oxide Crystal Growth from Cold Crucible (OCCC) using the raw material itself as the crucible [2]. However, since OCCC is designed for large-scale experiments, it is not suitable for composition screening; therefore, in this study, we used Floating Zone (FZ) method. According to DFT calculations, Hf forms a shallow donor level within $\beta\text{-Ga}_2\text{O}_3$ and Saleh *et al.* (2020) reported high carrier density in Hf-doped $\beta\text{-Ga}_2\text{O}_3$ grown by VGF method [3][4]. However, no studies have yet been reported on the growth of Hf-doped $\beta\text{-Ga}_2\text{O}_3$ single crystal using FZ. In addition, the report on optical properties of Hf-doped $\beta\text{-Ga}_2\text{O}_3$ are very few. In this study, we grew Hf-doped $\beta\text{-Ga}_2\text{O}_3$ single crystals using FZ and report on their optical and electrical properties.

Experiments: $\beta\text{-Ga}_2\text{O}_3$ and HfO_2 powder were uniformly mixed by milling with HfO_2 doping with various concentrations. During the crystal growth, the rotation rate was set to 30 rpm, and the vertical pull-down rate was 6 mm/h in 100% O_2 .

Results: Non-doped and Hf-doped $\beta\text{-Ga}_2\text{O}_3$ single crystals with a diameter of 4-5 mm were successfully obtained. Under UV light (254 nm) irradiation, the non-doped sample exhibited blue luminescence, whereas green luminescence was observed in the Hf-doped sample. Furthermore, in the PL spectra measured at 280 nm excitation, the Hf-doped sample showed broader emission and peak shift to 460 nm, compared to the non-doped

sample. Results such as XRD, and Hall effect measurements etc. will be reported on the day of the presentation.

Acknowledgements: We appreciate Takamasa Sugawara, Cooperative Research and Development Center for Advanced Materials, providing access to the Floating Zone Furnace.

[1] S. B. Reese, et al., *Joule* 3, 903-907 (2019)

[2] A. Yoshikawa, K. Kamada et al. *Sci. Rep.* 14, 14881 (2024)

[3] D. Chen et al. *Comput. Theor. Chem.*, 1241, 114906 (2024)

[4] M. Saleh et al., *Semicond. Sci. Technol.*, 35, 04LT01 (2020)

* Author for correspondence: akira.yoshikawa.d8@tohoku.ac.jp

IWGO-WeP-23 Exploration of Conductivity-Type Control in β -Ga₂O₃ through Nitrogen Doping, Haizhong Zhang, Fuzhou University, China

β -Ga₂O₃ is a next-generation ultra-wide-bandgap semiconductor with strong potential for power electronics and deep-ultraviolet photodetection owing to its ultra-wide bandgap and high critical breakdown field. However, its device performance remains far below the theoretical limit because intrinsic materials limitations, particularly the flat valence band and strong self-compensation induced by unintentional donors, continue to hinder precise control of epilayer quality and reliable p-type doping. Among the candidate dopants, nitrogen (N) is particularly attractive because its atomic radius is close to that of the host anion, making it a favorable compensating acceptor with minimal perturbation to the O²⁻ sublattice. To explore a viable route toward p-type β -Ga₂O₃, we adopted a strategy of first establishing high-quality epitaxial growth and then pursuing carrier control, and systematically investigated in situ N doping in β -Ga₂O₃ homoepilayers grown by metal-organic chemical vapor deposition (MOCVD). Using nitrous oxide (N₂O) as both the oxygen precursor and nitrogen source, together with trimethylgallium as the Ga precursor, we first suppressed unintentional donor incorporation through process optimization. This enabled the growth of a lightly N-doped layer on (001) β -Ga₂O₃ with a low background carrier concentration of $3.5 \times 10^{16} \text{ cm}^{-3}$ and a high electron mobility of $82.70 \text{ cm}^2 \text{ V}^{-1} \text{ s}^{-1}$. By further precisely regulating N incorporation, we drove the (001) homoepilayer from n-type conduction through a highly resistive state to p-type conduction, thereby obtaining a room-temperature p-type epilayer with a hole concentration of $1.08 \times 10^{18} \text{ cm}^{-3}$, a hole mobility of $0.47 \text{ cm}^2 \text{ V}^{-1} \text{ s}^{-1}$, and an acceptor activation energy of 0.168 eV. By combining first-principles calculations with experimental results, we further revealed an orientation-dependent N-doping mechanism on the (001) and (100) planes, arising from differences in the competitive adsorption of N and O on the two surfaces. The results show that the (001) plane is more suitable for precise control of N incorporation, whereas the (100) plane is more favorable for high-concentration N doping. Guided by this understanding, we further achieved precise in situ N doping on the (100) plane and obtained a homoepilayer with an N concentration as high as $1.13 \times 10^{20} \text{ cm}^{-3}$. Multiple Hall measurements together with Seebeck measurements confirmed p-type conduction, with a hole concentration of $9.15 \times 10^{18} \text{ cm}^{-3}$ and a hole mobility of $1.43 \text{ cm}^2 \text{ V}^{-1} \text{ s}^{-1}$.

IWGO-WeP-24 Re-Growth on Multi-Directional Fin Structures of (001) β -Ga₂O₃, Sai Krishna Anandan, Min-Yeong Kim, Arpit Nandi, Martin Kuball, University of Bristol, UK

Homoepitaxial growth of β -Ga₂O₃ focuses on conventional vertical growth on commercially available substrate orientations such as (001), (010), (201) and (110) [1]. Exploring lateral epitaxial growth, though limited, could increase the ability to design and implement new device structures, e.g. gate-all-around FETs, that benefit from anisotropy in electron transport and heat propagation within the β -Ga₂O₃ monoclinic structure. This work investigates the growth of β -Ga₂O₃ along the vertical sidewall of fins fabricated into (001) β -Ga₂O₃ substrates, along multiple in-plane directions like [010], [100], [140], [120], [110], [210], and [210]. The result shows anisotropy of regrowth surfaces depending on the crystallographic orientations of RIE etched side walls. Fig. 1(a) and Fig. 1(b) show FIB-SEM cross-sectional images along the [120] directional fin before and after growth, respectively, at a growth rate of 500 nm/h (vertical direction) for 30 mins at 930°C, 30 Torr, and a VI/III ratio of 1800. The increase in fin thickness on the fin side walls in Fig. 1(b) is used to assess the lateral growth rate on the sidewall. Fig. 1(c) represents the change in overgrowth thickness along the different sidewalls of fins under identical growth conditions. The highest lateral growth was observed along [140], [120], and [210] directional fins, exhibiting 50% of the vertical growth rate along (001). This variation is likely caused by anisotropy in atomic density on the sidewall planes leading to varying surface energies for nucleation. H₃PO₄ surface treatment has been proven to reduce

interface charge density (mitigating current degradation) in Trench Schottky Barrier Diodes and an increased stability of the device under high temperature operation [2]. Hence, regrowth on 10 min and 20 min H₃PO₄-treated side wall surfaces was compared to an untreated regrowth surface. Fig. 1(c) shows that H₃PO₄ treated samples (10 mins) exhibit reduced growth compared to the untreated surface on most surfaces apart of side walls is (010) fins; acid treatment may cause a reduction in nucleation sites and adsorption centers hindering growth kinetics [3].

IWGO-WeP-25 Surface Termination and Structural Stability of β -(Al_xGa_{1-x})₂O₃ (100) (X = 0 ~ 0.3) as-Cleaved Single Crystals, Ming-Chao Kao, Deutsches Elektronen-Synchrotron DESY (NanoLab), Germany

As demonstrated in our recent publication on APL [1] The surface structure of β -Ga₂O₃ single crystals cleaved along the (100) plane is investigated using synchrotron-based surface X-ray diffraction (SXRD) and atomic force microscopy (AFM). The results show the surface to consist of a single, so-called B-termination, which means that the crystal cleaves at planes formed by edge-sharing oxygen octahedra, thereby breaking the longest and weakest Ga–O bonds. Refinement of the atomic positions results in small displacements from the bulk structure, at most approximately 0.01 Å. AFM suggests that relatively large terraces form together with steps of half the a-axis length of approximately 0.6 nm, which means that terraces have the same atomic termination, related by the crystal symmetry. These results are important as a fundamental property of β -Ga₂O₃ when processed or used in various high-power semiconductor applications.

Building on our recent structural characterization of the cleaved β -Ga₂O₃ (100) surface, we now present initial results from synchrotron-based single-crystal X-ray diffraction (SCXRD) and X-ray reflectivity (XRR) measurements of β -(Al_xGa_{1-x})₂O₃ (100) single crystal substrates (x = 0 to 0.3). [2] These measurements provide new insight into the surface structure and bulk crystal properties of these Al-alloyed single crystals, which are critically important for high-quality epitaxial thin-film growth. Our results provide a comprehensive analysis of the lattice parameters, electron density, Al compositions, twinned domain, and surface structure of the alloyed β -(Al_xGa_{1-x})₂O₃ crystals. Furthermore, we propose several structural models, suggested by first-principles studies [3] and our PXRD-refined bulk model, which were subsequently used to fit the Crystal Truncation Rod (CTR) dataset and will reveal the key surface structural features of these alloyed single crystals. These findings will be discussed in detail at the conference. All investigated β -(Al_xGa_{1-x})₂O₃ single crystals shown in this study were grown using the Czochralski method at the Leibniz-Institut für Kristallzüchtung (IKZ). [2]

[1] Kao, Ming-Chao, et al., *Applied Physics Letters* 128.7 (2026).

[2] Galazka, Zbigniew, et al., *Journal of Applied Physics* 133.3 (2023).

[3] Mu, Sai, et al., *APL Materials* 8.9 (2020).

* Author for correspondence: vedran.vonk@desy.de

IWGO-WeP-26 Effect of the GaN Surface on n-Ga₂O₃/p-GaN Heterointerface Quality, Daniel Pennachio, US Naval Research Laboratory; Frank Kelly, Katie Gann, National Research Council Postdoctoral Fellow, residing at NRL; Emma Rocca, Michael Mastro, US Naval Research Laboratory

Gallium oxide is a promising ultrawide bandgap semiconductor due to its phenomenal electrical properties such as its high breakdown field and n-type conductivity. Importantly, compatibility with liquid-phase growth techniques allow large-area β -Ga₂O₃ substrates to be produced relatively inexpensively and early in the material's development. Despite these benefits, the lack of shallow p-type dopant and the material's low thermal conductivity hinder device performance. Both disadvantages may be resolved by forming heterostructures with compatible p-type semiconductors. This work explores epitaxy of n-type β -Ga₂O₃:Si via metalorganic chemical vapor deposition (MOCVD) on p-type GaN:Mg, with a focus on atomic configuration and associated defects of the heterointerface as a function of Ga₂O₃ growth initiation and substrate polarity.

This work investigates the effect of GaN surface modifications before Ga₂O₃ growth. Surface treatments include *ex situ* O₂ plasma oxidation or an *in situ* MOCVD Ga "flash" clean of the GaN surface [1]. The effects of the polarity of the GaN substrate and the inclusion of a low-temperature Ga₂O₃ nucleation layer are also studied in addition to the surface treatments. The interfacial structure and composition were measured using scanning transmission electron microscopy (STEM) and X-ray energy dispersive

Wednesday Evening, August 5, 2026

spectroscopy (EDS). All grown films exhibited rotational domains with the epitaxial alignment of $\text{Ga}_2\text{O}_3(-201)||\text{GaN}(0001)$. A 6-fold rotational alignment between the substrate and film were confirmed via X-ray diffraction (XRD). Fourier filtering and 4DSTEM were utilized to map grain alignments throughout the cross-sections, showing both vertical and horizontal grain boundaries, as well as various other defects. Predominant crystallographic alignments observed were $\text{Ga}_2\text{O}_3(-201)(0-10)||\text{GaN}(0001)[11-20]$ and $\text{Ga}_2\text{O}_3(-201)[1-32)||\text{GaN}(0001)[11-20]$. The film grown with *ex situ* oxidation but without a nucleation layer provided the largest lateral grain size as determined via atomic force microscopy (AFM) analysis of surface structure. This growth also exhibited relatively uniform lateral grain size throughout the film thickness in TEM. In contrast, films grown with a nucleation layer resulted in smaller lateral grain sizes near the interface, followed by wider grains near the film surface. For samples treated with *ex situ* oxidation, the interface showed a ~ 10 nm wide region containing voids, while samples grown without oxidation showed atomically abrupt interfaces.

[1] Katta, Abishek, et al. *Journal of Applied Physics* 135.7 (2024).

IWGO-WeP-27 p-GaN/n-Ga₂O₃ Diodes via MOCVD Selective Area Growth, Frank Kelly, Emma Rocco, Daniel Pennachio, James Lundh, Alan Jacobs, Tolen Nelson, Marko Tadjer, Michael Mastro, Naval Research Laboratory
Heteroepitaxy of n-Ga₂O₃ on p-type wide-bandgap semiconductors is a promising route for high-performance power rectifiers. Here we demonstrate p-GaN/n-Ga₂O₃ heterojunction diodes fabricated via MOCVD-based selective area growth. PECVD SiN_x was used as the growth mask material to enhance the surface diffusivity of Ga adatoms and prevent nucleation of polycrystalline material on the mask, a common issue with traditional SiO₂ masks. SiN_x layers were 90 nm thick and were patterned via wet etching with BOE. Growth was conducted at 800 °C with a growth pressure of 15 Torr and VI/III ratio of 890 in an Agnition Agilis 500 MOCVD reactor. SiH₄ was used as an n-type dopant source for Si. Growth temperature, pressure, and VI/III ratio were identified as important parameters to optimize to prevent polycrystalline Ga₂O₃ nucleation. Devices were fabricated by depositing Ti/Au contacts to the Ga₂O₃ and Pd/Au contacts to the p-GaN. Devices were tested in air prior to contact annealing and without passivation.

The fabricated diodes exhibit record-breaking performance of Ga₂O₃ devices produced via MOCVD-SAG, with current on/off ratios exceeding 10⁹ and the reverse bias current limited by the noise floor of the measurement system. Ideality values were around 3.5 and forward specific on resistance was high, suggesting improved performance can be obtained through contact annealing. Breakdown voltages were measured to be 50 V reverse bias for a 10 μm contact spacing, indicating breakdown through air rather than through the device. Mesas were non-uniform in thickness and doping due to excess unreacted Ga from the mask accumulating in growth windows. Plan-view scanning electron microscopy (SEM) of the device edge shows that the mask does not have crystallites and that the mesa edge has hexagonal faceting, attributed to the 6-fold rotational domains that β-Ga₂O₃ forms on c-plane GaN. Cross-sectional SEM shows lateral overgrowth and an increased thickness near the mask edge. Further study of the variation in doping level and its impact on device performance will be carried out and presented at the workshop.

*Author for correspondence: frank.p.kelly9.ctr@us.navy.mil

IWGO-WeP-28 Performance of MOCVD Grown Schottky Barrier Diodes with a Graded β-(Al,Ga)₂O₃ Cap, Cameron Gorsak, Frank Kelly, Jenifer Hajzus, Daniel Pennachio, Naval Research Laboratory; Katie Gann, Naval Research Laboratory, USA; Alan Jacobs, Emma Rocco, Michael Mastro, Naval Research Laboratory

β-Ga₂O₃ with its high critical electric field (E_{cr}) and controllable n-type doping, is an advantageous material for Schottky barrier diodes (SBDs) for compact, high-voltage, power conversion and distribution systems. A common failure mechanism in SBDs is electric field breakdown at the metal-semiconductor interface, where the field peaks under reverse bias. To further improve SBD performance, this work employs a β-(Al,Ga)₂O₃ cap, which provides a larger bandgap (E_g) and a correspondingly higher E_{cr} [1]. The corresponding decrease in electron affinity is predicted to increase the Schottky barrier height (Φ_b) to high work function metals. Previous work has demonstrated that a β-(Al,Ga)₂O₃ cap enhances SBD device performance by suppressing reverse leakage current via a higher Φ_b while simultaneously increasing the breakdown voltage (V_{br}) due to a higher E_{cr} [2]. The abrupt heterojunction, however, resulted in higher on resistance (R_{on}). To retain the benefits from the wider bandgap cap while minimizing

R_{on} , this work investigates the metalorganic chemical vapor deposition (MOCVD) of a compositional graded β-(Al,Ga)₂O₃ capped SBD.

An Agnition Agilis 500 MOCVD reactor is used to grow the UID drift region and graded β-(Al,Ga)₂O₃ cap on (010) Sn:β-Ga₂O₃ substrates using TEGa and O₂ precursors. The flow of TMAI is ramped to achieve the linearly graded β-(Al,Ga)₂O₃ layers. While the critical thickness for a commensurate, abrupt 20% β-(Al,Ga)₂O₃ film is limited to ≤ 30 nm [3], compositional grading offers a pathway to achieve higher Al content by distributing strain. This work presents a parametric investigation into the surface content of graded β-(Al,Ga)₂O₃ caps, including targeted compositions of 10%, 20%, and 30%. The initial device features a crack-free, ~ 15 nm graded cap with a surface Al content of $\sim 10\%$, as confirmed by scanning transmission electron microscopy energy dispersive X-ray spectroscopy. Both uncapped and capped surfaces exhibit as-grown roughness as low as ~ 1 nm RMS.

SBDs with 500 μm diameter Pt/Au Schottky contacts and backside Ti/Au ohmic contact are fabricated on the wafers. Results indicate that the β-(Al,Ga)₂O₃ devices exhibit a higher reverse V_{br} while maintaining a low $R_{on} \approx 0.01 \Omega\text{cm}^2$, comparable to the uncapped devices. This demonstrates the effectiveness of the graded cap in improving blocking performance without significantly increasing conduction losses. A direct comparison of key device parameters, including R_{on} and leakage current, will be presented.

References:

- [1] H. Peelaers et al., *APL* **112**(24), (2018).
- [2] P. Sundaram et al., *JVSTA* **40**(4), (2022).
- [3] J.S. Lundh et al., *APL* **123**(22), (2023).

IWGO-WeP-29 Vertical β-Ga₂O₃ U-Trench MOSFETs With N-ion-implanted Current Blocking Layer and Implanted Source, Jiawei Liu, Surajit Chakraborty, Walid Amir, Uttam Singiseti, University at Buffalo-SUNY

β-Ga₂O₃ has attracted significant attention as an ultra-wide-bandgap (UWBG) semiconductor for next-generation high-power and fast-switching. Among diverse device architectures, vertical MOSFETs are preferred in power electronics for their ability to mitigate surface effects and achieve scalable breakdown voltage (V_{br}) through drift layer thickness scaling. To compensate for the absence of p-type doping in Ga₂O₃, forming fin-type structures or introducing a current blocking layer (CBL) are the main methods to realize normally-off operation. Considering the requirement of high lithography resolution for fin structures, the CBL approach is investigated in this work.

The fabrication process started on commercially available Sn-doped (010) β-Ga₂O₃ substrates and ~ 10 μm HVPE-grown epitaxial layer with a doping concentration of $\sim 2 \times 10^{16} \text{ cm}^{-3}$. The box-shaped CBL with a thickness of approximately 800 nm was formed by N-ion implantation at multiple energy levels with specific doses. Afterward, the sample was annealed in an N₂ ambient to activate nitrogen ions and remove ion implantation damage. To form ohmic contacts, Si-ion implantation was then performed with a PECVD SiO₂ sacrificial layer to form a 0.2-μm-thick box profile followed by anneal in N₂ atmosphere. Ti/Au was then deposited on the front and backside, followed by anneal in N₂. The gate trench and mesa isolation regions were etched in BCl₃/Ar-base RIE and a SiO₂ layer was deposited by ALD as the gate dielectric layer, followed by gate metallization.

To analyze device behavior, the ohmic contact was first characterized, yielding a contact resistivity of $1.94 \times 10^{-6} \Omega\text{cm}^2$ and sheet resistance of 555.63 Ω/□ by CTLM measurements. Threshold voltage $V_{th} = 3.8$ V and the on/off ratio of 7.0×10^2 were extracted from the transfer characteristics measured at $V_{DS} = 5$ V. From the output characteristics, the highest current density of 50.0 A/cm² was obtained at $V_{GS} = 15$ V and $V_{DS} = 4$ V and the on resistance ($R_{on,sp}$) was extracted to be 56.9 mΩ·cm². Turn-on capacitance–voltage (C–V) measurements indicates sufficient gate control. However, the off-state C–V characteristics reveal the premature depletion of the drift layer. Breakdown measurements were performed at $V_{GS} = 0$ V and got a V_{br} of 342 V. The low V_{br} along with the low on/off ratio and the early depletion of the drift layer indicates the leakage issue in the CBL possibly caused by Si ion diffusion.

This study demonstrates an enhancement-mode β-Ga₂O₃ U-trench MOSFET with N-ion-doped CBL. Further optimization of the ion implantation, post-implantation annealing and the trench etching could be explored to solve the leakage.

IWGO-WeP-30 Donor Doping of β -Ga₂O₃ by Cl Ion Implantation, Katie Gann, Alan Jacobs, Frank Kelly, Emma Rocco, Cameron Gorsak, Marko Tadjer, Naval Research Laboratory; Rachael Myers-Ward, Naval Research Laboratory; Karl Hobart, Michael Mastro, Naval Research Laboratory

N-type doping in β -Ga₂O₃ has focused on substitutional impurities on Ga sites, such as Si. Chlorine substitution on O sites was proposed as a shallow donor, along with F,[1] in 2010 but has not been experimentally verified. To investigate Cl as an intentional donor, 500 nm UID β -Ga₂O₃ films grown by MOCVD on semi-insulating (010) substrates were implanted with either Si, Cl, or Si+Cl (at a 2:3 ratio to match the stoichiometry of Ga₂O₃) to concentrations of roughly 2×10^{19} , 3×10^{19} , and 5×10^{19} cm⁻³, respectively, to ~250 nm deep. Strain in the 020 XRD reflection of as-implanted samples varies for the different species and does not appear additive for the Si+Cl sample. Annealing was performed under a UHP Ar ambient at a reduced total pressure with P_{O₂}, P_{H₂O} < 10⁻⁶ bar, as both are known to be detrimental to activation of implanted Si, and likely for all n-type donors.[2]

Implant activation of Si served as baseline, where annealing for 10 minutes at 900, 925, and 950 °C yielded nearly full activation (~90%) with a mobility of ~60 cm²/Vs, confirming conditions are well optimized for Si implants compared to literature.[2] The Cl implanted samples exhibited increasing conductivity with temperature, not attributable to a change in mobility (~58 cm²/Vs), but rather to carriers increasing from ~2 to 10% of the implanted dose. The constant mobility suggests the increase in activation with temperature is likely not due to improved lattice recovery, with HRXRD confirming significant damage recovery by 900 °C. Literature suggests that implant damage primarily impacts the Ga sublattice, with the O sublattice remaining largely unperturbed. This may explain why dopants intended for Ga sites activate at relatively low temperatures, because Ga vacancies are formed via implant damage. However, for dopants intended for O sites to become active, higher annealing temperatures may be required for solute substitution. An activation energy of 2.1 eV from Cl activation anneals may be related to the formation of V_O necessary for Cl substitution. Temperature-dependent Hall measurements of the Cl-implanted samples (200-380K) reveal a carrier activation energy of ~12 meV, suggesting that a shallow impurity band was formed. Activation of the Si+Cl implanted samples show reduced activation and mobility compared to the Si-implanted samples, highlighting complicating factors from substituting on both sublattices and potentially the formation of compensating acceptors with the higher donor concentration.

[1] Varley, J. B., et al, (2010). *Applied Physics Letters*, 97(14).

[2] Gann, K. R., et al, (2024). *Journal of Applied Physics*, 135(1).

IWGO-WeP-31 Thermodynamic analysis of (Al_xGa_{1-x})₂O₃ MOCVD growth with TMA, O₂, and TMG and TEG as Ga precursors, Andri Dhora, Lund University, Sweden

Incorporating Al in β -Ga₂O₃ enhances its critical electric field and voltage-blocking capability. High quality, high purity β -(Al_xGa_{1-x})₂O₃ films with precise compositional control are required. MOCVD is a promising method for this goal [1], but challenges persist in achieving high growth rates while maintaining controlled conductivity and Al incorporation.

Numerous studies on MOCVD (Al_xGa_{1-x})₂O₃ growth are available, but clear guidelines for optimal conditions enabling high-purity and controlled Al incorporation are still lacking. We address this by performing a thermodynamic analysis of reactions between MO alkyls and O₂ during alloy growth with TMA, and either TEG or TMG as Ga precursors. For TEG, equilibrium partial pressures of 28 gaseous species were calculated from 24 chemical reactions and 4 constraints. For TMG, 29 gaseous species were analysed using 25 reactions and 4 constraints. These equilibrium partial pressures capture the reaction dynamics and clarify (Al_xGa_{1-x})₂O₃ growth behavior as a function of temperature, pressure, precursor supply, VI/III ratio, and the input gas-phase Al fraction (x_o).

The analysis shows that sufficient O₂ is required to fully combust MO-derived hydrocarbons and H₂, enabling high-purity growth at high rates. The required VI/III ratios differ as the precursors have different alkyl ligand compositions: above (21-x_o) for TEG and above 12 for TMG. In oxygen-rich regimes, the alloy composition (x) scales linearly with input Al fraction, whereas higher temperatures and oxygen-lean conditions enhance Al incorporation with an inverse dependence on VI/III ratio. Experimental data are well-reproduced by the thermodynamic model when accounting for differences in the kinetic growth efficiencies of the binary components under TMG and TEG; however, the TMG data points at higher TMA flow rates can be reproduced by assuming gas-phase losses, resulting in reduced effective precursor partial pressures at the growth interface.

[1] Bhuiyan, A.F.M., et al, *Journal of Applied Physics*, 133(21) (2023).

Wednesday Evening, August 5, 2026

+ Author for correspondence: andri.dhora@fysik.lu.se
[mailto:andri.dhora@fysik.lu.se]

IWGO-WeP-32 Effect of Ga Etching and Wet Acid Treatments on MOS Characteristics for Vertical β -Ga₂O₃ Power Devices, Akhila Mattapalli, Chinmoy Nath Saha, University of California at Santa Barbara; Carl Peterson, Steve Rebollo, Jim Speck, Sriram Krishnamoorthy, University of California Santa Barbara

Understanding the impact of trench/fin processing on MOS characteristics is key for realizing low-leakage, high field strength dielectrics for vertical trench diodes and transistors. We report on MOCVD Ga etching and wet chemical treatments (HF, HF & HCl, HF & heated H₃PO₄ (HP)) implemented on β -Ga₂O₃ trench structures and their effect on MOS leakage, breakdown and interface charge trapping. Gallium Oxide trenches of 2 or 5 μ m widths were fabricated with a footprint of 200 x 200 μ m² or 300 x 300 μ m² using a BCl₃ ICP-RIE dry etch process or TEGa Ga etch utilizing an MOCVD reactor (25 μ mol/min, 15 Torr, 800°C). We patterned [010] trenches with (100) sidewalls to minimize dry etch damage. The devices were fabricated on a 10 μ m (001) HVPE grown 10¹⁶ cm⁻³ doped drift layer on a Sn-doped conducting substrate. Planar MOS pads were also fabricated on the etched surface to distinguish between planar and sidewall leakage. After the trench etch (dry or Ga), the dry etched surfaces were treated with HF, HF & HCl, or HF & HP, and the Ga etch sample was treated with HF to remove the hard mask. Following trench definition and treatments, 55 nm Al₂O₃ gate oxide was deposited using plasma ALD, followed by Mo metal deposition. PR planarization was used to define the sidewall gate metal length. These steps were modeled after a typical vertical FinFET process. Current-voltage (J-V), capacitance-voltage (C-V), C-V hysteresis, reverse and forward breakdown measurements were carried out to characterize the trench MOS and planar MOS test structures.

All four samples had low baseline leakage (10⁻⁶ A/cm²), but the HF & HP and Ga etch samples had lower leakage compared to the HF and HF & HCl treated samples under higher forward voltage. C-V hysteresis measurements with a 5-min accumulation stress displayed reduced charge trapping in the Ga etch sample compared to the treated dry etch samples for planar MOS structures. The average trapped charge in the planar samples was 2.7, 6.3, 4.2, and 2.0 x 10¹¹ cm⁻² for Ga etch, HF & HP, HF, and HF & HCl respectively. The trench devices had similar trends, including a large device-to-device variation for the HF & HCl and HF samples. A 1.4 kV catastrophic breakdown was observed for the HP sample and 1.3 kV for the Ga Etch sample. An oxide breakdown field of 6.3 MV/cm was measured using forward I-V characteristics for Ga Etch planar samples with a 55 nm gate oxide. This study indicates that dry etch followed by heated H₃PO₄ treatment and trench etch using Ga precursor are promising approaches to realize low-leakage, high breakdown, low interface state density MOS junctions for vertical trench diodes and vertical transistors.

IWGO-WeP-33 High-Temperature Stability of Contacts to β -Ga₂O₃, Donivan R. Mouch, The Applied Research Lab at The Pennsylvania State University; Paul Kelemen, Sohyun Lee, Nathan S. Banner, Chan-Wen Chiu, Suzanne E. Mohney, Pennsylvania State University; Luke A. M. Lyle, The Applied Research Lab at The Pennsylvania State University

β -Ga₂O₃ is among the most promising candidates to replace Si in power electronics as it features an ultrawide band gap, shallow n-type dopants, and a large Baliga's figure of merit. It has the potential to surpass both SiC and GaN as a material for high power electronics due to the above considerations and presents the potential for scaling up manufacturing due to its ability to be grown from the melt. Wide and ultra-wide band gap semiconductors, like β -Ga₂O₃, offer the ability to operate at high voltages, high power, and high temperatures (> 300 °C). However, promising aspects of β -Ga₂O₃ can be limited, in part, due to the metal/semiconductor interface when high operating temperatures are required. The work examines the metallurgical stability of metallizations at elevated temperatures up to 700 °C.

This work explores the popular Ti/Au 20/100 nm and new Ti/TaSi₂/Ti/Pt 20/150/5/100 nm ohmic contacts for high-temperature applications. Ohmic contacts are annealed for 60 s at 100 °C increments in a rapid thermal annealing furnace, starting at 300 °C and increasing until failure. As deposited and annealed contacts are probed to determine specific contact resistances using the Cox-Strack method. In this work we demonstrated that by using the new Ti/TaSi₂/Ti/Pt ohmic contact, we can achieve a lower specific contact resistance by more than a factor of two after annealing at 500 °C. In addition to offering lower specific contact resistances, the Ti/TaSi₂/Ti/Pt ohmic contact continues to improve upon further annealing

up to 700 °C, while the Ti/Au contact is longer usable. We think that the failure mechanism of the Ti/Au, at 700 °C, may in part be caused by agglomeration of the Au layer. In addition, we will also present work on high-temperature stability of Schottky diodes to β -Ga₂O₃.

IWGO-WeP-34 Investigation of Temperature-Dependent Forward Transport Mechanism in kV class NiO/ β -Ga₂O₃ Heterojunction Diodes, Surajit Chakraborty, Deb Indronil Sajib, Uttam Singiseti, University at Buffalo-SUNY

Combining the ultra-wide bandgaps of p-NiO and n- β -Ga₂O₃ enables heterojunction diodes to achieve breakdown voltages exceeding 8 kV and power figures of merit (13.2 GW/cm²) [1]. In this study, we investigate the forward current behavior of sputtered p-NiO_x/n- β -Ga₂O₃ vertical rectifiers using temperature-dependent current–voltage (*I*–*V*–*T*) analysis, together with our developed analytical model and TCAD simulation incorporating Danielsson trap assisted interface recombination model [2].

We fabricated p-NiO_x/n- β -Ga₂O₃ HJD using RF reactive sputtering of a metallic Ni target for the NiO_x layer. The device schematic is illustrated in Fig. 1(a), with the process flow shown in Fig. 1(b). A bilayer NiO_x deposited with controlled Ar/O₂ ratios: the first layer is deposited at Ar/O₂ = 22/10 sccm (4.5 mT, 200 W, 100 nm), followed by a second layer at Ar/O₂ = 10/8 sccm (4 mT, 150 W, 100 nm), yielding sheet resistances of 171 k Ω /sq and 57.1 k Ω /sq, respectively. The doping concentration (*N_D*–*N_A*), extracted from C–V measurements, is $\sim 9 \times 10^{15}$ cm⁻³ which is depicted in Fig. 2. A small-area HJD (75 μ m diameter) with *V_{on}* \sim 1.97 V, an on-resistance of 16.3 m Ω /cm² achieves a breakdown voltage exceeding 3 kV (Instrument limit) showed in Fig. 3 and Fig. 4 respectively.

Temperature-dependent *I*–*V* measurements were conducted over a range from –33 °C to 250 °C to elucidate the forward conduction mechanism. To understand the mechanism, we developed both an analytical and TCAD model with interface recombination as the mechanism for current transport. This trend is in close agreement with the TCAD simulation model, as illustrated in Fig. 5. For all temperatures, *k_BT* \ll ΔE_c + *V_{bi}*, ruling out thermionic emission as the dominant transport mechanism. Furthermore, since *V_{ON}* \ll ΔE_c + *V_{bi}*, diffusion-limited transport is also unlikely. Silvaco TCAD simulations incorporating an interface trap level of approximately 0.4 eV below the NiO-side electrostatic potential successfully reproduce the *J*–*V* characteristics, showing close agreement with the experimental results depicted in Fig. 6 in different temperatures. Both the analytical and TCAD models predict the lower turn-on voltages than the voltage estimated from thermionic transport shown in Fig. 7. These results indicate that forward conduction is governed primarily by trap-assisted interface recombination.

IWGO-WeP-35 Group-III Flux Etching of β -(Al_xGa_{1-x})₂O₃ Heterostructures, Emma Rocco, Frank Kelly, J. S. Lundh, Daniel Pennachio, Katie Gann, Cameron Gorsak, Alan Jacobs, Marko Tadjer, Michael Mastro, U.S. Naval Research Laboratory

Group-III (Al, Ga) oxides have emerged as next-generation semiconductor materials for high-power applications owing to large bandgap energies and high critical electric field strengths. Realizing β -(Al_xGa_{1-x})₂O₃ power electronic devices require processing techniques for the fabrication of device architectures such as diodes and field effect transistors (FETs), including etching processes. Industry standard dry processes including inductively coupled plasma (ICP) etching have been developed for β -Ga₂O₃, utilizing SF₆, Cl₂, and BCl₃ chemistries. However, dry etching of β -Ga₂O₃ has been shown to result in subsurface damage. An alternative, Ga-flux etching of β -Ga₂O₃ has emerged as a potential damage-free technique and can be completed *in situ* via molecular beam epitaxy (MBE) and metal organic chemical vapor deposition (MOCVD). Ga-flux etch rates of β -Ga₂O₃ have been shown to vary based on the rate of Ga-flux, pressure, and crystal orientation, with etch rates as high as 140 nm/min and 30 nm/min reported for MOCVD and MBE flux etching, respectively. Etch rate has also been found to be dependent on feature size and pitch, with significant increase at the edge of mask openings due to precursor loading. To date, Ga-flux etching of β -(Al_xGa_{1-x})₂O₃ has yet to be reported, as well as the use of a combined Ga- and Al-flux.

In the present study, we investigate the impact of Ga to Al ratio, and group-III flux on the etch rate of β -(Al_xGa_{1-x})₂O₃ and Ga₂O₃ thin films. The structures under test are FETs consisting of O₃-MBE grown 21 nm β -(Al_{0.18}Ga_{0.82})₂O₃/250 nm Ga₂O₃ on (010) Ga₂O₃:Sn substrates (NCT, Japan). An SiO₂/SiN bi-layer mask is utilized and openings to the β -(Al_xGa_{1-x})₂O₃ are patterned via photolithography. Group-III flux etches were carried out in an Agnition Agilis 500 MOCVD system utilizing triethylgallium (TEGa) and trimethylaluminum (TMAI) as the Ga and Al precursors, respectively. A 24 min, Ga-flux only etch with TEGa flow rate of 35 μ mol/min resulted in etch

depths on the order of hundreds of nanometers, as measured by profilometry with an inverse relationship between etch depth and feature spacing. Characteristic crystallographic striations are seen via optical microscopy on the Ga₂O₃ surface following the etch for features with 5 μ m spacing. At increased feature spacings of 10 μ m and 15 μ m, incomplete removal of the Al-containing layer is observed by scanning electron microscopy and electron dispersive x-ray spectroscopy (SEM- EDX). This may indicate the formation of an Al or Al₂O₃ layer, inert to Ga-flux etching, resulting in micro-masking. Lower Ga- and group-III fluxes will be investigated for uniform volatilization of (Al_xGa_{1-x})₂O₃.

IWGO-WeP-36 Carrier Transport Across Wafer Bonded (001) -Ga₂O₃ Interfaces, Advait Gilankar, Arizona State University; Michael Liao, Piyush Shah, Apex Microdevices; Mark Goorsky, University of California Los Angeles; Nidhin Kurian Kalarickal, Arizona State University

Wafer bonding and heterogenous integration of β -Ga₂O₃ have been explored in the past to mitigate the low thermal conductivity of Ga₂O₃ [1]. However, homogeneous wafer bonding of Ga₂O₃ to Ga₂O₃ for active electrical transport across the bonded interface hasn't been explored so far. Achieving linear electrical transport across such homogeneously bonded interfaces with low interfacial resistance can open new design avenues for Ga₂O₃ power devices. In this work, we investigate electrical transport across bonded (001) Ga₂O₃ HVPE grown epilayers. Both samples underwent standard RCA SC-1 cleaning prior to being subjected to a plasma surface treatment. After plasma treatment, both samples were aligned face-to-face and \sim kPa pressure was applied to initiate the bond at room temperature. The bonded structure was then annealed up to 900 °C for bond strengthening. The top-side epilayer (EPI2) and substrate were then polished at an angle to obtain an inclined surface (Fig.1 a). After polishing, EPI2 exhibited an RMS surface roughness of \sim 0.25 nm. Off-axis XRD ϕ -scans revealed an in-plane rotational misalignment of \sim 5° between the two bonded epilayers. The electrical transport across interface was studied by fabricating Ni/Ga₂O₃ SBDs and Si implanted ohmic contacts (Ti/Au) at different locations along the incline (Fig.1 a). Diodes formed directly of EPI1 displayed high current density (\sim 10² A/cm²), while diodes located just near the start of the incline (diode B) displayed no current. As we move to the location of diode C (thicker EPI2), the devices turn-on with a low forward current density (\sim 10⁻¹ A-cm⁻²) indicating high interfacial resistance. The diodes formed on the substrate (diode D) show high reverse leakage but similar forward current densities (\sim 10⁻¹ A-cm⁻²). We attribute this behavior to a fixed negative charge at the bonded interface (\sim high 10¹¹ cm⁻²), supported by Silvaco TCAD simulations, which showed clear current suppression with increasing interfacial fixed negative charge density. Similar to the diodes, Si-implanted and annealed ohmic contacts (along the incline of EPI2) exhibited quasi-ohmic behavior with high resistance. We hypothesize that reducing the rotational misalignment can result in enhanced current transport across the homogenous bonded interface. This work was supported by the National Science Foundation under Grant No. NSF ECCS 2336397.

[1] M. Liao, *J. Vac. Sci. Technol. A* 41, 063203 (2023).

*Author for correspondence: agilanka@asu.edu

IWGO-WeP-37 High-Reflectance In-Plane Ga₂O₃/Air DBRs Fabricated by HEATE on (010) β -Ga₂O₃, SOTARO IJIMA, TAKAHASHI YUKI, Sophia Univ, Japan; AKIHIKO KIKUCHI, Sophia Univ / Sophia Semiconductor Research Institute, Japan

Ga₂O₃ has attracted increasing interest for electronic and photonic devices, owing to its wide bandgap energy (> 4.5 eV), excellent controllability of n-type conductivity, and availability of high-quality single-crystal substrates. We have previously developed a hydrogen environment anisotropic thermal etching (HEATE) technique enabling precise, high-aspect-ratio nanofabrication of GaN and Ga₂O₃ via hydrogen-assisted thermal decomposition combined with an ultrathin SiO₂ mask.

In this study, we demonstrate a novel photonic device application based on (010) β -Ga₂O₃. An in-plane high-Q resonator was fabricated by integrating a Ga₂O₃/air distributed Bragg reflector (DBR), designed for broadband high reflectance in the visible region, with a nanofluidic channel for dye injection. The reflectance characteristics of standalone Ga₂O₃/air DBR structures were also investigated.

The integrated resonator consists of a dye-solution reservoir (300 μ m \times 500 μ m), a nanofluidic channel transporting dye via capillary action, and a resonator section with DBRs on both sides of the channel. To secure optical paths for side excitation and observation of resonator characteristics, high-aspect-ratio structures with heights exceeding 10 μ m were formed approximately 50 μ m from the substrate edge.

Wednesday Evening, August 5, 2026

Fabrication was carried out on Fe-doped (010) β -Ga₂O₃ wafers. After forming SiO₂ nanomasks by electron-beam lithography and dry etching, HEATE processing was performed at 900°C under a hydrogen pressure of 100Pa for 330min. High-resolution SEM revealed vertically smooth DBR sidewalls along the thermodynamically stable (100) planes. The Ga₂O₃/air layer thicknesses were 217nm/410nm for the third-order DBR and 362nm/683nm for the fifth-order DBR, with deviations from the designed values within +4nm and -10nm. Side-view optical microscope observations using a 100× objective lens clearly resolved the 16μm-high DBR structures and nanofluidic channels, confirming suitability for side-excited resonator characterization.

For optical characterization, the third- and fifth-order standalone DBRs, both designed for a center wavelength of 547nm, were fabricated. Reflectance spectra measured using Fourier imaging microscopy agreed well with one-dimensional transfer-matrix simulations. Maximum reflectance and stopband widths (reflectance >90%) were 97% and 62nm for the third-order DBR, and 95% and 35nm for the fifth-order DBR, demonstrating excellent broadband reflectance performance.

Acknowledgement: Part of this study was supported by JSPS KAKENHI JP24K00950.

References: [1] R. Kita et al., Jpn. J. Appl. Phys., 54, 046501 (2015). [2] Y. Ooe et al., 80th JSAP Autumn meeting, 21p-B31-6 (2019).

IWGO-WeP-38 Phase-Dependent Photoluminescence of Near-Infrared Color Centers in Ga₂O₃, Keidai Toyoshima, The University of Tokyo, Japan; *Mathias Marchal*, Technical University of Denmark, Denmark; *Riena Jinno*, Satoshi Iwamoto, The University of Tokyo, Japan

Color centers are localized electronic states associated with point defects in crystals, and light emission from these defects produces photons at wavelengths corresponding to these levels and has attracted interest for quantum applications. Recently, luminescence originating from color centers has been reported in beta gallium oxide (β -Ga₂O₃). One example is the emission at 1316 nm, which lies in the telecom O-band. This emission is thought to originate from transition-metal-related defects; although Cu³⁺-related complex defects are candidates, their exact origin remains unknown. Furthermore, the Debye-Waller factor, which quantifies the fraction of emission into the zero-phonon line relative to the total emission and serves as an important figure of merit for quantum applications, has not yet been evaluated for these color centers, nor have their formations in different crystal polymorphs been systematically investigated. In this study, we determine the Debye-Waller factor and investigate the photoluminescence (PL) of various Ga₂O₃ samples.

The samples include Fe-doped and unintentionally doped (UID) β -Ga₂O₃ (010) substrates, as well as Sn-, Cu-, and Fe-doped and UID α -Ga₂O₃ thin films grown on c-plane sapphire substrates. α -Ga₂O₃ thin films were grown by mist chemical vapor deposition (mist CVD). The dopants were added at a concentration of 0.01 at.% relative to Ga. The film thickness was ~800 nm. PL was measured at 9 K using a liquid helium cryogenic system with pulsed laser excitation at a wavelength of 700 nm.

Sharp emission lines around 1312.5 and 1316 nm were observed in the Fe-doped and UID β -Ga₂O₃ substrates. The Debye-Waller factor of the emission from the β -Ga₂O₃ substrates was estimated to be ~6% for both samples. In contrast, no corresponding peaks were detected in the α -Ga₂O₃ thin films. A peak observed at ~1150 nm in the α -Ga₂O₃ films was also observed when only the sapphire substrate was measured, suggesting it originated from color centers within the substrate.

The observation of telecom-band emission in UID β -Ga₂O₃ suggests that unintended defect formation readily occurs, making precise defect control in the β -phase challenging. In contrast, the absence of such emissions in α -Ga₂O₃, even when intentionally doped with transition metals, suggests that the formation of these color centers depends on the specific crystal structure of the β -phase. The absence of such unintended emissions makes α -Ga₂O₃ as a relatively clean and promising host material. By elucidating the precise phase-dependent mechanism of these defects, future studies could enable the controlled introduction and precise tuning of quantum emitters within α -Ga₂O₃ matrices.

IWGO-WeP-39 Transmutation-doped β -Ga₂O₃ via Thermal Neutron Irradiation, Richard Barber, University of Missouri; *Marko Tadjer*, Evan Glaser, Naval Research Laboratory; *Marc Weber*, Washington State University; *Alison Hartman*, University of Missouri-Columbia; *Jaime Freitas*, *Steven Bennett*, *Mason Klemm*, *Alan Jacobs*, *Karl Hobart*, Naval Research Laboratory; *Kohei Sasaki*, *Akito Kuramata*, Novel Crystal Technology, Japan; *P. Shiv Halasyamani*, University of Houston; *Blaine Reid*, *John Brockman*, *John Gahl*, University of Missouri

Technology for doping control of β -Ga₂O₃ crystals via thermal neutron transmutation doping (NTD) is proposed for producing controllably Ge-doped ($\sim 10^{15}$ - 10^{17} cm⁻³ Ge donor concentration) β -Ga₂O₃ wafers for high-voltage applications. Thermal neutron capture by the stable isotopes of Ga, ⁶⁹Ga and ⁷¹Ga, produce the unstable isotopes ⁷⁰Ga and ⁷²Ga, which decay into stable ⁷⁰Ge and ⁷²Ge, forming shallow (E_c -28 meV) donors in Ga₂O₃.

NTD of Ga₂O₃ has been proposed by Logan et al. and demonstrated by Irvine et al. who have shown the transmutation of ^{69/71}Ga into stable ^{70/72}Ge via thermal neutron capture and decay at the OPAL research reactor in Australia [1, 2]. While successfully producing ^{70/72}Ge in β -Ga₂O₃, their work experienced significant challenges originating from the Ir impurities in the Ga₂O₃ wafers and the compensating point defects generated by fast neutrons. In our experiments, β -Ga₂O₃ wafer purity was significantly improved via growth in a crucible-free float zone (FZ) reactor. FZ crystals with diameter of about 8-10 mm were grown and subsequently prepared into polished (010) β -Ga₂O₃ wafers at Novel Crystal Technology, Japan.

In our presentation we will discuss the thermal neutron doping that we performed on Ga₂O₃ FZ grown samples. Point defect formation caused by the fast neutron component of the flux was characterized via electron paramagnetic resonance (EPR) spectroscopy and positron annihilation spectroscopy (PAS), demonstrating suppression of Ga-related vacancies under the irradiation and annealing conditions in these experiments. As a result, for 5×10^{13} n/s·cm² flux duration for 20 hrs, a 4.17×10^{17} cm⁻³ (0.511 ng/mol) concentration of ^{70/72}Ge was measured via inductively-coupled plasma mass spectroscopy (ICP-MS) and confirmed by electron paramagnetic resonance (EPR).

In these samples, a gallium vacancy related point defect concentration of $\sim 9 \times 10^{15}$ cm⁻³ was measured via positron annihilation spectroscopy (PAS) and a pre-irradiation Si concentration of $\sim 3 \times 10^{16}$ cm⁻³ was measured via secondary ion mass spectroscopy (SIMS). To our knowledge, this result is the first experimental demonstration of a ^{70/72}Ge-doped β -Ga₂O₃ crystal with a net thermal neutron transmuted donor concentration higher than the net vacancy concentration induced by the fast neutron component of the irradiation flux.

[1] C.P. Irvine et al., Physical Review Materials 6, no. 11 (2022): 114603

[2] J.V. Logan et al., Mater. Adv. 1, no. 1 (2020): 45-53.

IWGO-WeP-40 Optimizing β -Ga₂O₃ MOCVD Regrowth for Vertically Scaled Channels, Julian Gervasi-Saga, *Nabasinhu Das*, *Advait Gilankar*, *Nidhin Kurian Kalarickal*, School of Electrical, Computer and Energy Engineering, Arizona State University

Vertically scaled channels (Si delta doping, β -Ga₂O₃/(AlGa)₂O₃ modulation doping) are essential for realizing RF and mm-wave transistors based on β -Ga₂O₃. Contact regrowth using both MBE and MOCVD has proven highly effective for forming ohmic contacts to β -Ga₂O₃. While very low contact resistivity ($\sim 10^{-7}$ Ω·cm²) has been demonstrated for metal-n⁺⁺ β -Ga₂O₃ contacts [1], the **total contact resistance** (metal-to-channel) typically remains greater than 1 Ω·mm, particularly in vertically scaled channel architectures. This is nearly an order of magnitude higher than values routinely achieved in GaN (~ 0.1 Ω·mm) and must be reduced to minimize RC delays in high-frequency transistors. In this work, we investigate the impact of the source/drain recess etch and in-plane anisotropy on the total contact resistance.

The total contact resistance (R_c^{total}) comprises the metal-n⁺⁺ contact resistance ($R_c^{\text{n++}}$), the resistance between the metal and regrown layer ($R_s^{\text{n++}}$), and the interfacial resistance (R_{int}) between the regrown layer and channel. A source/drain recess etch, typically performed via ICP-RIE, exposes the channel sidewall prior to regrowth but can introduce etch-induced damage, particularly at the sidewalls, degrading the interfacial resistance. To evaluate this, we compare ICP-RIE etches and an in-situ TBCL etch and assess their impact on contact resistance. The epilayers were co-loaded β -Ga₂O₃ (010) MOCVD-grown Si delta-doped samples (sheet charge $\sim 1 \times 10^{13}$ cm⁻²) with a 30 nm cap. Four etch processes were studied: low-power BCl₃ ICP, low-power Cl₂ ICP, high-power BCl₃ ICP, and in-situ TBCL etching prior to regrowth. After regrowth, Ti/Au contacts were deposited

and annealed at 470 °C in N₂. Electrical characterization was performed using TLM. The low-power BCl₃ ICP etch yielded the lowest contact resistance (**0.54 Ω-mm**), followed by high-power BCl₃ (**2.44 Ω-mm**), low-power Cl₂ (**7.16 Ω-mm**), and in-situ TBCl (**12.08 Ω-mm**). The etch process significantly affected the sheet resistance of the regrown n⁺ layer, indicating defect formation originating at the etched surface. Pronounced in-plane anisotropy in contact resistance was also observed, primarily attributed to variations in R_{int}. TLM structures along [001] exhibited the highest resistance, while those along [100] showed the lowest. Our work highlights the critical role of recess etch processes and in-plane anisotropy in determining contact resistance in β-Ga₂O₃ devices.

This work is supported by the Army Research Office UWBG RF Center (W911NF2520005) and the National Science Foundation (NSF ECCS 2336397).

[1] A. Bhattacharyya et al., Appl. Phys. Express 14, 076502 (2021).
Author for correspondence: jgervass@asu.edu

IWGO-WeP-41 962 V Ga₂O₃ Schottky Power Diodes on (011) Substrate, Luoyuan Jiang, Md Mosarof Hossain Sarkar, Yibo Xu, Hongping Zhao, Wu Lu, Ohio State University

Gallium oxide (Ga₂O₃) has attracted increasing attention for high-voltage power devices due to its ultra-wide bandgap and large critical electric field. In particular, (011)-oriented β-Ga₂O₃ is considered promising for device applications because of lower dislocation density [1]. In this work, we show a Schottky diode with a breakdown voltage of 962 V on a (011) Ga₂O₃ substrate with significantly thinner drift layer thickness than reported devices with similar breakdown voltages.

The device structure consists of a 5.5-μm-thick drift layer grown by MOCVD at a growth rate of 5.5 μm/hr [2] on a (011)-oriented Ga₂O₃ substrate. To achieve a high breakdown voltage, a deep trench filled with SiO₂ in combination with a field plate is used for electric-field mitigation. Numerical simulations show that the structure with optimized trench depth and field plate geometry has a breakdown voltage of 1.4 kV, 800 V higher than the control structure without field management.

C-V measurements show that the average net donor concentration is ~1 × 10¹⁶ cm⁻³. The fabricated device with Ni/Au Schottky contacts exhibited a turn-on voltage of 0.98 V at 1 A/cm², an ideality factor of 1.11, and a specific on-resistance of 6.06 mΩ·cm². Temperature-dependent forward I-V measurements yielded a Schottky barrier height of 1.19 eV and a Richardson constant of 42.2 A/cm²/K². The leakage current density is 8.09 × 10⁻⁹ A/cm² at 100 V reverse bias, and the breakdown voltage is 962 V at a current density of 1 A/cm². At this voltage, the electrical field peaks at the anode edge with a value of 3.6 MV/cm. To our knowledge, the device has the thinnest drift layer thickness in comparison with reported Ga₂O₃ Schottky power diodes with a similar breakdown voltage. The results demonstrated from this work are promising for further scaling up the blocking voltage by increasing the drift layer thickness.

[1] B. Chen *et al*, CrystEngComm, 25, 2404–2409 (2023).

[2] M. M. H. Sarkar *et al*, ACS Appl. Electron. Mater. 8, 3, 1380–1389 (2026).

*Author for correspondence: jiang.2694@osu.edu
[mailto:jiang.2694@osu.edu]; lu.173@osu.edu

IWGO-WeP-42 Identifying the Origin of Emissions and Anisotropic Properties of Different Crystallographic Orientation Sn-Doped β-Ga₂O₃ Substrates, Kishor Upadhyaya, King Abdullah University of Science and Technology, India; Andres Hurtado, King Abdullah University of Science and Technology, Colombia; Hadeel Alamoudi, Iman Roqan, King Abdullah University of Science and Technology, Saudi Arabia

Photoluminescence (PL) and PL excitation (PLE) studies are necessary to understand the orientation dependent transition mechanisms and excitation pathways in β-Ga₂O₃. In this work, we address this gap by exploring the effect of Sn doping on the anisotropic optical properties of state-of-the-art quality (100), (010), and (001)-oriented single crystal Sn-doped β-Ga₂O₃ grown by EFG method (Novel crystal technology, Inc.). The absorption spectra of these Sn-doped β-Ga₂O₃ samples exhibit different behavior for different orientations with (100) and (100) orientations exhibiting an overlap between shallow and deep states with band edge states while (010) reveals a distinct separation between the shallow and deeper states. Raman spectroscopy indicates that the Sn substitution at octahedral Ga sites results in anisotropic vibrational behaviour by significantly altering B_g⁽⁵⁾ and A_g⁽⁹⁾ vibrational modes while suppressing A_g⁽⁹⁾ mode in (010) orientation whereas B_g⁽⁵⁾ is negligible in other two

orientations. PL spectra of Sn-doped films exhibit a broadband emission in the 2.5 eV-4.1 eV range with no band edge emission that is redshifted compared to their UID counterparts. PL and PLE measurements indicate such broadband emission is originated from UV, Blue and green components, while the contribution of each component is different for different orientation. Temperature-dependent photoluminescence (PL) measurements reveal red shift for all three orientations with (010) exhibiting the largest red shift of ~70 meV. PLE measurements at each component reveal the transitions related to such broad band for different orientation Sn-doped β-Ga₂O₃, which governed by dopant-related recombination paths as well as associated intrinsic defects and agrees with the absorption spectra. PLE spectra for (010) reveal additional peaks at 3.8 eV and 4.15 eV, which are not exhibited in other two orientations. PL obtained for different excitation energies corresponding to the peaks observed in PLE (3.35 eV - 4.95eV) reveal luminescence band due to even sub-band gap excitation energy of 3.35 eV. Such excitation-dependent PL correlates very well with the observed PLE peaks confirming the orientation dependent transitions. This is the first observation of emission from β-Ga₂O₃ with sub-band gap excitation. Time-resolved PL analysis shows that (010) exhibits fastest decay time of τ=22ms while (100) has the slowest decay time of τ=135ms further confirming the optical anisotropy. This study reveals origin of Sn-doped β-Ga₂O₃ broad emission, the related anisotropic properties and the effect of Sn incorporation in different orientation on the carrier recombination pathways.

International Workshop on Gallium Oxide and Related Materials (IWGO-6)

Room ESJ 0202 - Session IWGO-ThM1

Theory, Modeling, and Simulation

Moderators: Jinwoo Hwang, The Ohio State University, Joel Varley, Lawrence Livermore National Laboratory

8:00am IWGO-ThM1-1 Breakfast

8:30am IWGO-ThM1-7 Impact of Defects and Impurities on the Properties of Al₂O₃, Chris G. van de Walle, UCSB INVITED

Aluminum oxide (Al₂O₃) has a broad range of applications. Alloys of Al₂O₃ and Ga₂O₃ of course also serve as barrier layers in heterojunctions for Ga₂O₃-based devices. In metal-oxide-semiconductor (MOS) technologies, it can be used as a high-k gate dielectric, to passivate the surface of Si substrates, or as the tunneling layer of non-volatile flash memory devices. Al₂O₃ is also frequently used in superconducting qubits, as a tunneling barrier in the Josephson junction and/or as a substrate and capacitor dielectric.

Defects in the oxide layer affect the performance, for instance by leading to changes in threshold voltage. In quantum applications, the qubits are sensitive to defects in the substrate or in the tunnel barrier of the Josephson junction. Dielectric loss can also lead to decoherence. Enhanced control over devices thus requires a thorough understanding of the structural, electronic, and optical properties of potential defects and impurities.

We have performed first-principles calculations to elucidate these issues. For point defects, we focused on the dominant species, which are the oxygen and aluminum vacancies, and provided detailed characterization of their optical properties, which can aid experimental observation and identification [1]. For dielectric loss, we focused on mechanisms that could affect coherence at the operating frequencies of superconducting qubits, which are around about 5 GHz. We identified a mechanism by which charged defects or impurities can absorb electromagnetic radiation at GHz frequencies by emission of acoustic phonons [2]. Finally, for donor impurities, we have complemented our study of Si [3] with a comprehensive study of alternative impurities in both the corundum and monoclinic phase of Al₂O₃, identifying candidate dopants that are remarkably shallow in light of the very large band gap of this material.

Work performed in collaboration with J. L. Lyons, S. Mu, Y. Shin, S. Mu, M. Turiansky, J. B. Varley, H. Wang, M. Wang, D. Wickramaratne, and C. Wilhelmer, and supported by DOE, ONR and AFOSR.

[1] C. Wilhelmer, M. E. Turiansky, D. Waldhör, L. Cvitkovich, C. G. Van de Walle, and T. Grasser, *Phys. Rev. Mater.* **9**, 096202 (2025).

[2] M. E. Turiansky and C. G. Van de Walle, *APL Quantum* **1**, 026114 (2024).

[3] S. Mu, M. Wang, J. B. Varley, J. L. Lyons, D. Wickramaratne, and C. G. Van de Walle, *Phys. Rev. B* **105**, 155201 (2022).

8:55am IWGO-ThM1-12 GeO₂ and Ge_xSn_{1-x}O₂ Alloys: Emerging Ultra-Wide-Band-Gap Materials for Power Electronics, Emmanouil (Manos) Kioupakis, University of Michigan, Ann Arbor INVITED

In this talk, I will present recent advances by my research group, our collaborators, and the broader community on rutile GeO₂ and its alloys with SnO₂, a new UWBG semiconductor materials platform for power electronics. I will survey our first-principles investigations of the thermodynamic stability, electronic structure, defect physics, carrier transport, and thermal properties of rutile GeO₂ and Ge_xSn_{1-x}O₂ alloys. Complementing the theoretical insights, I will highlight recent experimental progress from our collaborators on the synthesis and characterization of GeO₂-based materials. These results provide critical validation of theoretical predictions and shed light on the practical challenges associated with materials quality and phase stability. Moreover, I will provide a brief overview of broader efforts by the global research community on rutile GeO₂ and its alloys SnO₂, spanning different growth techniques, doping strategies, and characterization approaches. This perspective will help identify key bottlenecks and opportunities for advancing these materials toward device applications.

9:20am IWGO-ThM1-17 Rutile Ge_xSn_{1-x}O₂ Alloys for Ultra-Wide Bandgap Electronics: Phase Stability and Bandgap Engineering, Alp Kurbay, University of Michigan, Ann Arbor; Yann Müller, EPFL, Switzerland; Xiao Zhang, University of Michigan, Ann Arbor; Anirudh Natarajan, EPFL, Switzerland; Emmanouil Kioupakis, University of Michigan, Ann Arbor

Ge_xSn_{1-x}O₂ alloys have recently attracted attention as candidate ultra-wide bandgap (UWBG) materials for power electronics due to their predicted ambipolar dopability, high carrier mobilities, and high thermal conductivity. Experiments show that these alloys can be grown as thin films over a wide composition range, have carrier mobilities that are insensitive to alloy disorder at low Ge content, and exhibit breakdown fields as high as 7.0 ± 1.4 MV/cm [1]. In this study, we perform a comprehensive investigation of the thermodynamic stability, structural parameters, and electronic properties of Ge_xSn_{1-x}O₂ alloys using first-principles atomistic calculations. The large positive mixing enthalpy produces a miscibility gap with a critical temperature above 2300 K, which agrees with the experimental phase diagram for bulk materials [2]. This indicates that the high solubilities observed in thin-film synthesis cannot be explained by the incoherent phase diagram alone. We demonstrate that coherency strain during epitaxial growth substantially alters phase stability, and calculations of the coherent spinodal show significant suppression of the miscibility gap, reducing the critical temperature to ≈ 900 K. Our calculations show that these alloys exhibit only weak short-range order, with a slight tendency for Ge–Sn nearest-neighbor clustering, and can be approximated as random solid solutions. Our calculated lattice parameters exhibit a nearly linear dependence on composition, consistent with Vegard's law and experimental measurements. Hybrid-functional calculations show a direct band gap at the Γ -point ranging from ~ 3.6 eV in SnO₂ to ~ 4.7 eV in GeO₂ with strong compositional bowing and light carrier effective masses. The calculated bandgaps in the Sn-rich region show a ~ 200 meV difference between thin films and bulk alloys, and we explore possible causes such as compressive strain and interfacial effects from the substrates. Our results reveal the thermodynamic origin of the metastability of Ge_xSn_{1-x}O₂ thin films and demonstrate the potential of this system for band-gap engineering in ultra-wide-bandgap oxide semiconductors [3].

[1] U. Mansur et al., *Phys. Status Solidi A*, 202501029 (2026).

[2] Watanabe, *J. Am. Ceram. Soc.* **66**, c104 (1983).

[3] Müller et al., arXiv:2601.12184, <https://doi.org/10.48550/arXiv.2601.12184>.

+Author for correspondence: akurbay@umich.edu.

9:35am IWGO-ThM1-20 Single Ga-Layer Reconstruction Mediates Ga₂O₃ Heteroepitaxy: A Multiscale Atomistic Study, Ilaria Bertoni, Aldo Ugolotti, Anna Marzegalli, Università degli Studi di Milano-Bicocca, Italy; Flyura Djurabekova, University of Helsinki, Finland; Leonida Miglio, Università degli Studi di Milano-Bicocca, Italy

Ga₂O₃ heteroepitaxy on c-plane sapphire displays a rich polymorphic competition, with different phases stabilizing depending on growth conditions [1]. Under high-temperature/ low-rate conditions—approaching quasi-equilibrium growth—largely relaxed β -Ga₂O₃ crystallites grow on sapphire, often mediated by a thin α wetting layer at the interface [2]. The coherent β /substrate interface is characterized by a strongly anisotropic mismatch strain, as large as $\sim 9\%$ along one of the two in-plane directions, thus making the observed stabilization of β without classical misfit dislocations particularly remarkable. The thermodynamic and atomistic mechanism behind this α/β sequence remains poorly understood.

Through a multiscale framework combining density functional theory, classical nucleation theory and continuum elasticity modeling, we show that α wetting of sapphire is thermodynamically driven by surface energetics, justifying the formation of a thin α interlayer of up to ~ 3 bilayers. Beyond this thickness, a crossover emerges: three-dimensional β islands, relaxing elastically through their free surfaces, become thermodynamically favored above a critical size, providing a purely thermodynamic rationale for the experimentally observed $\alpha \rightarrow \beta$ sequence.

Moreover, upon thermal activation, molecular dynamics simulations reveal a collective atomic rearrangement at the β/α interface that goes well beyond elastic relaxation, enabling near-complete strain release. This plastic reconstruction is confined to a single Ga atomic plane: as the β island expands toward its bulk lattice parameter, at the interface the relaxed β oxygen sublattice periodically overlaps with different sites of the underlying strained α sublattice, causing the interfacial Ga layer to respond to the local oxygen-sublattice environment by adopting an α -like or β -like coordination within the same atomic plane. The oxygen framework remains

perfectly crystalline across the interface, with strain accommodated entirely via this cation redistribution — a mechanism fundamentally distinct from dislocation-mediated relaxation.

This interfacial plasticity provides a permanent, size-independent strain-relief pathway that explains how β -Ga₂O₃ can stabilize on a strained α wetting layer even after island coalescence, consistent with experimental observations under quasi-equilibrium growth conditions.

[1] ACS Appl. Mater. Interfaces 17, 62261–62276 (2025)

[2] Applied Physics Express 8, 011101 (2015)

9:50am **IWGO-ThM1-23 Carrier Mobility in Ge_xSn_{1-x}O₂ Alloys from First Principles**, **Amanda Wang**, Alp Kurbay, Xiao Zhang, Nick Pant, Emmanouil Kioupakis, University of Michigan

SnO₂ and GeO₂ are both transparent conducting oxides in the rutile crystal structure, with band gaps of 3.6 eV and 4.7 eV, respectively. Alloying the two enables tunability of the band gap and of the lattice constants, as well as potential for ambipolar doping due to the predicted ambipolar dopability of GeO₂. However, a shortcoming of many semiconductor alloys is that the disordered potential landscape caused by the random arrangement of atoms results in carrier scattering, impeding mobility. Despite this, experiments have found high electron mobilities in Ge_xSn_{1-x}O₂ alloys that are insensitive to alloy composition, indicating a lack of alloy scattering [1,2]. In this work, we calculate the electron and hole mobilities in Ge_xSn_{1-x}O₂ alloys using first-principles electronic structure methods to predict the theoretical upper limit of mobility and examine the role of alloy scattering across the composition range. The carrier mobility limited by phonon- and ionized-impurity scattering is calculated for the binary end compounds, in good agreement with experimental measurements for SnO₂. To characterize the alloy scattering, we model random alloys using supercells and perform slab calculations to align the band edges across the composition range. The alloy scattering is combined with the phonon- and ionized-impurity scattering to determine the total alloy mobility. We find that the insensitivity of the band edges with respect to composition results in weak alloy scattering and high electron mobilities that are invariant to composition, especially in the range of low Ge composition, reproducing the trend from experiments as seen in Figure 1. This confirms that Ge_xSn_{1-x}O₂ alloys are promising wide-band-gap semiconductors with efficient carrier transport.

[1] Y. Nagashima, *et al.*, Chem. Mater. 34(24), 10842–10848 (2022).

[2] H. Takane, *et al.*, Phys. Rev. Mater. 6(8), 084604 (2022).

10:05am **IWGO-ThM1-26 Refractive Indices, Band-to-Band Transitions, and Ultraviolet Dielectric Functions of Unintentionally-Doped (x = 0 . . . 0.3) and Silicon Doped (x = 0 . . . 0.25) Single Crystal (100) β -(Al_xGa_{1-x})₂O₃**, **Preston Sorensen**, University of Nebraska - Lincoln; *Alyssa Mock*, Weber State University; *Megan Stokey*, Milwaukee School of Engineering; *Ufuk Kilic*, University of Nebraska - Lincoln; *Rafal Korlacki*, J. A. Woollam Co., Inc.; *Akhil Mauze*, *Yuewei Zhang*, *James Speck*, University of California Santa Barbara; *Zbigniew Galazka*, Leibniz Institute for Crystal Growth, Germany; *Vanya Darakchieva*, Lund University, Sweden; *Mathias Schubert*, University of Nebraska - Lincoln

The monoclinic beta phase of gallium oxide is an ultra-wide bandgap semiconductor that has been widely studied for potential use in high power switching applications. Advances in crystal growth techniques enable us to investigate high quality β -(Al_xGa_{1-x})₂O₃ films and bulk substrates. For the first time, the properties of unstrained bulk substrates are investigated, permitting for the decoupling of the effects of strain and the native properties of the lattice. Understanding the fundamental properties of the substrates also permits the investigation of compressive and tensile strain of epitaxial β -(Al_xGa_{1-x})₂O₃ or β -Ga₂O₃ on a different solid solution β -(Al_xGa_{1-x})₂O₃ crystal substrate, which has not yet been done.

Here, we study β -(Al_xGa_{1-x})₂O₃ (x = 0.05, 0.1, 0.15, 0.2, 0.25, and 0.3) and Silicon doped (x = 0.05, 0.1, 0.15, 0.2, and 0.25) both with (100) surface orientation. Bulk β -(Al_xGa_{1-x})₂O₃ crystals were grown by the Czochralski method using Ir crucibles and oxidizing atmosphere. We present model dielectric functions in the near ultraviolet to the vacuum ultraviolet. We investigate the changes in the optical bandgap and band-to-band transitions associated with the increasing aluminum concentration. We compare the results to our previous work done on an additional sample set of pseudomorphically strained β -(Al_xGa_{1-x})₂O₃ films on (010) β -Ga₂O₃, with aluminum molar content up to 21%. We contrast the data obtained from the doped samples to the unintentionally-doped samples to resolve the

effects of doping on free charge carrier concentration, bandgap, and higher photon energy band-to-band transitions.

International Workshop on Gallium Oxide and Related Materials (IWGO-6)

Room ESJ 0202 - Session IWGO-ThM2

Defects Science IV

Moderators: Emma Rocco, Naval Research Laboratory, **Chris G. van de Walle**, University of California Santa Barbara

10:50am **IWGO-ThM2-35 4D-STEM and Machine Learning Investigation of Defects and Polymorphism in Ultra Wide Band Gap Oxides and Nitrides**, **Jinwoo Hwang**, The Ohio State University

INVITED

Four dimensional scanning transmission electron microscopy (4D-STEM) has expanded the detector space of STEM, enabling efficient acquisition of electron nanodiffraction patterns with site specificity [1-4]. This capability allows detailed study of local defects and polymorphism in ultra wide band gap materials, including Ga₂O₃ and nitride based systems under active investigation. However, the massive data volume generated by 4D-STEM makes analysis inherently a big data problem, which bottlenecks the synthesis-characterization feedback loop that must be iterated multiple times to optimize thin film structure and properties. To address this, we incorporate machine learning analysis of 4D-STEM nanodiffraction data (Fig. 1a) to identify structural heterogeneity, bond anomalies, and phase separation in Ga₂O₃ films and II-IV-N₂ thin films. We demonstrate that this approach effectively identifies nanoscale polymorphs in Ga₂O₃, as well as structural distortion and different domains in MgSiN₂ based thin films. This combined 4D-STEM and machine learning framework enables fast throughput analysis of structure and defects in thin films [5], which is essential for accelerating the discovery and development of next generation materials for microelectronics in harsh environments. This presentation also includes high resolution STEM studies of twin boundaries in bulk Ga₂O₃ substrates, along with heterointerfaces involving emerging p-type materials such as LiGaO (Fig. 1b) [6,7].

[1] G. Calderon *et al.*, Acta Mater. 298, 121402 (2025).

[2] G. Calderon *et al.*, ACS Applied Materials & Interfaces 16, 55852 (2024).

[3] M. Abbasi *et al.*, APL Materials 11, 011102 (2023).

[4] S. Im *et al.*, Ultramicroscopy 195, 189 (2018).

[5] M. Zhu *et al.*, Scientific Reports 14, 4198 (2024).

[6] K. Zhang *et al.*, Phys. Status Solidi RRL 19 (12), 2500192 (2025).

[7] D. Yu *et al.*, APL Electron. Devices 1, 046104 (2025).

*Author for correspondence: hwang.458@osu.edu

11:15am **IWGO-ThM2-40 Bandgap Renormalization in Si-doped β -Ga₂O₃ Films**, **Takeyoshi Onuma**, **Kai Yamamoto**, **Kyohei Tanaka**, Kogakuin University, Japan; **Yoshiki Iba**, Tokyo University of Agriculture and Technology, Japan; **Junya Yoshinaga**, TAIYO NIPPON SANSO CORPORATION, Japan; **Yuma Terauchi**, Tokyo University of Agriculture and Technology, Japan; **Tomohiro Yamaguchi**, Kogakuin University, Japan; **Masataka Higashiwaki**, Osaka Metropolitan University/NICT, Japan; **Yuzaburo Ban**, TAIYO NIPPON SANSO ATI CORPORATION, Japan; **Yoshinao Kumagai**, Tokyo University of Agriculture and Technology, Japan; **Tohru Honda**, Kogakuin University, Japan

Burstein-Moss (BM) shift in β -Ga₂O₃ has been reported for single-crystal substrates [1], while bandgap renormalization (BGR) has been addressed for Si-doped films [2]. Recently, Yoshinaga *et al.* reported growth of Si-doped films by low-pressure hot-wall metal organic vapor phase epitaxy (MOVPE) [3]. In this study, optical spectra were measured for the MOVPE-grown Si-doped films to discuss BGR. 2.5–2.6- μ m-thick Si-doped films were grown on semi-insulating Fe-doped (010) substrates by inserting 1- μ m-thick undoped layer [3]. Room temperature carrier densities *n* were in a range from 1.77 \times 10¹⁶ to 1.29 \times 10¹⁹ cm⁻³. Polarized photoluminescence (PL) and PL excitation (PLE) spectra at 300 K are summarized in Fig. 1. All the PL spectra exhibited a peak around 3.35 eV (370 nm) due to donor-acceptor pair (DAP) emission involving Si donor [4]. A peak associated with the exciton transition at the Γ point was observed in the PLE spectra. The PLE peak energies are plotted as a function of *n* in Fig. 2. The BM and BGR shifts (Δ_{BM} and Δ_{BGR}) were calculated according to the *n*^{2/3} and *n*^{1/3} laws, respectively. As shown by the solid lines, the PLE peak energies were well reproduced by the Δ_{BGR} . The result implies the occurrence of BGR due to hybridization between band and Si levels. This work was supported by MIC under a grant

Thursday Morning, August 6, 2026

entitled “R&D of ICT Priority Technology (JPMI00316): Next-Generation Energy-Efficient Semiconductor Development and Demonstration Project (1st and 2nd periods) (in collaboration with MOEJ).” [1] N. Ueda et al., *APL* **71**, 933 (1997). [2] J. Zhang et al., *PRB* **106**, 205305 (2022). [3] J. Yoshinaga et al., *APEX* **18**, 055503 (2025). [4] T. Onuma et al., *JAP* **124**, 075103 (2018).

11:30am IWGO-ThM2-43 Formation and Stabilization of Ga Vacancies in β -(Al,Ga) $_2$ O $_3$: Effects of Al-alloying, Si-doping, and Proton Irradiation, Iuliia Zhelezova, Ilja Makkonen, University of Helsinki, Finland; Zbigniew Galazka, Leibniz-Institut für Kristallzüchtung, Germany; Filip Tuomisto, University of Helsinki, Finland

While *n*-type doping is readily achieved in β -Ga $_2$ O $_3$, its realization in wider bandgap β -(Al,Ga) $_2$ O $_3$ alloys remains challenging due to compensating defects. Here, we investigate cation vacancy formation in Si-doped β -(Al,Ga) $_2$ O $_3$ single crystals using positron annihilation spectroscopy. Eight Czochralski-grown compositions with Al contents of 0–25% were studied in undoped and Si-doped forms. Crystals were grown at Leibniz-Institut für Kristallzüchtung [1]. Residual Si concentrations in undoped samples are $2\text{--}3 \times 10^{17} \text{ cm}^{-3}$, while intentional doping yields $3\text{--}6 \times 10^{18} \text{ cm}^{-3}$. Hall measurements show *n*-type conductivity in undoped samples, whereas doping efficiency decreases with increasing Al content and the 25% alloy becomes insulating [1].

Temperature-dependent positron lifetime and 4D Doppler measurements [2] reveal clear differences between undoped and Si-doped materials. Undoped crystals exhibit strong anisotropy characteristic of β -Ga $_2$ O $_3$, while Si-doped samples show reduced anisotropy independent of Al content. Positron lifetimes are longer in Si-doped samples (190–220 ps) than in undoped ones (170–195 ps), indicating enhanced vacancy trapping. Si-doped alloys with 10–25% Al show nearly identical annihilation characteristics, consistent with dominant unrelaxed Ga vacancies. Undoped samples show signatures of split Ga-vacancy configurations, with unrelaxed vacancies appearing only at elevated temperatures for higher Al contents (20–25%). Below 100 K, negatively charged defects are observed only in Al-containing samples. The similar signatures of Si-doped alloys indicate that the insulating behavior of the 25% Al sample cannot be explained by Ga vacancies alone but likely involves additional acceptor-type defects.

To further probe defect formation, selected samples were subjected to 6 MeV proton irradiation. Undoped samples show increased lifetimes, reduced anisotropy, and decreased *W* $_2$ parameters, consistent with formation of unrelaxed Ga vacancies. In contrast, only minor changes occur in Si-doped samples, indicating that such vacancies are already dominant.

Overall, Al-alloying, Si-doping, and proton irradiation stabilize unrelaxed Ga vacancies and promote compensating defects, limiting doping efficiency and contributing to insulating behavior in β -(Al,Ga) $_2$ O $_3$.

[1] Z. Galazka et al., *JAP*, **133**, 035702 (2023).

[2] I. Zhelezova et al., *JAP*, **136**, 065702 (2024).

Author for correspondence: iuliia.zhelezova@helsinki.fi

11:45am IWGO-ThM2-46 Nitrogen-Doped (AlGa) $_2$ O $_3$ /n-Ga $_2$ O $_3$ Junctions Grown by Plasma-Assisted Molecular Beam Epitaxy, Kohki Tsujimoto, Toshiki Nakaoka, Yusuke Teramura, Shoma Takeda, Satoko Honda, Masataka Higashiwaki, Osaka Metropolitan University, Japan

Nitrogen (N)-doped (AlGa) $_2$ O $_3$ layers are effective in forming a large energy barrier in various Ga $_2$ O $_3$ device structures. For instance, a N-doped (AlGa) $_2$ O $_3$ back barrier is expected to significantly suppress leakage current at an interface between an epitaxial layer and a semi-insulating substrate in lateral Ga $_2$ O $_3$ field-effect transistors (FETs). In this study, we developed plasma-assisted molecular beam epitaxy (PAMBE) growth techniques of N-doped (AlGa) $_2$ O $_3$ thin films on Ga $_2$ O $_3$ (010) substrates and investigated their structural and electrical properties.

We first characterized structural properties of N-doped (AlGa) $_2$ O $_3$ layers with a N density of $4 \times 10^{19} \text{ cm}^{-3}$ and Al compositions of 0.06, 0.11, 0.15, and 0.18 by X-ray diffraction ω - 2θ measurement. (AlGa) $_2$ O $_3$ (020) peaks and clear fringe patterns were observed for all compositions, indicating high crystal quality and smooth epilayer/substrate interfaces.

To evaluate electrical properties, we fabricated vertical Schottky barrier diodes (SBDs) using the PAMBE-grown N-doped (AlGa) $_2$ O $_3$ layers on *n*-Ga $_2$ O $_3$ (010) substrates. The SBDs had Ni/Au Schottky anode electrodes on the N-doped (AlGa) $_2$ O $_3$ layer and a Ti/Au cathode ohmic electrode on the substrate backside. Note that a highly Si-doped *n* $^+$ -Ga $_2$ O $_3$ region (Si $\sim 3 \times 10^{19} \text{ cm}^{-3}$) was unintentionally formed at the epilayer/substrate interface due to Si contamination of the substrate surface.

The capacitance–voltage (*C*–*V*) characteristics of the N-doped (AlGa) $_2$ O $_3$ SBDs showed a monotonic decrease in *C* with decreasing *V* regardless of the Al composition, indicating that the depletion layer expanded into the substrate over the whole *V* range. This behavior was in contrast with that of a N-doped Ga $_2$ O $_3$ reference SBD (N = $4 \times 10^{19} \text{ cm}^{-3}$) in which the *C* remained nearly constant for *V* > –7 V and began to decrease for *V* < –7 V with decreasing *V*, indicating that a two-dimensional electron gas (2DEG) was formed at the epilayer/substrate interface due to the highly Si-doped *n* $^+$ -Ga $_2$ O $_3$ region, pinned the Fermi level, and prevented the depletion layer from expanding into the *n*-Ga $_2$ O $_3$ substrate for *V* < –7 V. This was because N deep acceptors in the N-doped Ga $_2$ O $_3$ layer compensated for only a small portion of the Si donors at the interface. This comparison demonstrates that the N-doped (AlGa) $_2$ O $_3$ layer is more effective to compensate for interface Si donors than the N-doped Ga $_2$ O $_3$ one and thus suggests that a N-doped (AlGa) $_2$ O $_3$ layer is more promising than a N-doped Ga $_2$ O $_3$ layer as a back barrier of lateral Ga $_2$ O $_3$ FETs.

This work was supported by JSPS KAKENHI Grant Number JP26H02143.

Friday Morning, August 7, 2026

International Workshop on Gallium Oxide and Related Materials (IWGO-6)

Room ESJ 0202 - Session IWGO-FrM1

Plenary Session III

Moderators: Shizuo Fujita, Kyoto University, Hongping Zhao, The Ohio State University

8:00am IWGO-FrM1-1 Breakfast

8:45am IWGO-FrM1-10 PLENARY: Scaling Ga₂O₃ Power Electronics: From 10 kV Devices to Megawatt Modules, *Yuhao Zhang*, The University of Hong Kong

INVITED

Benefiting from advances in large-diameter Ga₂O₃ wafers and processing technologies, Ga₂O₃ power device technology has made rapid progress in recent years. Reports of large-area, ampere-class Ga₂O₃ power devices have emerged worldwide, extending beyond fundamental research demonstrations to device packaging, circuit-level testing, and ruggedness evaluations. These milestones have established Ga₂O₃ as the only ultra-wide-bandgap (UWBG) semiconductor that has reached such critical steps toward practical commercialization and application.

This talk will introduce our recent progress on exploring Ga₂O₃ devices towards high-voltage, high-temperature, and high-power applications, addressing their critical barriers towards applications, and highlighting their potential to expand the frontier of power electronics.

Multidimensional device architectures—such as superjunction, FinFET, and multi-channel—can break the performance limit of 1D power devices and enable device performance improvements through geometrical scaling. To address the limitations in p-type doping in Ga₂O₃, we developed heterogeneous superjunctions based on charge-balanced NiO/Ga₂O₃ architectures. After the first demonstration of 2 kV Ga₂O₃ vertical superjunction devices [IEDM 23], we have demonstrated lateral NiO/Ga₂O₃ architectures superjunction diodes and transistors achieving breakdown voltages exceeding 10 kV and stable operation up to 250 °C [EDL 23, IEDM 24].

In parallel, scaling up current and power require advanced thermal management, particularly given the low thermal conductivity of Ga₂O₃. We explored the path of addressing the thermal challenge of Ga₂O₃ through packaging. We employed the junction-side cooling package to directly extract heat from the active junction and demonstrate a thermal resistance comparable to commercial SiC devices [T-PEL 21, EDL 22]. We then developed novel device-package interface designs for electrical-thermo-mechanical co-optimization, demonstrating the first ultra-wide bandgap power module capable of 1000 V, 200 A switching [IEDM 25]. Most recently, we upscale the power capacity of this module to megawatt and demonstrate its advantageous performance in pulsed power electronics applications [Nat. Commun. 26].

Reliability and robustness are also critical to power device applications. Despite the lack of effective p-type doping, we demonstrate the avalanche and surge robustness in NiO/Ga₂O₃ heterojunctions [Nat. Commun. 24], as well as good bipolar stability in this heterojunction [APL 25]. Overall, coordinated progress in device, packaging, and reliability is paving the way for deployment of Ga₂O₃ in next-generation power electronics.

9:30am IWGO-FrM1-19 Formation of High-Quality SiO₂/β-Ga₂O₃ MOS Structures: Design and Optimization of Post-Annealing Processes, *Heiji Watanabe, Kensei Maeda, Masahiro Hara, Takuma Kobayashi*, The University of Osaka, Japan

INVITED

The metal-oxide-semiconductor (MOS) structure is a fundamental component in electronic devices. Among various insulators, SiO₂ is regarded as the most suitable material for Ga₂O₃-based electronics owing to its sufficiently wide bandgap, excellent insulating properties, and high thermal stability. For MOSFET operation, electrical defects at the insulator/semiconductor interface not only act as scattering centers in the MOS channel but also play a critical role in determining reliability factors such as threshold-voltage stability. Therefore, improving the MOS interface quality remains an important research challenge. However, only a limited number of studies have reported on SiO₂/Ga₂O₃ MOS structures [1], and research and development in this area is still in its early stages.

The fabrication of Ga₂O₃-based MOS devices inevitably involves the deposition of insulating films, for which post-deposition annealing (PDA) in an oxygen atmosphere is widely employed to improve film quality. In our study, SiO₂ films were directly deposited on wet-cleaned β-Ga₂O₃(001) substrates by plasma-enhanced chemical vapor deposition. We first investigated the impact of PDA on the electrical properties of SiO₂/β-Ga₂O₃ MOS capacitors [2]. Although high-temperature PDA in O₂ ambient effectively reduced electrical defects at the interface, it also caused a decrease in the net donor density in Ga₂O₃, suggesting the formation of deep acceptor-type defects, likely associated with oxygen interstitials or gallium vacancies. However, subsequent annealing in N₂ ambient restored the donor density to its initial value. As a result, the combined O₂ and N₂ annealing process yielded a low interface-state density (D_{it}) of approximately 10^{11} cm⁻²eV⁻¹ near the conduction-band edge of Ga₂O₃. We also confirmed enhanced immunity to gate-bias stress, indicating improved long-term MOSFET reliability. Furthermore, we demonstrated the significant benefits of post-metallization forming-gas annealing (FG-PMA) for SiO₂/β-Ga₂O₃ MOS structures [3]. FG-PMA at relatively low temperatures below 400 °C effectively reduced both D_{it} and near-interface traps, leading to further improvements in device performance and long-term reliability. When FG-PMA was performed following the combined O₂ and N₂ annealing, an extremely low D_{it} in the low- 10^{10} cm⁻²eV⁻¹ range was achieved through hydrogen passivation of electrical defects in the SiO₂/β-Ga₂O₃ MOS system.

This work was partly based on results obtained from a project, JPNP22007, commissioned by NEDO.

[1] K. Kita *et al.*, ECS Trans. **92**, 59 (2019).

[2] T. Kobayashi *et al.*, Appl. Phys. Lett. **126**, 012108 (2025).

[3] K. Maeda *et al.*, Appl. Phys. Lett. **127**, 112107 (2025).

9:55am IWGO-FrM1-24 Analysis of Packaged Ga₂O₃ Schottky Barrier Diodes (SBDs) for AC Rectification at Industrial Voltages, *Jeremiah Williams*, KBR Inc.; *Nolan Hendricks, Joshua Piel*, AFRL; *Zachary Weber*, Ohio State University; *Aaron Adams, Weisong Wang*, KBR Inc.; *Kyle Liddy, Daniel Dryden*, AFRL; *Takekazu Masui, Higuchi Mitsuhiro*, NCT, Japan; *Ahmad Islam, Andrew Green*, AFRL

This work analyzes Ga₂O₃ Schottky Barrier Diodes (SBDs) as half-wave AC rectifiers for a 473 V_{RMS} (669 V_{peak}) sine wave (Fig. 1). Fundamentally, transmitting power through higher voltage allows for lower currents, which improves system-level efficiency by reducing Joule heating and the requisite conductor weight [1]. We evaluate Ga₂O₃ diodes as AC rectifiers, a basic power-handling function, in voltage-dominated power transfer at voltages approaching the standard 480 V_{RMS} used for heavy industry in the USA.

The Ga₂O₃ devices in this analysis are packaged prototypes fabricated by Novel Crystal Technologies (NCT). They are compared to SiC devices fabricated by GeneSiC. Both devices use a TO-247 package. Table 1 contains measured diode characteristics. For half-wave rectifier testing, the diode is placed in series with an AC power supply and a variable resistor (the load). The power supply is set to source a 480 V_{RMS}, 1 kHz sine wave. An oscilloscope is used to measure V_{in}, V_{load}, and I_{load}. A sine or piece-wise function is fit to the measured data using SciPy for analysis. The efficiency of the diode is analyzed by comparing the on-state input power to the on-state output power minus the off-state output power. Thus, an ideal diode with no leakage or on resistance would be 100% efficient.

The efficiency of both the SiC and Ga₂O₃ diodes is ≈ 98%, dropping slightly as current increases (Fig. 2). This high efficiency is consistent with the I-V behavior. When delivering power with a higher voltage and lower current, the impact of the diodes' on resistance is reduced while that of the built-in voltage (V_{bi}) is emphasized. Some series resistance is introduced from the test setup, but it is the same for each device. Package temperature is measured with the load dissipating 88 W, corresponding to 538 mA peak current. The Ga₂O₃ diode measures slightly hotter throughout this test, ending at 26.7 ± 0.2 °C compared to the SiC diode at 26.0 ± 0.2 °C after three minutes. These results show that, despite lagging in on-resistance, the system-level performance of Ga₂O₃ SBDs is comparable to commercial SiC devices for voltage-dominated power transfer at 45-88 W.

10:10am IWGO-FrM1-27 2.2 kV NiO Based JTE β-Ga₂O₃ Schottky Barrier Diode with Improved Reliability under High-Temperature Storage Stress, *Junpeng Wen, Xuanze Zhou, Guangwei Xu, Shibing Long*, University of Science and Technology of China

β-Ga₂O₃ power diodes have the potential in applications at high-temperature and high-voltage environments. The NiO based junction termination extension (JTE) can prevent the diodes' premature breakdown, fully

Friday Morning, August 7, 2026

leveraging the high E_c of β -Ga₂O₃. However, the reliability of β -Ga₂O₃Schottky barrier diode (SBD) featuring JTE under high-temperature storage stress (HTSS) warrants attention. In this study, a HTSS test at 250 °C was conducted on JTE-SBD and the changes in device performance over the storage time were investigated. During the test, the turn-on voltage (V_{on}) of diodes increased from 0.90 V to 1.10 V, while the breakdown voltage (BV) showed a phenomenon of first increasing and then decreasing. The C-V measurements shows that the carrier concentration (N_A) of NiO initially decreases and subsequently increases, leading to the variations of the peak electric field. To enhance the device reliability, a 300 °C-10 mins oxygen annealing process has been proposed. By this approach, the V_{on} of JTE-SBD only increased 0.10 V during the test. Due to the lower and more stable N_A of NiO, the average BV of the annealed JTE-SBD maintained 2231 V even after 124 hours HTSS. Finally, XPS spectra illustrates the reasons for the changes of N_A of NiO. This study enhances the understanding of the reliability of β -Ga₂O₃ and NiO, providing effective strategy for improving the stability of NiO/ β -Ga₂O₃ JTE-SBD.

10:25am **IWGO-FrM1-30 >1 GW/cm² β -Ga₂O₃ NiO_x Heterojunction Diodes on MOCVD-Grown (110) and (010) Epilayers, Carl Peterson, Yizheng Liu, Chinmoy Nath Saha, University of California Santa Barbara; Jacob H. Leach, Kyma Technologies Inc.; James S. Speck, Sriram Krishnamoorthy, University of California Santa Barbara**

We report on the creation of >1 GW/cm² NiO_x field-plated heterojunction diodes (FP-HJDs) on MOCVD-grown (110) and (010) drift layers achieving breakdown voltages of up to 7.58 kV and parallel-plane critical electric fields (E_{11}) of up to 4.14 MV/cm. MOCVD epilayers were grown on conductive Sn-doped β -Ga₂O₃ (010) and (110) substrates using TMGa, O₂, Ar carrier gas, and SiH₄ as the silicon dopant source. Intentionally Si doped 40 μ m and 6.2 μ m epitaxial films were grown on the (110) and (010) substrates respectively. The 40 μ m film was CMP polished for 1 hr. which smoothed the surface and reduced the epilayer thickness to ~25 μ m. The sample surface exhibited global variation in height, but locally smooth surfaces for devices. The anode for the circular field-plated HJDs was created by depositing a stack of 27 nm p⁺ NiO_x, 20 nm p⁺ NiO_x, and Ni/Au/Ni metal. Next, a 2 μ m deep self-aligned etch was performed via a BCl₃ ICP process to isolate the p-n junction. Finally, a 1 μ m thick SiO₂ FP dielectric, Ni/Au FP metal, and a Ti/Au backside Ohmic contact were deposited. High voltage C-V showed a flat N_D-N_A concentration of 2.5×10^{16} cm⁻³ and 5×10^{15} cm⁻³ for the (010) and (110) epilayers respectively. J-V measurements on the 6.2 μ m (010) epi resulted in J = 700 A/cm² at 4 V, HJD ideality factors of 1.29, V_{bi} of 2 V, rectification ratio of 10^{13} , and a differential specific on resistance ($R_{on,sp}$) value of 2.36 m Ω .cm². Breakdown on the (010) epi was 1.64 kV, leading to a E_{11} of 4.02 MV/cm and a PFOM of 1.14 GW/cm². J-V on the ~25 μ m (110) epi resulted in J = 100 A/cm² at 5.6 V, HJD ideality factors of 1.08, V_{bi} of 1.8 V, rectification ratio of 10^{10} , and a $R_{on,sp}$ value of 32.2 m Ω .cm². Breakdown on the (110) epi was 7.58 kV, leading to a E_{11} of 4.14 MV/cm and a PFOM of 1.78 GW/cm². HJD results on the (010) and (110) epilayers are state-of-the-art, with E_{11} and PFOM values rivaling those achieved on commercial HVPE (001) epilayers. Additionally, this is the first demonstration of devices on (110) epilayers, with the (110) results showing high promise for the material orientation.

International Workshop on Gallium Oxide and Related Materials (IWGO-6)

Room ESJ 0202 - Session IWGO-FrM2

Advanced Device Scaling and Fabrication Techniques II

Moderators: Samuel Graham, University of Maryland College Park, Uttam Singiseti, University of Buffalo

11:10am **IWGO-FrM2-39 High-Performance β -Ga₂O₃ Vertical Diodes and FinFETs with High Electric Field Strength, Sriram Krishnamoorthy, University of California at Santa Barbara**

INVITED

β -Ga₂O₃ holds immense potential for power device applications in the medium to high voltage regime, for power conversion using solid state transformers in AI data centers. **Trench Diodes:** We report on vertical Schottky barrier diodes (SBDs) based on β -Ga₂O₃ with trench architecture, featuring a high-permittivity dielectric RESURF structure. The incorporation of a trench geometry, coupled with the high-permittivity dielectric RESURF, effectively reduces the surface electric field at the metal-semiconductor junction. This reduction facilitates the use of a lower work-function anode contact, further diminishing the turn-on voltage. The combination of lower stored charge and a low forward voltage drop results in an excellent trade-

off between conduction and switching power loss, yielding a QCVF figure of merit comparable to commercial bare die SiC SBDs. **Heterojunction Diodes:** Integration of p-type oxides with Gallium Oxide offer a way to circumvent the lack of p-type Gallium Oxide to increase built-in potential of junctions with lightly doped Gallium Oxide drift layers. We report on > 3 kV NiO and Cr₂O₃ heterojunction diodes with promising performance. > 1 A devices can be realized and double pulse testing of high current diodes with record low reverse recovery charge and time indicate the promise of topology. **Vertical Transistors:** A β -Ga₂O₃-based multi-fin vertical FinFET featuring a thick field oxide layer at the trench bottom to enhance the breakdown voltage will be discussed. With novel edge termination, we report a vertical FinFET with strategies to reduce electric field crowding around device edges, leading to enhanced breakdown voltages. To reduce the gate capacitance for superior switching performance, vertical FinFETs with split gate design are also fabricated. The devices are fabricated on (001) β -Ga₂O₃ HVPE epilayers grown on Sn-doped substrates. This approach of utilizing a vertical FinFET with split gate presents a promising solution for vertical power switches with enhanced breakdown capabilities and better switching performance. Using high voltage C-V measurements the drift layer thickness was extracted to be 11 μ m, resulting in a record high average electric field of 3.1 MV/cm for the 3.4 kV FET, which is the *highest reported average electric field* (V_{BR}/L_{drift}) in any vertical power transistor, 3X the average fields in GaN and SiC vertical power transistors. Further improvements in β -Ga₂O₃ material and oxide quality will significantly enhance the performance of such devices with effective electric field management and edge termination.

11:35am **IWGO-FrM2-44 Diffusion Suppression of Mg and High Performance β -Ga₂O₃ Current Blocking Layers by N+Mg Co-Doping Approach, Fenfen Fenda Florena, Hironobu Miyamoto, Yuki Koishikawa, Hirofumi Shinohara, Kohei Sasaki, Akito Kuramata, NCT, Japan**

Deep acceptor doping is a promising strategy for forming current-blocking layers (CBLs) in β -Ga₂O₃ vertical power devices, where p-type doping is not feasible. By compensating donor concentrations, deep acceptors create high-resistivity regions that mimic p-type body layers. While single Mg or N implantation has been demonstrated for CBL formation, these approaches suffer from high leakage current and premature breakdown. In Mg-implanted CBLs, profile distortion due to Mg diffusion during high-temperature post-implantation annealing (PIA) limits performance. To overcome these limitations, a co-doping approach have been explored theoretically to induce shallow acceptor levels via donor-acceptor level repulsion effect. This work presents the first experimental demonstration of N+Mg co-doping in β -Ga₂O₃ achieving improved CBL performance.

Multi-energy N and Mg implantations were introduced into β -Ga₂O₃ to form CBL, followed by PIA. Figure 1 shows the depth profile of N and Mg as revealed by secondary ion mass spectrometry (SIMS) measurement. At 1/1 depth ratio of N/Mg, alteration of Mg profile was detected due to massive Mg diffusion toward epilayer/substrate interface. Impressively, a remarkable Mg profile stability was achieved by implanting N much deeper into region (N/Mg = 2/1). Suppression of leakage current was more prominent in N+Mg co-implanted CBL compared to its single counterpart (more than two orders of magnitude) as shown in Fig. 2. Moreover, higher N/Mg depth ratio led to increase in breakdown voltage from 2.0 kV to 2.5 kV. This paper is based on results obtained from a project, JPNP22007, commissioned by the New Energy and Industrial Technology Development Organization (NEDO).

11:50am **IWGO-FrM2-47 >3.3 kV Ga₂O₃ Monolithic Bidirectional Switch: Impact of NiO/Ga₂O₃ Interface Charges, Yuan Qin, Virginia Tech; Yuhao Zhang, The University of Hong Kong, China**

Bidirectional switches (BDSs), which block bipolar voltages in the off-state and conduct current in both directions in the on-state, are essential for AC power electronics [1]. Monolithic BDSs (MBDSs) with a shared drift region can reduce device area by about four times compared with solutions based on two discrete devices [2]. With its high critical electric field and superior thermal stability, ultra-wide-bandgap Ga₂O₃ is promising for high-voltage power devices, making it attractive for high-voltage power device applications. After earlier demonstrations of low-voltage Ga₂O₃ MBDSs [3], [4], we recently reported a JFET-based Ga₂O₃ MBDS with BV over 6.5 kV in both polarities [5]. However, its on-resistance (R_{on}) is still much higher than the ideal value predicted from channel resistivity analysis, and its reliability remains unclear.

This work investigates the R_{on} and reliability of a Ga₂O₃ MBDS, with a particular focus on the influence of NiO/Ga₂O₃ interface charges. The elevated R_{on} originates from the non-uniform current distribution caused by

Friday Morning, August 7, 2026

the NiO junction termination extension (JTE) and interfacial charges. Negative charges at the NiO/Ga₂O₃ interface are identified as the main factor responsible for the increased R_{on} . To assess the impact of these interface charges on long-term device reliability, reverse-bias stress tests at 3.3 kV were conducted. The minimal parametric drifts observed suggest that these interface charges correspond to deep-level traps and do not substantially affect the device's long-term performance. These findings offer valuable insights and guidelines for further optimizing the figure of merit of high-voltage lateral Ga₂O₃ devices.

[1] B. J. Baliga, IEEE Power Electron. Mag. **10**, 20(2023). [2] Y. Guo, IEEE Electron Device Lett. **46**, 556(2025). [3] P. Sharma, Appl. Phys. Lett. **125**, 253502(2024). [4] D. Chettri, Appl. Phys. Lett. **125**, 202104(2024). [5] Y. Qin, IEEE Electron Device Lett. **47**, 245(2026).

12:05pm IWGO-FrM2-50 Closing Remarks

Bold page numbers indicate presenter

— A —

Acharya, Krishna: IWGO-TuP-22, 28
 Adams, Aaron: IWGO-FrM1-24, 52; IWGO-TuP-40, **32**
 Afandi, Mohammad M.: IWGO-TuP-16, **26**
 Ahmadi, Elaheh: IWGO-TuP-34, 30
 Akhtar, Arub: IWGO-MoP-30, 13; IWGO-TuP-28, 29
 Akiba, Takayuki: IWGO-MoP-33, 14
 Alam, Sadikul: IWGO-MoM2-43, 2
 Alamoudi, Hadeel: IWGO-WeP-42, 48
 Albrecht, Martin: IWGO-TuP-28, 29
 Alem, Nasim: IWGO-MoA1-1, 4; IWGO-WeP-13, 40
 Alema, Fikadu: IWGO-WeP-15, 41
 Alonso-Orts, Manuel: IWGO-MoP-42, 16; IWGO-TuP-19, 27; IWGO-TuP-20, **27**; IWGO-TuP-30, 29
 Amano, Hiroshi: IWGO-MoP-29, 13
 Amir, Walid: IWGO-WeA-21, **37**; IWGO-WeP-29, 44
 An, Eun-Jeong: IWGO-MoP-22, 11; IWGO-TuP-11, **25**
 An, JuEun: IWGO-MoP-4, 7
 Anandan, Sai Kkrishna: IWGO-WeP-24, **43**
 Anderson, Travis: IWGO-MoP-14, 9
 Ando, Yuji: IWGO-MoP-36, 15
 Ansbro, Avery-Ryan: IWGO-MoP-25, **12**
 Arehart, Aaron: IWGO-MoA1-15, 5; IWGO-MoA1-9, 4
 Arnab, Aaditta: IWGO-MoA1-1, 4
 Asel, Tadj: IWGO-TuP-1, 23
 Asel, Thaddeus: IWGO-TuM2-37, 18; IWGO-TuP-13, 25; IWGO-WeM2-41, 34
 Ashraf, Huma: IWGO-TuP-31, 30; IWGO-TuP-34, 30

— B —

Bae, Sang-Jin: IWGO-MoP-22, 11; IWGO-TuP-11, 25
 Bae, Si-Young: IWGO-MoP-21, 11
 BAE, Si-Young: IWGO-TuP-23, 28
 Bag, Ankush: IWGO-TuP-18, 26
 Balog, Andrew: IWGO-WeP-13, 40
 Ban, Yuzaburo: IWGO-ThM2-40, 50
 Banner, Nathan S.: IWGO-WeP-33, 45
 Baraket, Mira: IWGO-MoP-13, 9
 Barber, Richard: IWGO-WeP-39, **47**
 Baunthiyal, Aman: IWGO-TuP-19, 27
 Beakes, Connor: IWGO-WeP-13, 40; IWGO-WeP-18, 41
 Bennett, Steven: IWGO-TuM2-42, 18; IWGO-WeP-39, 47
 Berini, Bruno: IWGO-WeP-3, 38
 Bertoni, Ilaria: IWGO-ThM1-20, **49**
 Bhat, Aditya K: IWGO-TuP-31, 30
 Bhattacharya, Debaditya: IWGO-MoM2-46, 2; IWGO-TuA1-12, **20**
 Bibilashvili, Amiran: IWGO-WeP-3, 38
 Bierwagen, Oliver: IWGO-MoM1-22, **1**
 Bin Anooz, Saud: IWGO-MoP-30, 13; IWGO-MoP-31, 13; IWGO-TuP-28, 29
 Bosch, Julien: IWGO-TuP-32, **30**
 Brand, Will: IWGO-WeP-15, **41**
 Braun, Jeffrey: IWGO-MoP-28, 13
 Breakfield, Jacob: IWGO-TuP-1, 23
 Brillson, Leonard: IWGO-WeP-16, 41
 Brockman, John: IWGO-WeP-39, 47
 Buchmaier, Wolfgang: IWGO-MoA1-6, 4
 Buontempo, Joshua: IWGO-MoM2-52, **2**; IWGO-WeP-10, **39**
 Burnett, Jay: IWGO-TuP-31, 30; IWGO-TuP-34, 30
 Butanovs, Edgars: IWGO-TuP-4, 23
 Butenko, Pavel: IWGO-WeP-5, **38**

— C —

Callahan, William: IWGO-TuP-33, **30**
 Callens, Gordon: IWGO-TuP-20, 27
 Cantin, Jean-Louis: IWGO-WeP-3, 38
 Cao, Haicheng: IWGO-TuP-36, 31
 Carver, Miranda: IWGO-MoA1-9, **4**
 Cavalero, Randal: IWGO-WeP-18, 41
 Chabak, Kelson: IWGO-WeP-4, 38
 Chakraborty, Surajit: IWGO-WeA-21, 37; IWGO-WeP-29, 44; IWGO-WeP-34, **46**
 Charnas, Adam: IWGO-TuP-13, 25
 Chettri, Dhanu: IWGO-TuP-36, 31
 Chiang, Chao-Ching: IWGO-MoP-14, 9
 Chikoidze, Ekaterine: IWGO-MoP-18, 10; IWGO-WeP-3, 38
 Chikoizde, Ekaterine: IWGO-WeM2-47, 35
 Chiu, Chan-Wen: IWGO-WeP-33, 45
 Choi, JungHun: IWGO-TuP-15, 26
 Chou, Ta-Shun: IWGO-MoP-30, 13; IWGO-MoP-31, 13; IWGO-TuP-28, **29**
 Chu, Ying-Hao: IWGO-TuP-25, 28
 Chujo, Taiki: IWGO-WeP-6, 39
 Chung, Roy: IWGO-TuP-17, 26
 Chung, Roy B.: IWGO-TuP-16, 26
 Colonel, Lucas: IWGO-TuM2-48, 18
 Consonni, Vincent: IWGO-TuP-32, 30
 Conway, Charlotte: IWGO-TuP-31, **30**
 Crnobrnja, Aleksa: IWGO-WeP-11, 40
 Czuba, Krzysztof: IWGO-MoP-23, 12

— D —

Darakchieva, Vanya: IWGO-ThM1-26, 50
 Das, Nabasindhu: IWGO-WeA-9, **36**; IWGO-WeP-40, 47
 DeLeon, Carlos: IWGO-WeP-16, **41**
 Dhar, Sarit: IWGO-TuP-37, **31**
 Dhasiyan, Arun Kumar: IWGO-MoP-27, **13**
 Dhora, Andri: IWGO-WeP-31, **45**
 Dipans, Eriks: IWGO-TuP-4, **23**
 Djurabekova, Flyura: IWGO-ThM1-20, 49
 Dobročka, Edmund: IWGO-MoP-34, 14
 Dong, Jiatong: IWGO-TuP-39, **32**
 Dryden, Daniel: IWGO-FrM1-24, 52; IWGO-MoP-40, **16**; IWGO-TuA2-33, 21; IWGO-WeM2-41, 34
 Dumont, Yves: IWGO-MoP-18, 10; IWGO-WeM2-47, 35; IWGO-WeP-3, 38
 Dutton, Benjamin: IWGO-WeP-12, 40; IWGO-WeP-13, 40; IWGO-WeP-18, **41**

— E —

Ebbing, Charles: IWGO-TuP-37, 31
 Ebihara, Kohei: IWGO-MoP-26, **12**
 Egbo, Kingsley: IWGO-TuA1-9, 20; IWGO-TuP-33, 30
 Eguchi, Masanori: IWGO-TuA2-30, **21**
 Eickhoff, Martin: IWGO-MoP-42, 16; IWGO-TuP-19, 27; IWGO-TuP-20, 27; IWGO-TuP-30, 29
 Elhajhasan, Mahmoud: IWGO-TuP-20, 27
 Eon, David: IWGO-TuM2-48, 18
 Ertekin, Elif: IWGO-MoA1-1, **4**
 Esteves, D.M.: IWGO-MoP-11, 9
 Etokoro, Kotaro: IWGO-TuP-29, **29**
 Evans, Prescott: IWGO-TuP-1, 23; IWGO-WeM2-41, 34

— F —

Falta, Jens: IWGO-TuP-19, 27
 Farzana, Esmat: IWGO-WeA-12, 36
 Febba, Davi: IWGO-TuP-33, 30
 Fenda Florena, Fenfen: IWGO-FrM2-44, **53**
 Ferreyra, Romualdo: IWGO-WeA-18, 37
 Feygelson, Boris: IWGO-TuP-9, 24
 Fiedler, Andreas: IWGO-MoP-30, 13; IWGO-MoP-31, 13; IWGO-TuP-28, 29; IWGO-WeM1-24, **33**

Florena, Fenfen Fenda: IWGO-MoA1-12, 4
 Freitas, Jaime: IWGO-WeP-39, 47
 Fu, Houqiang: IWGO-MoP-38, 15
 Fu, Pengyu: IWGO-WeA-6, 36
 Fujita, Shizuo: IWGO-MoP-35, 14; IWGO-MoP-36, **15**; IWGO-TuP-7, **24**
 — G —
 Gabrusenoks, Jevgenijs: IWGO-TuP-4, 23
 Gahl, John: IWGO-WeP-39, 47
 Galazka, Zbigniew: IWGO-MoM1-13, **1**; IWGO-ThM1-26, 50; IWGO-ThM2-43, 51; IWGO-TuP-28, 29
 Gallagher, James: IWGO-MoA1-18, **5**
 Gallarday, Pierre: IWGO-TuP-8, **24**; IWGO-WeM2-47, **35**
 Galyukov, Alex: IWGO-WeP-11, **40**
 Gann, Katie: IWGO-TuA2-24, 21; IWGO-TuM2-37, 18; IWGO-TuM2-42, 18; IWGO-TuP-9, **24**; IWGO-WeP-26, 43; IWGO-WeP-28, 44; IWGO-WeP-30, **45**; IWGO-WeP-35, 46
 Garland, Henry: IWGO-MoM2-49, 2
 Gaskins, John: IWGO-MoP-28, 13
 Geddis, Kale: IWGO-WeP-12, 40
 Gelineau, Guillaume: IWGO-TuM2-48, 18
 Genuist, Yann: IWGO-TuP-32, 30
 Gervassi-Saga, Julian: IWGO-WeP-40, **47**
 Ghadi, Hemant: IWGO-MoA1-15, 5; IWGO-MoA1-9, 4
 Ghosh, Saptarsi: IWGO-MoP-20, 11
 Gilankar, Advait: IWGO-WeP-36, **46**; IWGO-WeP-40, 47
 Glaser, Evan: IWGO-TuM2-42, 18; IWGO-WeP-39, 47
 Gołębiowska, Aneta: IWGO-MoP-23, 12
 Goorsky, Mark: IWGO-MoP-8, 8; IWGO-TuA1-15, 20; IWGO-WeP-36, 46
 Gopalan, Sanjay: IWGO-WeP-17, **41**
 Gordon, Mark: IWGO-WeM2-41, 34
 Gorsak, Cameron: IWGO-MoM2-52, 2; IWGO-TuA2-33, 21; IWGO-TuP-13, 25; IWGO-WeP-10, 39; IWGO-WeP-28, **44**; IWGO-WeP-30, 45; IWGO-WeP-35, 46
 Gray, Tia: IWGO-TuM2-42, 18; IWGO-WeP-9, 39
 Green, Andrew: IWGO-FrM1-24, 52; IWGO-TuA2-33, 21; IWGO-TuP-13, 25; IWGO-WeP-4, 38
 Green, Andy: IWGO-TuP-1, 23
 Greenberg, Benjamin: IWGO-TuP-9, 24
 Gregušová, Dagmar: IWGO-MoP-34, 14
 Grüneberg, Raimund: IWGO-MoP-30, 13
 Guemann, Filip: IWGO-MoP-34, **14**
 Gudelli, Vijay Kumar: IWGO-TuP-26, **28**
 Gurukrishna Vadlamudi, Sai: IWGO-MoP-34, 14
 Guza, Marcin: IWGO-MoP-23, 12
 — H —
 Haberland, Kolja: IWGO-MoP-30, **13**
 Hajzus, Jenifer: IWGO-WeP-28, 44
 Halasyamani, P. Shiv: IWGO-TuM2-42, 18; IWGO-WeP-39, 47
 Handwerg, Martin: IWGO-MoP-31, 13
 Haque, Aman: IWGO-MoP-14, 9
 Hara, Masahiro: IWGO-FrM1-19, 52
 Hartman, Alison: IWGO-WeP-39, 47
 Hasegawa, Sho: IWGO-TuM1-22, **17**; IWGO-TuM2-45, 18; IWGO-WeP-6, 39
 Hashimoto, Yasuhiro: IWGO-WeM2-50, 35
 Hassan, Mehidi: IWGO-MoM2-43, 2; IWGO-TuP-10, **25**
 Hatayama, Eito: IWGO-MoP-10, **8**

Author Index

- Haven, Drew: IWGO-MoM2-49, 2; IWGO-WeP-12, 40; IWGO-WeP-13, 40; IWGO-WeP-18, 41
- Hayashida, Tetsuro: IWGO-MoP-26, 12
- He, Shuwei: IWGO-WeA-6, 36
- Hendricks, Nolan: IWGO-FrM1-24, 52; IWGO-TuP-1, 23
- Hendzelek, Wojciech: IWGO-MoP-23, **12**
- Heron, John: IWGO-MoP-25, 12
- Hickman, Austin: IWGO-WeP-15, 41
- Higashiwaki, Masataka: IWGO-MoP-39, 15; IWGO-ThM2-40, 50; IWGO-ThM2-46, 51; IWGO-WeA-15, 37; IWGO-WeA-18, 37
- Hiraoka, Tomomi: IWGO-TuP-7, 24
- Ho, Ai: IWGO-TuP-25, **28**
- Hobart, Karl: IWGO-MoA1-18, 5; IWGO-TuA2-24, 21; IWGO-TuA2-36, 22; IWGO-TuM2-42, 18; IWGO-TuP-9, 24; IWGO-WeP-30, 45; IWGO-WeP-39, 47
- Hollar, Emerson: IWGO-WeA-12, **36**
- Honda, Satoko: IWGO-ThM2-46, 51
- Honda, Tohru: IWGO-MoP-33, 14; IWGO-ThM2-40, 50; IWGO-TuP-12, 25
- Hopkins, Patrick: IWGO-MoP-28, 13; IWGO-TuP-22, 28
- Hori, Masaru: IWGO-MoP-27, 13
- Horng, Ray Hua: IWGO-TuP-27, **29**
- Horng, Ray-Hua: IWGO-TuP-25, 28
- Hoshikawa, Keigo: IWGO-TuM1-28, 17
- Hu, Debo: IWGO-MoP-24, **12**
- Hurtado, Andres: IWGO-WeP-42, 48
- Hurtado, Andres E Castano: IWGO-TuP-26, 28
- Hušeková, Kristína: IWGO-MoP-34, 14
- Hwang, Jinwoo: IWGO-MoM2-43, 2; IWGO-ThM2-35, **50**; IWGO-TuP-10, 25; IWGO-TuP-6, 24
- I —
- Iba, Yoshiki: IWGO-ThM2-40, 50; IWGO-WeA-15, 37; IWGO-WeM2-50, **35**
- Igarashi, Takuya: IWGO-TuM1-12, 17; IWGO-WeP-6, 39
- IJIIMA, SOTARO: IWGO-WeP-37, **46**
- Ikeda, Hikaru: IWGO-MoP-36, 15; IWGO-TuP-7, 24
- Imai, Katsuhiko: IWGO-WeM2-35, 34; IWGO-WeM2-44, 34
- Imaida, Hayama: IWGO-TuP-38, 31
- Imanishi, Masayuki: IWGO-WeM2-38, 34; IWGO-WeP-20, 42; IWGO-WeP-21, 42
- Imhof, Aleksander: IWGO-MoP-41, **16**
- Inajima, Jin: IWGO-WeA-15, 37
- Isaacs-Smith, Tamara: IWGO-TuP-37, 31
- Ishida, Kentaro: IWGO-MoP-6, **8**
- Ishihara, Takuma: IWGO-MoP-7, 8
- Ishikawa, Mahiro: IWGO-MoP-7, **8**
- Ishikawa, Masato: IWGO-WeP-7, 39
- Ishikawa, Yukari: IWGO-MoA2-32, **6**; IWGO-TuA2-27, 21
- Ishiyama, Shota: IWGO-MoP-19, 10; IWGO-TuP-2, 23
- Ishizawa, Satoshi: IWGO-WeP-22, 42
- Islam, Ahmad: IWGO-FrM1-24, 52; IWGO-TuA2-33, 21
- Isobe, Yuki: IWGO-MoP-35, **14**; IWGO-MoP-36, 15; IWGO-TuP-29, 29
- Iwamoto, Satoshi: IWGO-WeM2-44, 34; IWGO-WeP-38, 47
- Izumi, Hirokazu: IWGO-MoP-35, 14
- J —
- Jacobs, Alan: IWGO-TuA2-24, **21**; IWGO-TuM2-42, 18; IWGO-TuP-9, 24; IWGO-WeP-27, 44; IWGO-WeP-28, 44; IWGO-WeP-30, 45; IWGO-WeP-35, 46; IWGO-WeP-39, 47
- Jang, MinSeok: IWGO-MoP-4, 7
- Jena, Debdeep: IWGO-MoM2-46, 2; IWGO-TuA1-12, 20
- Jeon, Dae-woo: IWGO-TuP-15, 26
- Jeon, Ho Jung: IWGO-MoP-16, 10
- JEONG, Seong-Min: IWGO-TuP-23, 28
- Jiang, Luoyuan: IWGO-WeP-41, **48**
- Jinno, Riena: IWGO-WeM2-44, **34**; IWGO-WeP-38, 47
- Jourdan, Fabien: IWGO-TuP-32, 30
- Joyce, David: IWGO-MoM2-49, 2; IWGO-WeP-12, 40; IWGO-WeP-13, 40; IWGO-WeP-18, 41
- Jung, Kwang-Hee: IWGO-MoP-22, 11; IWGO-TuP-11, 25
- Jung, Yusup: IWGO-TuP-3, 23; IWGO-WeP-1, 38
- K —
- Kakimoto, Koichi: IWGO-TuM1-25, 17
- Kalarickal, Nidhin Kurian: IWGO-WeP-36, 46; IWGO-WeP-40, 47
- Kamada, Kei: IWGO-TuM1-25, 17; IWGO-WeP-22, 42
- Kamimura, Takafumi: IWGO-WeA-15, 37
- Kamiński, Maciej: IWGO-MoP-23, 12
- Kanegae, Kazutaka: IWGO-MoP-10, 8; IWGO-TuP-2, 23; IWGO-WeP-2, 38
- Kaneko, Kentaro: IWGO-MoP-35, 14; IWGO-TuP-29, 29; IWGO-TuP-7, 24
- KANG, Chang-Mo: IWGO-TuP-23, 28
- Kang, Jinki: IWGO-WeP-8, 39
- Kang, Jin-Ki: IWGO-MoP-22, 11; IWGO-TuP-11, 25
- Kang, Myeonggyun: IWGO-WeP-22, **42**
- Kang, Taiyoung: IWGO-TuP-3, 23
- Kang, TaiYoung: IWGO-WeP-1, 38
- Kao, Ming-Chao: IWGO-WeP-25, **43**
- Karg, Alexander: IWGO-MoP-42, **16**; IWGO-TuP-19, 27; IWGO-TuP-20, 27; IWGO-TuP-30, **29**
- Kasu, Makoto: IWGO-TuA2-30, 21
- Katayama, Ryuji: IWGO-WeM2-38, 34
- Kato, Masashi: IWGO-MoP-19, 10; IWGO-MoP-7, 8; IWGO-TuP-2, 23
- Kato, Naofumi: IWGO-MoP-27, 13
- Katsube, Daiki: IWGO-MoA2-32, 6; IWGO-TuA2-27, **21**
- Kelemen, Paul: IWGO-WeP-33, 45
- Kelly, Frank: IWGO-WeP-26, 43; IWGO-WeP-27, **44**; IWGO-WeP-28, 44; IWGO-WeP-30, 45; IWGO-WeP-35, 46; IWGO-WeP-9, 39
- Kern, Deborah: IWGO-MoP-31, **13**
- Kezer, Pat: IWGO-MoP-25, 12
- KIKUCHI, AKIHIKO: IWGO-WeP-37, 46
- Kikuta, Daigo: IWGO-MoA1-12, 4
- Kilic, Ufuk: IWGO-ThM1-26, 50
- Kim, HeeJin: IWGO-MoP-4, 7
- Kim, Hyeong-Yun: IWGO-TuP-15, **26**
- Kim, HyoJung: IWGO-TuP-14, **26**
- Kim, Jung-Gon: IWGO-MoP-22, 11; IWGO-TuP-11, 25
- Kim, Ki Wook: IWGO-WeP-17, 41
- Kim, Min-Yeong: IWGO-MoP-38, 15; IWGO-WeP-24, 43; IWGO-WeP-4, 38
- Kim, Sanghun: IWGO-WeP-1, 38
- Kim, SangHun: IWGO-MoP-3, **7**
- Kioupakis, Emmanouil: IWGO-ThM1-17, 49; IWGO-ThM1-23, 50; IWGO-WeP-14, 40
- Kioupakis, Emmanouil (Manos): IWGO-ThM1-12, **49**
- Kishimoto, Eisho: IWGO-WeM2-38, 34
- Kita, Koji: IWGO-TuP-38, 31
- Kitahara, Masanori: IWGO-TuM1-25, **17**; IWGO-WeP-22, 42
- Kitzmler, Chase: IWGO-TuP-37, 31
- Klemm, Mason: IWGO-WeP-39, 47
- Kobayashi, Takuma: IWGO-FrM1-19, 52
- Kochurikhin, Vladimir: IWGO-TuM1-25, 17
- Köck, Anton: IWGO-TuP-8, 24
- Koishikawa, Yuki: IWGO-FrM2-44, 53
- Konishi, Keita: IWGO-TuM1-22, 17
- Konno, Shun: IWGO-WeA-18, 37
- Koo, Sang-Mo: IWGO-MoP-38, 15; IWGO-WeP-4, 38
- Koreishi, Kazuki: IWGO-MoP-37, **15**
- Korlacki, Rafal: IWGO-ThM1-26, 50
- Kosednar-Legenstein, Barbara: IWGO-TuP-8, 24
- Koshi, Kimiyoshi: IWGO-TuM1-12, 17; IWGO-TuM1-22, 17; IWGO-TuM2-45, 18; IWGO-WeP-6, 39
- Kozak, Iryna: IWGO-MoP-34, 14
- Kraker, Elke: IWGO-TuP-8, 24
- Krishnamoorthy, Sriram: IWGO-FrM1-30, 53; IWGO-FrM2-39, **53**; IWGO-MoA1-6, 4; IWGO-MoP-12, 9; IWGO-TuA1-6, 20; IWGO-WeA-6, 36; IWGO-WeP-32, 45; IWGO-WeP-9, 39
- Krohn, Matthew: IWGO-TuM2-42, 18
- Kuball, Martin: IWGO-TuA1-1, **20**; IWGO-TuP-18, 26; IWGO-TuP-31, 30; IWGO-WeP-24, 43
- Kumagai, Yoshinao: IWGO-MoP-39, 15; IWGO-ThM2-40, 50; IWGO-WeA-15, 37; IWGO-WeM1-19, **33**; IWGO-WeM2-50, 35
- Kuramata, Akito: IWGO-FrM2-44, 53; IWGO-TuA2-27, 21; IWGO-TuM1-12, **17**; IWGO-TuM1-22, 17; IWGO-TuM2-45, 18; IWGO-WeM2-38, 34; IWGO-WeP-39, 47; IWGO-WeP-6, 39
- Kurbay, Alp: IWGO-ThM1-17, **49**; IWGO-ThM1-23, 50
- Kusaba, Akira: IWGO-MoP-39, 15
- Kushitashvili, Zurab: IWGO-WeP-3, 38
- Kyoung, Sinsu: IWGO-TuP-3, 23
- Kyoung, SinSu: IWGO-MoP-3, 7; IWGO-WeP-1, 38
- L —
- Labed, Madani: IWGO-MoP-15, **10**; IWGO-MoP-16, 10
- Lamb, Dan: IWGO-MoP-20, 11
- Lang, Maik: IWGO-MoA1-15, 5; IWGO-TuP-13, 25
- Lavelle, Robert: IWGO-MoP-41, 16; IWGO-TuM2-42, 18; IWGO-WeP-12, 40; IWGO-WeP-13, **40**; IWGO-WeP-18, 41
- Lawson, Jacob: IWGO-TuP-37, 31
- Leach, Jacob: IWGO-MoA1-18, 5; IWGO-MoM2-38, **1**; IWGO-MoP-14, 9; IWGO-TuA2-36, 22
- Leach, Jacob H.: IWGO-FrM1-30, 53
- Lebedinsky, Alex: IWGO-TuM2-42, 18
- Lee, Channyung: IWGO-MoA1-1, 4
- Lee, Dong-Jin: IWGO-MoP-22, 11; IWGO-TuP-11, 25
- Lee, Dong-Jun: IWGO-WeP-8, **39**
- Lee, Eun-Seo: IWGO-TuP-11, 25
- LEE, Eun-Seo: IWGO-MoP-22, **11**
- Lee, Gyeong Ryl: IWGO-TuP-16, 26; IWGO-TuP-17, **26**
- Lee, HoJun: IWGO-MoP-4, 7
- Lee, JungBok: IWGO-MoP-4, **7**
- Lee, Sohyun: IWGO-WeP-33, 45
- Lee, Won-Jae: IWGO-TuP-11, 25
- LEE, Won-Jae: IWGO-MoP-22, 11
- Leitgeb, Verena: IWGO-TuP-8, 24
- Li, Cheng-Han: IWGO-TuP-25, 28
- Li, Jian: IWGO-TuP-1, 23; IWGO-WeM2-41, 34
- Li, Jian-Sian: IWGO-MoP-14, 9

Author Index

- Li, Qiliang: IWGO-MoP-38, 15; IWGO-WeP-4, 38
Li, Xiaohang: IWGO-TuP-36, 31
Liang, Yi: IWGO-MoP-25, 12
Liao, Michael: IWGO-MoP-8, **8**; IWGO-TuA1-15, **20**; IWGO-WeP-36, 46
Liddy, Kyle: IWGO-FrM1-24, 52; IWGO-WeP-4, 38
LIM, Jae-Hyeok: IWGO-TuP-23, **28**
Lin, Chia-Hung: IWGO-MoM2-43, 2; IWGO-TuA2-30, 21; IWGO-TuM1-12, 17; IWGO-WeM2-38, 34
Lindquist, Kurt: IWGO-WeP-12, **40**
Liu, Binzhi: IWGO-TuP-10, 25; IWGO-TuP-6, 24
Liu, Jiawei: IWGO-MoM2-43, 2; IWGO-WeA-21, 37; IWGO-WeP-29, **44**
Liu, Yizheng: IWGO-FrM1-30, 53; IWGO-MoP-12, **9**; IWGO-TuA1-6, **20**; IWGO-WeA-6, 36; IWGO-WeP-9, 39
Liudmila, Gushchina: IWGO-TuM1-25, 17
Llewelyn, Ciaran: IWGO-MoP-20, 11
Londhe, Manasi: IWGO-MoP-25, 12
Long, Shibing: IWGO-FrM1-27, 52
Lorenz, Katharina: IWGO-MoP-11, 9
Loske, Katharina: IWGO-MoP-14, **9**
Lu, Wu: IWGO-WeP-41, 48
Lundh, J. S.: IWGO-WeP-35, 46
Lundh, James: IWGO-TuA2-24, 21; IWGO-WeP-27, 44
Lundh, James Spencer: IWGO-TuM2-42, 18
Lyle, Luke: IWGO-WeP-12, 40; IWGO-WeP-13, 40; IWGO-WeP-18, 41
Lyle, Luke A. M.: IWGO-WeP-33, 45
— M —
Madeira, Florence: IWGO-TuM2-48, 18
Maeda, Kensei: IWGO-FrM1-19, 52
Maeda, Takuya: IWGO-TuP-35, 30
Mahadik, Nadeemullah: IWGO-MoA1-18, 5; IWGO-MoP-41, 16
Maimon, Ory: IWGO-MoP-38, 15; IWGO-WeP-4, 38
Mainali, Ganesh: IWGO-TuP-36, **31**
Maitra, Shreyasi: IWGO-MoP-20, 11
Makisako, Ryutarō: IWGO-MoP-36, 15
Makkonen, Ilja: IWGO-ThM2-43, 51
Mangum, John: IWGO-MoM2-49, 2
Marchal, Mathias: IWGO-WeP-38, 47
Marzegalli, Anna: IWGO-ThM1-20, 49
Masten, Hannah: IWGO-WeP-9, 39
Mastro, Michael: IWGO-MoA1-18, 5; IWGO-TuA2-24, 21; IWGO-TuP-9, 24; IWGO-WeP-26, 43; IWGO-WeP-27, 44; IWGO-WeP-28, 44; IWGO-WeP-30, 45; IWGO-WeP-35, 46
Masui, Takekazu: IWGO-FrM1-24, 52
Matsui, Shunya: IWGO-MoP-33, 14; IWGO-TuP-12, **25**
Matsuo, Daisuke: IWGO-WeA-18, 37
Mattapalli, Akhila: IWGO-WeP-32, **45**
Mauze, Akhil: IWGO-ThM1-26, 50
Mazen, Frédéric: IWGO-TuM2-48, 18
Mazzolini, Piero: IWGO-MoM1-22, 1
McGray, Craig: IWGO-TuA2-36, 22
McKnight, Grace: IWGO-MoA1-1, 4
Medjdoub, Farid: IWGO-WeP-3, 38
Meng, Lingyu: IWGO-MoA1-9, 4
Merrit, Joseph: IWGO-TuP-37, 31
Micottis, Tom: IWGO-MoP-32, **14**; IWGO-WeP-3, 38
Mičušik, Matej: IWGO-MoP-34, 14
Miglio, Leonida: IWGO-ThM1-20, 49
Milési, Frédéric: IWGO-TuM2-48, 18
Mitchell, Jacob: IWGO-TuP-31, 30
Mitchell, Lee: IWGO-TuM2-42, 18
Mitsuhito, Higuchi: IWGO-FrM1-24, 52
Mitterhuber, Lisa: IWGO-TuP-8, 24
Miyake, Hiroki: IWGO-MoP-5, 7; IWGO-TuP-5, 23
Miyamoto, Hironobu: IWGO-FrM2-44, 53; IWGO-MoA1-12, 4; IWGO-MoP-33, 14; IWGO-TuA2-27, 21; IWGO-TuP-12, 25; IWGO-TuP-35, 30
Mizui, Makoto: IWGO-TuM1-22, 17
Mizukoshi, Kensuke: IWGO-TuM1-28, 17
Mock, Alyssa: IWGO-ThM1-26, 50
Mohney, Suzanne E.: IWGO-WeP-33, 45
Mondal, Arnab: IWGO-TuP-18, 26
Monroy, Eva: IWGO-TuP-32, 30
Montserrat, Josep: IWGO-TuP-8, 24; IWGO-WeM2-47, 35
Mori, Yusuke: IWGO-WeM2-38, 34; IWGO-WeP-20, 42; IWGO-WeP-21, 42
Moriyama, Jun: IWGO-WeA-18, **37**
Moser, Neil: IWGO-WeP-4, 38
Mou, Shin: IWGO-TuP-1, **23**; IWGO-TuP-13, 25; IWGO-WeM2-41, 34
Mouck, Donivan R.: IWGO-WeP-33, **45**
Mudiyansele, Dinusha: IWGO-MoP-38, 15
Muller, David: IWGO-TuA1-12, 20; IWGO-TuM2-37, 18
Müller, Yann: IWGO-ThM1-17, 49
Munakata, Akihira: IWGO-TuP-35, **30**
Murakami, Kazuto: IWGO-WeM2-35, 34; IWGO-WeM2-44, 34
Murakami, Rikito: IWGO-WeP-22, 42
Muth, John: IWGO-WeP-17, 41
Myers-Ward, Rachael: IWGO-TuP-9, 24; IWGO-WeP-30, 45
Myren, Dominic: IWGO-TuA2-33, **21**
— N —
Nádaždy, Peter: IWGO-MoP-34, 14
Nair, Hari: IWGO-MoM2-52, 2; IWGO-TuA2-33, 21; IWGO-TuP-13, 25; IWGO-WeP-10, 39
Nakaniwa, Shotaro: IWGO-TuA2-30, 21
Nakano, Haru: IWGO-WeP-20, **42**
Nakaoka, Toshiki: IWGO-ThM2-46, 51
Nandi, Arpit: IWGO-TuP-18, **26**; IWGO-WeP-24, 43
Natarajan, Anirudh: IWGO-ThM1-17, 49
Nath Saha, Chinmoy: IWGO-WeP-32, 45; IWGO-WeP-9, 39
Neal, Adam: IWGO-TuP-1, 23; IWGO-TuP-13, **25**; IWGO-WeM2-41, 34
Nelson, Tolen: IWGO-WeP-27, 44
Niitsu, Kodai: IWGO-MoP-37, 15
Nishikawa, Tomoka: IWGO-WeM2-38, **34**
Nishinaka, Hiroyuki: IWGO-MoP-10, 8; IWGO-MoP-19, 10; IWGO-MoP-5, 7; IWGO-TuP-2, 23; IWGO-TuP-5, 23; IWGO-WeP-2, 38
Nishinoiri, Takashi: IWGO-TuM1-28, 17
Noesges, Brenton: IWGO-TuM2-37, 18; IWGO-TuP-1, 23; IWGO-WeM2-41, **34**
Noguchi, Munetaka: IWGO-MoP-26, 12
Nomoto, Kazuki: IWGO-MoM2-46, 2; IWGO-TuA1-12, 20
— O —
Oda, Osamu: IWGO-MoP-27, 13
O'Hayre, Ryan: IWGO-TuP-33, 30
Ohno, Yasuo: IWGO-TuP-7, 24
Ohtomo, Akira: IWGO-MoP-37, 15
Okuno, Hanako: IWGO-TuP-32, 30
O'Leary, Sean: IWGO-TuA2-36, 22
Onuma, Takeyoshi: IWGO-MoP-33, 14; IWGO-ThM2-40, **50**; IWGO-TuP-12, 25
O'Quinn, Eric: IWGO-TuP-13, 25
Oras, Sven: IWGO-TuP-4, 23
Oshima, Takayoshi: IWGO-MoP-1, **7**; IWGO-TuM2-51, **19**; IWGO-WeM2-35, 34; IWGO-WeM2-44, 34
Oshima, Yuichi: IWGO-TuM2-51, 19; IWGO-WeM2-35, **34**
Osinsky, Andrei: IWGO-WeP-15, 41
Overstreet, Cale: IWGO-MoA1-15, 5; IWGO-TuP-13, 25
Oya, Taisei: IWGO-TuP-21, 27
— P —
Pakes, Andrew: IWGO-MoP-20, 11
Pant, Nick: IWGO-ThM1-23, 50
Park, Jang Hyeok: IWGO-MoP-16, 10; IWGO-MoP-21, 11
Park, Ji-Hyeon: IWGO-TuP-15, 26
Park, Joonhui: IWGO-TuP-3, **23**
Park, Mi-Seon: IWGO-MoP-22, 11; IWGO-TuP-11, 25
Park, Taejun: IWGO-TuP-3, 23; IWGO-WeP-1, **38**
Park, Tae-Yong: IWGO-TuP-23, 28
Park, Young Min: IWGO-TuP-16, 26; IWGO-TuP-17, 26
Patel, Satyam: IWGO-WeP-19, **42**
Patnaik, Akash: IWGO-MoP-18, **10**; IWGO-WeP-3, 38
Pavlidis, Georges: IWGO-TuA2-33, 11
Peelaers, Hartwin: IWGO-MoA2-35, 6
Pennachio, Daniel: IWGO-TuA2-24, 21; IWGO-TuP-9, 24; IWGO-WeP-26, **43**; IWGO-WeP-27, 44; IWGO-WeP-28, 44; IWGO-WeP-35, 46
Peres, Marco: IWGO-MoP-11, 9
Perez Tomas, Amador Perez Tomas: IWGO-MoP-9, 8
Pérez-Tomás, Amador: IWGO-TuP-8, 24; IWGO-WeM2-47, 35
Petersen, Lynn: IWGO-TuM1-7, **17**
Peterson, Becky (R.L.): IWGO-WeP-19, 42
Peterson, Carl: IWGO-FrM1-30, **53**; IWGO-MoP-12, 9; IWGO-TuA1-6, 20; IWGO-WeP-32, 45
Peterson, Rebecca: IWGO-TuP-34, 30
Phiw-Ondee, Satjawoot: IWGO-TuP-30, 29
Philips, Bernard: IWGO-TuM2-42, 18
Pieczulewski, Naomi: IWGO-TuA1-12, 20; IWGO-TuM2-37, **18**
Piel, Joshua: IWGO-FrM1-24, 52
Piš, Igor: IWGO-MoP-34, 14
Pistner, Scott: IWGO-WeP-13, 40; IWGO-WeP-18, 41
Pohorelec, Ondrej: IWGO-MoP-34, 14
Pookpanratana, Sujitra: IWGO-MoP-38, **15**; IWGO-WeP-4, **38**
Popp, Adreas: IWGO-MoP-30, 13
Popp, Andreas: IWGO-MoP-31, 13; IWGO-TuP-28, 29
— Q —
Qin, Yuan: IWGO-FrM2-47, **53**
— R —
Raghuvansy, Sushma: IWGO-MoP-42, 16; IWGO-TuP-19, 27
Ramdin, Daram: IWGO-TuP-13, 25; IWGO-WeM2-41, 34
Ramesh, Madhav: IWGO-TuA1-12, 20
Rebollo, José: IWGO-TuP-8, 24; IWGO-WeM2-47, 35
Rebollo, Steve: IWGO-MoA1-6, **4**; IWGO-WeP-32, 45
Redwing, Joan: IWGO-WeP-13, 40
Rehm, Jana: IWGO-MoP-30, 13; IWGO-TuP-28, 29
Reid, Blaine: IWGO-WeP-39, 47

Author Index

- Reilly, Caroline: IWGO-MoA1-18, 5; IWGO-MoM2-38, 1; IWGO-MoP-14, 9; IWGO-TuA2-36, **22**
- Reimann, Christian: IWGO-MoA1-18, 5
- Ren, Fan: IWGO-MoP-14, 9
- Reyes, Jessica: IWGO-MoP-28, 13
- Ribault, Thomas: IWGO-MoP-18, 10; IWGO-WeP-3, **38**
- Rim, You Seung: IWGO-MoP-15, 10; IWGO-MoP-16, 10; IWGO-MoP-21, 11
- Ringel, Steven: IWGO-MoA1-15, 5; IWGO-MoA1-9, 4
- Roberts, Kerry: IWGO-TuP-31, 30; IWGO-TuP-34, 30
- Rocco, Emma: IWGO-TuA2-36, 22; IWGO-TuP-9, 24; IWGO-WeP-26, 43; IWGO-WeP-27, 44; IWGO-WeP-28, 44; IWGO-WeP-30, 45; IWGO-WeP-35, **46**
- Rohnke, Marcus: IWGO-TuP-20, 27
- Ronning, Carsten: IWGO-TuP-20, 27
- Roqan, Iman: IWGO-MoP-11, 9; IWGO-TuP-39, 32; IWGO-WeP-42, 48
- Roqan, Iman S: IWGO-TuP-26, 28
- Rosenauer, Andreas: IWGO-MoP-42, 16; IWGO-TuP-19, 27; IWGO-TuP-20, 27; IWGO-TuP-30, 29
- Roth, Adrien: IWGO-TuM2-48, **18**
- Roussel, Hervé: IWGO-TuP-32, 30
- S —
- Sacchi, Anna: IWGO-MoM2-49, 2; IWGO-TuA1-9, 20; IWGO-TuP-22, **28**; IWGO-TuP-33, 30
- Sadowski, Oskar: IWGO-MoP-23, 12
- Saha, Chinmoy: IWGO-MoP-12, 9; IWGO-TuA1-6, 20
- Saha, Chinmoy Nath: IWGO-FrM1-30, 53; IWGO-WeA-6, **36**
- Saha, Niloy Chandra: IWGO-TuA2-30, 21
- Saito, Aoi: IWGO-MoP-5, **7**
- Sajib, Deb Indronil: IWGO-WeP-34, 46
- Sakaguchi, Ryoichi: IWGO-TuM1-22, 17; IWGO-WeP-6, 39
- Sakai, Ryuji: IWGO-MoP-26, 12
- Sakamoto, Isao: IWGO-TuM1-22, 17
- Sanyal, Indraneel: IWGO-MoP-20, **11**
- sarigiannidou, Eirini: IWGO-TuP-32, 30
- Sarkar, Md Mosarof Hossain: IWGO-MoM2-43, **2**; IWGO-TuP-6, 24; IWGO-WeP-41, 48
- Sarkar, Md. Mosarof Hossain: IWGO-WeA-21, 37
- Sartel, Corine: IWGO-WeM2-47, 35
- Sartel, Corinne: IWGO-MoP-18, 10; IWGO-WeP-3, 38
- Sasaki, Kohei: IWGO-FrM2-44, 53; IWGO-MoA1-12, 4; IWGO-MoA2-32, 6; IWGO-MoM2-43, 2; IWGO-MoP-33, 14; IWGO-MoP-7, 8; IWGO-TuA2-27, 21; IWGO-TuA2-30, 21; IWGO-TuM1-12, 17; IWGO-TuM1-22, 17; IWGO-TuM2-45, 18; IWGO-TuP-12, 25; IWGO-TuP-35, 30; IWGO-WeM1-10, **33**; IWGO-WeM2-38, 34; IWGO-WeP-39, 47; IWGO-WeP-6, 39
- Sato, Koji: IWGO-MoA2-32, 6
- Sato, Makoto: IWGO-TuA2-30, 21
- Saurabh, Kumar: IWGO-TuM2-42, 18
- Scarpulla, Michael: IWGO-MoA1-1, 4
- Schlom, Darrell: IWGO-TuA1-12, 20; IWGO-TuM1-17, **17**
- Schlom, Darrell G.: IWGO-MoM2-46, 2
- Schmidbauer, Martin: IWGO-MoP-31, 13
- Schowalter, Marco: IWGO-MoP-42, 16; IWGO-TuP-19, 27; IWGO-TuP-20, 27; IWGO-TuP-30, 29
- Schubert, Mathias: IWGO-ThM1-26, 50; IWGO-TuA1-12, 20
- Schulte, Kevin: IWGO-MoM2-49, 2
- Scott, Ethan: IWGO-MoP-28, **13**
- Seacat, Sierra: IWGO-MoA2-35, **6**
- Séguret, Andy: IWGO-TuP-32, 30
- Seike, Ichiro: IWGO-TuP-5, **23**
- Senevirathna, M. K. Indika: IWGO-MoM2-46, 2
- Senevirathna,, Indika: IWGO-TuA1-12, 20
- Sepelak, Nicholas: IWGO-WeM2-41, 34
- Shah, Piyush: IWGO-MoP-8, 8; IWGO-TuA1-15, 20; IWGO-WeP-36, 46
- Shimazaki, Takumi: IWGO-WeP-7, 39
- Shimazoe, Kazuki: IWGO-MoP-19, **10**; IWGO-MoP-7, 8; IWGO-TuP-2, **23**
- Shimizu, Naohiro: IWGO-MoP-27, 13
- Shimizu, Shigenori: IWGO-TuM1-28, 17
- Shin, Hee Won: IWGO-MoP-21, **11**
- Shin, Kanghee: IWGO-MoP-16, **10**
- SHIN, Yun-Ji: IWGO-TuP-23, 28
- Shinagawa, Ryo: IWGO-WeP-6, 39
- Shinohara, Hirofumi: IWGO-FrM2-44, 53
- Shintani, Michihiro: IWGO-MoP-10, 8
- Shivamade Gowda, Shivashree: IWGO-TuP-22, 28
- Shoji, Yasuhiro: IWGO-TuM1-25, 17
- Shrestha, Pragya: IWGO-WeP-4, 38
- Shuai, Quentin: IWGO-MoA1-15, 5
- Singiseti, Uttam: IWGO-MoM2-43, 2; IWGO-WeA-1, **36**; IWGO-WeA-21, 37; IWGO-WeP-29, 44; IWGO-WeP-34, 46
- Smeaton, Michelle: IWGO-TuP-22, 28
- Smirnov, Andrey: IWGO-WeP-11, 40
- Smith, Matthew: IWGO-TuP-31, 30
- Snyder, David: IWGO-WeP-13, 40; IWGO-WeP-18, 41
- Solay, Leo Raj: IWGO-TuP-36, 31
- Soma, Takuto: IWGO-MoP-37, 15
- Sorensen, Preston: IWGO-ThM1-26, **50**; IWGO-TuA1-12, 20
- Speck, James: IWGO-MoA1-6, 4; IWGO-MoP-12, 9; IWGO-ThM1-26, 50
- Speck, James S.: IWGO-FrM1-30, 53; IWGO-WeA-6, 36
- Speck, Jim: IWGO-WeP-32, 45
- Splawn, Heather: IWGO-MoA1-18, 5; IWGO-MoM2-38, 1; IWGO-TuA2-36, 22
- Spurgeon, Steven R.: IWGO-TuP-22, 28
- Staerz, Anna: IWGO-TuP-33, 30
- Steele, Jacob: IWGO-MoM2-46, **2**; IWGO-TuA1-12, 20
- Stevanovic, Vladan: IWGO-TuP-22, 28
- Stokey, Megan: IWGO-ThM1-26, 50
- Strods, Edvards: IWGO-TuP-4, 23
- Suda, Jun: IWGO-MoP-36, 15
- Suzumi, Hisato: IWGO-WeP-22, 42
- Sugaya, Hidetaka: IWGO-MoP-36, 15
- Szerling, Anna: IWGO-MoP-23, 12
- T —
- Tadger, Marko: IWGO-MoA1-18, 5; IWGO-MoP-14, 9; IWGO-MoP-28, 13; IWGO-MoP-41, 16; IWGO-TuA1-6, 20; IWGO-TuA2-36, 22; IWGO-TuM2-42, **18**; IWGO-WeP-27, 44; IWGO-WeP-30, 45; IWGO-WeP-35, 46; IWGO-WeP-39, 47; IWGO-WeP-9, **39**
- Taishi, Toshinori: IWGO-MoP-6, 8; IWGO-TuM1-28, 17
- Takahashi, Hidemasa: IWGO-MoP-36, 15
- Takane, Hitoshi: IWGO-MoA1-12, **4**
- Takayama, Hajime: IWGO-MoP-10, 8
- Takeda, Shoma: IWGO-ThM2-46, 51
- Takeda, Tomoki: IWGO-MoP-27, 13
- Takemura, Shinya: IWGO-WeA-18, 37
- Tamura, Atsushi: IWGO-TuP-38, **31**
- Tan, Chee Keong: IWGO-MoP-17, 10
- Tanaka, Katsuhisa: IWGO-MoP-35, 14; IWGO-MoP-36, 15; IWGO-TuP-29, 29; IWGO-TuP-7, 24
- Tanaka, Kohei: IWGO-WeA-18, 37
- Tanaka, Kyohei: IWGO-ThM2-40, 50
- Tanaka, Rina: IWGO-MoP-26, 12
- Tang, Xiao: IWGO-TuP-31, 30
- Tanikawa, Hayato: IWGO-WeP-2, **38**
- Tanikawa, Tomoyuki: IWGO-WeM2-38, 34
- Ľapajna, Milan: IWGO-MoP-34, 14
- Tarenko, Jaroslaw: IWGO-MoP-23, 12
- Taube, Andrzej: IWGO-MoP-23, 12
- Taya, Masaki: IWGO-MoP-26, 12
- Tellekamp, Brooks: IWGO-TuP-22, 28; IWGO-TuP-33, 30
- Tellekamp, M Brooks: IWGO-MoM2-49, **2**
- Tellekamp, M. Brooks: IWGO-TuA1-9, 20
- Teo, K.B.K: IWGO-MoP-20, 11
- Teramura, Yusuke: IWGO-ThM2-46, 51; IWGO-WeA-15, 37
- Terauchi, Yuma: IWGO-ThM2-40, 50; IWGO-WeA-15, 37; IWGO-WeM2-50, 35
- Thompson, Michael: IWGO-TuM2-37, 18
- Togashi, Rie: IWGO-MoP-39, **15**; IWGO-WeP-7, **39**
- Tomida, Taketoshi: IWGO-TuM1-25, 17
- Tomita, Takahiro: IWGO-WeM2-35, 34; IWGO-WeM2-44, 34
- Toyoshima, Keida: IWGO-WeP-38, **47**
- Trausa, Annamarija: IWGO-TuP-4, 23
- Tripathi, Pushpanshu: IWGO-MoM2-52, 2; IWGO-WeP-10, 39
- Troutot, Nicolas: IWGO-TuM2-48, 18
- Tsujimoto, Kohki: IWGO-ThM2-46, **51**; IWGO-WeA-15, 37
- Tuomisto, Filip: IWGO-ThM2-43, 51
- U —
- Ueda, Tetsuzo: IWGO-MoP-36, 15
- Ueda, Yuki: IWGO-MoM2-43, 2; IWGO-TuM1-22, 17; IWGO-TuM2-45, **18**; IWGO-WeP-6, **39**
- Ugolotti, Aldo: IWGO-ThM1-20, 49
- Uno, Kazuyuki: IWGO-TuP-21, **27**
- Upadhyaya, Kishor: IWGO-MoP-11, **9**; IWGO-TuP-26, 28; IWGO-WeP-42, **48**
- Usami, Shigeyoshi: IWGO-WeM2-38, 34; IWGO-WeP-20, 42; IWGO-WeP-21, **42**
- Usui, Kosuke: IWGO-WeA-18, 37
- V —
- Van de Walle, Chris: IWGO-MoP-12, 9
- van de Walle, Chris G.: IWGO-ThM1-7, **49**
- Vanjari, Sai Charan: IWGO-TuP-31, 30
- Varley, Joel: IWGO-MoA1-1, 4; IWGO-MoA2-27, **5**
- Vellvehí i Llovet, Aniol: IWGO-MoP-9, **8**
- Vellvehí, Aniol: IWGO-TuP-8, 24; IWGO-WeM2-47, 35
- Vellvehí, Miquel: IWGO-TuP-8, 24; IWGO-WeM2-47, 35
- Vogt, Patrick: IWGO-MoP-42, 16; IWGO-TuP-30, 29
- Volant, Marty: IWGO-TuP-32, 30
- Voss, Kay-Obbe: IWGO-MoA1-15, 5; IWGO-TuP-13, 25
- W —
- Wakamatsu, Takeru: IWGO-MoP-35, 14; IWGO-MoP-36, 15; IWGO-TuP-29, 29; IWGO-TuP-7, 24
- Wakimoto, Daiki: IWGO-TuA2-27, 21
- Walsby, Edward: IWGO-TuP-34, 30
- Wan, Hsiao-Hsuan: IWGO-MoP-14, 9
- Wang, Amanda: IWGO-ThM1-23, **80**
- Wang, Haitao: IWGO-MoP-29, 13
- Wang, Haochen: IWGO-MoP-12, 9
- Wang, Jia: IWGO-MoP-29, 13

Author Index

- Wang, Jin: IWGO-WeA-6, 36
Wang, Weisong: IWGO-FrM1-24, 52
Wang, Yan: IWGO-MoP-17, **10**
Wang, Zhenwei: IWGO-WeA-15, **37**; IWGO-WeA-18, 37
Watahiki, Tatsuro: IWGO-MoP-26, 12
Watanabe, Heiji: IWGO-FrM1-19, **52**
Watanabe, Hiroshi: IWGO-MoP-26, 12
Watanabe, Shinya: IWGO-TuM1-12, 17; IWGO-TuM1-22, 17
Weber, Marc: IWGO-WeP-39, 47
Weber, Zach: IWGO-TuP-1, 23
Weber, Zachary: IWGO-FrM1-24, 52
Welp, Eric: IWGO-WeP-13, 40
Wen, Junpeng: IWGO-FrM1-27, **52**
Wickramaratne, Darshana: IWGO-TuA2-24, 21; IWGO-TuM2-42, 18
Widiez, Julie: IWGO-TuM2-48, 18
Wierzbicka, Justyna: IWGO-MoP-23, 12
Williams, Jeremiah: IWGO-FrM1-24, **52**
Williams, Martin Samuel: IWGO-MoP-42, 16; IWGO-TuP-19, **27**; IWGO-TuP-20, 27; IWGO-TuP-30, 29
Winchester, Andrew: IWGO-MoP-38, 15
Wojcicka, Aleksandra: IWGO-TuP-24, **28**
Wójcicka, Aleksandra: IWGO-MoP-23, 12
Woodward, Jeffrey: IWGO-TuP-9, 24
Wu, Mingxuan: IWGO-TuP-6, 24
Wzorek, Marek: IWGO-MoP-23, 12
— X —
Xiao, Shiyu: IWGO-WeM2-35, 34; IWGO-WeM2-44, 34
Xing, Huili, 2
Xing, Huili Grace: IWGO-TuA1-12, 20
Xu, Guangwei: IWGO-FrM1-27, 52
Xu, Yibo: IWGO-WeP-41, 48
Xu, Zhiyu: IWGO-MoP-29, **13**
— Y —
Yamaguchi, Tomohiro: IWGO-MoP-33, 14; IWGO-ThM2-40, 50
Yamamoto, Kai: IWGO-ThM2-40, 50
Yamamoto, Yuki: IWGO-MoP-35, 14; IWGO-TuM1-28, **17**
Yamaoka, Yu: IWGO-TuM1-22, 17
Yamashita, Yusuke: IWGO-MoA1-12, 4
Yang, Juchen: IWGO-WeA-6, 36
Yao, Yongzaho: IWGO-MoA2-32, 6
Yao, Yongzhao: IWGO-MoM1-27, **1**; IWGO-TuA2-27, 21
Yao, Yuzhou: IWGO-WeA-6, 36
Yasuda, Harunobu: IWGO-MoP-33, **14**; IWGO-TuP-12, 25
Yatskiv, Roman: IWGO-MoP-2, **7**; IWGO-TuP-41, **32**
Ymaguchi, Tomohiro: IWGO-TuP-12, 25
Yokota, Yuui: IWGO-WeP-22, 42
Yoo, GeonWook: IWGO-TuP-14, 26
Yoon, SiSung: IWGO-TuP-14, 26
Yoshikawa, Akira: IWGO-TuM1-25, 17; IWGO-WeP-22, 42
Yoshimatsu, Kohei: IWGO-MoP-37, 15
Yoshinaga, Junya: IWGO-ThM2-40, 50; IWGO-WeA-15, 37; IWGO-WeM2-50, 35
Yoshino, Masao: IWGO-WeP-22, 42
Young, Matthew: IWGO-MoM2-49, 2
Yousf, Nuzhat: IWGO-TuP-36, 31
Yu, Dong su: IWGO-MoM2-43, 2
Yu, Dong Su: IWGO-MoA1-9, 4; IWGO-TuP-6, **24**
Yu, Dongsu: IWGO-WeA-21, 37
YUKI, TAKAHASHI: IWGO-WeP-37, 46
Yun, Ho-Gyun: IWGO-MoP-22, 11; IWGO-TuP-11, 25
— Z —
Zakutayev, Andriy: IWGO-MoM2-49, 2; IWGO-TuA1-9, **20**; IWGO-TuP-22, 28; IWGO-TuP-33, 30
Zhai, Xin: IWGO-TuP-34, **30**
Zhang, Haizhong: IWGO-WeP-23, **43**
Zhang, Kaitian: IWGO-TuP-6, 24; IWGO-WeP-16, 41
Zhang, Xiao: IWGO-ThM1-17, 49; IWGO-ThM1-23, 50; IWGO-WeP-14, **40**
Zhang, Yuewei: IWGO-ThM1-26, 50
Zhang, Yuhao: IWGO-FrM1-10, **52**; IWGO-FrM2-47, 53
Zhao, Hingping: IWGO-WeA-21, 37
Zhao, Hongping: IWGO-MoA1-9, 4; IWGO-MoM2-43, 2; IWGO-TuP-6, 24; IWGO-WeP-16, 41; IWGO-WeP-41, 48
Zhao, Yanzhen: IWGO-MoA1-15, **5**
Zhelezova, Iuliia: IWGO-ThM2-43, **51**
Zheng, Yunlin: IWGO-MoP-18, 10; IWGO-WeP-3, 38
Zhou, Xuanze: IWGO-FrM1-27, 52